MATHEMATICAL STUDY OF RISK IN FINANCIAL MARKETS

A thesis submitted to

DELHI TECHNOLOGICAL UNIVERSITY

for the award of the degree of

DOCTOR OF PHILOSOPHY

in

MATHEMATICS

by

GIFTY MALHOTRA

(Enrollment No. : 2K14/Ph.D/AM/06)

under the supervision of

Prof. R.Srivastava

and

Prof. H.C.Taneja

DEPARTMENT OF APPLIED MATHEMATICS

DELHI TECHNOLOGICAL UNIVERSITY

(Formerly Delhi College of Engineering)

DELHI-110042, INDIA

July, 2019

DECLARATION

I declare that the research work reported in this thesis entitled "**Mathematical Study Of Risk In Financial Markets**" for the award of the degree of *Doctor of Philosophy in Mathematics* has been carried out by me under the supervision of *Prof. R.Srivastava* and *Prof. H.C.Taneja*, Department of Applied Mathematics, Delhi Technological University, Delhi, India.

The research work embodied in this thesis, except where otherwise indicated, is my original research. This thesis has not been submitted by me earlier in part or full to any other University or Institute for the award of any degree or diploma.

This thesis does not contain other person's data, graphs or other information unless specifically acknowledged.

Date :

(Gifty Malhotra)
Enrollment No. : 2K14/Ph.D/AM/06
Department of Applied Mathematics
Delhi Technological University
Delhi - 110042, India

DELHI TECHNOLOGICAL UNIVERSITY

(Formerly Delhi College of Engineering)

Shahbad Daulatpur, Bawana Road, Delhi-110042, India

CERTIFICATE

This is to certify that the thesis entitled **"Mathematical Study Of Risk In Financial Markets"** submitted by **Ms. Gifty Malhotra** with enrollment number **2K14/Ph.D/AM/06** in the Department of Applied Mathematics, Delhi Technological University, Delhi, India for the award of the degree of *Doctor of Philosophy in Mathematics*, is a record of original research work carried out by her under our guidance and supervision.

We have read this thesis and that, in our opinion, it is fully adequate in scope and quality as a thesis for the degree of Doctor of Philosophy in Mathematics.

To the best of our knowledge, the work reported in this thesis is original and has not been submitted partially or fully to any other university or institution in any form for the award of any degree or diploma.

(Prof. R.Srivastava)
Supervisor
Department of Applied Mathematics
Delhi Technological University
Delhi-110042, India

(Prof. H.C.Taneja)
Co-Supervisor
Department of Applied Mathematics
Delhi Technological University
Delhi-110042, India

(Prof. Sangita Kansal)
Head
Department of Applied Mathematics
Delhi Technological University
Delhi-110042, India

ACKNOWLEDGEMENTS

I have received encouragement and support from lots of people during my Ph.D. work. It is the time to express my sincere gratitude to all of them.

First and foremost, I would like to thank the Almighty for holding my hands throughout this journey and giving me hope, strength and opportunities to complete this research work.

I wish to express my sincere gratitude to my respected supervisors Prof. R.Srivastava and Prof. H.C.Taneja, Department of Applied Mathematics, Delhi Technological University (DTU), Delhi for their inspiring guidance and support during my research work, and for giving me the freedom to explore my own ideas. It is indeed a great pleasure for me to work under their supervision. I appreciate all their contributions of time and ideas to make my Ph.D. experience productive and stimulating.

I sincerely thank to Prof. Sangita Kansal, Head, Department of Applied Mathematics, DTU, for providing me the necessary facilities and valuable suggestions during the progress of the work.

I extend my sincere thanks to Prof. H.C.Taneja as Dean (Academic, PG), DTU, for his everlasting support and guidance. My sincere thanks to all the faculty members of Department of Applied Mathematics and other Departments of DTU for their constant support and encouragement.

I gratefully acknowledge the academic branch and administration of DTU for providing the suitable environment and facilities to carry out my research work. I would like to thank Mr. Akhil, Ms. Nisha, Mr. Anurag and Mr. Sumit, the office staff of Department of Applied Mathematics, DTU, for their all kinds of support.

I acknowledge my heartfelt thanks to all my teachers from my childhood for pouring their precious knowledge and for inculcating in me the love for 'Mathematics'. I express my gratitude to my mentors Dr. Amrit Pal Singh Virk and Ms. Rupneet Kaur for giving me confidence to follow my dream of doing research in mathematics. I am ineffably indebted to my friends Ms. Monika Singh and Mr. Aditya Kumar Mourya for always believing in me and for their constant affirmation and encouragement during my Ph.D. work.

My time at DTU was enjoyable due to some very good friends and groups that became a part of my life. I am grateful to my seniors Dr. Virendra Kumar, Dr. Vijay Singh, Dr. Pankaj Kumar, Dr. Richa Thapliyal, Dr. Rashmi Jain, Dr. Saloni Rathi and Dr. Minakshi Dhamija for their unconditional support and encouragement. I would like to thank Dr. Milan Srivastava, Dr. Anjali Singh, Dr. Kanika Khatter, Ms. Mamata Sahu and Ms. Charu Arora for all the good times we spent together.

I am thankful to Mr. Abhishek Kumar, Mr. Ram Pratap and Mr. Ajay Kumar for always helping me in the need of hour. I thank Ms. Mridula Mundalia, Ms. Ritu Goel, Ms. Kanica Goel, Ms. Shweta Goel and Mr. Aniket Goel for their joyful company and wonderful memories. I express my sincere thanks to all other research scholars of Department of Applied Mathematics, DTU.

I wish to record my profound gratitude to my family who has provided me all kinds of support and help for my academic achievements, and for their constant love and care. I am extremely thankful to my father for always giving me the freedom to make my own choices and to pursue my passion. I also acknowledge with deep sense of reverence, my gratitude towards my mother for all her sacrifices, prayers, blessings and for always being there for me.

I would like to express my thanks to my brother Mr. Lovish Malhotra, my sister-in-law Ms. Shaina Malhotra, my cute niece Saisha Malhotra and our dearest Appy for their heartiest cooperation and affection.

I gratefully acknowledge University Grants Commission (UGC), Government of India, for providing me research fellowship (JRF and SRF).

I want to express my thanks to all of them who have not been mentioned here but supported, encouraged and inspired me during my Ph.D. work.

Date : **(GIFTY MALHOTRA)**

Place : Delhi, India

Dedicated To . . .

Satguru "Sai"

and

my parents Mrs. Gulshan Malhotra and Mr. Babu Ram Malhotra

Blessed to have their love, encouragement and endless support

Contents

Abstract

In 1973, a significant breakthrough came in the history of pricing options when Fischer Black and Myron Scholes proposed a valuation formula for the pricing of European call options based on the geometric Brownian motion model of the stock price dynamics. This option pricing model was further developed by Robert C. Merton in the same year, and was named as the "Black-Scholes option pricing model". Despite its landmark success in the option pricing theory, the model has certain biases like the assumptions of constant volatility and Gaussian distribution of asset log-returns. In practice, the volatility is not constant and the asset log-return distributions are non-Gaussian in nature characterized by heavy tails and high peaks. A wide range of research has been done to revise and upgrade classical Black-Scholes model. The relaxation of constant volatility assumption led to the modeling of dynamic volatility. A natural extension is to regard the volatility as a continuous time stochastic process which gave rise to the stochastic volatility modeling. Stochastic volatility models allow the volatility to fluctuate randomly and are able to incorporate many empirical characteristics of volatility namely volatility smile, mean-reversion and leverage to name a few. These models are further extended to consider either multiple factors of volatility or to include the jumps in the stock price or volatility process.

Volatility is a standard measure of risk, which is a statistical tool to measure the dispersion of asset returns from their mean over a given time period. An alternate measure of risk can be entropy, since it also measures the randomness. Shannon(1948) in his mathematical theory of communication, used entropy as a measure of information which laid the foundation of the field of information theory. Entropy has broad applications in finance too especially in the portfolio selection, asset pricing and time series analysis. The principle of maximum entropy has extensively been used in finance. Furthermore, the concept of entropy is of great help in analysing the stock market since it captures the uncertainty and disorder

of the time series without imposing any constraints on the theoretical probability distribution.

The thesis entitled **"Mathematical Study of Risk in Financial Markets"** is devoted to the execution of stochastic volatility modeling and entropy approach for the option pricing and the analysis of asset log-return series. We have proposed a multifactor stochastic volatility model with a fast and a slow mean-reverting factors of volatility, where the slow volatility factor is approximated with a quadratic arc. Using this model, the pricing formulae and the implied volatility smiles are obtained for the European and Asian options. The accuracy of these option pricing formulae is also established. We have also shown that the multifactor stochastic volatility models outperform the stochastic volatility jump diffusion models, by comparing the two extensions of Heston stochastic volatility model.

In addition, the option pricing and analysis of asset log-return series is conducted using entropy measures. The concept of approximation of slow volatility factor is infused with the entropy maximization. For this, we have proposed to calibrate the risk-neutral density function of the future asset price by maximizing a two-parameter entropy with an additional variance constraint, where the quadratic arc expression of volatility is considered. The calibrated density function is used to price the European call options for different strikes. We have also proposed a two-parameter permutation entropy and its extensions viz. two-parameter multiscale permutation entropy and two-parameter weighted multiscale permutation entropy to analyse the asset log-return series.

List of Abbreviations

ATM	$At-The-Money$
BM	$Brownian\ Motion$
CIR	$Cox-Ingersoll-Ross$
EPO	$End\ Point\ Overlapping$
GAO	$Geometric\ Asian\ Option$
GBM	$Geometric\ Brownian\ Motion$
HSV	$Heston\ Stochastic\ Volatility$
ITM	$In-The-Money$
$LMMR$	$Log\ Moneyness\ to\ Maturity\ Ratio$
MEP	$Maximum\ Entropy\ Principle$
MPE	$Multiscale\ Permutation\ Entropy$
$MPE_{\alpha,\beta}$	$Two\ Parameter\ Multiscale\ Permutation\ Entropy$
MRE	$Mean\ Relative\ Error$
$MRPE$	$Multiscale\ Renyi\ Permutation\ Entropy$
MSV	$Multifactor\ Stochastic\ Volatility$
NoO	$Non\ Overlapping$
OTM	$Out-The-Money$
OU	$Ornstein-Uhlenbeck$
PDE	$Partial\ Differential\ Equation$
$p.d.f.$	$Probability\ Density\ Function$
PE	$Permutation\ Entropy$
$PE_{\alpha,\beta}$	$Two\ Parameter\ Permutation\ Entropy$
RPE	$Renyi\ Permutation\ Entropy$
$S.D.$	$Standard\ Deviation$
SDE	$Stochastic\ Differential\ Equation$
SVJ	$Stochastic\ Volatility\ Jump$

$WMPE$	*Weighted Multiscale Permutation Entropy*
$WMPE^{v}_{\alpha,\beta}$	*Two Parameter Weighted Multiscale Permutation Entropy*
$WMPE^{w}_{\alpha,\beta}$	*Two Parameter New Weighted Multiscale Permutation Entropy*
$WMRPE$	*Weighted Multiscale Renyi Permutation Entropy*
$WPE^{v}_{\alpha,\beta}$	*Two Parameter Weighted Permutation Entropy*
$WPE^{w}_{\alpha,\beta}$	*Two Parameter New Weighted Permutation Entropy*

List of Figures

List of Tables

Chapter 1

Introduction and Literature Survey

In this thesis, we have worked on the stochastic volatility models in the continuous time scenario where the stock price and the volatility dynamics is given by the stochastic differential equations (SDEs). The chapter begins with the basic introduction to stochastic (or random) processes and stochastic calculus. The stochastic volatility models are used to price options and to calibrate the volatility surface so next we have defined the option and volatility. Starting from the Black-Scholes model to price the European options, we have discussed its development up to the multifactor stochastic volatility models. A brief literature on Asian option pricing is also given. Along with the stochastic volatility modeling, we have also worked on asset pricing and time series analysis of asset log-return series using entropy measures, therefore, some important entropy measures and the principle of maximum entropy is given along with the relevant literature on these topics. At the end, the outline of the work reported in this thesis is given.

The field of financial mathematics is concerned with the development and analysis of mathematical models that can be used for the valuation of investments in the financial assets. There are mainly two types of assets which are traded in a financial market namely risky and risk free. Risky assets include a stock, stock index, foreign currency, gold, a commodity or any asset whose future value is unknown today. Risk free assets include bank deposit or bond issued by government, a financial institute or a company. An investor invests in the financial market to get the maximum return on his investment. For the more potential return on an investment, an investor has to take more risk because risk and return are related to each other. So, for making large and quick gain a person speculates and trades in the risky financial assets which attract a huge amount of risk because of their random dynamics. A good understanding of asset dynamics is essential to make a significant financial decision. Along with this, one should have a sound knowledge of the measures of risk and the ways to manage or hedge this risk. The standard measure of risk is volatility which is a statistical tool to measure the dispersion of asset returns from their mean over a given time period. An alternate measure of risk can be entropy, since it also measures the randomness. This work is devoted to the study of these two aspects for the option pricing and time series analysis of asset log-return series. Here, we present the necessary material required for the understanding of the work carried out in the upcoming chapters of this thesis.

In Section 1.1, stochastic processes and their basic properties have been discussed. In Section 1.2, we have given a review of some basic topics of stochastic calculus such as SDEs, stochastic integral and Ito lemma. In Section 1.3, the concept of option and volatility has been explained. The well renowned Black-Scholes model and the extensions of this model for the pricing of European options have also been discussed in this section by giving the suitable literature review. In Section 1.4, a review on Asian option pricing has been given. In Section 1.5, entropy as a measure of risk has been discussed and its applications in financial asset pricing and time series analysis are reviewed. The outline of the research work reported in the thesis has been given in Section 1.6.

1.1 Stochastic Processes

To depict the random movements of the asset (say stock) prices mathematically, the concept of stochastic processes plays an important role.

By Lefebvre [76], $p.47$: "Suppose that with each element s of a sample space S of some random experiment E, we associate a function $X(t,s)$, where t belongs to $T \subset \mathbb{R}$. The set $\{X(t,s) : t \in T\}$ is called a stochastic (or random) process". With a fixed s and varying t, this stochastic process is a sample path and with a fixed t and varying s, this is a random variable. Alternatively, a stochastic process is also denoted as $\{X(t) : t \in T\}$ or $\{X_t : t \in T\}$ without explicitly mentioning s.

By Ross [103], $p.41$: "A stochastic process $\underline{X} = \{X(t), t \in T\}$ is a collection of random variables. That is, for each t in the index set T, $X(t)$ is a random variable". Here, the parameter t, which varies over the index set (or parameter space) T, is usually interpreted as time. The range (or collection of all possible values) of random variable X_t where $t \in T$ is interpreted as the state space of stochastic process.

- A stochastic process $\{X_t : t \in T\}$ is categorized as a discrete-time or a continuous-time stochastic process depending on whether its parameter space T is discrete or continuous. Similarly, based on the state space, which can be discrete or continuous, a stochastic process is categorized as a discrete-state or a continuous-state stochastic process.

1.1.1 Some Properties of Stochastic Processes

- A stochastic process $\{X_t : t \in T\}$ has the **independent increments** if for all non negative integers n and for all $h_0 < h_1 < ... < h_n \in T$, the random variables $X_{h_1} - X_{h_0}$, $X_{h_2} - X_{h_1}, ..., X_{h_n} - X_{h_{n-1}}$ are independent.
  It has the **stationary increments** if for $0 \leq h < t$, the distribution of $X_t - X_h$ is same as that of $X_{(t-h)} - X_0$.

- The given stochastic process $\{X_t : t \in T\}$ will be a **Markov process** if

$$P\{a_1 < X_t \leq b_1 \mid X_{h_0} = x_0,\, X_{h_1} = x_1, ...,\, X_{h_n} = x_n\} = P\{a_1 < X_t \leq b_1 \mid X_{h_n} = x_n\} \tag{1.1.1}$$

  where $h_0 < h_1 < ... < h_n < t$. This represents that the probability of future

state, when the current state is given, is not affected by any supplementary knowledge of the previous information. In finance and economics, a continuous-state Markov process under certain conditions becomes a **Diffusion process**.

- The stochastic process $\{X_t : t \in T\}$ will be a **martingale** if its expected value, $E(X_t)$ exists for all t and for any $h_0 < h_1 < ... < h_n \in T$,

$$E(X_{h_n} \mid X_{h_0} = x_0,\, X_{h_1} = x_1, ..., X_{h_{n-1}} = x_{n-1}) \;=\; x_{n-1} \tag{1.1.2}$$

- Martingales are like fair games. If X_t represents the fortune of a player at time t, then the martingale property ensures that his average fortune at the next play given the current fortune is independent of the past fortunes.

The history of modeling stock prices with stochastic processes started in 1900 when Louis Bachelier [5] proposed the very basic model for the stock price dynamics. He defined Brownian motion mathematically and used the one dimensional version of Brownian motion to model stock price dynamics.

1.1.2 Brownian Motion

An English botanist Robert Brown in 1827 observed the highly irregular movements of the grains of the pollen suspended in the liquid or gas, which is now known as the *Brownian motion* (BM). Mathematically, BM is a continuous-time and continuous-state stochastic process $\{B_t : t \geq 0\}$, satisfying certain properties given below:

(i) $B_0 = 0$;

(ii) The increments of B_t are independent and stationary ;

(iii) The increments $B_{t+s} - B_s$ has the normal distribution $\mathcal{N}(0, \sigma^2 t)$.

The sample path B_t is always continuous for $t > 0$. This mathematical description of BM was given by the great mathematician Norbort Wiener in his series of work beginning from 1918. Here, σ^2 is the variance parameter of the process.

- The stochastic process $W_t = \frac{B_t}{\sigma}$ is the **standard Brownian motion** or **Wiener process**. Its distribution is $\mathcal{N}(0,t)$.

- The stochastic process $X_t = \mu t + \sigma W_t$ is called the BM with drift (or mean) μ and variance σ^2. Here $-\infty < \mu < \infty$ and $\sigma > 0$ are constants.

- BM is a diffusion process. Also, the standard Brownian motion W_t is a martingale but the BM X_t with drift μ is not a martingale.

BM, being normally distributed, can take negative values with positive probabilities. As the stock prices cannot be negative so the geometric Brownian motion was suggested by Samuelson [106] as a refinement of BM to represent the stock price dynamics.

1.1.3 Geometric Brownian Motion

A stochastic process $\{Y_t : t \geq 0\}$, defined as $Y_t = e^{X_t}$, is the *geometric Brownian motion* (GBM) where X_t is the BM with drift coefficient μ and diffusion coefficient σ. It is sometimes given in the generalized form as $Y_t = Y_0 e^{X_t}$.

- Geometric Brownian motion is not Gaussian, instead it has lognormal distribution. It is always non negative, thus it provides a realistic model to depict the dynamics of stock prices.

- The quantity $X_t = \ln(\frac{Y_t}{Y_0})$ is referred as the logarithmic growth of stock price. It has the normal distribution $\mathcal{N}(\mu t + \ln(Y_0), \sigma^2 t)$.

- Geometric Brownian motion is helpful in modeling the percentage changes instead of the absolute changes in the price.

To model the price fluctuations (or movements), among all the stochastic processes, BM is the most widely used stochastic process. As BM has the continuous sample paths so it retains the continuous behaviour throughout the stock price dynamics. However, empirically, prices do not move continuously and rather have jumps in their movements. This discontinuous behaviour is more prominent at time scales ranging between several days and several months. For details, one may refer to Cont and Tankov [23] and Gatheral [48]. To accommodate the discontinuous patterns in the stock price dynamics, Poisson process is the basic process. So next we define Poisson and Compound Poisson Process, which are the stochastic processes with the discontinuous paths.

1.1.4 Poisson and Compound Poisson Process

A **Poisson process** is a continuous-time and discrete-state stochastic process. Let $\{N_t, t \geq 0\}$ specifies the number of events which has occurred upto time t (i.e. a counting process). By Ross [103], $p.59,\ 87$: "The counting process $\{N(t), t \geq 0\}$ is said to be a Poisson process having rate $\lambda,\ \lambda > 0$, if:

(i) $N(0) = 0$.

(ii) The process has independent increments.

(iii) The number of events in any interval of length t is Poisson distributed with mean λt.

and, a stochastic process $\{X(t), t \geq 0\}$ is said to be a **compound Poisson process** if it can be represented, for $t \geq 0$, by

$$X(t) = \sum_{i=1}^{N(t)} X_i$$

where $\{N(t), t \geq 0\}$ is a Poisson process, and $\{X_i,\ i = 1, 2, ...\}$ is a family of independent and identically distributed random variables that is independent of the process $\{N(t) : t \geq 0\}$".

Along with these stochastic processes, few other stochastic processes which have been used in the succeeding chapters to capture the volatility movements are the **Ornstein-Uhlenbeck** (OU) process and a square bessel process named as the **Cox-Ingersoll-Ross** (CIR) process. The SDEs governed by these processes are discussed in the next subsection. For detailed study of these processes one may refer to Lefebvre [76].

1.2 Stochastic Calculus

As already mentioned, the Brownian motion (BM) is the most accepted model to capture random movements in the stock price dynamics. Although, the BM has continuous sample paths, but these paths are no where differentiable and are of unbounded variation. The classical calculus could not be applied to such functions so this gave rise to a new calculus known as the stochastic calculus. Stochastic calculus can be thought of as the calculus of stochastic processes.

By Shreve [70], $p.128$: "Stochastic calculus grew out of the need to assign meaning to ordinary differential equations involving continuous stochastic processes". Here, we give a brief review of certain topics of stochastic calculus. For more insights to these topics one may refer to [29, 34, 70, 84, 93].

1.2.1 Stochastic Differential Equations

In the continuous time modeling, the dynamics of stock price is described by a stochastic differential equation (SDE). By Øksendal [93], $p.2$: " ... equation we obtain by allowing randomness in the coefficients of a differential equation is called a stochastic differential equation". It is explained as below.

Consider a stochastic process X_t, and a partition $0 = h_0 < h_1 < ... < h_n = t$ of the time interval $[0,t]$. Then, the difference equation

$$X_{h_{i+1}} - X_{h_i} = \mu(h_i, X_{h_i})(h_{i+1} - h_i) + \sigma(h_i, X_{h_i})(W_{h_{i+1}} - W_{h_i});\ \ i = 0, 1, ..., n-1, \quad (1.2.1)$$

as the increments $h_{i+1} - h_i \to 0$, is transformed to

$$dX_t = \mu(t, X_t)dt + \sigma(t, X_t)dW_t \quad (1.2.2)$$

This is the general form of a SDE where the first term on the right side is deterministic with drift μ and the second term is a random term with diffusion σ. W_t represents the standard Brownian motion. It must be noted that as BM is no where differentiable so dW_t just represents the increment $W_{t+dt} - W_t$ on the interval $[t, t+dt]$, and $(dW_t)^2 = (W_{t+dt} - W_t)^2 = dt$ is the quadratic variation of W_t. Also,

$$dW_t dt = 0, \quad (dt)^2 = 0 \quad (1.2.3)$$

For proof one may refer to Mikosch [84]. The method to find the solution of SDEs will be discussed in Subsection 1.2.3.

Eq.$(1.2.2)$ can be expressed as an integral

$$X_t = X_0 + \int_0^t \mu(h, X_h)dh + \int_0^t \sigma(h, X_h)dW_h \quad (1.2.4)$$

here $\int_0^t \sigma(h, X_h)dW_h$ is the integral with respect to the standard Brownian motion W_t and is known as the stochastic integral. The stochastic integral and its existence is discussed in the next subsection.

1.2.2 Stochastic Integral

Definition of stochastic integral requires the understanding of certain terms which are firstly defined here.

Definition 1.1. $\sigma-$***algebra:*** *By Øksendal [93], p.7: "If Ω is a given set, then a $\sigma-$algebra $\mathscr{F}$ on Ω is a family $\mathscr{F}$ of subsets of Ω with the following properties:*

(i) $\phi \in \mathscr{F}$

(ii) $F \in \mathscr{F} \Rightarrow F^C \in \mathscr{F}$, *where* $F^C = \Omega \setminus F$ *is the complement of* F *in* Ω

(iii) $A_1, A_2, \ldots \in \mathscr{F} \Rightarrow A := \cup_{i=1}^{\infty} A_i \in \mathscr{F}$".

A "$\sigma-$algebra generated by a stochastic process X_t" is denoted by $\sigma(X_t)$ and is the smallest $\sigma-$algebra containing all the information about the structure of X_t.

Definition 1.2. ***Filtration:*** *For the continuous time parameter $t \in [0,T]$, the collection $\{\mathscr{F}_t\}$ of $\sigma-$algebras is said to be a filtration if $\mathscr{F}_s \subset \mathscr{F}_t$, $\forall\, 0 \leq s < t$.*

Filtration is used to track the information flow over time. For a stochastic process X_t, the filtration $\mathscr{F}_t = \sigma(X_s, s \leq t)$ is the smallest filtration containing the past information of this process till time t and is called the natural filtration of X_t.

Definition 1.3. ***Adapted Process:*** *If for any stochastic process X_t and a filtration $\mathscr{F}_t$, $\sigma(X_t) \subset \mathscr{F}_t$, then the stochastic process X_t is an adapted process with respect to this filtration.*

The natural filtration of a stochastic process is the smallest filtration to which it is adapted. Also if a stochastic process X_t is an adapted process with respect to some filtration $\mathscr{F}_t$, then X_t is called $\mathscr{F}_t-$measurable. For the existence of the stochastic integral of a process X_t with respect to the standard Brownian motion W_t, X_t must belong to L^2 class of functions which is defined below.

Definition 1.4. *A stochastic process $\{X_t : 0 \leq t \leq T\}$ belongs to $L^2[0,T]$ class of functions if:*

(i) X_t *is $\mathscr{F}_t-$measurable where $\mathscr{F}_t$ is the natural filtration of W_t;*

(ii) $E\left(\int_0^T X_t^2 dt\right) < \infty$.

Now we define the stochastic integral.

Definition 1.5. ***Stochastic Integral:*** *Let $X_t \in L^2[0,T]$ and $0 = h_0 < h_1 < ... < h_n = T$. For $h_i \leq h^* \leq h_{i+1};\ 0 \leq i \leq n-1$, let $X_{h^*} = X_{h_i}$ (i.e. its value at left end point of the interval $[h_i, h_{i+1}]$). Then the limit $lim_{n\to\infty} \sum_{i=0}^{n-1} X_{h_i}[W_{h_{i+1}} - W_{h_i}]$ is denoted by $\int_0^T X_t dW_t$, and is the stochastic integral of the process X_t with respect to standard Brownian motion W_t.*

This stochastic integral is also called the Ito integral and it was introduced by Ito [65, 66]. There is also one another type of stochastic integral called the Stratonovich integral, but we have confined ourselves only to the Ito integrals throughout this work.

Next, we discuss the *Ito lemma* which can be thought of as the chain rule of the stochastic calculus. Ito lemma is required for solving stochastic integral and the SDEs.

1.2.3 Ito Lemma

Let $g(x)$ be a real valued function having continuous second order derivative, then for the standard Brownian motion $\{W_t : t \geq 0\}$, the formula

$$g(W_t) - g(W_s) = \int_s^t g^{'}(W_u)dW_u + \frac{1}{2}\int_s^t g^{''}(W_u)(dW_u)^2, \quad 0 \leq s < t \tag{1.2.5}$$

is called the Ito lemma or Ito formula. By the quadratic variation of Brownian motion W_t, the squared differential $(dW_u)^2$ becomes dt. The integral $\int_s^t g^{'}(W_u)dW_u$ is the Ito's stochastic integral of $g^{'}(W_u)$.

Intuitively, in terms of SDEs, Eq.(1.2.5) can be written as

$$dg(W_t) = g^{'}(W_t)dW_t + \frac{1}{2}g^{''}(W_t)dt \tag{1.2.6}$$

Ito lemma can also be extended to a function $g(t,x)$ having the continuous second order partial derivatives as

$$g(t,W_t) - g(s,W_s) = \int_s^t g_t(u,W_u)dt + \int_s^t g_x(u,W_u)dW_u + \frac{1}{2}\int_s^t g_{xx}(u,W_u)(dW_u)^2, \quad 0 \leq s < t \tag{1.2.7}$$

As $(dW_u)^2 = dt$, Eq.(1.2.7) becomes

$$g(t,W_t) - g(s,W_s) = \int_s^t \left(g_t(u,W_u) + \frac{1}{2}g_{xx}(u,W_u)\right)dt + \int_s^t g_x(u,W_u)dW_u \quad 0 \leq s < t \tag{1.2.8}$$

and equivalently

$$dg(t,W_t) = \left(g_t(t,W_t) + \frac{1}{2}g_{xx}(t,W_t)\right)dt + g_x(t,W_t)dW_t \tag{1.2.9}$$

Further, let a stochastic process X_t has the dynamics given by

$$dX_t = a_1(t,x)dt + a_2(t,x)dW_t \tag{1.2.10}$$

and Y_t be another stochastic process such that $Y_t = f(t,X_t)$. Then by Ito lemma, the SDE of Y_t will be

$$dY_t \;=\; df(t,X_t) \;=\; f_t dt + f_x dX_t + \frac{1}{2}f_{xx}(dX_t)^2 \tag{1.2.11}$$

Using Eqs.(1.2.3) and (1.2.10) in (1.2.11), we get

$$df(t,X_t) = \left(f_t + a_1 f_x + \frac{1}{2}a_2^2 f_{xx}\right)dt + a_2 f_x dW_t \tag{1.2.12}$$

1.2.4 Some Important Stochastic Differential Equations

- **Geometric Brownian Motion (GBM):** Consider a SDE

$$dX_t = \mu X_t dt + \sigma X_t dW_t^x \tag{1.2.13}$$

here $-\infty < \mu < \infty$ and $\sigma > 0$ are the constants. It is to be noticed that the superscript x in the standard Brownian motion W_t^x corresponds to the process X_t. This convention is useful to avoid the confusion when more than one SDEs are given in the model.

The SDE (1.2.13) is explicitly solvable by Ito lemma. Its solution is $X_t = X_0 e^{(\mu - \frac{\sigma^2}{2})t + \sigma W_t^x}$, which is the GBM with initial value X_0. So, Eq.(1.2.13) represents the SDE of the GBM and is used to model the stock price evolution. It is also called the lognormal model for the stock price dynamics.

In the stochastic volatility models (which will be discussed in Subsection 1.3.4), the volatility dynamics is given by a stochastic process and the most commonly used stochastic processes are the OU and CIR process.

The SDEs governed by these processes are given next.

- **Ornstein-Uhlenbeck (OU) Process:** OU Process is a diffusion process with SDE

$$dY_t = k(m - Y_t)dt + bdW_t^y \tag{1.2.14}$$

This SDE can also be solved explicitly using Ito's lemma. Its solution is

$$Y_t = m + (Y_0 - m)e^{-kt} + b\int_0^t e^{-k(t-s)}dW_s^y \tag{1.2.15}$$

here Y_0 is the initial value of process at $t = 0$. k, m and b are the positive constants. OU process is one of the simplest *mean-reverting* process. In simple words, a process is mean-reverting if it moves about some average value over time. Eq.(1.2.14) has k as the mean-reversion rate with m as the long-run or invariant mean. OU process has the normal distribution $\mathcal{N}(m+(Y_0-m)e^{-kt}, \frac{b^2}{2k}(1-e^{-2kt}))$. Its long-run distribution is $\mathcal{N}(m, \frac{b^2}{2k})$, which is obtained when $t \to \infty$.

- **Cox-Ingersoll-Ross (CIR) Process:** CIR process is also a diffusion process. Its SDE is given as

$$dY_t = k(m - Y_t)dt + b\sqrt{Y_t}dW_t^y \tag{1.2.16}$$

This process is also mean-reverting with m as the long-run mean and mean-reversion rate k. It is different from OU process with $\sqrt{Y_t}$ term in the diffusion coefficient. Condition $b^2 \leq 2km$ ensures that if the process has started with a positive value it will remain positive throughout. The long-run distribution of CIR process is the gamma distribution.

Lognormal process is not mean-reverting but OU and CIR processes are mean-reverting. These processes are used to model volatility dynamics in the stochastic volatility models as discussed in the next section.

1.3 Option Pricing and Volatility

After discussing the stock price dynamics governed by the stochastic processes and their corresponding SDEs, we review the literature on option pricing and volatility dynamics in this section.

1.3.1 Volatility

Volatility dynamics is an important topic of research within the domain of financial mathematics because it is closely linked with the stock price dynamics. In Eq.(1.2.13), we have seen that the volatility (σ) appears in the SDE governing the stock prices. This volatility is called actual or instantaneous volatility. Basically, volatility is the standard measure of risk. In the financial markets, it is a statistical tool to measure the dispersion of asset returns from their mean over a given time period.

By Hull and Basu [63], $p.353$: *"The volatility, σ, of a stock is a measure of our uncertainty about the returns provided by the stock".* Alternatively, volatility indicates the magnitude of the asset price fluctuations. Commonly, higher the volatility, riskier the particular security. There are two types of volatility used in the securities analysis: historical and implied volatility.

- **Historical volatility** refers to the price fluctuations exhibited by the security (e.g. stock) over time. It is thus a standard deviation (S.D.) calculated from the past data defined as follows:
  Consider the stock price data, $S_0, S_1, ..., S_n$ with $\Delta t = t_i - t_{i-1};\ \ i = 1, 2, ..., n$ as the length of the sampling interval. The estimated volatility σ, from this historical stock price data, is the standard deviation of the logarithmic returns per unit time given as

$$\hat{\sigma} = \frac{\sqrt{V}}{\sqrt{\Delta t}}$$

  where $V = \frac{1}{n-1}\sum_{i=1}^{n}(X_i - \bar{X})^2$ is the variance of logarithmic returns $X_i = \log(\frac{S_i}{S_{i-1}})$ from the mean $\bar{X} = \frac{1}{n}\sum_{i=1}^{n} X_i$.

- **Implied volatility** refers to the future volatility of a stock. It is calculated from an option pricing model. Gatheral [48] defined "Implied volatility is the volatility input to the Black-Scholes formula that generates the market price".

For the better understanding of implied volatility and empirical characteristics of volatility, we next define option and give the Black-Scholes model for pricing European options.

1.3.2 Option

Option is a financial security (contract) whose value is derived from (or depends on) an underlying security (stock, stock index, foreign currency etc.). It is a contract giving the option buyer (or holder) a right to buy or sell a specified underlying asset in future by a fixed date and at a fixed price which is decided when the contract is initiated. This fixed price is known as the "strike price or exercise price" and the fixed date is known as the "maturity or expiration date".

Since an option gives its holder a right without any obligation, the holder needs to pay some amount in the beginning of the contract to the option seller (or writer) to get this right. This amount is called the *'premium or price of the option'*.

Options are the most traded financial securities and can be used to manage risk. For e.g. If an investor buys a risky asset (say a stock), its future is not known today. Its price can fall in the future and the investor may have to born the loss. Instead of buying a stock if a person buys a call option on that stock, he gets the right to wait and buy this asset in future (without any obligation) if its price increases the strike price. If the price does not reach the agreed price, he can exit the contract without exercising his right. In this case, his loss will be the premium amount only which was paid at the beginning of the contract.

Any option can be categorized as a **"call option"** or a **"put option"** depending upon, whether the holder gets the right to buy or the right to sell respectively without any obligation. An option can be either exercised only at maturity (European option) or at any time up to maturity (American option). These options are also called the vanilla options. Vanilla options are the path-independent options because these options are independent of the historical prices of the underlying assets.

The options which depend on the price history of the underlying assets are called the path-dependent options, viz; binary or digital option, lookback option, barrier option, compound option or Asian option etc. Path-dependent options are also called the exotic options. The exotic options may either have the European or American type expiration. In this thesis, we have considered the path-independent European options and in the path-dependent options we have considered only Asian options with European type expiration.

Here, we consider the European call options only. Asian options will be covered in the Section 1.4.

For a European call option, the payoff (or the value of option at maturity T) is given as:

$$h(X_T) \; = \; (X_T - K)^+ \; = \; max(X_T - K, 0) \tag{1.3.1}$$

where X_T is stock price at maturity and K is the strike price.

The European call option is said to be "in-the-money" (ITM) if $X_T > K$, "at-the-money" (ATM) if $X_T = K$ and "out-the-money" (OTM) if $X_T < K$. The buyer of a call option exercises his right only if he gets some benefit, which is possible when $X_T > K$, otherwise he'll not exercise his right. This results in the payoff given in Eq.(1.3.1).

The most interesting question is 'To get this right without obligation, How much one should pay for an option contract?'. Every option pricing model tries to find out the fair price of an option.

Before 1970s, there was not any standard way to price the options. Most of the previous work on the valuation of options include Sprenkle [111], Ayrus [4], Boness [15], Samuelson [105], Baumol et al. [10] and Chen [18], but none were widely accepted until the significant breakthrough by Fischer Black, Myron Scholes and Robert Merton during 1970s.

1.3.3 The Black-Scholes Model for Option Pricing

In 1973, there came a revolution in the field of options trading when Fischer Black and Myron Scholes [14] and Robert C. Merton [82] published their work on 'Pricing options'. Black and Scholes [14] gave an option pricing formula for the European options which was further developed by Merton [82] in the same year. Black-Scholes model became a milestone in the field of modern finance and for their contribution Myron Scholes and Robert C. Merton received the "Nobel prize in Economics" in 1997. Due to his sudden demise in 1995, Fischer Black could not share this prize.

The Black-Scholes model assumes that the market is complete, stock pays no dividend and follows a GBM. Volatility and risk free rate of interest are constant through out the option period. The model gives the formula for the pricing of European call options. This model is explained as follows:

Let X_t be the price of the underlying asset at time t, whose dynamics is governed

by the geometric Brownian motion given as

$$dX_t = \mu X_t dt + \sigma X_t dW_t^x \tag{1.3.2}$$

where W_t^x is the standard Brownian motion, $-\infty < \mu < \infty$ is the growth term (drift) and $\sigma > 0$ is the volatility. Let B_t be the bond price at time t and r be the risk free interest rate, then the dynamics of B_t is given as:

$$dB_t = rB_t dt$$

Let the price of the European call option at time t be $C(x,t)$, where $x = X_t$. This price satisfies the partial differential equation (PDE)

$$\frac{\partial C}{\partial t} + rx\frac{\partial C}{\partial x} + \frac{1}{2}\sigma^2 x^2 \frac{\partial^2 C}{\partial x^2} - rC = 0 \tag{1.3.3}$$

with the terminal condition

$$h(X_T) = (X_T - K)^+ \tag{1.3.4}$$

This PDE is called the **Black-Scholes PDE** or Black-Scholes equation. For its derivation one may refer Luenberger [79], $p.353$. This equation can also be written as

$$\mathscr{L}_{BS} C = 0$$

where

$$\mathscr{L}_{BS} = \frac{\partial}{\partial t} + \frac{1}{2}\sigma^2 x^2 \frac{\partial^2}{\partial x^2} + r(x\frac{\partial}{\partial x} - .) \tag{1.3.5}$$

is Black-Scholes operator for the European options. The solution of this equation gives the Black-Scholes formula for pricing options, mentioned next.

Black-Scholes Formula: The European call option price, at time t, is obtained in the closed form as

$$C(X_t, t, T, r, \sigma, K) = X_t N(w_1) - Ke^{-r(T-t)} N(w_2) \tag{1.3.6}$$

here

$$w_1 = \frac{\log(\frac{X_t}{K}) + (r + \frac{1}{2}\sigma^2)(T-t)}{\sigma\sqrt{T-t}}$$

$$w_2 = w_1 - \sigma\sqrt{T-t} \tag{1.3.7}$$

with the strike price K, maturity T and the current time t. $N(.)$ represents the cumulative distribution function (CDF) of the standard normal random variable.

The European call and put option prices on an underlying asset X_t, with same strike price K and expiration time T are related with **"Put-Call parity formula"** given as

$$C_t - P_t = X_t - Ke^{-r(T-t)} \tag{1.3.8}$$

here, C_t and P_t represents the prices of call and put option respectively at time t with risk free interest rate r. Black-Scholes formula had a major impact on the market as the investors began to feel more comfortable in trading options.

Along with the Black-Scholes PDE approach to obtain the Black-Scholes formula, there is another approach to obtain the Black-Scholes option pricing formula which is given below.

Risk-Neutral Pricing: We here discuss an alternate approach to derive the Black-Scholes formula which was introduced by Harrison and Pliska [56]. This is the pricing under a risk- neutral probability measure. A risk-neutral probability is a probability under which the expected return on a risky investment is equal to the return on a risk free investment. It is different from the actual probability because in the real world the future price of a risky security is a random quantity. The risk-neutral probability measure is also called the **equivalent martingale measure**.

Risk-neutral probability measure is important because it helps to find the fair price of an option. The existence of the equivalent martingale measure ensures that the market is arbitrage free (i.e. without an initial investment there can not be a guaranteed risk free profit) and vice versa (by first fundamental theorem of finance). According to second fundamental theorem of finance, "an arbitrage free market is complete iff there exists a unique equivalent martingale measure". The risk-neutral probability measure can be obtained using *"Randon-Nikodym Theorem"* and *"Girsanov's Theorem"*. For these theorems one can refer to Karatzas and Shreve [70] and Mikosch [84].

A stochastic process is a martingale if its SDE has no drift term. Next, it is shown that the discounted stock price becomes a martingale under the risk-neutral probability measure.

Let the stock price X_t follows the geometric Brownian motion given by Eq.(1.3.2).

The SDE of $\tilde{X}_t = e^{-rt}X_t$, which is the discounted stock price process, is obtained using Ito's formula and is given as

$$\begin{aligned} d\tilde{X}_t &= -re^{-rt}X_t dt + e^{-rt}(\mu X_t dt + \sigma X_t dW_t^x) \\ &= \tilde{X}_t((\mu - r)dt + \sigma dW_t^x) \end{aligned} \tag{1.3.9}$$

here the drift term $\mu - r$ does not vanish under the real probability measure P(say). But, on letting $\phi = \frac{\mu - r}{\sigma}$, there exists a risk-neutral probability measure P^* (by Girsanov's theorem) under which $W_t^* = W_t^x + \int_0^t \phi ds$ is a standard Brownian motion. Thus

$$d\tilde{X}_t = \sigma \tilde{X}_t dW_t^* \tag{1.3.10}$$

and $\tilde{X}_t$ becomes a martingale under this risk-neutral probability measure P^*. Under P^*, the drift term in the dynamics of stock price X_t given in Eq.(1.3.2) will be r.

In the Black-Scholes framework, a replicating portfolio in stock and bond is considered for the call prices. So, let there be a self-financing portfolio (a_t, b_t) with value $V_t = a_t X_t + b_t B_t$ at time t. Its value at maturity will be $V_T = h(X_T)$ which is the payoff of the call option contract. Then

$$dV_t = a_t dX_t + b_t dB_t, \tag{1.3.11}$$

because the portfolio is self-financing. The discounted portfolio process $\tilde{V}_t = e^{-rt}V_t$ will become a martingale under the risk-neutral probability measure P^* giving

$$\tilde{V}_t = E^*[\tilde{V}_T | \mathscr{F}_t]$$

this gives

$$\tilde{V}_t = E^*[e^{-rT}V_T | \mathscr{F}_t]$$

also as $V_T = h(X_T)$, thus

$$\tilde{V}_t = E^*[e^{-rT}h(X_T) | \mathscr{F}_t]$$

which gives that

$$V_t = E^*[e^{-r(T-t)}h(X_T) | \mathscr{F}_t] \tag{1.3.12}$$

where $\mathscr{F}_t = \sigma(W_s^x, s \leq t)$ and E^* is risk-neutral expectation under the probability

measure P^*. Thus, the value of European call option at any time t is given by

$$C(X_t,t) = E^*[e^{-r(T-t)}h(X_T)|\mathscr{F}_t] \tag{1.3.13}$$

which upon solving gives the Black- Scholes formula (1.3.6).

Eq.(1.3.13) can be written as

$$C(X_t,t) = E^*[e^{-r(T-t)}h(X_T)|X_t] \tag{1.3.14}$$

The Feynmann-Kac Formula: This formula establishes a link between the two approaches discussed above. Let the dynamics of stock price X_t be given by Eq.(1.3.2). By Feynmann-Kac formula, the solution of PDE (1.3.3) subject to the boundary condition (1.3.4) is given by Eq.(1.3.14) and vice versa.

The generalized form of Feynmann-Kac formula is also available and is applied to the case when the model has more than one SDEs, as in the stochastic volatility models. Its extended version is given in Subsection 1.3.4 for the multifactor stochastic volatility models.

Next, we return to the implied volatility. If $C_{BS}(X_t,t,T,r,\sigma,K)$ is the Black-Scholes call option price given by Eq.(1.3.6) and C_{mkt} is the actual call price quoted in the market, then the implied volatility I is the volatility input to C_{BS}, such that

$$C_{BS}(X_t,t,T,r,I,K) = C_{mkt} \tag{1.3.15}$$

By changing K and T, the implied volatility also changes. The implied volatility plot with respect to strike price for a fixed expiration time is called *volatility smile*. Similarly, the variation of the implied volatility with respect to maturity time for a fixed strike is called the *term structure of volatility*. The variation of implied volatility with both strike price K and maturity T is known as implied volatility surface. The variation of volatility violates the Black-Scholes assumption of constant volatility. Implied volatility surface is better expressed in terms of log moneyness to time to maturity ratio (LMMR). Moneyness is generally reperesented as $\frac{K}{X_t}$ and time to maturity is given as $\tau = T-t$. For a better insight to this topic, one may refer to Gatheral [48] and Hafner [55].

Despite its landmark success in option pricing, Black-Scholes formula has significant biases. The model assumes volatility to be constant and asset log-

return distribution as Gaussian. In practice, the log-return distributions are non-Gaussian in nature characterised by heavy tails and high peaks and volatility tends to vary in terms of the strike price and expiry. Enormous work has been done to revise and upgrade the classical Black-Scholes model. The relaxation of constant volatility assumption consequently led to the modeling of evolution of dynamic volatility.

1.3.4 Evolution of Dynamic Volatility Modeling

Volatility is not constant and has many empirical characteristics like volatility smile and skew, mean-reversion, leverage, volatility clustering, variation on different time scales etc.(refer to [48,55,85]). There has been a logical progress in the field of volatility modeling by the development of new models as an improvement of the existing ones. Time dependent volatility models ($\sigma = f(t)$) (Merton [82]) were able to capture the variation of option prices with maturity dates. The local volatility models ($\sigma = f(t, X_t)$) (Cox and Ross [25], Derman and Kani [28], Dupire [30]) also addressed volatility smiles and leverage effect (correlation of stock price and volatility), whereas stochastic volatility models ($\sigma = f(Y_t)$) were able to assimilate all the features of local volatility models and some other empirical volatility characteristics like mean-reversion and volatility clustering (autocorrelation of volatility). In this thesis, we have worked on the stochastic volatility models and their extensions. So we start with the general representation of the stochastic volatility models.

Stochastic Volatility Model (One Factor): The general representation of the single factor stochastic volatility model is given below. The dynamics of stock price process X_t is given by

$$\frac{dX_t}{X_t} = \mu dt + \sigma dW_t^x$$

where, $\sigma = f(Y_t)$ and Y_t is the stochastic volatility factor whose dynamics is given by

$$dY_t = a(Y_t)dt + b(Y_t)dW_t^y \tag{1.3.16}$$

here, $a(Y_t)$ and $b(Y_t)$ are some functions of Y_t. The standard Brownain motions W_t^x and W_t^y have the correlation structure $E[dW_t^x.dW_t^y] = \rho dt$ where, ρ represents

a correlation between them.

Some of the most notable single factor stochastic volatility models are given in Ball and Roma [7], Heston [59], Hull and white [64], Scott [107] and Stein and Stein [112]. Hull and White [64] considered the volatility dynamics (1.3.16) to follow lognormal process (1.2.13), Scott [107] and Stein and Stein [112] considered the volatility dynamics to follow OU process (1.2.14), whereas, Ball and Roma [7] and Heston [59] considered volatility dynamics to follow CIR process (1.2.16). As stated by Gatheral [48], "in these single factor stochastic volatility models, Heston model [59] is the most popular because of the existence of a fast and easily implemented quasi closed form solution of the European options", the Heston stochastic volatility model is given below.

Heston Stochastic Volatility Model: Let P^* be the risk-neutral probability measure, r be the risk free rate of interest. Under P^*, the dynamics of stock price X_t is as follows:

$$dX_t = rX_t dt + \sigma X_t dW_t^x$$

where $\sigma = \sqrt{Y_t}$ such that

$$dY_t = \alpha(m - Y_t)dt + \beta\sqrt{Y_t}dW_t^y \tag{1.3.17}$$

and $E[dW_t^x . dW_t^y] = \rho dt$. This is the required Heston stochastic volatility model. Clearly, the dynamics of Y_t is given by the CIR process (1.2.16). Y_t represents the stochastic variance of the stock. The positive constants α, m and β satisfy $2\alpha m \geq \beta^2$ to ensure that Y_t remains positive for all t. This model is solved using Fourier transform technique to give the semi analytic pricing formula for the European options. Using this model, the pricing formula of the European call option at time t is given as:

$$C(X_t, Y_t, t) = X_t P_1 - Ke^{-r(T-t)}P_2 \tag{1.3.18}$$

where K is the strike price and T is the maturity time. Also, for $j = 1, 2$ and with $x = X_t$, $y = Y_t$ and $s = ln(x)$,

$$P_j(s, y, t, T, K) = \frac{1}{2} + \frac{1}{\pi}\int_0^\infty Re\left[\frac{e^{-i\phi \ln K} f_j(s, y, t, T, \phi)}{i\phi}\right] d\phi, \tag{1.3.19}$$

The characteristic function f_j of P_j is

$$f_j(s,y,t,\phi,t+\tau) = e^{D(\tau,\phi)+E(\tau,\phi)y+i\phi s} \tag{1.3.20}$$

where $\tau = T-t$. The other terms are

$$D(\tau,\phi) = r\phi i\tau + \frac{\alpha m}{\beta^2}\left[(b_j - \rho\beta\phi i + d_j)\tau - 2ln\left(\frac{1-g_j e^{d_j\tau}}{1-g_j}\right)\right]; \tag{1.3.21}$$

$$E(\tau,\phi) = \frac{b_j - \rho\beta\phi i + d_j}{\beta^2}\left(\frac{1-e^{d_j\tau}}{1-g_j e^{d_j\tau}}\right); \tag{1.3.22}$$

with

$$g_j = \frac{b_j - \rho\beta\phi i + d_j}{b_j - \rho\beta\phi i - d_j};$$

$$d_j = \sqrt{(\rho\beta\phi i - b_j)^2 - \beta^2(2u_j\phi i - \phi^2)};$$

and

$$u_1 = \frac{1}{2},\ u_2 = \frac{-1}{2},\ b_1 = \alpha - \rho\beta,\ b_2 = \alpha. \tag{1.3.23}$$

Stochastic volatility models (one factor) are unable to completely capture the dynamics of volatility. These models can generate the volatility smile but its time-varying nature remains unexplained by these models (refer to [22, 41]). Also, the one factor stochastic volatility models like Heston stochastic volatility model does not fit the short term implied volatility surface. So there arose a necessity to carry out more profound work in this direction. In the literature, the shortcomings of these models have been addressed by the addition of jumps to the stock price process (e.g. stochastic volatility jump diffusion models [9, 80, 95, 108]). These models are important to explain the distributional characteristics of return and implied volatility smile/skew of options. Jumps are added to the stochastic volatility model which improves its pricing performance for the short-term options [6]. The stochastic volatility jump diffusion model of Bates [9] is given below.

Stochastic Volatility Jump Diffusion Model: Bates [9] introduced the stochastic volatility jump diffusion (SVJ) model by including proportional lognormal jumps in the SDE governing the stock prices, in the Heston model.

The stock price dynamics, under the risk-neutral probability measure P^* was considered as

$$dX_t = (r - \lambda\bar{k})X_t dt + \sigma X_t dW_t^x + dZ_t$$

where $\sigma = \sqrt{Y_t}$, such that

$$dY_t = \alpha(m - Y_t)dt + \beta\sqrt{Y_t}dW_t^y \tag{1.3.24}$$

and $E[dW_t^x.dW_t^y] = \rho dt$. The jump size k was assumed to have the lognormal distribution with expected value $\bar{k}$. Z_t was a compound Poisson process with rate λ. An alternate and relatively recent approach in the context of option pricing is the consideration of multifactor stochastic volatility models to address the shortcomings of one factor stochastic volatility models. These models can be contemplated as a natural extension of one factor stochastic volatility models. In these models, volatility has several factors varying at different time scales (e.g. [35, 38, 39, 87]).

Alizadeh et al. [1] found the evidence of two factors in volatility, out of which one was highly persistent and another was quickly mean-reverting. Extending this idea, Fouque et al. [39] proposed a multifactor stochastic volatility model with two factors of volatility, out of which one was a fast scale mean-reverting factor and another was a slow scale factor of volatility. Christoffersen et al. [22] had empirically shown that the two-factor models improve one factor models both in term structure and moneyness dimension. A general representation of a two-factor stochastic volatility model is given below.

Stochastic Volatility Model (Two Factors): Under P^*, let the dynamics of stock price X_t be

$$dX_t = rX_t dt + \sigma_t X_t dW_t^x$$

where $\sigma_t = f(Y_t, Z_t)$ with

$$dY_t = a_1(Y_t)dt + b_1(Y_t)dW_t^y$$

$$dZ_t = a_2(Z_t)dt + b_2(Z_t)dW_t^z \tag{1.3.25}$$

here Y_t is the fast scale volatility factor and Z_t is the slow scale volatility factor. $a_1(Y_t)$ and $b_1(Y_t)$ are some functions of Y_t. $a_2(Z_t)$ and $b_2(Z_t)$ are some functions

of Z_t. The three standard Brownian motions, W_t^x, W_t^y and W_t^z have the correlation structure as:

$$E[dW_t^x.dW_t^y] = \rho_{xy}dt,\ \ E[dW_t^x.dW_t^z] = \rho_{xz}dt,\ \ E[dW_t^y.dW_t^z] = \rho_{yz}dt$$

Using this model, the price of the European call option at time t, with payoff $h(X_T)$ is given as

$$C(X_t,Y_t,Z_t,t) = E^*[e^{-r(T-t)}h(X_T)|X_t,Y_t,Z_t]$$

By the Feynmann-Kac formula, $C(X_t,Y_t,Z_t,t)$ will satisfy the PDE

$$\frac{\partial C}{\partial t} + \mathscr{L}C - rC = 0 \tag{1.3.26}$$

with the boundary condition

$$C(X_T,Y_T,Z_T,T) = h(X_T)$$

here

$$\begin{aligned}\mathscr{L} &= rx\frac{\partial}{\partial x} + a_1\frac{\partial}{\partial y} + a_2\frac{\partial}{\partial z} + \frac{1}{2}\sigma_t^2x^2\frac{\partial^2}{\partial x^2} + \frac{1}{2}b_1^2\frac{\partial^2}{\partial y^2} + \frac{1}{2}b_2^2\frac{\partial^2}{\partial z^2}\\ &+ \rho_{xy}(\sigma x)(b_1)\frac{\partial^2}{\partial x\partial y} + \rho_{xz}(\sigma x)(b_2)\frac{\partial^2}{\partial x\partial z} + \rho_{yz}(b_1)(b_2)\frac{\partial^2}{\partial y\partial z}\end{aligned} \tag{1.3.27}$$

Because of the stochastic volatility consideration, this PDE does not give the closed form solution and can be solved either by using numerical methods or the analytic methods (perturbation techniques).

In particular, the multifactor stochastic volatility model of Fouque et al. [39] is given here, which considers the two factors of volatility.

“The dynamics of stock price process X_t and of the volatility factors Y_t and Z_t is

$$dX_t = \mu X_t dt + \sigma_t X_t dW_t^x$$

where, $\sigma_t = f(Y_t,Z_t)$ and

$$dY_t = \frac{1}{\varepsilon}(m - Y_t)dt + \frac{\nu\sqrt{2}}{\sqrt{\varepsilon}}dW_t^y$$

$$dZ_t = \delta c(Z_t)dt + \sqrt{\delta}g(Z_t)dW_t^z$$

Y_t follows OU process with rate of mean-reversion $\frac{1}{\varepsilon}$, long run mean m and volatility of volatility $\frac{\nu\sqrt{2}}{\sqrt{\varepsilon}}$ ". W_t^x, W_t^y and W_t^z have the correlation structure as given above. They considered the diffusion of slow volatility factor Z_t resulting from a simple time change where $c(Z_t)$ and $g(Z_t)$ are smooth functions of Z_t. They used the singular and regular perturbations to derive the option pricing formula for the European options. The approxiate option price thus obtained is perturbed around the Black-Scholes price. The option pricing formula obtained by them is independent of fast volatility factor but depends on the slow volatility factor. Thus the dynamics of slow factor of volatility can not be ignored. The approximation of this slow volatility factor is the base of Chapters 2 and 3 where we have used the perturbation methods of Fouque et al. [41] to solve the pricing PDE and to prove the accuracy of our results.

Along with this, to analyze the pursuance of stochastic volatility jump diffusion (SVJ) models versus multifactor stochastic volatility (MSV) models, in the pricing of European options and in the market implied volatility fit, a comparative study is done in Chapter 6.

1.4 A Brief on Asian Options

Asian options, first introduced in 1987, (also known as average-price or average-rate options) are the path-dependent options such that their payoff depends upon the average of the underlying asset price over the option period. Asian options are much attractive because these are generally less volatile and provide a cheaper way of hedging than their path-independent counterparts. These options are commonly traded in the currency and the commodity markets.

Asian options are mainly of two types: **"fixed strike"** and **"floating strike"** with payoffs $max\,(A_T - K, 0)$ and $max\,(X_T - A_T, 0)$ respectively. Here, A_T is the mean of the underlying asset price over the time period $[0, T]$. Mostly, the averaging of the underlying asset price in these options can either be arithmetic or geometric. The geometric Asian options (GAOs) are more attractive than the arithmetic one because their closed form solutions similar to the Black-Scholes formula are available.

- The continuous arithmetic average is given as:

$$A_T = \frac{1}{T}\int_0^T X_t dt$$

- The continuous geometric average is given as:

$$A_T = exp\left(\frac{1}{T}\int_0^T \ln X_t dt\right)$$

1.4.1 The Black-Scholes Formula for Geometric Asian Options

GBM follows lognormal distribution. The sum of lognormally distributed random variables does not have any formal representation but their product remains lognormal. So the pricing formula for the Asian options with geometric average can be analytically derived in the Black-Scholes framework.

Let the underlying stock price has the dynamics

$$dX_t = \mu X_t dt + \sigma_t X_t dW_t^x$$

and $G_{[0,t]}$ be the geometric average of asset prices in the time interval $[0,t]$ such that

$$G_{[0,t]} = exp\left(\frac{1}{t}\int_0^t \ln X_\tau d\tau\right) \tag{1.4.1}$$

The Black-Scholes PDE for the GAOs using Feynmann-Kac formula is given as

$$\frac{\partial B}{\partial t} + \frac{1}{2}\sigma^2 x^2 \frac{\partial^2 B}{\partial x^2} + rx\frac{\partial B}{\partial x} + \frac{G}{t}\ln(\frac{x}{G})\frac{\partial B}{\partial G} - rB = 0 \tag{1.4.2}$$

On solving, this equation gives the Black-Scholes price (B) for GAOs. Kwok [75] used the risk-neutral valuation approach to deduce the pricing formula for the fixed strike geometric Asian call options and PDE approach to obtain the pricing formula for floating strike GAOs. We here simply give the pricing formulae derived by Kwok [75].

Let $B^{fl}(t,x,G)$ be the price of the floating strike GAO call, where $x = X_t$. The transformation $s = \ln x$ and $u = t\ln\frac{G}{x}$ is used to get

$$B^{fl}(t,x,G) = e^s\left[N(d_1) - e^{\frac{u}{T}-Q}N(d_2)\right] \tag{1.4.3}$$

where $N(.)$ is the CDF of the standard normal variate,

$$d_1 = \frac{-u + (r + \frac{\overline{\sigma}^2}{2})\frac{T^2 - t^2}{2}}{\overline{\sigma}\sqrt{\frac{T^3 - t^3}{3}}},$$

$$d_2 = d_1 - \frac{\overline{\sigma}}{T}\sqrt{\frac{T^3 - t^3}{3}},$$

and

$$Q = (r + \frac{\overline{\sigma}^2}{2})\frac{T^2 - t^2}{2T} - \frac{\overline{\sigma}^2}{6T^2}(T^3 - t^3), \tag{1.4.4}$$

with payoff function

$$h(S_T, U_T) = e^{S_T} max(1 - e^{\frac{U_T}{T}}, 0). \tag{1.4.5}$$

Similarly, for the fixed strike GAO call

$$B_0^{fix} = e^{s + \frac{u}{T} - Q} N(\hat{d}_1) - Ke^{-r(T-t)} N(\hat{d}_2) \tag{1.4.6}$$

where $N(.)$ is the CDF of the standard normal variate. Q is given by Eq.(1.4.4) and

$$\hat{d}_2 = \frac{\frac{u}{T} + s - \ln K + (r - \frac{\overline{\sigma}^2}{2})\frac{(T-t)^2}{2T}}{\frac{\overline{\sigma}}{T}\sqrt{\frac{(T-t)^3}{3}}},$$

$$\hat{d}_1 = \hat{d}_2 + \frac{\overline{\sigma}}{T}\sqrt{\frac{(T-t)^3}{3}}, \tag{1.4.7}$$

with payoff function

$$h(S_T, U_T, K) = max(e^{S_T + \frac{U_T}{T}} - K, 0). \tag{1.4.8}$$

Asian options have extensively been studied in literature. For the arithmetic Asian options pricing, numerical approximations are given by Turnbull and Wakeman [116], Laplace transform formulae are derived by Geman and Yor [49], bounds are given by Rogers and Shi [102], Monte carlo and Laplace inversion formula is compared by Fu et al. [44] and a one-dimensional PDE is derived by Vecer [118]. The dimension reduction technique by Vecer [119] is generalized by Fouque and Han [36] by considering random volatility. The spectral expansions are discussed by Linetsky [78]. The pricing based on Fourier-Cosine expansion is given by Huang et al. [60] etc.

For the GAOs, explicit expressions of price are derived by Angus [2], Kemna and Vorst [71] and Zhang [126] under the Black-Scholes framework, by Kim and

Wee [72] under the Heston stochastic volatility model, by Peng [96] using constant elasticity of variance model, by Wong and Cheung [120] using the perturbation techniques in a single factor stochastic model and by Hubalek and Sgarra [62] using Barndorff-Nielsen and Shephard model under a stochastic volatility jump model framework etc.

Next, we give a review on the entropy measures and some concepts of information theory which have been used in Chapters 4 and 5 of this thesis.

1.5 Entropy: A Measure of Risk

Shannon [109], in his mathematical theory of communication, used entropy as a measure of information which laid the foundation of the field of information theory. Entropy has been used widely in a number of fields like communication, coding theory, physics, economics etc. It has broad applications in finance too specially in portfolio selection [13, 61, 77, 91, 98], asset pricing [3, 42, 94, 104, 114] and time series analysis [86, 92, 101, 122]. "The principle of maximum entropy" given by Jaynes [68], "The principle of minimum cross entropy" given by Kullback and Leibler [74], and the "Entropy pricing theory" given by Gulko [52–54], are some of the significant concepts of information theory which have extensively been used in finance.

Entropy has been used as a tool to capture the irregularities in a time series. For a given financial time series, high values of Shannon entropy depicts that there is a high uncertainty and thus the behaviour of time series is highly unpredictable, whereas the low entropy value depicts that there is less uncertainty and hence high predictability of the time series [11]. Volatility gives one way to measure the risk in a financial investment. Another way can be the use of entropy which is also a measure of uncertainty. Entropy can be a good tool to analyse the financial market data because it measures the uncertainty of a given time series without depending on the theoretical probability measure. Entropy has been explored as a measure of risk in many studies [12, 21, 43, 50, 67, 97]. The review of the applications of entropy in finance is given in Zhou [129].

In this thesis, we have explored the asset pricing and analysis of asset log-return series using entropy measures, in Chapters 4 and 5 respectively.

The basic entropy measures and the principle of maximum entropy used in this work are given in the next subsections.

1.5.1 Some Entropy Measures

Some of the entropy measures used in this thesis are:

Shannon Entropy: If $X = (x_1, x_2, ..., x_n)$ are the outcomes of a random experiment with probability distribution $P = (p_1, p_2, ..., p_n)$ satisfying $0 \leq p_i \leq 1$ and $\sum_{i=1}^{n} p_i = 1$, then the average amount of uncertainty associated with the outcomes of random experiment X, denoted by $H(P)$, is given as:

$$H(P) = -\sum_{i=1}^{n} p_i \log p_i \tag{1.5.1}$$

where $0 \log 0 = 0$ and logarithm is considered with base 2. This is called the Shannon entropy associated with the random experiment X.

For a continuous random variable (r.v.) X, with p.d.f. $p(x)$, it is defined as:

$$H(p) = -\int_0^\infty p(x) \log p(x) dx \tag{1.5.2}$$

Some of the most notable extensions of Shannon entropy are given below.

Rényi Entropy: The Rényi entropy [100], for the continuous r.v. X with the p.d.f. $p(x)$ is defined as

$$H_\alpha(p) = \frac{1}{1-\alpha} \log \left(\int_0^\infty p^\alpha(x) dx \right) \tag{1.5.3}$$

It has the order α, where $\alpha \geq 0$ and $\alpha \neq 1$. As $\alpha \to 1$, the expression of Shannon entropy given in Eq.$(1.5.2)$ is obtained.

Tsallis Entropy: Tsallis entropy [115] of order α, where $\alpha(\neq 1)$ is a positive real number, for a continuous r.v. X with the p.d.f. $p(x)$ is defined as

$$H_\alpha(p) = \frac{1}{\alpha - 1} \left(1 - \int_0^\infty p^\alpha(x) dx \right) \tag{1.5.4}$$

as $\alpha \to 1$, the Shannon entropy $(1.5.2)$ is obtained. Havrda and Charvát entropy [57] is also similar to the Tsallis entropy.

Varma Entropy: Varma [117] generalized the Rényi's entropy (1.5.3) to a two-parameter entropy named as Varma entropy with order α and type β. This two-parameter entropy is given by

$$H_{\alpha,\beta}(p) = \frac{1}{\beta-\alpha}\log\int_0^\infty p^{\alpha+\beta-1}(x)dx \tag{1.5.5}$$

with $\beta \geq 1,\ \beta-1 < \alpha < \beta$ and $\alpha+\beta \neq 2$. Clearly, $\alpha+\beta > 1$. For $\beta = 1$, Rényi entropy (1.5.3) is obtained. So Rényi entropy becomes a particular case of Varma entropy.

Along with these entropies some other entropies which have been used in this thesis are discussed below.

Permutation Entropy: Bandt and Pompe [8] introduced an entropy measure to analyse the complexity of an arbitrary time series based on the comparison of neighbouring values and named it as the permutation entropy. It is explained as follows:

Consider a time series $\{x_i\}_{i=1}^N$ with length N. From this series, a vector $X_k(m,\tau) = (x_k, x_{k+\tau}, ..., x_{k+(m-1)\tau}), k = 1,2,...,N-(m-1)\tau$ is taken, with embedding dimension m and time delay τ. As m different numbers can be ordered in $m!$ ways, so each vector is assigned a pattern out of the $m!$ possible ordinal patterns $\{\pi_l\}_{l=1}^{m!}$. The permutation entropy of this series is defined as

$$H(m,\tau,P) = -\sum_{l=1}^{m!} p(\pi_l)\log p(\pi_l) \tag{1.5.6}$$

where, the relative frequencies $p(\pi_l)$ are given by

$$p(\pi_l) = \frac{||\{k:\ k \leq N-(m-1)\tau,\ \ (x_k, x_{k+\tau}, ..., x_{k+(m-1)\tau})\ \ has\, the\, ordinal\, pattern\, \pi_l\}||}{N-(m-1)\tau} \tag{1.5.7}$$

$||.||$ represents the number of elements in the set. This entropy is called the permutation entropy.

Permutation entropy is a simple, fast and robust measure to capture complexity of a system and it is easily applicable on any regular, chaotic, noisy or reality based time series. For the permutation entropy analysis of the financial time series, one may refer to [58, 69, 127, 130].

Multiscale Entropy: Most of the time series have inherited multiple time scales. The financial time series also fluctuates on the multiple time scales. As already discussed in Section1.3, in the recent years, multiple time scales in volatility dynamics have been found and studied. To capture the multiple time scales inherent in healthy physiological dynamics, Costa et al. [24] gave the concept of multiscale entropy which is given below.

Let $\{x_i\}_{i=1}^N$ be a discrete time series having length N. The multiple time scales are included by constructing a coarse grained series $\{y_r^s\}$ with scale factor s, given as

$$y_r^s = \frac{1}{s} \sum_{i=(r-1)s+1}^{rs} x_i, \quad 1 \leq r \leq \left[\frac{N}{s}\right] \tag{1.5.8}$$

This series is obtained from the original time series $\{x_i\}_{i=1}^N$ by taking average over the non-overlapping windows of length s. For the scale factor $s = 1$, the time series (1.5.8) becomes the original time series $\{x_i\}_{i=1}^N$. The length of each new series $\{y_r^s\}$, obtained after coarse graining, is equal to the greatest integer less than or equal to $\frac{N}{s}$. For each such coarse grained series, obtained at different values of s, Costa et al. [24] calculated the sample entropy (SampEn) [101] and named the procedure as the multiscale entropy. Multiscale entropy has been an efficient tool for the analysis of the complex time series. For its applications in the analysis of the financial time series, one may refer to [81,92,99,121–123,128] etc.

Weighted Permutation Entropy: Despite of the fact that the permutation entropy (see Eq.(1.5.6)) is an efficient tool to study the complexity of any non-linear time series, it has certain limitations. Permutation entropy only retains the order structure of a pattern and is unable to capture its amplitude information. To capture this amplitude information, Fadlallah et al. [32] extended the permutation entropy procedure to the weighted permutation entropy by introducing a weighting scheme based on the variance of each neighbouring vectors.

For defining weighted permutation entropy, we rewrite relative frequencies given in Eq.(1.5.7) as

$$p(\pi_l) = \frac{\sum_{k \leq N-(m-1)\tau} I_{A_l}(X_k(m,\tau))}{\sum_{k \leq N-(m-1)\tau} I_B(X_k(m,\tau))} \tag{1.5.9}$$

where $I_Y(Z)$ denotes the indicator function such that $I_Y(z) = 1$ if $z \in Y$ otherwise $I_Y(z) = 0$, for each element z of Z. A_l is the set of all those vectors which have the ordinal pattern π_l. B is the set of all those vectors which have ordinal patterns in

the set $\{\pi_l\}_{l=1}^{m!}$.

Fadlallah et al. [32], assigned weights to each neighbouring vector and defined the weighted relative frequencies as

$$p_v(\pi_l) = \frac{\sum_{k\leq N-(m-1)\tau} I_{A_l}(X_k(m,\tau))v_k}{\sum_{k\leq N-(m-1)\tau} I_B(X_k(m,\tau))v_k} \tag{1.5.10}$$

where,

$$v_k = \frac{1}{m}\sum_{h=1}^{m}(x_{k+(h-1)\tau} - \overline{X}_k(m,\tau))^2$$

and $\overline{X}_k(m,\tau)$ is the mean (arithmetic) of the vector $X_k(m,\tau)$. Thus, the weighted permutation entropy is defined as

$$H(m,\tau,P) = -\sum_{l=1}^{m!} p_v(\pi_l)\log p_v(\pi_l) \tag{1.5.11}$$

The concept of permutation entropy is extended to a two-parameter permutation entropy for the asset log-return time series analysis in Chapter 5. The two-parameter permutation entropy is also extended to include the multiscales and weights in that chapter.

Next, the principle of maximum entropy is given.

1.5.2 Principle of Maximum Entropy

Jaynes [68] gave the "Principle of maximum entropy". This principle is briefly explained here. The objective of this principle is to obtain an unknown probability density function $p(x)$ that maximizes the given entropy $H(p)$, under some constraints such as:

$$\int_0^\infty p(x)dx = 1, \tag{1.5.12}$$

and some more constraints of the type

$$\int_0^\infty G(x)p(x)dx = M, \tag{1.5.13}$$

where M is the expected value of $G(x)$, which is any continuous function of X. The Lagrange method is used to solve this problem.

Cozzolino and Zahner [26] used the the principle of maximum entropy to provide a probability distribution of the future stock price with known mean and variance.

They derived variance assuming the stationary and independent increments for the stock price process. Buchen and Kelly [17] applied the MEP for the maximization of Shannon entropy to construct the "risk-neutral density function of the future asset price" using prices of the path-independent options. Alternatively, Neri and Schneider [88] obtained the localization of the maximum entropy distribution for an asset from the call and digital option prices by applying the results of Csiszar [27] and compared their results to Buchen and Kelly [17]. Neri and Schneider [89] obtained that "in the family of the entropy maximizing densities, the Buchen-Kelly density is the unique continuous density with the greatest entropy". All these studies considered the maximization of the Shannon entropy. Also, Brody et al. [16] maximized the one-parameter Rényi entropy considering only mean constraint neglecting the effect of volatility on the price distribution. We have proposed the maximization of two-parameter Varma entropy with the inclusion of volatility constraint in Chapter 4.

1.6 Outline of the Work Done

Motivated by the above discussion, in this thesis, we have proposed a multifactor stochastic volatility model by approximating the slow volatility factor. Using this model the pricing formulae and the implied volatility smiles are obtained for the European and Asian options. We have done a comparative study between a multifactor stochastic volatility model and a stochastic volatility jump model for the pricing and capturing implied volatility of European options. We have also applied the entropy measures in the option pricing and time series analysis of asset log-return series. The principle of maximum entropy is used to calibrate the risk-neutral probability density function by maximizing two-parameter (Varma) entropy and this maximum entropy density function is used to price European options. The two-parameter permutation entropy is proposed and is used to analyse the financial time series of asset log-returns.

This thesis comprises of six chapters including the current chapter on introduction and literature survey. The work reported in the subsequent chapters is as follows.

In Chapter 2, we have proposed a new multifactor stochastic volatility model

where the slow volatility factor, which is the persistent factor of volatility, is approximated by a quadratic arc. Using this model, the pricing formula for the European call options is obtained and implied volatility surface is also calibrated. The perturbation technique is used to obtain the approximate expression for the European option price. The notion of a modified Black-Scholes price is introduced. The approximated price is perturbed around the modified Black-Scholes price. An expression of the modified price is also obtained in terms of the Black-Scholes price. The effect of this modification on pricing is explained. The accuracy of the approximate option pricing formula is established, and its computational cost is also discussed. The pricing formula obtained by our model is very simple and contains only one unknown parameter which is estimated from the calibrated market implied volatilities, using the linear relationship of implied volatilities with log moneyness to maturity ratio. For the estimation of model parameter, data of S&P 500 index European options over the period of 6 months is used with different maturities and strike prices.

The work reported in this chapter has been published in a research article **"Quadratic Approximation of the Slow Factor of Volatility in a Multifactor Stochastic Volatility Model, *Journal of Futures Markets*, 38, 607-624 (2018)"**.

In Chapter 3, we have extended the model proposed in Chapter 2, for the pricing of geometric Asian options. In this case, the model contains an additional random term arising due to the consideration of geometric average of the asset prices. Using this model, the pricing formulae for the continuous geometric Asian options (GAOs) (both floating and fixed strike) are obtained. For this, the asymptotic expansion of the price function is considered and the first order price approximation is derived using the perturbation techniques for both floating and fixed strike GAOs. The zeroth order term in the price approximation is named as the modified Black-Scholes price for the GAOs. The expression of the modified price is also given in respect of the Black-Scholes price for the Asian options. The accuracy of the approximate option pricing formulae is also established. The unknown parameters in the pricing formulae are estimated by capturing the European and Asian volatility smiles together. For the numerical illustration, the S&P 500 index data of geometric Asian call options with the floating strike is considered for the period of 6 months. The approximated price is compared with

the price of the floating strike GAOs obtained in the Black-Scholes framework.

The work reported in this chapter has been communicated under the title **"Pricing of the Geometric Asian Options Under a Multifactor Stochastic Volatility Model"**. A part of this work has been presented in '*FIM&ISME 2017*' conference held at Kitakyushu International Conference Center, Kitakyushu, Japan, August 25-28, 2017.

In Chapter 4, we applied the quadratic arc approximation of the slow volatility factor proposed in Chapter 2, as a constraint in the entropy maximization procedure. For this, two-parameter Varma entropy is maximized using the principle of maximum entropy with the available options data, to calibrate the risk-neutral density function of the future asset prices. Entropy maximization is subjected to the expectation and the variance constraints. For the second order moment (variance) constraint, the volatility is assumed to be mean-reverting and following a quadratic path. The desired power law distribution is verified for the density function obtained, which contains both the entropy parameters. Presence of two parameters provide additional degrees of freedom. The calibrated density function is used to price the European call options for different strikes. The results thus obtained are also discussed for the one parameter Rényi and Tsallis entropies. The density function is calibrated using the data of European options on S&P 500 and FTSE 100 index with two different maturities and the corresponding strike prices. *MATLAB2012b* is used for the numerical analysis. The maximization of Varma entropy with additional volatility constraint gives the improved market fit in comparison to the Rényi and Shannon entropy.

The work reported in this chapter has been published in a research article **"Calibration of the Risk-Neutral Density Function by Maximization of a Two-Parameter Entropy, *Physica A*, 513, 45-54 (2019)"**.

In Chapter 5, a two-parameter permutation entropy is proposed and is used to obtain a two-parameter multiscale permutation entropy and a two-parameter weighted multiscale permutation entropy. The multiscale procedure captures the complexity of a financial time series on the multiple time scales, with the additional amplitude information obtained by including weights. In the multiscale analysis, we have introduced a new procedure for the averaging. Also, for calculating the

weights of the neighbouring vectors, a new weighting scheme is proposed. An empirical analysis is conducted on S&P 500 index data by comparing the two parametric entropies at different values of embedding dimensions, scales and entropy parameters. The consideration of two parameters give additional degrees of freedom to the system and improve the result. The effect of change of entropy parameters is also discussed.

The work reported in this chapter has been communicated in two research papers titled **"Two-Parameter Multiscale Permutation Entropy of a Financial Time Series"** and **"Analysis of Financial Time Series Using a Two-Parameter Weighted Multiscale Permutation Entropy"**.

In Chapter 6, we study and compare two models, one stochastic volatility jump model and another multifactor stochastic volatility model proposed in the literature, on the basis of their pricing performance and implied volatility fit to the market data. For this we consider "stochastic volatility jump model of Yan and Hanson" [124] and a "multifactor stochastic volatility model of Fouque and Lorig" [37]. Both the models are the extensions of Heston model, one by adding jumps in the stock price dynamics where jump amplitudes have log-uniform distribution, and other by considering a mean-reverting fast factor of volatility in addition to the CIR process. The parameters of Heston model, stochastic volatility jump model and multifactor stochastic volatility model are calibrated by non-linear least squares optimization. The S&P 500 index European call options data is used for the empirical analysis. The implied volatility fit of all the three models are compared at different time to maturity and for different log moneyness. The pricing performance of these models is compared by comparing their mean relative error with respect to the market data.

This work has been communicated under the title **"Comparative Study of a Stochastic Volatility Jump Model and a Multifactor Stochastic Volatility Model"**

Finally, the work reported in this thesis is concluded. The further scope of this work is given, followed by bibliography and a list of papers, published in journals and presented at various national and international conferences.

Chapter 2

Quadratic Approximation of the Persistent Volatility Factor

In this chapter[1]*, a new multifactor stochastic volatility model is proposed by approximating the slow volatility factor with a quadratic arc. The perturbation technique is used to obtain the approximate expression for the European option price. The notion of a modified Black-Scholes price is introduced. A simplified expression for the European option price, perturbed around the modified Black-Scholes price, is obtained. An expression of modified price is also obtained in terms of the Black-Scholes price. The effect of this modification on pricing is explained. The accuracy of the approximate option pricing formula is established, and its computational cost is also discussed.*

[1]The work reported in this chapter has been published in a research article "**Quadratic Approximation of the Slow Factor of Volatility in a Multifactor Stochastic Volatility Model,** ***Journal of Futures Markets*****, 38, 607-624, (2018)**".

2.1 Introduction

As discussed in detail in the previous chapter, the stochastic volatility modeling is a robust improvement of the classical Black-Scholes model. Multifactor stochastic volatility models are efficient to explain the time varying nature of volatility which the single factor stochastic volatility models are unable to capture. Multifactor stochastic volatility models have been ratified and studied in many papers [1, 22, 39, 41].

Fouque et al. [39] proposed a multifactor model with one fast mean-reverting stochastic volatility factor and the other slowly varying stochastic volatility factor. They have shown that the slow varying volatility factor is essential for the options with longer maturity and used the perturbation analysis in the context of pricing options.

The persistence of volatility should be given importance and must be incorporated in any volatility model [31]. Also, the multifactor stochastic volatility models give better results for the options with medium to longer maturity [33]. Therefore, the slow factor of volatility, which is highly persistent, is important and its dynamics cannot be ignored.

In the perturbation analysis given by Fouque et al. [39], the approximate option price depends upon the slow factor of volatility but is independent of the fast factor. They considered that the slow volatility factor follows a diffusion process resulting from a simple time change, as mentioned in Subsection 1.3.4 of the previous chapter.

In the present chapter, a new multifactor stochastic volatility model is proposed to give importance to the slow factor of volatility by taking it mean-reverting and approximating it by a quadratic arc. Also, using this model, a much simplified formula for the pricing of European call option is derived. The notion of a modified Black-Scholes operator is introduced. The modification factor is the real essence of this work improving the price of the European options. The accuracy and the computational cost of the approximate option pricing formula is explained. The implied volatility surface is also calibrated.

The rest of the chapter is organized as follows: The multifactor stochastic volatility (MSV) model has been introduced in Section 2.2. The PDE governing option price and the asymptotic expansion of price has been discussed in Sections

2.3 and 2.4 respectively. Section 2.5 gives the approximate price of the European call option. The accuracy of the approximate option price has been given in Section 2.6. In Section 2.7, the calibration of the implied volatility has been given. The computational cost of using price approximation formulae has also been explained in this section. The conclusion has been given in Section 2.8.

2.2 Model Under Consideration

Let X_t be the price of an underlying asset (non-dividend paying), P^* be the risk-neutral probability measure, and r be the risk-free rate of interest. Under P^*, the dynamics of X_t is given as

$$dX_t = rX_t dt + \sigma X_t dW_t^x \tag{2.2.1}$$

where

$$\sigma = f(Y_t, Z_t) \tag{2.2.2}$$

is the stochastic volatility which is assumed to be bounded and driven by two factors Y_t and Z_t which are respectively the fast scale and the slow scale factors of volatility. W_t^x is a standard Brownian motion. The dynamics of the fast volatility factor Y_t is considered as

$$dY_t = \frac{1}{\varepsilon}(m - Y_t)dt + \frac{\nu\sqrt{2}}{\sqrt{\varepsilon}}dW_t^y \tag{2.2.3}$$

which is an Ornstein-Uhlenbeck (OU) process with the long-run distribution $\mathcal{N}(m, \nu^2)$ and is reverting on the short time scale ε around its long-run mean value m with $1/\varepsilon$ as its rate of mean-reversion. Its volatility of volatility (vol-vol) parameter is $\frac{\nu\sqrt{2}}{\sqrt{\varepsilon}}$. W_t^y is also a standard Brownian motion. W_t^x and W_t^y have the correlation structure:

$$E[dW_t^x . dW_t^y] = \rho_{xy} dt$$

where ρ_{xy} represents a correlation between the two standard Brownian motions. The volatility being mean-reverting, keeps on fluctuating randomly around its long-run mean value. During the slow reverting mode, the volatility takes a longer time to come back to its long-run mean, moving randomly.

For instance, the S&P 500 index historical volatility data of period one year,

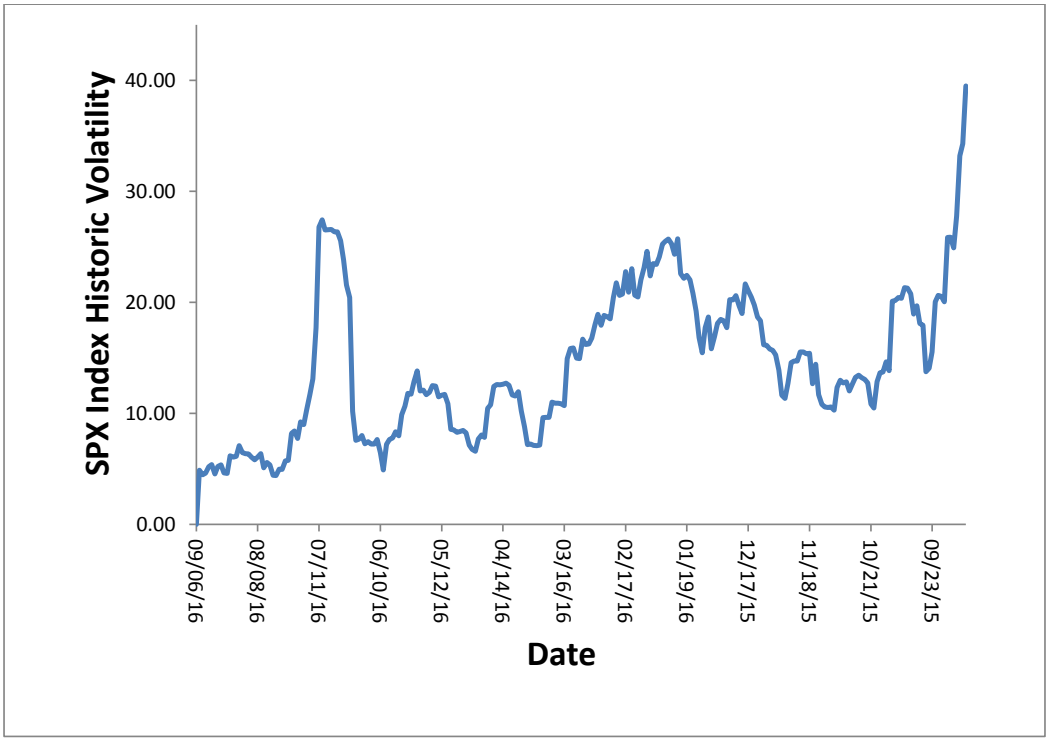

Figure 2.1: Mean-reverting historic volatility of S&P 500 index from September $8, 2015$ to September $6, 2016$.

which is mean- reverting around 20% (say) is given in Fig.2.1. A parabola is fitted to smooth out the random movement of the slow factor of volatility for one period of mean-reversion. So a quadratic arc approximation is considered to capture the slow volatility factor, given as

$$Z_t = \mathscr{A}t^2 + \mathscr{B}t + \mathscr{C} + \alpha_t \tag{2.2.4}$$

where $\mathscr{A}, \mathscr{B}$ and $\mathscr{C}$ are the unknown constants with $\mathscr{A} \neq 0$; α_t is the error term in the approximation of Z_t . This choice of quadratic approximation is justified by the fact that any diffusion process may be reduced to Eq.(2.2.4).

For example, if Z_t is an Ornstein-Uhlenbeck (OU) process given as

$$dZ_t = k(m^{'} - Z_t)dt + \eta dW_t^z \tag{2.2.5}$$

W_t^z is also a standard Brownian motion. It has the correlation with W_t^x and W_t^y as

$$E[dW_t^x.dW_t^z] = \rho_{xz}dt$$

$$E[dW_t^y.dW_t^z] = \rho_{yz}dt$$

and the correlation coefficients ρ_{xy}, ρ_{xz} and ρ_{yz} are such that $\rho_{xy}^2 < 1, \rho_{xz}^2 < 1, \rho_{yz}^2 < 1$ and $1 + 2\rho_{xy}\rho_{xz}\rho_{yz} - \rho_{xy}^2 - \rho_{xz}^2 - \rho_{yz}^2 > 0$ for the positive definiteness of the covariance matrix of the three Brownian motions. Z_t has the long-run distribution $\mathcal{N}(m^{'}, \frac{\eta^2}{2k})$ and is reverting on a long time scale $1/k$ around its long-run mean value $m^{'}$. The rate of mean-reversion for Z_t is k and its vol-vol parameter is η.

On solving Eq.(2.2.5) using Ito lemma, Z_t can be written explicitly in terms of its initial value Z_0 as

$$Z_t = m^{'} + (Z_0 - m^{'})e^{-kt} + \eta \int_0^t e^{-k(t-s)} dW_s^z$$

On expanding e^{-kt} term

$$Z_t = m^{'} + (Z_0 - m^{'})(1 - kt + \frac{k^2t^2}{2!} + ...) + \eta \int_0^t e^{-k(t-s)} dW_s^z$$

After rearranging the terms, we get

$$Z_t = \left[\frac{(Z_0 - m^{'})}{2} k^2\right] t^2 + [-k(Z_0 - m^{'})]t + Z_0 + \delta_t + \beta_t \tag{2.2.6}$$

Comparing it with Eq.(2.2.4), we obtain

$$\mathscr{A} = \frac{(Z_0 - m^{'})}{2} k^2,$$

$$\mathscr{B} = -(Z_0 - m^{'})k,$$

$$\mathscr{C} = Z_0,$$

and

$$\alpha_t = \delta_t + \beta_t$$

δ_t is the truncation error, and the term β_t involving η is the randomness in the value of the slow factor of volatility Z_t. To assure that $\mathscr{A} \neq 0$, it is assumed that $Z_0 \neq m^{'}$. Also, it is assumed that the error term α_t is negligible, since the truncation error δ_t can be neglected because of the small value of k. The expected value of the random term β_t which involves η is zero, so it can also be neglected.

The approximated value of Z_t is a function of t. So

$$\frac{\partial}{\partial z} = \left(\frac{1}{2\mathscr{A}t + \mathscr{B} + \zeta_t}\right) \frac{\partial}{\partial t} \tag{2.2.7}$$

and

$$\frac{\partial^2}{\partial z^2} = \frac{1}{(2\mathscr{A}t + \mathscr{B} + \zeta_t)^2}\left[\frac{\partial^2}{\partial t^2} - \left(\frac{2\mathscr{A} + \zeta_t^{'}}{2\mathscr{A}t + \mathscr{B} + \zeta_t}\right)\frac{\partial}{\partial t}\right] \tag{2.2.8}$$

where

$$\zeta_t = \frac{\partial \alpha_t}{\partial t}$$

These expressions will be needed for pricing in the proceeding sections. So our multifactor stochastic volatility model under the risk-neutral probability measure P^*, which is already chosen by the market is

$$dX_t = rX_t dt + \sigma X_t dW_t^x$$

$$dY_t = \frac{1}{\varepsilon}(m - Y_t)dt + \frac{\nu\sqrt{2}}{\sqrt{\varepsilon}}dW_t^y$$

$$Z_t = \mathscr{A}t^2 + \mathscr{B}t + \mathscr{C} + \alpha_t$$

where

$$\mathscr{A} = \frac{(Z_0 - m^{'})}{2}k^2,$$

$$\mathscr{B} = -(Z_0 - m^{'})k,$$

$$\mathscr{C} = Z_0 \tag{2.2.9}$$

here Z_t has been obtained by considering the diffusion process

$$dZ_t = k(m^{'} - Z_t)dt + \eta dW_t^z$$

Next, the pricing equation for the European options is obtained.

2.3 Pricing Equation

The price of the European call option, under the risk-neutral probability measure P^*, is the conditional expectation of the discounted payoff $h(X_T)$, which is given as:

$$P^{\varepsilon}(t,x,y,z) = E^*\{e^{-r(T-t)}h(X_T)|X_t = x, Y_t = y, Z_t = z\}, \tag{2.3.1}$$

Using the Feynman-Kac formula, given in Eq.(1.3.27) of previous chapter, $P^{\varepsilon}(t,x,y,z)$ satisfies the following parabolic PDE:

$$\mathscr{L}^{\varepsilon}P^{\varepsilon}(t,x,y,z)=0 \tag{2.3.2}$$

with the boundary condition

$$P^{\varepsilon}(T,X_T,Y_T,Z_T)=h(X_T)$$

where $\mathscr{L}^{\varepsilon}$ is given by:

$$\mathscr{L}^{\varepsilon}=\frac{1}{\varepsilon}\mathscr{L}_0+\frac{1}{\sqrt{\varepsilon}}\mathscr{L}_1+\mathscr{L}_2 \tag{2.3.3}$$

with

$$\mathscr{L}_0=(m-y)\frac{\partial}{\partial y}+\nu^2\frac{\partial^2}{\partial y^2} \tag{2.3.4}$$

$$\mathscr{L}_1=\rho_{xy}\nu\sqrt{2}f(y,z)x\frac{\partial^2}{\partial x\partial y}+\rho_{yz}\nu\sqrt{2}\eta\frac{\partial^2}{\partial y\partial z} \tag{2.3.5}$$

and

$$\mathscr{L}_2=\frac{\partial}{\partial t}+\frac{1}{2}f^2(y,z)x^2\frac{\partial^2}{\partial x^2}+r(x\frac{\partial}{\partial x}-.)+\rho_{xz}\eta f(y,z)x\frac{\partial^2}{\partial x\partial z}+\frac{1}{2}\eta^2\frac{\partial^2}{\partial z^2}+k(m^{'}-z)\frac{\partial}{\partial z} \tag{2.3.6}$$

Substituting for $\frac{\partial}{\partial z}$ and $\frac{\partial^2}{\partial z^2}$ from Eqs.(2.2.7) and (2.2.8) in Eqs.(2.3.5) and (2.3.6) and solving, we get

$$\mathscr{L}_1=\nu\sqrt{2}\left[\rho_{xy}f(y,z)x\frac{\partial^2}{\partial x\partial y}+\frac{\rho_{yz}}{2\mathscr{A}t+\mathscr{B}+\zeta_t}\eta\frac{\partial^2}{\partial y\partial t}\right] \tag{2.3.7}$$

and

$$\begin{aligned}\mathscr{L}_2=&\left[1+\frac{k(m^{'}-z)}{2\mathscr{A}t+\mathscr{B}+\zeta_t}-\frac{1}{2}\eta^2\frac{2\mathscr{A}+\zeta_t^{'}}{(2\mathscr{A}t+\mathscr{B}+\zeta_t)^3}\right]\frac{\partial}{\partial t}+\frac{1}{2}f^2(y,z)x^2\frac{\partial^2}{\partial x^2}+r(x\frac{\partial}{\partial x}-.)\\&+\left(\frac{\rho_{xz}\eta f(y,z)x}{2\mathscr{A}t+\mathscr{B}+\zeta_t}\right)\frac{\partial^2}{\partial x\partial t}+\frac{1}{2}\eta^2\frac{1}{(2\mathscr{A}t+\mathscr{B}+\zeta_t)^2}\frac{\partial^2}{\partial t^2}\end{aligned} \tag{2.3.8}$$

where $z=Z_t$ is given by Eq.(2.2.6).

From Eqs.(2.3.2) and (2.3.3) we have,

$$(\frac{1}{\varepsilon}\mathscr{L}_0+\frac{1}{\sqrt{\varepsilon}}\mathscr{L}_1+\mathscr{L}_2)P^{\varepsilon}(t,x,y,z)=0 \tag{2.3.9}$$

This is the required pricing equation with solution P^{ε}.

2.4 Asymptotic Expansion

The asymptotic expansion of P^ε in powers of $\sqrt{\varepsilon}$ is

$$P^\varepsilon = P_0 + \sqrt{\varepsilon}P_1 + \varepsilon P_2 + ... \tag{2.4.1}$$

Using it in Eq.(2.3.9) gives

$$(\frac{1}{\varepsilon}\mathscr{L}_0 + \frac{1}{\sqrt{\varepsilon}}\mathscr{L}_1 + \mathscr{L}_2)(P_0 + \sqrt{\varepsilon}P_1 + \varepsilon P_2 + ...) = 0 \tag{2.4.2}$$

A similar expansion is considered in Fouque et al. [40] for the one factor and in Fouque et al. [39] for the two factors of volatility. The expansion, only in the powers of $\sqrt{\varepsilon}$, is considered here because the slow factor of volatility is approximated.

Terms of order $\frac{1}{\varepsilon}$:

$$\mathscr{L}_0 P_0 = 0$$

here $\mathscr{L}_0$ is given in Eq.(2.3.4) and it contains the partial derivatives with respect to y. This implies that

$$P_0 = P_0(t,x,z) \tag{2.4.3}$$

which is independent of y, but depending on z, the slow factor of volatility.

Terms of order $\frac{1}{\sqrt{\varepsilon}}$:

$$\mathscr{L}_1 P_0 + \mathscr{L}_0 P_1 = 0$$

as P_0 is independent of y, and $\mathscr{L}_1$ given in Eq.(2.3.7) contains partial derivatives with respect to y in each term, thus $\mathscr{L}_1 P_0 = 0$. This results in to

$$\mathscr{L}_0 P_1 = 0$$

which gives

$$P_1 = P_1(t,x,z) \tag{2.4.4}$$

which is again independent of y, but depending on z, the slow factor of volatility.

Terms of order 1:

$$\mathscr{L}_2 P_0 + \mathscr{L}_1 P_1 + \mathscr{L}_0 P_2 = 0$$

since P_1 is independent of y thus $\mathscr{L}_1 P_1 = 0$, this gives

$$\mathscr{L}_0 P_2 + \mathscr{L}_2 P_0 = 0 \tag{2.4.5}$$

It is a "Poisson equation" in P_2 with respect to y with the Fredholm solvability condition

$$E_y[\mathscr{L}_2 P_0] = 0$$

as P_0 is independent of y, therefore, it can be written as

$$E_y[\mathscr{L}_2] P_0 = 0 \tag{2.4.6}$$

where $E_y[\mathscr{L}_2]$ is the average of $\mathscr{L}_2$ with respect to the invariant (or long run) distribution of process Y_t, which is $\mathscr{N}(m, v^2)$. For simplification, the error term involving truncation and randomness is neglected in Eq.(2.2.6) assuming $\delta_t \to 0$ and the vol-vol parameter of $Z_t, \eta \approx 0$. Therefore, Eqs.(2.3.7) and (2.3.8) are reduced to

$$\mathscr{L}_1 = v\sqrt{2}\left[\rho_{xy} f(y,z) x \frac{\partial^2}{\partial x \partial y}\right] \tag{2.4.7}$$

and

$$\mathscr{L}_2 = \left[1 + \frac{1 - kt + \frac{k^2 t^2}{2}}{1 - kt}\right]\frac{\partial}{\partial t} + \frac{1}{2} f^2(y,z) x^2 \frac{\partial^2}{\partial x^2} + r(x\frac{\partial}{\partial x} - .)$$

On taking

$$\frac{1 - kt + \frac{k^2 t^2}{2}}{1 - kt} = \gamma$$

with $kt \neq 1$ and $\gamma \neq 0$ gives

$$\mathscr{L}_2 = [1 + \gamma]\frac{\partial}{\partial t} + \frac{1}{2} f^2(y,z) x^2 \frac{\partial^2}{\partial x^2} + r(x\frac{\partial}{\partial x} - .) \tag{2.4.8}$$

and

$$E_y[\mathscr{L}_2] = [1 + \gamma]\frac{\partial}{\partial t} + \frac{1}{2}\overline{\sigma}^2(z) x^2 \frac{\partial^2}{\partial x^2} + r(x\frac{\partial}{\partial x} - .) \tag{2.4.9}$$

where

$$\overline{\sigma}(z) = E_y[f(y,z)]$$

which is a function of the slow factor of volatility.

The operator $E_y[\mathscr{L}_2]$ differs from the Black-Scholes operator given in Eq.(1.3.5) in the coefficient of $\frac{\partial}{\partial t}$, so $E_y[\mathscr{L}_2]$ is named as a $\gamma-$modified Black-Scholes operator with volatility $\overline{\sigma}(z)$. Therefore, in Eq.(2.4.6), P_0 is a modified Black-Scholes price.

To obtain the expression of P_0, Eq.(2.4.6) is solved. We write operator $E_y[\mathscr{L}_2]$ as

$$E_y[\mathscr{L}_2] = \mathscr{L}_{BS}(\overline{\sigma}(z)) + \gamma\frac{\partial}{\partial t}$$

where $\mathscr{L}_{BS}(\overline{\sigma}(z))$ is the Black-Scholes operator given in Eq.(1.3.5) with volatility $\overline{\sigma}(z)$.

Let $P_0(t,x,z) = b(t)Q_0(t,x,\overline{\sigma}(z))$, where $Q_0(t,x,\overline{\sigma}(z))$ is the Black-Scholes price satisfying $\mathscr{L}_{BS}Q_0 = 0$. So Eq.(2.4.6) gives

$$\left[\mathscr{L}_{BS} + \gamma\frac{\partial}{\partial t}\right](b(t)Q_0) = 0, \tag{2.4.10}$$

that is,

$$b(t)\mathscr{L}_{BS}Q_0 + Q_0\mathscr{L}_{BS}(b(t)) + \gamma b(t)\frac{\partial Q_0}{\partial t} + \gamma Q_0\frac{\partial b(t)}{\partial t} = 0 \tag{2.4.11}$$

as $\mathscr{L}_{BS}Q_0 = 0$ and $\mathscr{L}_{BS}(b(t)) = \frac{\partial b(t)}{\partial t}$, the above equation reduces to

$$Q_0\frac{\partial b(t)}{\partial t} + \gamma b(t)\frac{\partial Q_0}{\partial t} + \gamma Q_0\frac{\partial b(t)}{\partial t} = 0 \tag{2.4.12}$$

that is,

$$(1+\gamma)Q_0\frac{\partial b(t)}{\partial t} + \gamma b(t)\frac{\partial Q_0}{\partial t} = 0 \tag{2.4.13}$$

this implies,

$$\left(\frac{1+\gamma}{\gamma}\right)\left(\frac{1}{b(t)}\right)\frac{\partial b(t)}{\partial t} + \frac{1}{Q_0}\frac{\partial Q_0}{\partial t} = 0 \tag{2.4.14}$$

After solving this equation, the expression of P_0 in terms of the Black-Scholes price Q_0 is obtained as

$$P_0(t,x,z) = \frac{|kt-2|^{\frac{a-2r}{k}}e^{\frac{2r-a}{k(|kt-2|)}}}{e^{\frac{(2r-a)t}{2}}}Q_0(t,x,\overline{\sigma}(z)) \tag{2.4.15}$$

where $kt \neq 2$ for $0 \leq t \leq T$ and a is the constant satisfying

$$a = 2r - \frac{\gamma\frac{\partial Q_0}{\partial t}}{(1+\gamma)Q_0[\frac{k^2t^2-2kt+2}{2(kt-2)^2}]} \tag{2.4.16}$$

$\frac{\partial Q_0}{\partial t}$ is the Black-Scholes theta (one of the Greeks) and $a \neq 2r$ for $0 \leq t < T$. Equality holds at maturity to satisfy the boundary condition

$$P_0(T, X_T, Z_T) = h(X_T)$$

Also, from Eqs.(2.4.5) and (2.4.6)

$$\mathscr{L}_0 P_2 = -[\mathscr{L}_2 P_0 - E_y[\mathscr{L}_2]P_0]$$

giving

$$P_2 = -\mathscr{L}_0^{-1}[\mathscr{L}_2 - E_y[\mathscr{L}_2]]P_0 \tag{2.4.17}$$

Terms of order $\sqrt{\varepsilon}$:

$$\mathscr{L}_0 P_3 + \mathscr{L}_2 P_1 + \mathscr{L}_1 P_2 = 0$$

which is a "Poisson equation" in P_3 with respect to y, with the Fredholm solvability condition:

$$E_y[\mathscr{L}_2 P_1 + \mathscr{L}_1 P_2] = 0$$

that is

$$E_y[\mathscr{L}_2]P_1 + E_y[\mathscr{L}_1 P_2] = 0$$

thus

$$E_y[\mathscr{L}_2]P_1 = -E_y[\mathscr{L}_1 P_2]$$

Considering the expression of P_2 from Eq.(2.4.17), we get

$$E_y[\mathscr{L}_2]P_1 = \mathscr{G} P_0 \tag{2.4.18}$$

where

$$\mathscr{G} = E_y[\mathscr{L}_1 \mathscr{L}_0^{-1}[\mathscr{L}_2 - E_y[\mathscr{L}_2]]]$$

This expression is further simplified by considering the value of $\mathscr{L}_0$, $\mathscr{L}_1$, $\mathscr{L}_2$ and $E_y[\mathscr{L}_2]$ from Eqs.(2.3.4), (2.4.7), (2.4.8) and (2.4.9) respectively. Firstly, we get that

$$\mathscr{L}_2 - E_y[\mathscr{L}_2] = \frac{1}{2}(f^2(y,z) - \overline{\sigma}^2(z))x^2 \frac{\partial^2}{\partial x^2} \tag{2.4.19}$$

On taking ϕ as the solution of

$$\mathscr{L}_0\phi_{y,z} = f^2(y,z) - \overline{\sigma}^2(z) \tag{2.4.20}$$

we obtain that

$$\mathscr{L}_0^{-1}[\mathscr{L}_2 - E_y[\mathscr{L}_2]] = \frac{1}{2}\phi_{y,z}x^2\frac{\partial^2}{\partial x^2}$$

thus

$$\mathscr{L}_1\mathscr{L}_0^{-1}[\mathscr{L}_2 - E_y[\mathscr{L}_2]] = \frac{\nu\rho_{xy}}{\sqrt{2}}f\frac{\partial\phi}{\partial y}x\frac{\partial}{\partial x}x^2\frac{\partial^2}{\partial x^2} \tag{2.4.21}$$

this gives

$$\mathscr{G} = \frac{\nu\rho_{xy}}{\sqrt{2}}E_y[f\frac{\partial\phi}{\partial y}]x\frac{\partial}{\partial x}x^2\frac{\partial^2}{\partial x^2} \tag{2.4.22}$$

For the first order price approximation, the expression for P_1 is also needed along with that of P_0. The following theorem is developed to obtain the expression of P_1.

Theorem 2.1. *Let $A(t,x,z)$ be a function which satisfies*

$$E_y[\mathscr{L}_2]A(t,x,z) = D(t,x,z) \tag{2.4.23}$$

with $A(T,x,z) = 0$ and $D(t,x,z)$ be a function which satisfies $E_y[\mathscr{L}_2]D(t,x,z) = 0$. Then the solution of Eq.(2.4.23) *is*

$$A(t,x,z) = -\left(\int_t^T \frac{d\tau}{1+\gamma}\right)D(t,x,z)$$

where, $1+\gamma = \frac{(2-kt)^2}{2(1-kt)}$.

Proof. Let

$$A(t,x,z) = -\left(\int_t^T \frac{d\tau}{1+\gamma}\right)D(t,x,z)$$

Clearly

$$A(T,x,z) = 0$$

Also, as

$$(1+\gamma)\frac{\partial A}{\partial t} = D(t,x,z) - \left(\int_t^T \frac{d\tau}{1+\gamma}\right)(1+\gamma)\frac{\partial D(t,x,z)}{\partial t}$$

and

$$\left[\frac{1}{2}\overline{\sigma}^2(z)x^2\frac{\partial^2}{\partial x^2} + r(x\frac{\partial}{\partial x} - .)\right]A(t,x,z) = -\left(\int_t^T \frac{d\tau}{1+\gamma}\right)\left[\frac{1}{2}\overline{\sigma}^2(z)x^2\frac{\partial^2}{\partial x^2} + r(x\frac{\partial}{\partial x} - .)\right]D(t,x,z)$$

therefore

$$E_y[\mathscr{L}_2]A(t,x,z) = D(t,x,z) - \left(\int_t^T \frac{d\tau}{1+\gamma}\right)E_y[\mathscr{L}_2]D(t,x,z)$$

As $E_y[\mathscr{L}_2]D(t,x,z) = 0$, thus

$$E_y[\mathscr{L}_2]A(t,x,z) = D(t,x,z)$$

This completes the proof of the Theorem 2.1. □

Now, as P_1 satisfies Eq.(2.4.18) and $P_1(T,x,z) = 0$. Also, $E_y[\mathscr{L}_2]$ and $\mathscr{G}$ commute with each other, giving

$$E_y[\mathscr{L}_2](\mathscr{G}P_0) \;=\; \mathscr{G}E_y[\mathscr{L}_2](P_0) \;=\; 0$$

therefore, by the Theorem 2.1

$$P_1 = -\left(\int_t^T \frac{d\tau}{1+\gamma}\right)(\mathscr{G}P_0)$$

On substituting the value of $1+\gamma$

$$P_1 = 2\left(\int_t^T \frac{k\tau - 1}{(k\tau - 2)^2}d\tau\right)\mathscr{G}P_0$$

It can be easily solved to give

$$P_1(t,x,z) = 2\left[\frac{1}{k}\log\left|\frac{kT-2}{kt-2}\right| + \frac{T-t}{(kT-2)(kt-2)}\right]\mathscr{G}P_0 \tag{2.4.24}$$

which is a unique solution of Eq.(2.4.18) with the boundary condition

$$P_1(T,X_T,Z_T) = 0$$

2.5 Approximate Option Price

From the above calculation, a first-order approximated option price is obtained and is given as

$$P^{\varepsilon} \approx \hat{P}^{\varepsilon} = P_0 + \sqrt{\varepsilon} P_1$$

that is

$$P^{\varepsilon} \approx \hat{P}^{\varepsilon} = P_0 + \sqrt{\varepsilon}\left(2\left[\frac{1}{k}\log\left|\frac{kT-2}{kt-2}\right| + \frac{T-t}{(kT-2)(kt-2)}\right]\mathscr{G}\right)P_0 \tag{2.5.1}$$

where P_0 is given by Eq.(2.4.15).

Now, Eq.(2.5.1) can be written as

$$P^{\varepsilon} \approx (1+g)\left[Q_0 + \sqrt{\varepsilon}\left(2\left[\frac{1}{k}\log\left|\frac{kT-2}{kt-2}\right| + \frac{T-t}{(kT-2)(kt-2)}\right]VD_1D_2\right)Q_0\right] \tag{2.5.2}$$

here

$$\begin{aligned} V &= \frac{\nu\rho_{xy}}{\sqrt{2}}E_y[f\frac{\partial\phi}{\partial y}] \\ D_1 &= x\frac{\partial}{\partial x} \\ D_2 &= x^2\frac{\partial^2}{\partial x^2} \end{aligned} \tag{2.5.3}$$

Eq.(2.5.2) gives the required approximated price, where

$$1+g = b(t) = \frac{|kt-2|^{\frac{a-2r}{k}}e^{\frac{2r-a}{k(|kt-2|)}}}{e^{\frac{(2r-a)t}{2}}} \tag{2.5.4}$$

such that g converges to zero at maturity. $(1+g)$ is named as a modification factor. This modification factor significantly improves the pricing in comparison to the Black-Scholes price.

2.6 Accuracy of the Approximate Option Pricing Formula

We have considered the case of non-smooth payoff function for the European option. We observed that the case of smooth payoff is straightforward. In Fouque

et al. [39, 40], the error in the price approximation of the European call option has an upper bound $c(\varepsilon + \varepsilon|\log\varepsilon|)$, where c is some constant. For the model under consideration, we have proved our results on the same lines.

Suppose that $P^{\varepsilon,\delta}$ be the slightly smoothed (or regularized) price with smoothing parameter δ, and $s = \ln x$ be the log stock price. For this smoothed option, the payoff function is

$$\begin{aligned} H^{\delta}(s) &= P_0(T-\delta, s, K, T, \overline{\sigma}(z)) \\ &= (1+g)Q_0(T-\delta, s, K, T, \overline{\sigma}(z)) \end{aligned}$$

where the Black-Scholes price Q_0 is obtained at volatility $\overline{\sigma}(z)$, which is a function of the slow volatility factor z. $(1+g)$ represents a modification factor given in Eq.(2.5.4).

If $\hat{P}^{\varepsilon,\delta}$ is the first order approximation to $P^{\varepsilon,\delta}$ then

$$P^{\varepsilon,\delta} \approx \hat{P}^{\varepsilon,\delta} = P_0^{\delta} + \sqrt{\varepsilon} P_1^{\delta}$$

where

$$P_0^{\delta} = (1+g)Q_0(t-\delta, s, K, T, \overline{\sigma}(z)) \tag{2.6.1}$$

and

$$P_1^{\delta} = 2\left[\frac{1}{k}\log\left|\frac{kT-2}{kt-2}\right| + \frac{T-t}{(kT-2)(kt-2)}\right]\mathscr{G}P_0^{\delta} \tag{2.6.2}$$

The accuracy of the price approximation is established by the theorem given below.

Theorem 2.2. *If $f(y,z)$ is positive and bounded, then at a fixed $t < T, s, y, z \in \mathbb{R}$, the approximated option price $\hat{P}^{\varepsilon}$ satisfies*

$$|P^{\varepsilon}(t,s,y,z) - \hat{P}^{\varepsilon}(t,s,z)| \leq c\left[\left(\varepsilon + \varepsilon^{\frac{1}{2}}\right)\left(1 + \varepsilon^{\frac{1}{4}}\right) + \varepsilon|\log(\varepsilon)|\right]$$

for some constant c.

The proof of the theorem depends on the three results which are given below as lemmas.

Lemma 2.1. *For a fix point (t,s,y,z) with $t<T$, there exist constants $\varepsilon_1>0,\ \delta_1>0$ and $c_1>0$ so that*

$$|P^{\varepsilon}(t,s,y,z)-P^{\varepsilon,\delta}(t,s,y,z)|\le c_1\delta$$

for all $0<\delta<\delta_1$ and $0<\varepsilon<\varepsilon_1$.

Proof. This lemma shows that for a small δ, the difference of the regularized and the unregularized price is small.

Consider a new stochastic process $\tilde{S}_t$ given by

$$d\tilde{S}_t=\left(r-\frac{1}{2}\tilde{f}(t,y,z)^2\right)dt+\tilde{f}(t,y,z)(\rho dW_t^y+\sqrt{1-\rho^2}d\hat{W}_t^s)$$

here ρ represents ρ_{sy}. ρ_{sz} and ρ_{yz} are taken as zero for simplification. W_t^y and $\hat{W}_t^s$ are the Brownian motions independent of each other, and

$$\tilde{f}(t,y,z)=\begin{cases} f(y,z), & \text{if } t<T\\ \overline{\sigma}(z), & \text{if } t\ge T.\end{cases}$$

Therefore, we write

$$P^{\varepsilon,\delta}(t,s,y,z)=E^*_{t,s,y,z}[e^{-r(T+\delta-t)}H(\tilde{S}_{T+\delta})]$$

and

$$P^{\varepsilon}(t,s,y,z)=E^*_{t,s,y,z}[e^{-r(T-t)}H(\tilde{S}_T)]$$

this implies that

$$\begin{aligned}
&P^{\varepsilon}(t,s,y,z)-P^{\varepsilon,\delta}(t,s,y,z)\\
&\quad=E^*_{t,s,y,z}[e^{-r(T-t)}H(\tilde{S}_T)]-E^*_{t,s,y,z}[e^{-r(T+\delta-t)}H(\tilde{S}_{T+\delta})]\\
&\quad=E^*_{t,s,y,z}[E^*_{t,s,y,z}\{e^{-r(T-t)}H(\tilde{S}_T)-e^{-r(T+\delta-t)}H(\tilde{S}_{T+\delta})\}|(W_u^y)_{t\le u\le T}]\\
&=E^*_{t,s,y,z}[E^*_{t,s,y,z}\{e^{-r(T-t)}H(\tilde{S}_T)|(W_u^y)_{t\le u\le T}\}-E^*_{t,s,y,z}\{e^{-r(T+\delta-t)}H(\tilde{S}_{T+\delta})|(W_u^y)_{t\le u\le T}\}]
\end{aligned}\tag{2.6.3}$$

The distribution of $\tilde{S}_T$ conditional on the path of $(W_u^y)_{t\le u\le T}$ is $\mathcal{N}(\mu_s,\overline{\sigma}^2_{\rho,s}(T-t))$, where

$$\mu_s=\tilde{S}_t+r(T-t)+\rho\int_t^T\tilde{f}(u,y,z)dW_u^y-\frac{1}{2}\int_t^T\tilde{f}^2(u,y,z)du$$

and

$$\overline{\sigma}^2_{\rho,s}(T-t) = (1-\rho^2)\int_t^T \tilde{f}^2(u,y,z)du$$

It is rearranged as

$$-\frac{1}{2}\int_t^T \tilde{f}^2(u,y,z)du = -\frac{\overline{\sigma}^2_{\rho,s}(T-t)}{2} - \frac{\rho^2}{2}\int_t^T \tilde{f}^2(u,y,z)du$$

This gives

$$\mu_s = \tilde{S}_t + \left(r - \frac{\overline{\sigma}^2_{\rho,s}}{2}\right)(T-t) + \xi_{t,T}$$

where

$$\xi_{t,T} = \rho\int_t^T \tilde{f}(u,y,z)dW^y_u - \frac{\rho^2}{2}\int_t^T \tilde{f}^2(u,y,z)du$$

therefore

$$\begin{aligned} E^*_{t,s,y,z}\{e^{-r(T-t)}H(\tilde{S}_T)|(W^y_u)_{t\le u\le T}\} &= P_0(t,\tilde{S}_t+\xi_{t,T},K,T,\overline{\sigma}_{\rho,s}) \\ &= (1+g)Q_0(t,\tilde{S}_t+\xi_{t,T},K,T,\overline{\sigma}_{\rho,s}) \end{aligned} \tag{2.6.4}$$

Similarly, the conditional distribution of $\tilde{S}_{T+\delta}$ given the path of $(W^y_u)_{t\le u\le T}$ is $\mathcal{N}(\mu_{s,\delta}, \overline{\sigma}^2_{\rho,s,\delta}(T-t))$, where

$$\mu_{s,\delta} = \tilde{S}_t + r\delta + \left(r - \frac{\overline{\sigma}^2_{\rho,s,\delta}}{2}\right)(T-t) + \xi_{t,T}$$

and

$$\overline{\sigma}^2_{\rho,s,\delta}(T-t) = \overline{\sigma}^2_{\rho,s}(T-t) + \overline{\sigma}^2\delta$$

therefore

$$\begin{aligned} E^*_{t,s,y,z}\{e^{-r(T-t)}H(\tilde{S}_{T+\delta})|(W^y_u)_{t\le u\le T}\} &= P_0(t,\tilde{S}_t+\xi_{t,T}+r\delta,K,T,\overline{\sigma}_{\rho,s,\delta}) \\ &= (1+g)Q_0(t,\tilde{S}_t+\xi_{t,T}+r\delta,K,T,\overline{\sigma}_{\rho,s,\delta}) \end{aligned} \tag{2.6.5}$$

Using Eqs.(2.6.4) and (2.6.5) in Eq.(2.6.3), we get

$$\begin{aligned} &P^{\varepsilon}(t,s,y,z) - P^{\varepsilon,\delta}(t,s,y,z) \\ &= E^*_{t,s,y,z}[(1+g)Q_0(t,\tilde{S}_t+\xi_{t,T},K,T,\overline{\sigma}_{\rho,s}) - (1+g)Q_0(t,\tilde{S}_t+\xi_{t,T}+r\delta,K,T,\overline{\sigma}_{\rho,s,\delta})] \\ &= (1+g)E^*_{t,s,y,z}[Q_0(t,\tilde{S}_t+\xi_{t,T},K,T,\overline{\sigma}_{\rho,s}) - Q_0(t,\tilde{S}_t+\xi_{t,T}+r\delta,K,T,\overline{\sigma}_{\rho,s,\delta})] \end{aligned} \tag{2.6.6}$$

Given the assumption that $kt \neq 2$, $(1+g)$ will always be finite for a finite t. Also, under the assumption of bounded $f(y,z)$ and using the explicit expression of the Black-Scholes formula for the European options, we have easily obtained that

$$|P^{\varepsilon}(t,s,y,z) - P^{\varepsilon,\delta}(t,s,y,z)| \leq c_1\delta$$

with some constant c_1 and some small δ. □

Lemma 2.2. *For a fix point (t,s,y,z) with $t < T$, there exist constants $\varepsilon_2 > 0$, $\delta_2 > 0$ and $c_2 > 0$ so that*

$$|\hat{P}^{\varepsilon,\delta}(t,s,z) - \hat{P}^{\varepsilon}(t,s,z)| \leq c_2\delta$$

for all $0 < \delta < \delta_2$ and $0 < \varepsilon < \varepsilon_2$.

Proof. This lemma shows that for a small δ, the difference of the regularized and the un-regularized first-order price approximation is small. Consider

$$\begin{aligned}
&\hat{P}^{\varepsilon,\delta}(t,s,z) - \hat{P}^{\varepsilon}(t,s,z) \\
&= \left[1 + 2\left(\frac{1}{k}\log\left|\frac{kT-2}{kt-2}\right| + \frac{T-t}{(kT-2)(kt-2)}\right)\sqrt{\varepsilon}VD_1D_2\right](P_0^{\delta} - P_0) \\
&= (1+g)\left[1 + 2\left(\frac{1}{k}\log\left|\frac{kT-2}{kt-2}\right| + \frac{T-t}{(kT-2)(kt-2)}\right)\sqrt{\varepsilon}VD_1D_2\right](Q_0^{\delta} - Q_0)
\end{aligned}$$

D_1 and D_2 in terms of log stock price s will be

$$\begin{aligned}
D_1 &= \frac{\partial}{\partial s} \\
D_2 &= \frac{\partial^2}{\partial s^2} - \frac{\partial}{\partial s}
\end{aligned} \tag{2.6.7}$$

The expression of V is given in Eq.(2.5.3). From Eq.(2.4.20), which is a Poisson equation in $\phi_{y,z}$ with bounded expression on right side, we used the bounds on the solution of the Poisson equation to get that

$$|V^{\varepsilon}| \leq d_1\sqrt{\varepsilon}$$

for some d_1. Here, $V^{\varepsilon} = \sqrt{\varepsilon}V$

also,

$$P_0^{\delta}(t,s,z) = P_0(t-\delta,s,z) = (1+g)Q_0(t-\delta,s,z)$$

For any $t < T$, Q_0 and the derivatives of Q_0 with respect to s, are differentiable in t.

$(1+g)$ is also differentiable in t under the assumption $kt \neq 2$. So for any fixed (t,s,y,z), where $t < T$

$$|\hat{P}^{\varepsilon,\delta}(t,s,z) - \hat{P}^{\varepsilon}(t,s,z)| \leq c_2\delta$$

for some given c_2 and small δ. □

Lemma 2.3. *For a fix point (t,s,y,z) with $t < T$, there exist constants $\varepsilon_3 > 0$, $\delta_3 > 0$ and $c_3 > 0$ such that*

$$|P^{\varepsilon,\delta}(t,s,y,z) - \hat{P}^{\varepsilon,\delta}(t,s,z)| \leq c_3\left[\left(\varepsilon + \frac{\varepsilon}{\delta}\right)\left(1+\sqrt{\frac{\varepsilon}{\delta}}\right) + \varepsilon|\log(\delta)|\right]$$

for all $0 < \delta < \delta_3$ and $0 < \varepsilon < \varepsilon_3$.

Proof. This lemma shows that for a small δ, the difference of the regularized price and its corresponding regularized first-order price approximation is small.

Let $P^{\varepsilon,\delta} = P_0^\delta + \sqrt{\varepsilon}P_1^\delta + \varepsilon P_2^\delta + \varepsilon^{\frac{3}{2}}P_3^\delta - R^{\varepsilon,\delta}$

where $R^{\varepsilon,\delta}$ is the error or the residual in the approximation of the regularized problem. Considering the operator $\mathscr{L}^\varepsilon$ from Eq.(2.3.3)

$$\begin{aligned}\mathscr{L}^\varepsilon R^{\varepsilon,\delta} &= \left(\frac{1}{\varepsilon}\mathscr{L}_0 + \frac{1}{\sqrt{\varepsilon}}\mathscr{L}_1 + \mathscr{L}_2\right)(P_0^\delta + \sqrt{\varepsilon}P_1^\delta + \varepsilon P_2^\delta + \varepsilon^{\frac{3}{2}}P_3^\delta - P^{\varepsilon,\delta}) \\ &= \frac{1}{\varepsilon}\mathscr{L}_0P_0^\delta + \frac{1}{\sqrt{\varepsilon}}(\mathscr{L}_1P_0^\delta + \mathscr{L}_0P_1^\delta) + (\mathscr{L}_2P_0^\delta + \mathscr{L}_1P_1^\delta + \mathscr{L}_0P_2^\delta) \\ &+ \sqrt{\varepsilon}(\mathscr{L}_2P_1^\delta + \mathscr{L}_1P_2^\delta + \mathscr{L}_0P_3^\delta) + \varepsilon(\mathscr{L}_2P_2^\delta + \mathscr{L}_1P_3^\delta) + \varepsilon^{\frac{3}{2}}(\mathscr{L}_2P_3^\delta) - \mathscr{L}^\varepsilon P^{\varepsilon,\delta}\end{aligned}$$

Terms of order $\frac{1}{\varepsilon}, \frac{1}{\sqrt{\varepsilon}}, 1$ and $\sqrt{\varepsilon}$ becomes zero as already shown in Section 2.4. Also, $\mathscr{L}^\varepsilon P^{\varepsilon,\delta} = 0$ by Eq.(2.3.2), therefore

$$\mathscr{L}^\varepsilon R^{\varepsilon,\delta} = \varepsilon(\mathscr{L}_2P_2^\delta + \mathscr{L}_1P_3^\delta) + \varepsilon^{\frac{3}{2}}(\mathscr{L}_2P_3^\delta) = M^{\varepsilon,\delta} \tag{2.6.8}$$

As terms of order 1 are zero, therefore, we easily obtain that

$$P_2^\delta = -\frac{\phi_{y,z}}{2}D_2P_0^\delta$$

$\phi_{y,z}$ and D_2 are given by Eqs.(2.4.20) and (2.6.7) respectively. Also, term of order $\sqrt{\varepsilon}$ is zero, thus

$$P_3^\delta = \frac{\nu\rho_{sy}}{\sqrt{2}}\psi_{y,z}D_1D_2P_0^\delta - \frac{\phi_{y,z}}{2}D_2P_1^\delta$$

here $\psi_{y,z}$ is the solution of

$$\mathscr{L}_0\psi_{y,z} = f(y,z)\phi'_{y,z} - E_y[f\phi']$$

therefore

$$\mathscr{L}_2 P_2^\delta = -\frac{1}{4}(f^2(y,z) - \overline{\sigma}^2(z))\phi_{y,z} D_2 D_2 P_0^\delta$$

$$\mathscr{L}_1 P_3^\delta = \nu^2\rho_{sy}^2 f(y,z)\psi'_{y,z} D_1 D_1 D_2 P_0^\delta - \frac{\nu}{\sqrt{2}}\rho_{sy} f(y,z)\phi'_{y,z} D_1 D_2 P_1^\delta$$

and

$$\mathscr{L}_2 P_3^\delta = \frac{1}{2}(f^2(y,z) - \overline{\sigma}^2(z))\left[\frac{\nu}{\sqrt{2}}\rho_{sy}\psi_{y,z} D_2 D_1 D_2 P_0^\delta - \frac{1}{2}\phi_{y,z} D_2 D_2 P_1^\delta\right]$$

Using these in Eq.(2.6.8) and after further simplification we get

$$\begin{aligned} M^{\varepsilon,\delta} = (1+g)\Bigg[\varepsilon\Bigg(&\sum_{i=1}^{4} g_i^{(1)}(y,z)\frac{\partial^i}{\partial s^i}Q_0^\delta + \sum_{i=1}^{6} g_i^{(2)}(y,z)\frac{\partial^i}{\partial s^i}Q_0^\delta \\ &+ (T-t)\sum_{i=1}^{6} g_i^{(3)}(y,z)\frac{\partial^i}{\partial s^i}Q_0^\delta\Bigg) + \varepsilon^{\frac{3}{2}}\Bigg(\sum_{i=1}^{5} g_i^{(4)}(y,z)\frac{\partial^i}{\partial s^i}Q_0^\delta \\ &+ \sum_{i=1}^{7} g_i^{(5)}(y,z)\frac{\partial^i}{\partial s^i}Q_0^\delta + (T-t)\sum_{i=1}^{7} g_i^{(6)}(y,z)\frac{\partial^i}{\partial s^i}Q_0^\delta\Bigg)\Bigg] \end{aligned}$$

Now, at time T

$$\begin{aligned} R^{\varepsilon,\delta}(T) &= \varepsilon P_2^\delta(T,s,y,z) + \sqrt{\varepsilon}P_3^\delta(T,s,y,z) \\ &= H^{\varepsilon,\delta}(s,y,z) \end{aligned}$$

Using the expression of P_2^δ and P_3^δ , the above terminal condition is further simplified to get

$$\begin{aligned} H^{\varepsilon,\delta}(s,y,z) = (1+g)\Bigg[&\varepsilon\Bigg(\sum_{i=1}^{2} h_i^{(1)}(y,z)\frac{\partial^i}{\partial s^i}Q_0^\delta(T,s,z)\Bigg) \\ &+ \varepsilon^{\frac{3}{2}}\Bigg(\sum_{i=1}^{3} h_i^{(2)}(y,z)\frac{\partial^i}{\partial s^i}Q_0^\delta(T,s,z)\Bigg)\Bigg] \end{aligned}$$

The probabilistic representation of $\mathscr{L}^\varepsilon R^{\varepsilon,\delta} = M^{\varepsilon,\delta}$ with the payoff $H^{\varepsilon,\delta}(s,y,z)$ is

$$R^{\varepsilon,\delta} = E^*_{t,s,y,z}\left[e^{-r(T-t)}H^{\varepsilon,\delta}(S_T,Y_T,Z_T) - \int_t^T e^{-r(u-t)}M^{\varepsilon,\delta}(u,S_u,Y_u,Z_u)du\right]$$

Using the expression of $M^{\varepsilon,\delta}$ given above,

$$\left|E^*_{t,s,y,z}\left[\int_t^T e^{-r(u-t)}M^{\varepsilon,\delta}(u,S_u,Y_u,Z_u)du\right]\right| \leq d_2\left[\left(\varepsilon+\frac{\varepsilon}{\delta}\right)\left(1+\sqrt{\frac{\varepsilon}{\delta}}\right)+\varepsilon|\log(\delta)|\right]$$

and

$$\left|E^*_{t,s,y,z}\left[e^{-r(T-t)}H^{\varepsilon,\delta}(S_T,Y_T,Z_T)\right]\right| \leq d_2\left[\varepsilon\left(1+\sqrt{\frac{\varepsilon}{\delta}}\right)\right]$$

for some constant d_2. Therefore, for a fixed $t<T$

$$\begin{aligned}|P^{\varepsilon,\delta}(t,s,y,z)-\hat{P}^{\varepsilon,\delta}(t,s,z)| &= |\varepsilon P_2^\delta+\varepsilon^{\frac{3}{2}}P_3^\delta-R^{\varepsilon,\delta}| \\ &\leq c_3\left[\left(\varepsilon+\frac{\varepsilon}{\delta}\right)\left(1+\sqrt{\frac{\varepsilon}{\delta}}\right)+\varepsilon|\log(\delta)|\right]\end{aligned}$$

where P_2^δ and P_3^δ can also be shown to be bounded for $t<T$. □

Next, Theorem 2.2 is proved using these lemmas.

Taking $\hat{\delta}=\min(\delta_1,\delta_2,\delta_3)$ and $\hat{\varepsilon}=\min(\varepsilon_1,\varepsilon_2,\varepsilon_3)$. For a fixed (t,s,y), and for $0<\delta<\hat{\delta}$ and $0<\varepsilon<\hat{\varepsilon}$

$$\begin{aligned}|P^\varepsilon-\hat{P}^\varepsilon| &\leq |P^\varepsilon-P^{\varepsilon,\delta}|+|P^{\varepsilon,\delta}-\hat{P}^{\varepsilon,\delta}|+|\hat{P}^{\varepsilon,\delta}-\hat{P}^\varepsilon| \\ &\leq 2c_4\delta+c_3\left[\left(\varepsilon+\frac{\varepsilon}{\delta}\right)\left(1+\sqrt{\frac{\varepsilon}{\delta}}\right)+\varepsilon|\log(\delta)|\right] \qquad (2.6.9)\end{aligned}$$

where $c_4=\max(c_1,c_2)$.

On taking $\delta=\varepsilon^{\frac{1}{2}}$,

$$|P^\varepsilon-\hat{P}^\varepsilon| \leq c\left[\left(\varepsilon+\varepsilon^{\frac{1}{2}}\right)\left(1+\varepsilon^{\frac{1}{4}}\right)+\varepsilon|\log(\varepsilon)|\right] \qquad (2.6.10)$$

This proves the required accuracy of the approximate option pricing formula.

2.7 Calibration of the Implied Volatility

From the approximate option pricing formula (2.5.2), the only parameter which is to be estimated is V. Its value is obtained employing the calibration of the European smiles.

Assume the asymptotic expansion for the market implied volatility function I as

$$I=I_0+\sqrt{\varepsilon}I_1+\varepsilon I_2+\ldots \qquad (2.7.1)$$

For convenience, I is attained by equating the modified Black-Scholes price with our market price P^{ε}. i.e.

$$P_0(t,x,I) = P^{\varepsilon}(t,x,z,\overline{\sigma}(z))$$

here

$$P_0(t,x,I) = (1+g)Q_0(t,x,I)$$

where Q_0 is the classical Black-Scholes price.

Considering the Taylor series expansion of $P_0(t,x,I)$ about I_0 and the asymptotic expansion of P^{ε} to get

$$P_0(I_0) + \frac{\partial P_0(I_0)}{\partial \sigma}\sqrt{\varepsilon}I_1 + ... = P_0(\overline{\sigma}(z)) + \sqrt{\varepsilon}P_1(\overline{\sigma}(z)) + ... \tag{2.7.2}$$

Comparing the coefficients of ε^0 on both sides, we get

$$P_0(I_0) = P_0(\overline{\sigma}(z))$$

this gives

$$I_0 = \overline{\sigma}(z) \tag{2.7.3}$$

where $\overline{\sigma}(z)$ depends upon the slow volatility factor z.

Also, on using the relation $x^2\frac{\partial^2 P_0}{\partial x^2} = \frac{1}{\overline{\sigma}(T-t)}\frac{\partial P_0}{\partial \sigma}$, terms of order $\sqrt{\varepsilon}$ gives

$$\begin{aligned}\frac{\partial P_0(I_0)}{\partial \sigma}I_1 &= P_1(\overline{\sigma}(z)) \\ &= \frac{2}{(T-t)\overline{\sigma}}\left[\frac{1}{k}\log\left|\frac{kT-2}{kt-2}\right| + \frac{T-t}{(kT-2)(kt-2)}\right]VD_1\frac{\partial P_0(I_0)}{\partial \sigma}\end{aligned} \tag{2.7.4}$$

As $P_0 = (1+g)Q_0$, therefore the above equation will be reduced to

$$\frac{\partial Q_0(I_0)}{\partial \sigma}I_1 = \frac{2}{(T-t)\overline{\sigma}}\left[\frac{1}{k}\log\left|\frac{kT-2}{kt-2}\right| + \frac{T-t}{(kT-2)(kt-2)}\right]VD_1\frac{\partial Q_0(I_0)}{\partial \sigma} \tag{2.7.5}$$

For the Black-Scholes price Q_0, the direct computation gives

$$D_1\frac{\partial Q_0}{\partial \sigma} = \big(1 - \frac{d_1}{\overline{\sigma}\sqrt{T-t}}\big)\frac{\partial Q_0}{\partial \sigma}$$

and

$$d_1 = \frac{\log(\frac{x}{K}) + (r + \frac{\overline{\sigma}^2}{2})(T-t)}{\overline{\sigma}\sqrt{T-t}}$$

so that

$$1-\frac{d_1}{\overline{\sigma}\sqrt{T-t}}=\frac{\log(\frac{K}{x})-(r-\frac{\overline{\sigma}^2}{2})(T-t)}{\overline{\sigma}^2(T-t)}$$

therefore, Eq.(2.7.5) gives

$$I_1=\frac{2}{(T-t)}\left[\frac{1}{k}\log\left|\frac{kT-2}{kt-2}\right|+\frac{T-t}{(kT-2)(kt-2)}\right]\frac{V}{\overline{\sigma}^3}\left[\frac{\log(\frac{K}{x})}{(T-t)}-\left(r-\frac{\overline{\sigma}^2}{2}\right)\right] \tag{2.7.6}$$

It can be written in the linear form as

$$I_1=p\left[\frac{\log(\frac{K}{x})}{(T-t)}\right]+q$$

more precisely

$$\sqrt{\varepsilon}I_1=I_1^{\varepsilon}=p^{\varepsilon}\left[\frac{\log(\frac{K}{x})}{(T-t)}\right]+q^{\varepsilon} \tag{2.7.7}$$

where

$$p^{\varepsilon}=\frac{2}{(T-t)}\left[\frac{1}{k}\log\left|\frac{kT-2}{kt-2}\right|+\frac{T-t}{(kT-2)(kt-2)}\right]\frac{\sqrt{\varepsilon}V}{\overline{\sigma}^3} \tag{2.7.8}$$

and

$$\begin{aligned}q^{\varepsilon}&=-\frac{2}{(T-t)}\left[\frac{1}{k}\log\left|\frac{kT-2}{kt-2}\right|+\frac{T-t}{(kT-2)(kt-2)}\right]\frac{\sqrt{\varepsilon}V}{\overline{\sigma}^3}\left(r-\frac{\overline{\sigma}^2}{2}\right)\\&=-p^{\varepsilon}\left(r-\frac{\overline{\sigma}^2}{2}\right)\end{aligned} \tag{2.7.9}$$

So the approximated value of the implied volatility I is given as

$$I\approx I_0+I_1^{\varepsilon}=p^{\varepsilon}\left[\frac{\log(\frac{K}{x})}{(T-t)}\right]+q^{\varepsilon}+\overline{\sigma}(z) \tag{2.7.10}$$

which is a function of "log moneyness to maturity ratio (LMMR)". V^{ε} can be written in terms of p^{ε} as

$$V^{\varepsilon}=\frac{p^{\varepsilon}\overline{\sigma}^3}{\frac{2}{(T-t)}[\frac{1}{k}\log|\frac{kT-2}{kt-2}|+\frac{T-t}{(kT-2)(kt-2)}]}. \tag{2.7.11}$$

p^{ε} and q^{ε} are estimated by calibrating the implied volatility surface and using the linear relation of I with LMMR given in Eq.(2.7.10).

The implied volatility data of S&P 500 index on January 4, 2016 for the options with maturities lying between 18 days to 158 days (both the days inclusive) and

moneyness ranging from 80% to 120% has been considered for the estimation of the values of p^{ε} and q^{ε}, refer to Fig.2.2.

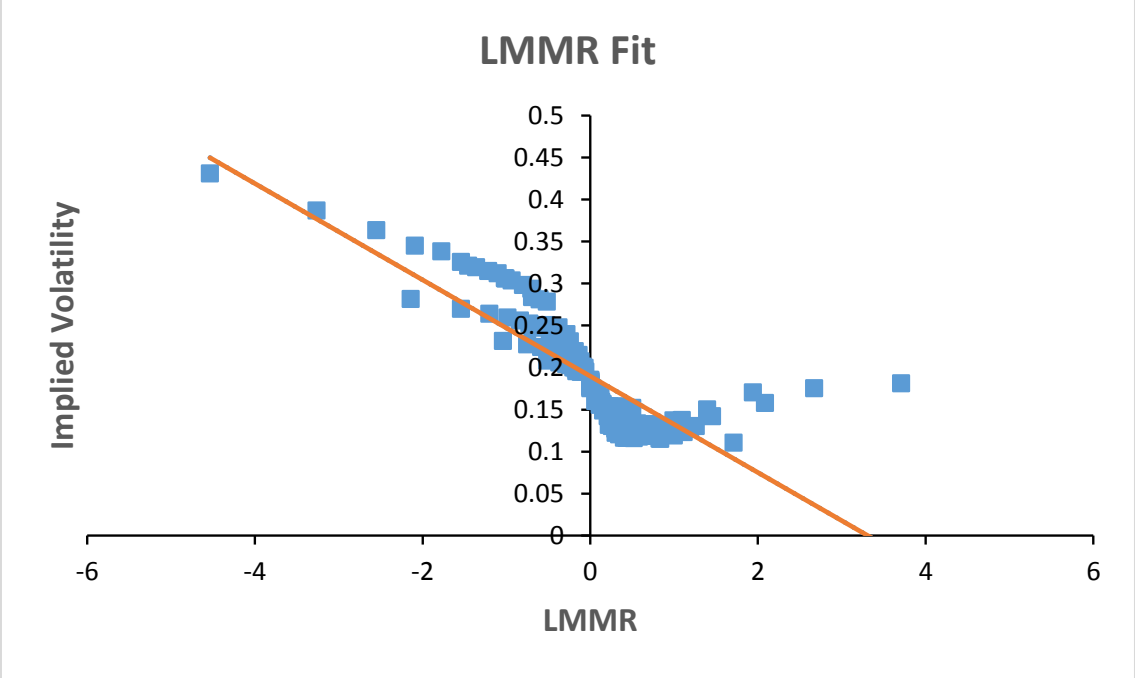

Figure 2.2: S&P 500 index implied volatilities as a function of LMMR.

The line $p^{\varepsilon}(\text{LMMR}) + q^{\varepsilon} + \overline{\sigma}$ gives the estimated value of parameters p^{ε} and $q^{\varepsilon} + \overline{\sigma}$. So with the linear regression, it is found that $p^{\varepsilon} = -0.0573$ and $q^{\varepsilon} + \overline{\sigma} = 0.1897$. Consequently, $V^{\varepsilon} = 0.0008$.

Now, as V^{ε} is obtained, inputting it with all the other parameters in Eq.(2.5.2), the approximate option price of the European option is obtained.

For instance, setting the parameters

$$x = 100, K = 80, T - t = 1, r = 0.0264, \overline{\sigma} = 0.1892, k = 1$$

we get, $(1+g) = 1.0561$ and the approximated option price as 24.2647. Its relative error with the Black-Scholes price is found to be 0.0633.

The computational cost of these formulae is explained in terms of run-time efficiency. The multifactor stochastic volatility models though represent a realistic scenario of the actual market, yet face the difficulty of implementation and execution because of a large number of parameters involved as compared to the corresponding single-factor models. In the proposed model, as the slow factor of volatility is approximated, so the pricing formula gets simplified in a

multifactor scenario, reducing the unknown number of parameters to one. This parameter is estimated from the implied volatility surface. $MATLAB2012b$ is used to obtain the desired results. The computation time with this model is of the order 10^{-4} seconds, which is quite fast. So the computational complexity is almost negligible and hence the computational cost. This makes the proposed model and the derived option pricing formula computationally more efficient.

2.8 Conclusion

Using the quadratic approximation of the slow factor of volatility in a multifactor stochastic volatility model, a first order approximated price of the European option is obtained which is perturbed around a modified Black-Scholes price. The accuracy of the approximate option pricing formula is established, and the computational cost of using this formula is also discussed. With this approximation, the calculations get simplified and the results obtained are easy to implement in a multifactor stochastic volatility scenario. The consideration of the slow factor of volatility as only time-dependent, has produced a result which is significant to the literature since it provides a different and simplified setup for the multifactor stochastic volatility models. This multifactor model is extended to price the geometric Asian options in the next chapter.

Chapter 3

Pricing of the Geometric Asian Options

In this chapter[1]*, the pricing formulae for the continuous geometric Asian options (GAOs) are obtained using the multifactor stochastic volatility model framework proposed in the previous chapter. The asymptotic expansion of the price function is considered and the first order price approximation is derived using the perturbation techniques for both floating and fixed strike GAOs. The zeroth order term in the price approximation is the modified Black-Scholes price for the GAOs. This modified price is expressed in respect of the Black-Scholes price for the Asian options. The accuracy of the approximate option pricing formulae is also established.*

---

[1]The work reported in this chapter has been communicated under the title **"Pricing of the Geometric Asian Options Under a Multifactor Stochastic Volatility Model".** Some of this work is presented in UGC sponsored 'NSRDMS-2017' held at MDU Rohtak from March $07-08, 2017$ and in 'FIM & ISME 2017' held at Kitakyushu International Conference Center, Kitakyushu, Japan from August $25-28, 2017$.

3.1 Introduction

In the previous chapter, the quadratic approximation of the slow volatility factor was proposed which gave a much simplified multifactor stochastic volatility model. The approximate pricing formula for the European option (path-independent) was derived using this multifactor stochastic volatility model. In the present chapter, we extend that model to obtain the approximate pricing formulae for the Asian options with European type expiration which are more complicated in comparison to the path-independent European options.

As explained in Section 1.4 of Chapter 1, Asian options are the path-dependent options such that their payoff depends upon the average of the underlying asset price over the option period. The averaging of the underlying asset price in Asian options is usually arithmetic or geometric. The Black-Scholes formulae for the pricing of fixed and floating strike GAOs are given in Eqs.(1.4.3) to (1.4.8). GAOs have also been used to approximate the arithmetic Asian option prices (for instance, see Turnbull and Wakeman [116]). In general, the trading of the Asian options is in a discrete way but to consider the continuous sampling, it can be approximated through the daily sampling [126]. Here the continuously sampled GAOs are considered.

We have already elucidated in Chapters 1 and 2 that the constant volatility assumption of the Black-Scholes framework does not hold good in the actual market scenario. This consequently provided a path for the development of the dynamic volatility modeling which has been progressed in a logical way addressing the shortcomings of the previous models. For the GAOs, the pricing formulae has also been obtained in the framework of stochastic volatility models (refer to Kim and Wee [72] and Wong and Cheung [120]). The literature on the arithmetic and geometric Asian option pricing is given in Section 1.4 of Chapter 1.

For the pricing of the GAOs, Wong and Cheung [120] considered a stochastic volatility model with only fast mean-reverting factor of volatility, and using asymptotic expansions they derived the approximate pricing formulae for the continuous GAOs. We here intend to consider the pricing of GAOs in a multifactor stochastic volatility framework by approximating the slow factor of volatility using a quadratic (parabolic) arc. The pricing formulae for the floating and fixed strike continuous GAOs are derived using this model. The accuracy of these formulae

is also established.

This chapter is organized as follows: The multifactor stochastic volatility model to be considered for pricing has been discussed in Section 3.2. Pricing equation and the asymptotic expansion of continuous GAOs have been derived in Sections 3.3 and 3.4 respectively. In Section 3.5, the first order approximated option pricing formulae have been given. Accuracy of the approximated formulae has been discussed in Section 3.6. The model parameter has been estimated from the market by capturing the European and the Asian volatility smiles together in Section 3.7. The conclusion has been given in Section 3.8.

3.2 Model Specification

The approximated price of the floating and fixed strike GAOs is obtained by extending the multifactor stochastic volatility model proposed in the previous chapter. The Asian options are the path-dependent options such that the geometric average of the underlying asset prices over the option period is required additionally for the pricing under the GAO setup.

Let the price of an asset (non-dividend paying) at time t be X_t. The geometric average of these prices, considered in the interval $[0,t]$, is denoted by $G_{[0,t]}$ and is expressed as a stochastic process, given below.

$$G_{[0,t]} = exp\left(\frac{1}{t}\int_0^t S_\tau d\tau\right) \tag{3.2.1}$$

where $S_t = \ln X_t$.

Let P^* be the risk-neutral probability measure. Under P^* the dynamics of asset price X_t is

$$dX_t = rX_t dt + f(Y_t, Z_t)X_t dW_t^x \tag{3.2.2}$$

where Y_t and Z_t are respectively the fast and the slow mean-reverting factors of stochastic volatility $f(Y_t, Z_t)$ with their dynamics given by

$$dY_t = \frac{1}{\varepsilon}(m - Y_t)dt + \frac{\nu\sqrt{2}}{\sqrt{\varepsilon}}dW_t^y \tag{3.2.3}$$

and

$$Z_t = \mathscr{A}t^2 + \mathscr{B}t + \mathscr{C} + \alpha_t \tag{3.2.4}$$

here

$$\mathscr{A} = \frac{(Z_0 - m')}{2} k^2$$
$$\mathscr{B} = -(Z_0 - m')k$$
$$\mathscr{C} = Z_0 \tag{3.2.5}$$

which is obtained by considering the following OU diffusion for the slow volatility factor Z_t

$$dZ_t = k(m' - Z_t)dt + \eta dW_t^z \tag{3.2.6}$$

The standard Brownian motions W_t^x, W_t^y and W_t^z have the correlation structure:

$$E[dW_t^x . dW_t^y] = \rho_{xy} dt$$

$$E[dW_t^x . dW_t^z] = \rho_{xz} dt$$

$$E[dW_t^y . dW_t^z] = \rho_{yz} dt$$

where ρ_{xy}, ρ_{xz} and ρ_{yz} are such that $\rho_{xy}^2 < 1, \rho_{xz}^2 < 1, \rho_{yz}^2 < 1$ and $1 + 2\rho_{xy}\rho_{xz}\rho_{yz} - \rho_{xy}^2 - \rho_{xz}^2 - \rho_{yz}^2 > 0$ for the positive definiteness of the covariance matrix of the three Brownian motions.

So the above system of equations from Eq.(3.2.1) to Eq.(3.2.4) specify the multifactor stochastic volatility model to be considered for the pricing of GAOs. Here an additional source of randomness is present to represent the geometric averaging of the underlying asset price, thus this model extends the model introduced in the previous chapter. The pricing equation is given in the next section.

3.3 PDE for the Pricing of Geometric Asian Options

Let $C^\varepsilon(t,x,y,z,G)$ be the price of a continuous GAO call with payoff $h(X_T, G_{[0,T]})$ (Notation C_{fl}^ε and C_{fix}^ε is used for floating and fixed strike GAOs respectively). Using the Feynmann-Kac formula given in Eq.(1.3.27) of Chapter 1, the PDE

for the price comes out to be

$$\left(\frac{\partial}{\partial t}+\frac{1}{2}f^2(y,z)x^2\frac{\partial^2}{\partial x^2}+r(x\frac{\partial}{\partial x}-.)+\rho_{xz}\eta f(y,z)x\frac{\partial^2}{\partial x\partial z}+\frac{1}{2}\eta^2\frac{\partial^2}{\partial z^2}\right.$$
$$+k(m^{'}-z)\frac{\partial}{\partial z}+\frac{G}{t}\ln(\frac{x}{G})\frac{\partial}{\partial G}+\frac{1}{\varepsilon}[(m-y)\frac{\partial}{\partial y}+\nu^2\frac{\partial^2}{\partial y^2}]$$
$$\left.+\frac{1}{\sqrt{\varepsilon}}[\rho_{xy}\nu\sqrt{2}f(y,z)x\frac{\partial^2}{\partial x\partial y}+\rho_{yz}\nu\sqrt{2}\eta\frac{\partial^2}{\partial y\partial z}]\right)C^{\varepsilon}=0 \tag{3.3.1}$$

with the boundary conditions

$$C^{\varepsilon}_{fl}(T,X_T,Y_T,Z_T,G_{[0,T]})=h(X_T,G_{[0,T]}),$$
$$C^{\varepsilon}_{fix}(T,X_T,Y_T,Z_T,G_{[0,T]},K)=h(K,G_{[0,T]}) \tag{3.3.2}$$

for the floating and fixed strike GAOs respectively. K is the strike price. Using the transformation $s=\ln x$ and $u=t\ln\frac{G}{x}$ in Eq.(3.3.1) and after solving, we get

$$\left[\frac{\partial}{\partial t}+\frac{1}{2}f^2(y,z)\left(\frac{\partial}{\partial s}-t\frac{\partial}{\partial u}\right)^2+\left(r-\frac{1}{2}f^2(y,z)\right)\left(\frac{\partial}{\partial s}-t\frac{\partial}{\partial u}\right)-r\right.$$
$$+\rho_{sz}\eta f(y,z)\left(\frac{\partial}{\partial s}-t\frac{\partial}{\partial u}\right)\frac{\partial}{\partial z}+\frac{1}{2}\eta^2\frac{\partial^2}{\partial z^2}+k(m^{'}-z)\frac{\partial}{\partial z}+\frac{1}{\varepsilon}[(m-y)\frac{\partial}{\partial y}+\nu^2\frac{\partial^2}{\partial y^2}]$$
$$\left.+\frac{1}{\sqrt{\varepsilon}}[\rho_{sy}\nu\sqrt{2}f(y,z)\left(\frac{\partial}{\partial s}-t\frac{\partial}{\partial u}\right)\frac{\partial}{\partial y}+\rho_{yz}\nu\sqrt{2}\eta\frac{\partial^2}{\partial y\partial z}]\right]C^{\varepsilon}(t,s,y,z,u)=0$$

It can be written as

$$\mathscr{L}^{\varepsilon}_a C^{\varepsilon}(t,s,y,z,u)=0 \tag{3.3.3}$$

where subscript 'a' specifies the Asian options with

$$\mathscr{L}^{\varepsilon}_a=\frac{1}{\varepsilon}\mathscr{L}^a_0+\frac{1}{\sqrt{\varepsilon}}\mathscr{L}^a_1+\mathscr{L}^a_2$$

This operator is different from the operator $\mathscr{L}^{\varepsilon}$ given in Eq.(2.3.3) for the European options such that

$$\mathscr{L}^a_0=(m-y)\frac{\partial}{\partial y}+\nu^2\frac{\partial^2}{\partial y^2} \tag{3.3.4}$$

$$\mathscr{L}^a_1=\nu\sqrt{2}\left[\rho_{sy}f(y,z)\left(\frac{\partial}{\partial s}-t\frac{\partial}{\partial u}\right)\frac{\partial}{\partial y}+\rho_{yz}\eta\frac{\partial^2}{\partial y\partial z}\right] \tag{3.3.5}$$

and

$$\mathscr{L}_2^a = \frac{\partial}{\partial t} + \frac{1}{2}f^2(y,z)\left(\frac{\partial}{\partial s} - t\frac{\partial}{\partial u}\right)^2 + \left(r - \frac{1}{2}f^2(y,z)\right)\left(\frac{\partial}{\partial s} - t\frac{\partial}{\partial u}\right) - r$$
$$+\rho_{sz}\eta f(y,z)\left(\frac{\partial}{\partial s} - t\frac{\partial}{\partial u}\right)\frac{\partial}{\partial z} + \frac{1}{2}\eta^2\frac{\partial^2}{\partial z^2} + k(m' - z)\frac{\partial}{\partial z} \tag{3.3.6}$$

Since the slow factor of volatility Z_t is approximated by a quadratic arc given in Eq.(3.2.4), therefore, as specified in Eqs.(2.2.7) and (2.2.8)

$$\frac{\partial}{\partial z} = \left(\frac{1}{2\mathscr{A}t + \mathscr{B} + \zeta_t}\right)\frac{\partial}{\partial t}$$

and

$$\frac{\partial^2}{\partial z^2} = \frac{1}{(2\mathscr{A}t + \mathscr{B} + \zeta_t)^2}\left[\frac{\partial^2}{\partial t^2} - \left(\frac{2\mathscr{A} + \zeta_t'}{2\mathscr{A}t + \mathscr{B} + \zeta_t}\right)\frac{\partial}{\partial t}\right]$$

where

$$\zeta_t = \frac{\partial \alpha_t}{\partial t}$$

On substituting for $\frac{\partial}{\partial z}$ and $\frac{\partial^2}{\partial z^2}$ in Eqs.(3.3.5) and (3.3.6), we get

$$\mathscr{L}_1^a = \nu\sqrt{2}\left[\rho_{sy}f(y,z)\left(\frac{\partial}{\partial s} - t\frac{\partial}{\partial u}\right)\frac{\partial}{\partial y} + \frac{\rho_{yz}}{2\mathscr{A}t + \mathscr{B} + \zeta_t}\eta\frac{\partial^2}{\partial y \partial t}\right] \tag{3.3.7}$$

and

$$\mathscr{L}_2^a = \left(1 + \frac{k(m' - z)}{2\mathscr{A}t + \mathscr{B} + \zeta_t} - \frac{1}{2}\eta^2\frac{2\mathscr{A} + \zeta_t'}{(2\mathscr{A}t + \mathscr{B} + \zeta_t)^3}\right)\frac{\partial}{\partial t} + \frac{1}{2}f^2(y,z)\left(\frac{\partial}{\partial s} - t\frac{\partial}{\partial u}\right)^2$$
$$+\left(r - \frac{1}{2}f^2(y,z)\right)\left(\frac{\partial}{\partial s} - t\frac{\partial}{\partial u}\right) - r + \frac{\rho_{sz}\eta f(y,z)}{2\mathscr{A}t + \mathscr{B} + \zeta_t}\left(\frac{\partial}{\partial s} - t\frac{\partial}{\partial u}\right)\frac{\partial}{\partial t}$$
$$+\frac{1}{2}\eta^2\frac{1}{(2\mathscr{A}t + \mathscr{B} + \zeta_t)^2}\frac{\partial^2}{\partial t^2} \tag{3.3.8}$$

So the required pricing equation is (3.3.3) where $\mathscr{L}_0^a, \mathscr{L}_1^a$ and $\mathscr{L}_2^a$ are given by Eqs.(3.3.4), (3.3.7) and (3.3.8) respectively.

3.4 Asymptotic Price Approximation

We consider the asymptotic expansion of the Asian call option price C^ε in the powers of $\sqrt{\varepsilon}$ as

$$C^\varepsilon = C_0 + \sqrt{\varepsilon}C_1 + \varepsilon C_2 + \ldots \tag{3.4.1}$$

(for i = 0,1,2,..., the notation C_i^{fl} and C_i^{fix} is used for the floating and fixed strike continuous GAOs respectively). Putting this in the pricing equation (3.3.3) to get

$$\mathscr{L}_a^{\varepsilon}(C_0+\sqrt{\varepsilon}C_1+\varepsilon C_2+...)=0$$

this gives

$$(\frac{1}{\varepsilon}\mathscr{L}_0^a+\frac{1}{\sqrt{\varepsilon}}\mathscr{L}_1^a+\mathscr{L}_2^a)(C_0+\sqrt{\varepsilon}C_1+\varepsilon C_2+...)=0 \tag{3.4.2}$$

Equating the terms of various orders equal to zero to get

Terms of order $\frac{1}{\varepsilon}$:

$$\mathscr{L}_0^a C_0=0 \tag{3.4.3}$$

Terms of order $\frac{1}{\sqrt{\varepsilon}}$:

$$\mathscr{L}_0^a C_1+\mathscr{L}_1^a C_0=0 \tag{3.4.4}$$

Terms of order 1:

$$\mathscr{L}_0^a C_2+\mathscr{L}_1^a C_1+\mathscr{L}_2^a C_0=0 \tag{3.4.5}$$

Terms of order $\sqrt{\varepsilon}$:

$$\mathscr{L}_0^a C_3+\mathscr{L}_1^a C_2+\mathscr{L}_2^a C_1=0 \tag{3.4.6}$$

and so on. Eq.(3.4.3), using the expression of $\mathscr{L}_0^a$ given in Eq.(3.3.4), implies that the zeroth order term C_0 is independent of the fast volatility factor y but depends on z, the slow factor of volatility. Thus,

$$C_0=C_0(t,s,z,u) \tag{3.4.7}$$

In Eq.(3.4.4), $\mathscr{L}_1^a C_0=0$ because C_0 is independent of y. Therefore, we get that

$$\mathscr{L}_0^a C_1=0$$

which gives that the first order term C_1 in the price approximation is independent of y but depends on z. That is,

$$C_1=C_1(t,s,z,u) \tag{3.4.8}$$

For the first order price approximation, the expressions of C_0 and C_1 are required. Firstly, the expression of C_0 is obtained.

Since C_1 is independent of y, hence $\mathscr{L}_1^a C_1 = 0$ and Eq.(3.4.5) reduces to

$$\mathscr{L}_0^a C_2 + \mathscr{L}_2^a C_0 = 0 \tag{3.4.9}$$

As discussed in previous chapter, it is a "Poisson equation" in C_2 with respect to y and admits a solution only if the centering condition holds:

$$E_y[\mathscr{L}_2^a C_0] = 0$$

now, as C_0 is independent of y, this gives that

$$E_y[\mathscr{L}_2^a] C_0 = 0 \tag{3.4.10}$$

here $E_y[\mathscr{L}_2^a]$ is the average of operator $\mathscr{L}_2^a$ considering the invariant distribution of y. The expression of $\mathscr{L}_2^a$ in Eq.(3.3.8) is bit complicated. Therefore, for simplification, we neglect the error term in the approximation of the slow volatility factor assuming negligible truncation error and η almost zero as considered in Section 2.4 of the previous chapter. So Eq.(3.3.8) is reduced to the simplified form:

$$\mathscr{L}_2^a = \left(1 + \tfrac{1-kt+\frac{k^2t^2}{2}}{1-kt}\right)\tfrac{\partial}{\partial t} + \tfrac{1}{2}f^2(y,z)\left(\tfrac{\partial}{\partial s} - t\tfrac{\partial}{\partial u}\right)^2 + \left(r - \tfrac{1}{2}f^2(y,z)\right)\left(\tfrac{\partial}{\partial s} - t\tfrac{\partial}{\partial u}\right) - r$$

As defined in the previous chapter,

$$\frac{1-kt+\frac{k^2t^2}{2}}{1-kt} = \gamma \tag{3.4.11}$$

with $kt \neq 1$ and $\gamma \neq 0$. This gives

$$\mathscr{L}_2^a = (1+\gamma)\frac{\partial}{\partial t} + \frac{1}{2}f^2(y,z)\left(\frac{\partial}{\partial s} - t\frac{\partial}{\partial u}\right)^2 + \left(r - \frac{1}{2}f^2(y,z)\right)\left(\frac{\partial}{\partial s} - t\frac{\partial}{\partial u}\right) - r \tag{3.4.12}$$

It is worth noticing that

$$\mathscr{L}_2^a = \mathscr{L}_{BSA} + \gamma\frac{\partial}{\partial t}$$

where $\mathscr{L}_{BSA}$ is the "Black-Scholes operator for the Asian options". $\mathscr{L}_2^a$ is named as a $\gamma-$modified Black-Scholes operator for the GAOs. Thus,

$$E_y[\mathscr{L}_2^a] = (1+\gamma)\frac{\partial}{\partial t} + \frac{1}{2}\overline{\sigma}^2(z)\left(\frac{\partial}{\partial s} - t\frac{\partial}{\partial u}\right)^2 + \left(r - \frac{1}{2}\overline{\sigma}^2(z)\right)\left(\frac{\partial}{\partial s} - t\frac{\partial}{\partial u}\right) - r \tag{3.4.13}$$

is the $\gamma-$modified Black-Scholes operator for the GAOs with the effective volatility $\overline{\sigma}(z)$. The solution of Eq.(3.4.10) gives the zeroth order term C_0 of the price approximation and is named as the modified Black-Scholes price for the Asian options.

We proceed on the lines of method given in the Eqs.(2.4.10) to (2.4.14) of the previous chapter to obtain the expression of the modified Black-Scholes price C_0 for the geometric Asian call options in terms of the Black-Scholes price B_0 for the GAO call.

Let for the floating strike options

$$C_0^{fl}(t,s,z,u) = \beta^{fl}(t)B_0^{fl}(t,s,\overline{\sigma}(z),u)$$

and for the fixed strike options

$$C_0^{fix}(t,s,z,u) = \beta^{fix}(t)B_0^{fix}(t,s,\overline{\sigma}(z),u)$$

It can be expressed (collectively for floating and fixed strike GAOs) as

$$C_0^{fl,fix}(t,s,z,u) = \beta^{fl,fix}(t)B_0^{fl,fix}(t,s,\overline{\sigma}(z),u)$$

or simply

$$C_0(t,s,z,u) = \beta(t)B_0(t,s,\overline{\sigma}(z),u) \tag{3.4.14}$$

where after simplification

$$\beta(t) = \left[\left(\frac{2-kT}{2-kt}\right)^{\frac{2}{k}} e^{(T-t)\frac{(2-kt)(2-kT)+2}{(2-kt)(2-KT)}}\right]^M \tag{3.4.15}$$

with $kt \neq 2$ for $0 < t \leq T$ and

$$M = \left(\frac{1}{B_0}\right)\frac{\partial B_0}{\partial t} \tag{3.4.16}$$

here $\frac{\partial B_0}{\partial t}$ is the Black-Scholes theta for the GAOs. It has the different expressions for floating and fixed strike GAOs. $\beta(t) = 1$ at maturity to satisfy the boundary condition

$$C_0^{fl}(T,S_T,Z_T,U_T) = h(S_T,U_T)$$

or

$$C_0^{fix}(T,S_T,Z_T,U_T,K) = h(K,S_T,U_T)$$

After obtaining the expression for C_0 we intend to find C_1. For this, consider Eq.(3.4.6), which is a "Poisson equation" in C_3 with respect to y and admits a solution only if the following centering condition holds

$$E_y[\mathscr{L}_2^a C_1 + \mathscr{L}_1^a C_2] = 0$$

this implies that

$$E_y[\mathscr{L}_2^a]C_1 + E_y[\mathscr{L}_1^a C_2] = 0 \tag{3.4.17}$$

From Eq.(3.4.9), $\mathscr{L}_0^a C_2 = -\mathscr{L}_2^a C_0$. It can be expressed as

$$\mathscr{L}_0^a C_2 = -(\mathscr{L}_2^a C_0 - E_y[\mathscr{L}_2^a]C_0)$$

thus

$$C_2 = -(\mathscr{L}_0^a)^{-1}(\mathscr{L}_2^a - E_y[\mathscr{L}_2^a])C_0$$

Putting it in Eq.(3.4.17) and after solving on the lines of Eqs.(2.4.19) to (2.4.21) of previous chapter, we get that

$$E_y[\mathscr{L}_2^a]C_1 = \mathscr{G}_a C_0$$

where

$$\mathscr{G}_a = V\left[\left(\frac{\partial}{\partial s} - t\frac{\partial}{\partial u}\right)^3 - \left(\frac{\partial}{\partial s} - t\frac{\partial}{\partial u}\right)^2\right] \tag{3.4.18}$$

and

$$V = \frac{\rho_{sy}\nu}{\sqrt{2}} E_y\left[f(y,z)\frac{\partial \phi(y,z)}{\partial y}\right] \tag{3.4.19}$$

$\phi(y,z)$ is the solution of

$$\mathscr{L}_0^a \phi(y,z) = f^2(y,z) - \overline{\sigma}^2(z) \tag{3.4.20}$$

Now, for the floating strike GAO call, the differentials of the zeroth order term C_0^{fl} satisfies

$$\frac{\partial^{i+j} C_0^{fl}}{\partial u^i \partial s^j} = \frac{\partial^i C_0^{fl}}{\partial u^i} \tag{3.4.21}$$

where $i, j = 0, 1, 2, \ldots$. This is obtained using the Black-Scholes formula for the floating strike geometric Asian call options given in Section 1.4 of Chapter 1.

For the floating strike GAO call, Eq.(3.4.14) is

$$C_0^{fl} = \beta^{fl}(t) B_0^{fl}$$

which gives

$$C_0^{fl} = \beta^{fl}(t) e^s \left[N(d_1) - e^{\frac{u}{T} - Q} N(d_2) \right] \tag{3.4.22}$$

where

$$d_1 = \frac{-u + (r + \frac{\overline{\sigma}^2}{2}) \frac{T^2 - t^2}{2}}{\overline{\sigma} \sqrt{\frac{T^3 - t^3}{3}}},$$

$$d_2 = d_1 - \frac{\overline{\sigma}}{T} \sqrt{\frac{T^3 - t^3}{3}}$$

and

$$Q = (r + \frac{\overline{\sigma}^2}{2}) \frac{T^2 - t^2}{2T} - \frac{\overline{\sigma}^2}{6T^2} (T^3 - t^3) \tag{3.4.23}$$

with payoff function

$$h(S_T, U_T) = e^{S_T} max(1 - e^{\frac{U_T}{T}}, 0) \tag{3.4.24}$$

$\beta^{fl}(t)$ is given in Eq.(3.4.15). It is clear from Eq.(3.4.22) that $\frac{\partial C_0^{fl}}{\partial s} = C_0^{fl}$ thus $\frac{\partial^j C_0^{fl}}{\partial s^j} = C_0^{fl}$ for every $j = 0, 1, 2, \ldots$. This results in Eq.(3.4.21). Therefore for the floating strike GAO, Eq.(3.4.18) is reduced to

$$\mathscr{G}_a^{fl} = -V \left[t \frac{\partial}{\partial u} - 2t^2 \frac{\partial^2}{\partial u^2} + t^3 \frac{\partial^3}{\partial u^3} \right]$$

Similarly for the fixed strike GAO, Eq.(3.4.14) becomes

$$C_0^{fix} = \beta^{fix}(t) B_0^{fix}$$

Using the Black-Scholes formula for the pricing of fixed strike GAO call, given in Section 1.4 of Chapter 1,

$$C_0^{fix} = \beta^{fix}(t) \left[e^{s + \frac{u}{T} - Q} N(\hat{d}_1) - K e^{-r(T-t)} N(\hat{d}_2) \right] \tag{3.4.25}$$

where, $\beta^{fix}(t)$ is given in Eq.(3.4.15) and Q is given in Eq.(3.4.23). Also,

$$\hat{d}_2 = \frac{\frac{u}{T} + s - \ln K + (r - \frac{\overline{\sigma}^2}{2}) \frac{(T-t)^2}{2T}}{\frac{\overline{\sigma}}{T} \sqrt{\frac{(T-t)^3}{3}}}$$

and

$$\hat{d_1} = \hat{d_2} + \frac{\overline{\sigma}}{T}\sqrt{\frac{(T-t)^3}{3}} \tag{3.4.26}$$

with the payoff function

$$h(S_T, U_T) = max(e^{S_T + \frac{U_T}{T}} - K, 0) \tag{3.4.27}$$

For the fixed strike GAOs

$$\frac{\partial C_0^{fix}}{\partial s} = \frac{\partial}{\partial s}(\beta^{fix}(t) B_0^{fix}) = \beta^{fix}(t)\frac{\partial B_0^{fix}}{\partial s} + B_0^{fix}\frac{\partial \beta^{fix}(t)}{\partial s}$$

$$= T\left(\beta^{fix}(t)\frac{\partial B_0^{fix}}{\partial u} + B_0^{fix}\frac{\partial \beta^{fix}(t)}{\partial u}\right) = T\frac{\partial C_0^{fix}}{\partial u}$$

thus $\frac{\partial^j C_0^{fix}}{\partial s^j} = T^j \frac{\partial^j C_0^{fix}}{\partial u^j}$. This results in

$$\frac{\partial^{i+j} C_0^{fix}}{\partial u^i \partial s^j} = T^j \frac{\partial^{i+j} C_0^{fix}}{\partial u^{i+j}} \tag{3.4.28}$$

where $i, j = 0, 1, 2, \ldots$. The corresponding $\mathscr{G}_a^{fix}$ will be

$$\mathscr{G}_a^{fix} = V\left[(T-t)^3\frac{\partial^3}{\partial u^3} - (T-t)^2\frac{\partial^2}{\partial u^2}\right]$$

Having the expressions of $\mathscr{G}_a^{fl}$ and $\mathscr{G}_a^{fix}$, C_1 is obtained for the floating and fixed strike GAO using Theorem 3.1 given below.

Theorem 3.1. *If function $A(t,s,z,u)$ satisfies*

$$E_y[\mathscr{L}_2^a]A(t,s,z,u) = \sum_{v=1}^{n} f_v(t) D_v(t,s,z,u)$$

with

$$A(T, S_T, Z_T, U_T) = 0$$

and $D_v(t,s,z,u)$ satisfies the PDE $E_y[\mathscr{L}_2^a]D(t,s,z,u) = 0$ for every $v = 1,2,\ldots,n$, then A(t,s,z,u) will be of the form

$$A(t,s,z,u) = -\sum_{v=1}^{n}\left(\int_t^T \frac{f_v(\tau)}{1+\gamma} d\tau\right) D_v(t,s,z,u)$$

where $1+\gamma = \frac{(2-kt)^2}{2(1-kt)}$ considering γ from equation (3.4.11).

Proof. The theorem is proved here for the modified Black-Scholes operator $E_y[\mathscr{L}_2^a]$ which satisfies

$$E_y[\mathscr{L}_2^a] = [1+\gamma]\frac{\partial}{\partial t} + \frac{1}{2}\overline{\sigma}^2(z)\left(\frac{\partial}{\partial s} - t\frac{\partial}{\partial u}\right)^2 + \left(r - \frac{1}{2}f^2(y,z)\right)\left(\frac{\partial}{\partial s} - t\frac{\partial}{\partial u}\right) - r$$

Here the case $n = 1$ is considered only and the proof will be parallel for any other value of n. Consider

$$A(t,s,z,u) = -\left(\int_t^T \frac{f(\tau)}{1+\gamma}d\tau\right)D(t,s,z,u)$$

Clearly

$$A(T,s,z,u) = 0.$$

Also as

$$(1+\gamma)\frac{\partial A}{\partial t} = f(t)D(t,s,z,u) - \left(\int_t^T \frac{f(\tau)}{1+\gamma}d\tau\right)(1+\gamma)\frac{\partial D}{\partial t}$$

and

$$\left(\frac{\partial}{\partial s} - t\frac{\partial}{\partial u}\right)^i A = -\left(\int_t^T \frac{f(\tau)}{1+\gamma}d\tau\right)\left(\frac{\partial}{\partial s} - t\frac{\partial}{\partial u}\right)^i D,\ \forall i$$

Therefore

$$\begin{aligned} E_y[\mathscr{L}_2^a]A(t,s,z,u) &= f(t)D(t,s,z,u) - \left(\int_t^T \tfrac{f(\tau)}{1+\gamma}d\tau\right)E_y[\mathscr{L}_2^a]D(t,s,z,u) \\ &= f(t)D(t,s,z,u) \end{aligned}$$

because $E_y[\mathscr{L}_2^a]D(t,s,z,u) = 0$. This completes the proof of Theorem 3.1. □

Now, $E_y[\mathscr{L}_2^a]C_1 = \mathscr{G}_a C_0$ gives

$$E_y[\mathscr{L}_2^a]C_1^{fl} = -V\left[t\frac{\partial}{\partial u} - 2t^2\frac{\partial^2}{\partial u^2} + t^3\frac{\partial^3}{\partial u^3}\right]C_0^{fl}$$

and

$$E_y[\mathscr{L}_2^a]C_1^{fix} = V\left[(T-t)^3\frac{\partial^3}{\partial u^3} - (T-t)^2\frac{\partial^2}{\partial u^2}\right]C_0^{fix}$$

and the u-differentials of C_0 are interchangeable with the modified Black-Scholes operator $E_y[\mathscr{L}_2^a]$, so it is clear that the u-differentials of C_0^{fl} and C_0^{fix} will satisfy $E_y[\mathscr{L}_2^a]D(t,s,z,u) = 0$. Thus by above theorem,

$$C_1^{fl} = V\left[\left(\int_t^T \frac{\tau}{1+\gamma}d\tau\right)\frac{\partial}{\partial u} - 2\left(\int_t^T \frac{\tau^2}{1+\gamma}d\tau\right)\frac{\partial^2}{\partial u^2} + \left(\int_t^T \frac{\tau^3}{1+\gamma}d\tau\right)\frac{\partial^3}{\partial u^3}\right]C_0^{fl} \tag{3.4.29}$$

and

$$C_1^{fix} = V\left[\left(\int_t^T \frac{(T-\tau)^2}{1+\gamma}d\tau\right)\frac{\partial^2}{\partial u^2} - \left(\int_t^T \frac{(T-\tau)^3}{1+\gamma}d\tau\right)\frac{\partial^3}{\partial u^3}\right]C_0^{fix} \tag{3.4.30}$$

These expressions are simplified to give

$$C_1^{fl} = V\left[I_1\frac{\partial}{\partial u} - 2I_2\frac{\partial^2}{\partial u^2} + I_3\frac{\partial^3}{\partial u^3}\right]C_0^{fl} \tag{3.4.31}$$

and

$$C_1^{fix} = V\left[I_4\frac{\partial^2}{\partial u^2} - I_5\frac{\partial^3}{\partial u^3}\right]C_0^{fix} \tag{3.4.32}$$

where

$$\begin{aligned}
I_0 &= \tfrac{-2}{k}\left[k(T-t)(\tfrac{1}{(2-kT)(2-kt)}) + \ln\tfrac{2-kT}{2-kt}\right] \\
I_1 &= \tfrac{-2}{k^2}\left[k(T-t)(1+\tfrac{2}{(2-kT)(2-kt)}) + 3\ln\tfrac{2-kT}{2-kt}\right] \\
I_2 &= \tfrac{-2}{k^3}\left[\tfrac{k^2}{2}(T^2-t^2) + k(T-t)(3+\tfrac{4}{(2-kT)(2-kt)}) + 8\ln\tfrac{2-kT}{2-kt}\right] \\
I_3 &= \tfrac{-2}{k^4}\left[\tfrac{k^3}{3}(T^3-t^3) + \tfrac{3k^2}{2}(T^2-t^2) + 8k(T-t)(1+\tfrac{1}{(2-kT)(2-kt)}) + 20\ln\tfrac{2-kT}{2-kt}\right] \\
I_4 &= I_2 - 2TI_1 + T^2I_0 \\
I_5 &= -I_3 + 3TI_2 - 3T^2I_1 + T^3I_0
\end{aligned} \tag{3.4.33}$$

Clearly, C_1^{fl} and C_1^{fix} satisfy the boundary condition

$$C_1(T, S_T, Z_T, U_T) = 0$$

Collectively for floating and fixed strike GAO

$$C_1^{fl,fix} = U^{fl,fix}C_0^{fl,fix}$$

The expression of U is given in Eqs.(3.4.31) and (3.4.32) for the floating and fixed strike GAOs respectively.

3.5 First Order Approximated Price

The first order approximation to the asymptotic expansion of the GAO call price $C^{\varepsilon}_{fl,fix}$ (combined for floating and fixed strike options) denoted as $\hat{C}^{\varepsilon}_{fl,fix}$, is given

as

$$C^{\varepsilon}_{fl,fix} \approx \hat{C}^{\varepsilon}_{fl,fix} = C_0^{fl,fix} + \sqrt{\varepsilon} C_1^{fl,fix} \tag{3.5.1}$$

where $C_0^{fl,fix}$ is given by Eq.(3.4.14) and $C_1^{fl,fix}$ is given by Eqs.(3.4.31) and (3.4.32) for floating and fixed strike options respectively. Unlike Wong and Cheung [120], where the approximate price was perturbed around the Black-Scholes price for the GAOs, here the first order approximated price is perturbed around the modified Black-Scholes price $C_0^{fl,fix}$ for both floating and fixed strike options. The price is modified by a modification factor $\beta(t)$ given in Eq.(3.4.15). The prices are calculated at the effective volatility $\overline{\sigma}(z)$ which is estimated by the quadratic arc.

3.6 Accuracy of the Price Approximation

The accuracy of the first order price approximation formula (3.5.1) is discussed in this section for the non-smooth pay-off of floating and fixed strike geometric Asian options. The method employed here is on the lines of the method used in Section 2.6 of the preceding chapter where the accuracy of the first order pricing formula is given for the European options. The non-smooth payoff h is regularized by replacing it with modified Black-Scholes formula for the GAOs with time to maturity $\Delta > 0$ and volatility $\overline{\sigma}(z)$ given as

$$\begin{aligned} h^{\Delta}(s,z,u) &= C_{MA}(\Delta, s, u, \overline{\sigma}(z)) \\ &= \beta(\Delta) B_A(\Delta, s, u, \overline{\sigma}(z)) \end{aligned} \tag{3.6.1}$$

where C_{MA} is the modified Black-Scholes price and B_A is the Black-Scholes price for GAOs obtained at volatility $\overline{\sigma}(z)$. $\beta(\Delta)$ is the modification factor. Corresponding to the regularized pay-off h^{Δ}, the regularized option price $C^{\varepsilon,\Delta}$ satisfies

$$\mathscr{L}_a^{\varepsilon} C^{\varepsilon,\Delta} = 0$$

where

$$C^{\varepsilon,\Delta}(T,s,y,z,u) = h^{\Delta}(s,z,u)$$

and its first order price approximation $\hat{C}^{\varepsilon,\Delta}$ is

$$\hat{C}^{\varepsilon,\Delta} = C_0^{\Delta} + \sqrt{\varepsilon} C_1^{\Delta}$$

with

$$C_0^{\Delta}(t,s,z,u) = C_0(t-\Delta,s,z,u) = C_{MA}(T-t+\Delta,s,u,\overline{\sigma}(z))$$

and

$$C_1^{\Delta}(t,s,z,u) = U^{\Delta}C_0^{\Delta}(t,s,z,u)$$

The accuracy of the first order approximated price is established by the theorem given below.

Theorem 3.2. *Let the volatility function $f(y,z)$ is measurable and bounded away from zero. Then for a fixed $t(<T), s,y,z,u \in \mathbb{R}$, the accuracy of first order approximated price for the GAO is given as*

$$|C^{\varepsilon}(t,s,y,z,u) - \hat{C}^{\varepsilon}(t,s,z,u)| \leq b(\varepsilon^{\frac{1+c}{2}})$$

for $c<1$ and some constant b.

The proof of this theorem is a direct implication of three lemmas given below.

Lemma 3.1. *Fix the point (t,s,y,z,u) where $t<T$, there exist constants $\Delta_1>0, \varepsilon_1>0$ and $\overline{b}_1>0$ so that*

$$|C^{\varepsilon}(t,s,y,z,u) - C^{\varepsilon,\Delta}(t,s,y,z,u)| \leq \overline{b}_1\Delta$$

for all $0<\varepsilon\leq\varepsilon_1$ and $0<\Delta\leq\Delta_1$.

Proof. This lemma gives that the difference in actual price C^{ε} and the regularized price $C^{\varepsilon,\Delta}$ is small. Proof of this lemma is on the lines of Lemma 2.1 of Chapter 2. As the payoff functions (3.4.24) and (3.4.27) involve both S_T and U_T, therefore, the joint distribution of S_T and U_T is required for the risk valuation argument. To reduce the complexity, instead of considering the joint distribution of S_T and U_T, we have considered the joint distribution of $\ln X_T$ and $\ln G_{[0,T]}$. For the simplification, it is considered that $\rho_{sy}=\rho$, $\rho_{yz}=0$ and $\rho_{sz}=0$. The proof involves the consideration of the dynamics of a new stochastic process $\ln\overline{X}_t$ which is analogous to the process $\ln X_t$ such that

$$d\ln\overline{X}_t = \left(r - \frac{1}{2}\overline{f}(t,y,z)^2\right)dt + \overline{f}(t,y,z)(\rho dW_t^y + \sqrt{1-\rho^2}d\tilde{W}_t^x)$$

W_t^y and $\tilde{W}_t^x$ are the Brownian motions independent of each other and

$$\overline{f}(t,y,z) = \begin{cases} f(y,z), & \text{if } t<T \\ \overline{\sigma}(z), & \text{if } t\geq T. \end{cases}$$

Using the risk-neutral valuation under the expectation E^*,

$$C^{\varepsilon}(t,x,y,z,G) - C^{\varepsilon,\Delta}(t,x,y,z,G)$$
$$= E^*_{t,x,y,z,G}[e^{-r(T-t)}h(\overline{X}_T, \overline{G}_{[0,T]})] - E^*_{t,x,y,z,G}[e^{-r(T-t+\Delta)}h(\overline{X}_{T+\Delta}, \overline{G}_{[0,T+\Delta]})] \quad (3.6.2)$$

this implies that

$$C^{\varepsilon}(t,x,y,z,G) - C^{\varepsilon,\Delta}(t,x,y,z,G) = E^*_{t,x,y,z,G}[E^*_{t,x,y,z,G}\{e^{-r(T-t)}h(\overline{X}_T, \overline{G}_{[0,T]})|(W^y_p)_{t\le p\le T}\}$$
$$-E^*_{t,x,y,z,G}\{e^{-r(T-t+\Delta)}h(\overline{X}_{T+\Delta}, \overline{G}_{[0,T+\Delta]})|(W^y_p)_{t\le p\le T}\}] \quad (3.6.3)$$

The joint distribution of random vector $[\ln\overline{X}_T, \ln\overline{G}_{[0,T]}]$ given the path of $(W^y_p)_{t\le p\le T}$ is a multivariate normal distribution having a 2-dimensional vector $[\mu_x, \mu_G]$ as the mean vector and a 2×2 covariance matrix

$$\begin{bmatrix} \overline{\sigma}^2_{\rho,x}(T-t) & \overline{\sigma}^2_{\rho,x}\frac{(T-t)^2}{2T} \\ \overline{\sigma}^2_{\rho,x}\frac{(T-t)^2}{2T} & \overline{\sigma}^2_{\rho,x}\frac{(T-t)^3}{3T^2} \end{bmatrix}$$

where

$$\mu_x = \ln\overline{X}_t + \left(r - \frac{\overline{\sigma}^2_{\rho,x}}{2}\right)(T-t) + \lambda_{t,T},$$

$$\mu_G = \frac{t}{T}\ln\overline{G}_{[0,t]} + \frac{1}{T}\left(\ln\overline{X}_t(T-t) + \left(r - \frac{\overline{\sigma}^2_{\rho,x}}{2}\right)\frac{(T-t)^2}{2} + \int_t^T \lambda_{t,q}dq\right),$$

$$\overline{\sigma}^2_{\rho,x}(T-t) = (1-\rho^2)\int_t^T \overline{f}^2(p,y,z)dp$$

and

$$\lambda_{t,T} = \rho\int_t^T \overline{f}(p,y,z)dW^y_p - \frac{\rho^2}{2}\int_t^T \overline{f}^2(p,y,z)dp$$

Similarly, the joint distribution of random vector $[\ln\overline{X}_{T+\Delta}, \ln\overline{G}_{[0,T+\Delta]}]$ given the path of $(W^y_p)_{t\le p\le T}$, is a multivariate normal distribution having a 2-dimensional vector $[\mu_{x,\Delta}, \mu_{G,\Delta}]$ as the mean vector and a 2×2 covariance matrix

$$\begin{bmatrix} \overline{\sigma}^2_{\rho,x,\Delta}(T-t) & \overline{\sigma}^2_{\rho,x,G,\Delta}\frac{(T-t)^2}{2T} \\ \overline{\sigma}^2_{\rho,x,G,\Delta}\frac{(T-t)^2}{2T} & \overline{\sigma}^2_{\rho,G,\Delta}\frac{(T-t)^3}{3T^2} \end{bmatrix}$$

where

$$\mu_{x,\Delta} = \ln\overline{X}_t + \left(r - \frac{\overline{\sigma}^2_{\rho,x,\Delta}}{2}\right)(T-t) + r\Delta + \lambda_{t,T},$$

$$\mu_{G,\Delta} = \frac{t}{T}\ln \overline{G}_{[0,t]} + \frac{1}{T}\left(\ln \overline{X}_t (T-t+\Delta) + \left(r - \frac{\overline{\sigma}^2_{\rho,x,G,\Delta}}{2}\right)\frac{(T-t)^2}{2} + \int_t^T \lambda_{t,q} dq + r\Delta(T-t+\frac{\Delta}{2})\right),$$

with

$$\overline{\sigma}^2_{\rho,x,\Delta}(T-t) = \overline{\sigma}^2_{\rho,x}(T-t) + \overline{\sigma}^2\Delta$$

$$\overline{\sigma}^2_{\rho,x,G,\Delta}(T-t)^2 = \overline{\sigma}^2_{\rho,x}(T-t+\Delta)^2 + \rho^2\overline{\sigma}^2\Delta^2$$

and

$$\overline{\sigma}^2_{\rho,G,\Delta}(T-t)^3 = \overline{\sigma}^2_{\rho,x}(T-t+\Delta)^3 + \rho^2\overline{\sigma}^2\Delta^3$$

The prices C^ε and $C^{\varepsilon,\Delta}$ involves $\beta(t)$ which will be always finite for a finite t. Also, under the assumption of bounded $f(y,z)$ and using the expression of Black-Scholes price for GAOs given in Section 1.4 of Chapter 1, it is easily obtained that

$$|C^\varepsilon(t,x,y,z,G) - C^{\varepsilon,\Delta}(t,x,y,z,G)| \leq \overline{b}_1\Delta$$

for some constant $\overline{b}_1$ and some small Δ. □

Lemma 3.2. *Fix the point (t,s,y,z,u) where $t < T$, there exist constants $\Delta_2 > 0, \varepsilon_2 > 0$ and $\overline{b}_2 > 0$ so that*

$$|\hat{C}^\varepsilon(t,s,z,u) - \hat{C}^{\varepsilon,\Delta}(t,s,z,u)| \leq \overline{b}_2\Delta$$

for all $0 < \varepsilon \leq \varepsilon_2$ and $0 < \Delta \leq \Delta_2$.

Proof. This lemma gives that the difference in approximated price C^ε and its corresponding regularized price $C^{\varepsilon,\Delta}$ is small. Proof of this lemma is straightforward and on the lines of Lemma 2.2 of Chapter 2. From Eqs.(3.4.14), (3.4.31), (3.4.32) and (3.5.1), for the floating and fixed strike GAOs call, the difference

$$\begin{aligned}&\hat{C}^\varepsilon_{fl,fix}(t,s,z,u) - \hat{C}^{\varepsilon,\Delta}_{fl,fix}(t,s,z,u)\\ &\quad= \left(1 + L_1^{fl,fix}\frac{\partial}{\partial u} + L_2^{fl,fix}\frac{\partial^2}{\partial u^2} + L_3^{fl,fix}\frac{\partial^3}{\partial u^3}\right)(C_0^{fl,fix} - C_0^{fl,fix,\Delta}) \qquad (3.6.4)\end{aligned}$$

where for $i = 1,2,3$ and $j = 0,1,...,5$, $L_i^{fl,fix}$ involves I_j and V with their expressions given in (3.4.33) and (3.4.19) respectively. $V^\varepsilon = \sqrt{\varepsilon}V$ is bounded. Also for $kt \neq 2$, the modification factor $\beta(t)$, the Black-Scholes price for Asian options and its successive derivatives w.r.t u are bounded in $t < T$, therefore the same holds for the modified Black-

Scholes price of GAOs. So it is easily obtained that

$$|\hat{C}^{\varepsilon}(t,s,z,u) - \hat{C}^{\varepsilon,\Delta}(t,s,z,u)| \leq \bar{b}_2\Delta$$

for some constant $\bar{b}_2$ and small Δ. □

Lemma 3.3. *Fix the point (t,s,y,z,u) where $t < T$, there exist constants $\Delta_3 > 0, \varepsilon_3 > 0$ and $\bar{b}_3 > 0$ so that*

$$|C^{\varepsilon,\Delta}(t,s,y,z,u) - \hat{C}^{\varepsilon,\Delta}(t,s,z,u)| \leq \bar{b}_3\varepsilon^{\frac{1+c}{2}}$$

for all $0 < \varepsilon \leq \varepsilon_3$, any $c < 1$ and uniformly in $\Delta \leq \Delta_3$

Proof. This lemma gives that the difference in regularized price $C^{\varepsilon,\Delta}$ and the corresponding regularized first order price approximation $\hat{C}^{\varepsilon,\Delta}$ is small. Its proof is on the lines of Lemma $B.3$ of Fougue et al. [38], which has been proved for the European options. All the assumptions given in Subsection 2.1 of Fougue et al. [38] clearly holds in case of GAO where the volatility factors are considered to follow OU process.

Consider $C^{\varepsilon,\Delta} = C_0^{\Delta} + \sqrt{\varepsilon}C_1^{\Delta} + \varepsilon C_2^{\Delta} + \varepsilon\sqrt{\varepsilon}C_3^{\Delta} - R^{\varepsilon,\Delta}$, where $R^{\varepsilon,\Delta}$ is the residual for the regularized problem such that

$$\mathscr{L}_a^{\varepsilon} R^{\varepsilon,\Delta} = K^{\varepsilon,\Delta}$$

with

$$\begin{aligned} K^{\varepsilon,\Delta} &= \mathscr{L}_a^{\varepsilon}(C_0^{\Delta} + \sqrt{\varepsilon}C_1^{\Delta} + \varepsilon C_2^{\Delta} + \varepsilon\sqrt{\varepsilon}C_3^{\Delta} - C^{\varepsilon,\Delta}) \\ &= \varepsilon(\mathscr{L}_2^a C_2^{\Delta} + \mathscr{L}_1^a C_3^{\Delta}) + \varepsilon\sqrt{\varepsilon}(\mathscr{L}_2^a C_3^{\Delta}) \end{aligned} \tag{3.6.5}$$

where

$$C_2^{\Delta} = -\frac{1}{2}\phi(y,z)D_2C_0^{\Delta}$$

$$C_3^{\Delta} = \frac{\mu}{\sqrt{2}}\rho\psi_1(y,z)D_1D_2C_0^{\Delta} - \frac{1}{2}\phi(y,z)D_2C_1^{\Delta}$$

$$D_1 = \left(\frac{\partial}{\partial s} - t\frac{\partial}{\partial u}\right)$$

$$D_2 = \left(\frac{\partial}{\partial s} - t\frac{\partial}{\partial u}\right)^2 - \left(\frac{\partial}{\partial s} - t\frac{\partial}{\partial u}\right)$$

and $\psi_1(y,z)$ is the solution of

$$\mathscr{L}_0^a\psi(y,z) = f\phi' - E_y[f\phi']$$

On substituting these values in (3.6.5) and solving for the floating and fixed strike GAOs, we get

$$K_{fl}^{\varepsilon,\Delta} = \beta^{fl}\Bigg[\varepsilon\Bigg(\sum_{i=1}^{6}\chi_{i,0}^{fl}(t,T,y,z)\frac{\partial^i}{\partial u^i} + (T-t)\sum_{i=1}^{6}\chi_{i,1}^{fl}(t,T,y,z)\frac{\partial^i}{\partial u^i}\Bigg) + \varepsilon\sqrt{\varepsilon}\Bigg(\sum_{i=1}^{7}\chi_{i,2}^{fl}(t,T,y,z)\frac{\partial^i}{\partial u^i} + (T-t)\sum_{i=1}^{7}\chi_{i,3}^{fl}(t,T,y,z)\frac{\partial^i}{\partial u^i}\Bigg)\Bigg]B_0^{\Delta} \tag{3.6.6}$$

and

$$\begin{aligned} K_{fix}^{\varepsilon,\Delta} = \beta^{fix}\Bigg[&\varepsilon\Bigg(\sum_{i=1}^{6}\chi_{i,0}^{fix}(t,T,y,z)\frac{\partial^i}{\partial u^i} + (T-t)\sum_{i=1}^{2}\chi_{i,1}^{fix}(t,T,y,z)\frac{\partial^i}{\partial u^i} \\ &+(T-t)^2\sum_{i=1}^{5}\chi_{i,2}^{fix}(t,T,y,z)\frac{\partial^i}{\partial u^i} + (T-t)^3\sum_{i=1}^{6}\chi_{i,3}^{fix}(t,T,y,z)\frac{\partial^i}{\partial u^i}\Bigg) \\ &+\varepsilon\sqrt{\varepsilon}\Bigg(\sum_{i=1}^{4}\chi_{i,4}^{fl}(t,T,y,z)\frac{\partial^i}{\partial u^i} + (T-t)\sum_{i=1}^{5}\chi_{i,5}^{fl}(t,T,y,z)\frac{\partial^i}{\partial u^i} \\ &+(T-t)^2\sum_{i=1}^{5}\chi_{i,6}^{fl}(t,T,y,z)\frac{\partial^i}{\partial u^i} + (T-t)^3\sum_{i=1}^{6}\chi_{i,7}^{fl}(t,T,y,z)\frac{\partial^i}{\partial u^i} \\ &+(T-t)^4\sum_{i=1}^{7}\chi_{i,8}^{fl}(t,T,y,z)\frac{\partial^i}{\partial u^i} + (T-t)^5\sum_{i=1}^{7}\chi_{i,9}^{fl}(t,T,y,z)\frac{\partial^i}{\partial u^i}\Bigg)\Bigg]B_0^{\Delta} \end{aligned} \tag{3.6.7}$$

Also at maturity,

$$\begin{aligned} R^{\varepsilon,\Delta}(T) &= \varepsilon C_2^{\Delta}(T,s,y,z,u) + \varepsilon\sqrt{\varepsilon}C_3^{\Delta}(T,s,y,z,u) \\ &= Q^{\varepsilon,\Delta}(s,y,z,u) \ \ (say) \end{aligned}$$

On considering the value of C_2^{Δ} and C_3^{Δ} for both floating and fixed strike GAO at maturity, it is easily obtained that

$$Q_{fl,fix}^{\varepsilon,\Delta}(s,y,z,u) = \beta^{fl,fix}\Bigg[\varepsilon\sum_{i=1}^{2}q_{i,0}^{fl,fix}(T,y,z)\frac{\partial^i}{\partial u^i} + \varepsilon\sqrt{\varepsilon}\sum_{i=1}^{3}q_{i,1}^{fl,fix}(T,y,z)\frac{\partial^i}{\partial u^i}\Bigg]B_0^{\Delta}$$

Clearly for fixed strike options this value is zero. Using this terminal condition, residual $R^{\varepsilon,\Delta}$ has the probabilistic representation

$$R^{\varepsilon,\Delta} = E^*_{t,s,y,z,u}\Bigg[e^{-r(T-t)}Q^{\varepsilon,\Delta} - \int_t^T e^{-r(\tau-t)}K^{\varepsilon,\Delta}d\tau\Bigg]$$

Using Lemma $B.4$ of [38], for both fixed and floating strike options at a fixed $t < T$,

$$\Bigg|E^*_{t,s,y,z,u}\Bigg[Q^{\varepsilon,\Delta}(S_T,Y_T,Z_T,U_T)]\Bigg| \leq b_3\varepsilon^{\frac{1+c}{2}}$$

and

$$\left| E^*_{t,s,y,z,u}\left[\int_t^T e^{-r(\tau-t)} K^{\varepsilon,\Delta}(s,y,z,u)d\tau \right] \right| \leq c_3 \varepsilon^{\frac{1+c}{2}}$$

therefore,

$$|C^{\varepsilon,\Delta}(t,s,y,z,u) - \hat{C}^{\varepsilon,\Delta}(t,s,z,u)| = |\varepsilon C_2^{\Delta} + \varepsilon\sqrt{\varepsilon} C_3^{\Delta} - R^{\varepsilon,\Delta}|$$

where C_2^{Δ} and C_3^{Δ} are bounded for $t < T$ giving

$$|C^{\varepsilon,\Delta}(t,s,y,z,u) - \hat{C}^{\varepsilon,\Delta}(t,s,z,u)| \leq \overline{b}_3 \varepsilon^{\frac{1+c}{2}}$$

for some $\overline{b}_3$ and $c < 1$. □

Using Lemmas 3.1, 3.2 and 3.3, the proof of Theorem 3.2 is straightforward. Consider a fixed point (t,s,y,z,u). Taking $\overline{\varepsilon} = \min(\varepsilon_1, \varepsilon_2, \varepsilon_3)$ and $\overline{\Delta} = \min(\Delta_1, \Delta_2, \Delta_3)$.

$$\begin{aligned} |C^{\varepsilon} - \hat{C}^{\varepsilon}| &\leq |C^{\varepsilon} - C^{\varepsilon,\Delta}| + |C^{\varepsilon,\Delta} - \hat{C}^{\varepsilon,\Delta}| + |\hat{C}^{\varepsilon,\Delta} - \hat{C}^{\varepsilon}| \\ &\leq \overline{b}_1\Delta + \overline{b}_2\Delta + \overline{b}_3(\varepsilon^{\frac{1+c}{2}}) \\ &\leq 2max(\overline{b}_1, \overline{b}_2)\Delta + \overline{b}_3(\varepsilon^{\frac{1+c}{2}}) \end{aligned}$$

Let $\overline{b}_4 = max(\overline{b}_1, \overline{b}_2)$ and on taking $\Delta = \varepsilon$, we get

$$\begin{aligned} |C^{\varepsilon} - \hat{C}^{\varepsilon}| &\leq 2\overline{b}_4\varepsilon + \overline{b}_3(\varepsilon^{\frac{1+c}{2}}) \\ &\leq b(\varepsilon^{\frac{1+c}{2}}) \end{aligned} \tag{3.6.8}$$

This completes the required proof.

3.7 Estimation of Model Parameter

After establishing the accuracy of the approximated pricing formula of GAOs, we intend to estimate V (given in Eq.(3.4.19)), the only parameter required for the implementation of the approximate formulae. The fixed strike put options and floating strike call options have the positive *vegas*. Therefore, the volatility smiles can be captured for these options unlike the fixed strike call and floating strike put options which may have the negative *vegas*. The European and Asian smiles are captured together on the lines of the method given in Wong and Cheung [120]. The European smiles with the model under consideration have already been obtained in Chapter 2.

Firstly, the case of floating strike call options is considered. Assume the asymptotic expansion for the market implied volatility (I) of the floating strike options. that is,

$$I^{fl} = I_0^{fl} + \sqrt{\varepsilon} I_1^{fl} + \varepsilon I_2^{fl} + ...$$

The implied volatility I^{fl} is obtained by matching the modified Black-Scholes price for Asian options with the price C_{fl}^{ε} of GAO. This gives

$$C_{fl}^{\varepsilon}(t,s,z,u,\overline{\sigma}(z)) = C_0^{fl}(t,s,z,u,\sigma = I^{fl})$$

Consider the Taylor expansion of the modified Black-Scholes price C_0^{fl} about I_0^{fl} and the asymptotic expansion of C_{fl}^{ε} given in Eq.(3.4.1) to get

$$C_0^{fl}(\overline{\sigma}(z)) + \sqrt{\varepsilon} C_1^{fl}(\overline{\sigma}(z)) + ... = C_0^{fl}(I_0^{fl}) + \frac{\partial C_0^{fl}(I_0^{fl})}{\partial \sigma} \sqrt{\varepsilon} I_1^{fl} + ...$$

Matching the terms of order zero and ε on both side to get

$$I_0^{fl} = \overline{\sigma}(z)$$

and

$$I_1^{fl} = \left(\frac{\partial C_0^{fl}(I_0^{fl})}{\partial \sigma} \right)^{-1} C_1^{fl}(\overline{\sigma}(z))$$

The first order approximated value of implied volatility is

$$I^{fl} \approx I_0^{fl} + \sqrt{\varepsilon} I_1^{fl}$$

For I_1^{fl}, consider the expression of C_1^{fl} from Eq.(3.4.31) and on rearranging the terms

$$I^{fl} \approx \overline{\sigma}(z) + \sqrt{\varepsilon} \left[\left(\frac{\partial C_0^{fl}(\overline{\sigma}(z))}{\partial \sigma} \right)^{-1} \left(p_{fl} \frac{(r\overline{\sigma}(z))(I_1 \frac{\partial}{\partial u} - 2I_2 \frac{\partial^2}{\partial u^2} + I_3 \frac{\partial^3}{\partial u^3}) C_0^{fl}}{\frac{1}{(T-t)} [\frac{1}{k} \log |\frac{kT-2}{kt-2}| + \frac{T-t}{(kT-2)(kt-2)}]} + q_{fl} \right) \right]$$

which gives

$$(I^{fl} - \overline{\sigma}(z)) \left(\frac{\partial C_0^{fl}(\overline{\sigma}(z))}{\partial \sigma} \right) \approx p_{fl}^{\varepsilon} \left(\frac{(r\overline{\sigma}(z))(I_1 \frac{\partial}{\partial u} - 2I_2 \frac{\partial^2}{\partial u^2} + I_3 \frac{\partial^3}{\partial u^3}) C_0^{fl}}{\frac{1}{(T-t)} [\frac{1}{k} \log \frac{2-kT}{2-kt} + \frac{T-t}{(2-kT)(2-kt)}]} \right) + q_{fl}^{\varepsilon}$$

where $p^{\varepsilon}_{fl} = \sqrt{\varepsilon} p_{fl}$ and $q^{\varepsilon}_{fl} = \sqrt{\varepsilon} q_{fl}$. The expressions of $\frac{\partial C_0^{fl}}{\partial u}, \frac{\partial^2 C_0^{fl}}{\partial u^2}, \frac{\partial^3 C_0^{fl}}{\partial u^3}$ and $\frac{\partial C_0^{fl}}{\partial \sigma}$ are given as

$$\frac{\partial C_0^{fl}}{\partial u} = -\beta^{fl}(t)\frac{e^{s+\frac{u}{T}-Q}}{T}N(d_2)$$

$$\frac{\partial^2 C_0^{fl}}{\partial u^2} = \frac{\beta^{fl}(t)}{T}\left[\frac{\partial C_0^{fl}}{\partial u} + \frac{e^{s+\frac{u}{T}-Q}\phi(d_2)}{\overline{\sigma}\sqrt{\frac{T^3-t^3}{3}}}\right]$$

$$\frac{\partial^3 C_0^{fl}}{\partial u^3} = \frac{\beta^{fl}(t)}{T}\left[\frac{\partial^2 C_0^{fl}}{\partial u^2} + e^{s+\frac{u}{T}-Q}\left(\frac{\phi(d_2)}{\overline{\sigma}T\sqrt{\frac{T^3-t^3}{3}}} + \frac{d_2\phi(d_2)}{\overline{\sigma}^2\frac{T^3-t^3}{3}}\right)\right]$$

and

$$\frac{\partial C_0^{fl}}{\partial \overline{\sigma}} = \beta^{fl}(t)e^{s+\frac{u}{T}-Q}\left[\frac{1}{T}\sqrt{\frac{T^3-t^3}{3}}\phi(d_2) + \frac{\overline{\sigma}(T-t)^2(T+2t)N(d_2)}{6T^2}\right]$$

where, $N(.)$ and $\phi(.)$ are respectively the cumulative distribution function and the probability density function for the standard normal variate.

p^{ε}_{fl} and q^{ε}_{fl} are estimated using the simple linear regression and the value of V is obtained from

$$V = \frac{p_{fl}(2r\overline{\sigma})}{\frac{2}{(T-t)}[\frac{1}{k}\log\frac{2-kT}{2-kt} + \frac{T-t}{(2-kT)(2-kt)}]} \tag{3.7.1}$$

Similarly, for the fixed strike put options

$$(I^{fix} - \overline{\sigma}(z))\left(\frac{\partial P_0^{fix}(\overline{\sigma}(z))}{\partial \sigma}\right) \approx p^{\varepsilon}_{fix}\left(\frac{(r\overline{\sigma}(z))(I_4\frac{\partial^2}{\partial u^2} - I_5\frac{\partial^3}{\partial u^3})P_0^{fix}}{\frac{1}{(T-t)}[\frac{1}{k}\log\frac{2-kT}{2-kt} + \frac{T-t}{(2-kT)(2-kt)}]}\right) + q^{\varepsilon}_{fix}$$

where $p^{\varepsilon}_{fix} = \sqrt{\varepsilon} p_{fix}$ and $q^{\varepsilon}_{fix} = \sqrt{\varepsilon} q_{fix}$. The expressions of $\frac{\partial^2 P_0^{fix}}{\partial u^2}, \frac{\partial^3 P_0^{fix}}{\partial u^3}$ and $\frac{\partial P_0^{fix}}{\partial \sigma}$ are given as:

$$\frac{\partial P_0^{fix}}{\partial u} = -\beta^{fix}(t)\frac{e^{s+\frac{u}{T}-Q}}{T}N(-\hat{d_1})$$

$$\frac{\partial^2 P_0^{fix}}{\partial u^2} = \frac{\beta^{fix}(t)}{T}\left[\frac{\partial P_0^{fix}}{\partial u} + \frac{e^{s+\frac{u}{T}-Q}\phi(\hat{d_1})}{\overline{\sigma}\sqrt{\frac{(T-t)^3}{3}}}\right]$$

$$\frac{\partial^3 P_0^{fix}}{\partial u^3} = \frac{\beta^{fix}(t)}{T}\left[\frac{\partial^2 P_0^{fix}}{\partial u^2} + e^{s+\frac{u}{T}-Q}\left(\frac{\phi(\hat{d_1})}{\overline{\sigma}T\sqrt{\frac{(T-t)^3}{3}}} - \frac{\hat{d_1}\phi(\hat{d_1})}{\overline{\sigma}^2\frac{(T-t)^3}{3}}\right)\right]$$

and

$$\frac{\partial P_0^{fix}}{\partial \overline{\sigma}} = \beta^{fix}(t)e^{s+\frac{u}{T}-Q}\left[\frac{1}{T}\sqrt{\frac{(T-t)^3}{3}}\phi(\hat{d_1}) + \frac{\overline{\sigma}(T-t)^2(T+2t)N(-\hat{d_1})}{6T^2}\right]$$

where $N(.)$ and $\phi(.)$ are respectively the cumulative distribution function and the probability density function for the standard normal variate.

p^{ε}_{fix} and q^{ε}_{fix} are estimated using the simple linear regression and the value of V is obtained from

$$V = \frac{p_{fix}(2r\overline{\sigma})}{\frac{2}{(T-t)}[\frac{1}{k}\log\frac{2-kT}{2-kt} + \frac{T-t}{(2-kT)(2-kt)}]} \tag{3.7.2}$$

Numerical Illustration: The data of S&P 500 index GAOs with the floating strike is considered for the period January $4,2016$ to July $4,2016$ with the initial stock price $X_0 = 2013.99$. The other parameters are $k = 2, r = 0.0264, \varepsilon = 0.001, Z_0 = 0.1834, m^{'} = 0.20$. $\overline{\sigma}(z)$ is estimated from the quadratic arc $\mathscr{A}t^2 + \mathscr{B}t + \mathscr{C}$. $T-t$ ranges from 0.01 to 0.5. Firstly, V is calibrated from data. For this, consider Eq.(3.7.1) which is written as

$$\mathscr{Y} \approx p^{\varepsilon}_{fl}\mathscr{X} + q^{\varepsilon}_{fl} \tag{3.7.3}$$

Using the simple linear regression with the least square approach, values of p^{ε}_{fl} and q^{ε}_{fl} are estimated from Fig.3.1.

The estimated p^{ε} is 0.6367 and the corresponding V^{ε} is calculated from (3.7.1) which lies in the range -0.009 to -0.003 for different $T-t$ values. With this calibrated V , the approximated price of the floating strike GAO is obtained from (3.5.1). The modification factor β^{fl} is in the range 0.7 to 1.5 for the different values of $T-t$. This approximated price is compared with the Black-Scholes price for the floating strike GAOs with volatility 0.1834 against the moneyness G/x shown in Fig.3.2.

The effect of modification factor β on the pricing of floating strike GAO is clearly visible in Fig.3.2. For the data set under consideration, first order approximate prices are improved than the Black-Scholes prices and the difference is more prominent for moneyness G/x greater than 1.

The calculations get simplified with the quadratic arc approximation of the persistent volatility factor. The formulae obtained are straight forward and easy to implement. *MATLAB2012b* and *Excel2013* are used for numerical computations. The run time of this model is also very small and it takes a fraction of second to obtain the results.

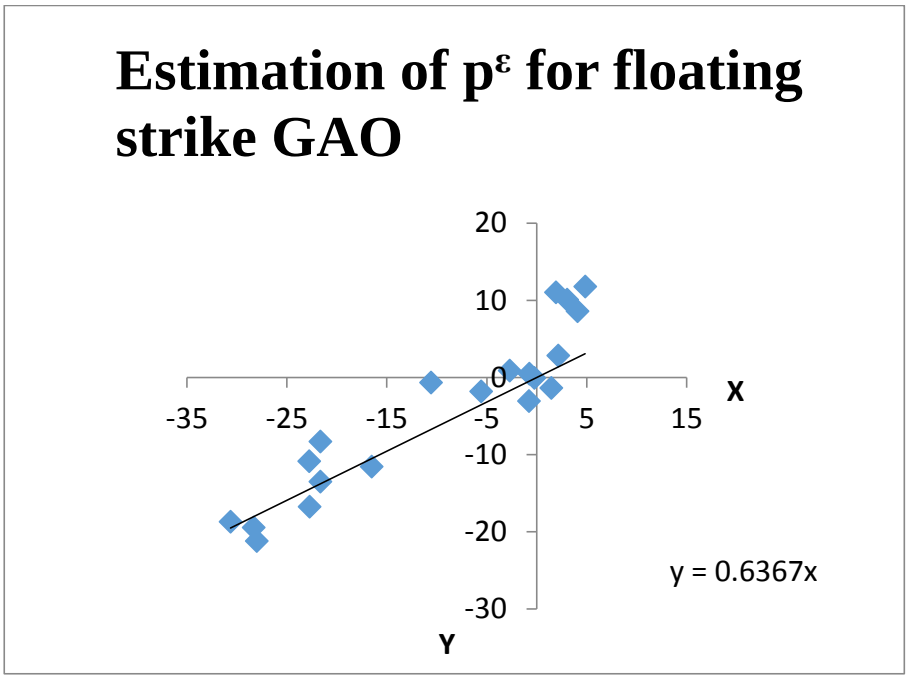

Figure 3.1: Estimation of p^{ε} using the market data of S&P 500 index implied volatility for the options with different maturities from January 04, 2016 to July 04, 2016.

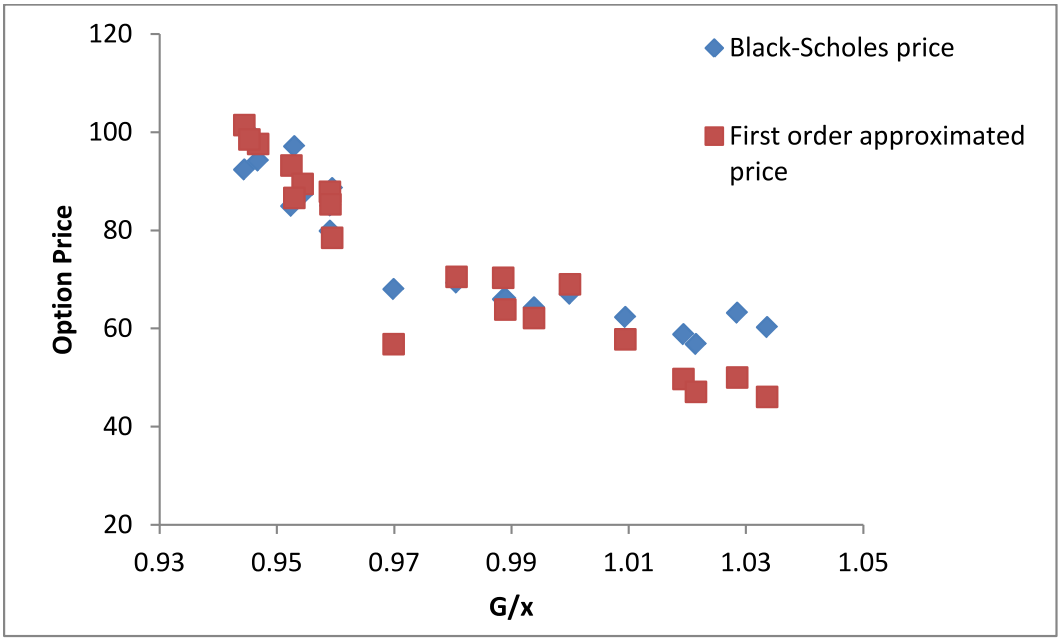

Figure 3.2: The comparison of first-order approximated price of floating strike GAO with the Black-Scholes price of floating strike GAO against the moneyness G/x.

3.8 Conclusion

A first order approximated price expression for floating and fixed strike GAO is obtained in a multifactor stochastic volatility framework where slow volatility factor is approximated by a quadratic arc. The approximated price is perturbed around the modified Black-Scholes price for the Asian options. The accuracy of the approximated formulae is established and the model parameter V is calibrated by collectively considering the Asian and the European volatility smiles. The first order approximate price for the floating strike GAO is obtained and compared with the corresponding Black-Scholes price using the S&P 500 index Asian options data. The proposed model gives the improved results for the data set under consideration in comparison to the Black-Scholes prices.

The quadratic arc expression of the slow volatility factor is quite important. So in the next chapter this expression is used as a constraint for the maximization of a two-parameter entropy to calibrate the risk-neutral density function.

Chapter 4

Calibration of the Risk-Neutral Density Function by Maximization of a Two-Parameter Entropy

---

In this chapter[1]*, a two-parameter entropy is maximized to calibrate the risk-neutral density function of the future asset price using options data subject to the expectation and the variance constraints. In the variance constraint, the volatility is assumed to be mean-reverting and following a quadratic path as proposed in Chapter 2. The desired power law distribution is verified for the density function obtained, containing both the entropy parameters, giving additional degrees of freedom. The calibrated density function is used to price the European call options for different strikes. The results thus obtained are also discussed for the one-parameter Rényi and Tsallis entropies.*

---

[1]The work reported in this chapter has been published in a research article "**Calibration of the Risk-Neutral Density Function by Maximization of a Two-Parameter Entropy, *Physica A*, 513, 45-54 (2019)**".

4.1 Introduction

Shannon [109], in his mathematical theory of communication, used entropy as a measure of information which laid the foundation of the field of information theory. Entropy has broad applications in the field of finance including asset pricing, portfolio selection and time series analysis. Out of these, one of the important aspects is to obtain the risk-neutral density function for the future asset price from the limited information available, using the principle of maximum entropy (or the maximum entropy principle (MEP)) given in Subsection 1.5.2 of Chapter 1.

Most of the literature on MEP consider the maximization of the Shannon entropy which gives the lognormal distribution of the future asset price. As the asset price distribution follows the power law [45,46,51], Brody et al. [16] extended the results of Buchen and Kelly [17] and proposed to use Rényi entropy to calibrate the risk-neutral price distribution. They maximized the one-parameter Rényi entropy instead of the Shannon entropy using market data of options on FTSE 100 futures, and obtained the power law distribution for the future asset price. They have also shown that the maximization of the Rényi entropy and maximization of the Havrda-Charvát entropy (or the Tsallis entropy), under the same constraints, is equivalent. The actual distribution of the underlying stock is not lognormal but is high peaked having fat tails, so the maximization of Rényi entropy seems relevant to the real market scenario.

While the calibration of the risk-neutral probability density function from the option prices, Brody et al. [16] considered only the mean constraint, neglecting the effect of volatility on the price distribution. The correlation between the volatility and stock price effects the distribution of the stock prices [64], so when the risk-neutral density function of the future asset price is calibrated using the options data, this correlation can not be neglected. To incorporate this effect of volatility structure on the terminal distribution of the stock price a second order moment constraint should be imposed on the system.

In the present chapter, we propose to consider the variance constraint along with the mean constraint in maximising the two-parameter Varma entropy [117]. While calibrating the risk-neutral density function from the option prices, the volatility would be considered to follow a quadratic path. Consideration of the two independent parameters provides an additional degree of freedom in

the application, and the volatility constraint makes the system realistic as its correlation with the stock price effects the terminal distribution of the stock price. Thus, this problem becomes more general and realistic.

This chapter proceeds as follows: A two-parameter entropy has been maximized to obtain the power law distribution of the future price of an asset in Section 4.2. The calibration of the risk-neutral density function has been discussed in Section 4.3 using S&P 500 index and FTSE 100 index call option data. Using this density function, the option prices at different strikes have been obtained and compared with the market data of S&P 500 index and FTSE 100 index in Section 4.4. The discussion on the results and contribution to the literature has also been given in this section. The conclusion has been presented in Section 4.5.

4.2 Two-Parameter Entropy Maximization

The two-parameter Varma entropy associated with the underlying asset price, already given in Section 1.5.1 of Chapter 1 is

$$H_{\alpha,\beta} = \frac{1}{\beta-\alpha}\log\int_0^\infty p^{\alpha+\beta-1}(x)dx \tag{4.2.1}$$

with $\beta \geq 1$, $\beta-1<\alpha<\beta$ and $\alpha+\beta\neq 2$. Clearly $\alpha+\beta>1$. For $\beta=1$, Rényi entropy of order α is obtained. The problem of interest is to find the unknown density function $p(x)$ that maximizes the expression (4.2.1) under the normalization constraint:

$$\int_0^\infty p(x)dx = 1 \tag{4.2.2}$$

and some additional constraints of the type

$$\int_0^\infty G(x)p(x)dx = M \tag{4.2.3}$$

where M is the expectation of any continuous function $G(x)$ of random variable X. The expression of $G(x)$ in Eq.(4.2.3) will be taken as x, x^2 and $(x-K_j)^+, j=1,2,...,n$ to specify $(n+2)$ constraints in the next section. Thus, Eqs.(4.2.2) and (4.2.3) taken together will comprise total $(n+3)$ constraints.

The Lagrange method is used to solve this problem such that

$$\frac{\partial}{\partial p}\left[\frac{1}{\beta-\alpha}\log\int_0^\infty p^{\alpha+\beta-1}(x)dx-\lambda\left(\int_0^\infty p(x)dx-1\right)-\gamma\left(\int_0^\infty G(x)p(x)dx-M\right)\right]=0 \tag{4.2.4}$$

where λ and γ are the Lagrange multipliers. Eq.(4.2.4) on simplification gives

$$\frac{\alpha+\beta-1}{\beta-\alpha}\frac{p^{\alpha+\beta-2}(x)}{\int_0^\infty p^{\alpha+\beta-1}(x)dx}-\lambda-\gamma G(x)=0 \tag{4.2.5}$$

Given only two constraints, the value of Lagrange multipliers can be obtained analytically. Like for λ, on multiplying both sides of Eq.(4.2.5) by $p(x)$, integrating from 0 to ∞ and using Eqs.(4.2.2) and (4.2.3), we get

$$\lambda=\frac{\alpha+\beta-1}{\beta-\alpha}-\gamma M \tag{4.2.6}$$

When a large number of constraints are given as in the next section, the numerical methods are preferred over the analytical approach to obtain the value of the Lagrange multipliers from the constraint equations. The expression of $p(x)$ obtained from Eq.(4.2.5) is

$$p(x)=\frac{1}{H}\left[\lambda+\gamma G(x)\right]^{\frac{1}{\alpha+\beta-2}} \tag{4.2.7}$$

This is the resulting maximum entropy distribution, where

$$\frac{1}{H}=\left(\frac{\beta-\alpha}{\alpha+\beta-1}\int_0^\infty p^{\alpha+\beta-1}(x)dx\right)^{\frac{1}{\alpha+\beta-2}} \tag{4.2.8}$$

As the procedure of entropy maximization is explained, the calibration of the risk-neutral density function using option prices is discussed in the next section.

4.3 Calibration of the Risk-Neutral Density Function

We assume the market to be complete. The unknown risk-neutral density function $p(x)$ for the underlying asset price is calibrated by maximizing the Varma entropy given in Eq.(4.2.1) subject to the normalization constraint (4.2.2), the first order

moment (or the mean) constraint

$$\int_0^\infty xp(x)dx = S_0 e^{rT}, \tag{4.3.1}$$

that is, the risk-neutral expectation of the price of the underlying asset at maturity time $t = T$ is the time value of the initial asset price S_0 with the risk free constant rate of interest r. The second order moment constraint

$$\int_0^\infty x^2 p(x)dx = \sigma_T^2 + (S_0 e^{rT})^2, \tag{4.3.2}$$

here, the volatility is considered to follow the mean-reverting quadratic path as proposed in Chapter 2, such that its value at the terminal time T is

$$\sigma_T = AT^2 + BT + C \tag{4.3.3}$$

where the expressions of A, B and C, as obtained in Chapter 2, are given by

$$A = \frac{(\sigma_0 - m)k^2}{2},\ B = -(\sigma_0 - m)k,\ C = \sigma_0 \tag{4.3.4}$$

here σ_0 is the initial value of volatility σ_t, m is the long-run mean and k is the rate of mean-reversion of the volatility. In addition to these three constraints, the constraints compatible with the multiple call prices C_j where $j = 1, 2, ..., n$, are given by

$$\int_0^\infty (x - K_j)^+ p(x)dx = C_j e^{rT} \tag{4.3.5}$$

here $\{K_j\}_{j=1}^n$ are the strike prices which are assumed to satisfy $0 < K_1 < K_2 < ... < K_n$.

As in the previous section, the Lagrange method is used here for solving this problem. The respective Lagrangian is

$$\begin{aligned} L = \frac{1}{\beta - \alpha} \log \int_0^\infty p^{\alpha+\beta-1}(x)dx - \lambda \left(\int_0^\infty p(x)dx - 1 \right) - \gamma_0 \left(\int_0^\infty xp(x)dx - S_0 e^{rT} \right) \\ - \gamma_1 \left(\int_0^\infty x^2 p(x)dx - V_T \right) - \sum_{j=1}^n \xi_j \left(\int_0^\infty (x - K_j)^+ p(x)dx - C_j e^{rT} \right) \end{aligned} \tag{4.3.6}$$

where

$$V_T = (AT^2 + BT + C)^2 + (S_0 e^{rT})^2 \tag{4.3.7}$$

with A, B and C given by Eq.(4.3.4). λ, γ_0, γ_1 and ξ_j, $(j = 1,2,...,n)$, denote the Lagrange multipliers relative to the constraints $(4.2.2), (4.3.1), (4.3.2)$ and $(4.3.5)$ respectively. The Lagrangian L satisfies

$$\frac{\partial}{\partial p}\left[\frac{1}{\beta-\alpha}\log\int_0^\infty p^{\alpha+\beta-1}(x)dx-\lambda\left(\int_0^\infty p(x)dx-1\right)-\gamma_0\left(\int_0^\infty xp(x)dx-S_0e^{rT}\right)\right.$$
$$\left.-\gamma_1\left(\int_0^\infty x^2p(x)dx-V_T\right)-\sum_{j=1}^{n}\xi_j\left(\int_0^\infty(x-K_j)^+p(x)dx-C_je^{rT}\right)\right]=0$$

which on simplification gives

$$\frac{\alpha+\beta-1}{\beta-\alpha}\frac{p^{\alpha+\beta-2}(x)}{\int_0^\infty p^{\alpha+\beta-1}(x)dx}-\lambda-\gamma_0x-\gamma_1x^2-\sum_{j=1}^{n}\xi_j(x-K_j)^+=0$$

this implies,

$$p(x)=\left(\frac{\beta-\alpha}{\alpha+\beta-1}\int_0^\infty p^{\alpha+\beta-1}(x)dx\left[\lambda+\gamma_0x+\gamma_1x^2+\sum_{j=1}^{n}\xi_j(x-K_j)^+\right]\right)^{\frac{1}{\alpha+\beta-2}}$$

On taking $H=\left(\frac{\beta-\alpha}{\alpha+\beta-1}\int_0^\infty p^{\alpha+\beta-1}(x)dx\right)^{\frac{1}{2-\alpha-\beta}}$ as the normalization factor,

$$p(x)=\frac{1}{H}\left[\lambda+\gamma_0x+\gamma_1x^2+\sum_{j=1}^{n}\xi_j(x-K_j)^+\right]^{\frac{1}{\alpha+\beta-2}}$$

which can be further written as

$$p(x)=\left[\overline{\lambda}+\overline{\gamma_0}x+\overline{\gamma_1}x^2+\sum_{j=1}^{n}\overline{\xi_j}(x-K_j)^+\right]^{\frac{1}{\alpha+\beta-2}} \tag{4.3.8}$$

where $\overline{\lambda}=\frac{\lambda}{H^{\alpha+\beta-2}}$, $\overline{\gamma_0}=\frac{\gamma_0}{H^{\alpha+\beta-2}}$, $\overline{\gamma_1}=\frac{\gamma_1}{H^{\alpha+\beta-2}}$ and $\overline{\xi_j}=\frac{\xi_j}{H^{\alpha+\beta-2}}$ for $j=1,2,...,n$.

This is the required power law expression for the density function (risk-neutral) of the future asset price. The new set of variables (will be called the normalized Lagrange multipliers) $\overline{\lambda}$, $\overline{\gamma_0}$, $\overline{\gamma_1}$ and $\overline{\xi_j}$, $(j = 1,2,...,n)$, are obtained by solving the constraints $(4.2.2), (4.3.1), (4.3.2)$ and $(4.3.5)$ numerically.

The inclusion of the second order moment constraint has made the system complex. Before applying the numerical procedures, the constraint equations are further simplified. For this, putting the value of $p(x)$ from Eq.$(4.3.8)$ in Eq.$(4.2.2)$

to get

$$\int_0^{\infty}\left[\overline{\lambda}+\overline{\gamma_0}x+\overline{\gamma_1}x^2+\sum_{j=1}^{n}\overline{\xi_j}(x-K_j)^+\right]^{\frac{1}{\alpha+\beta-2}}dx=1 \tag{4.3.9}$$

For $0<K_1<K_2<...<K_n$, The integral $(4.3.9)$ splits in $n+1$ integrals as

$$\begin{aligned}&\int_0^{K_1}\left(\overline{\lambda}+\overline{\gamma_0}x+\overline{\gamma_1}x^2\right)^{\frac{1}{\alpha+\beta-2}}dx+\int_{K_1}^{K_2}\left(\overline{\lambda}+\overline{\gamma_0}x+\overline{\gamma_1}x^2+\overline{\xi_1}(x-K_1)\right)^{\frac{1}{\alpha+\beta-2}}dx\\&+\int_{K_2}^{K_3}\left(\overline{\lambda}+\overline{\gamma_0}x+\overline{\gamma_1}x^2+\overline{\xi_1}(x-K_1)+\overline{\xi_2}(x-K_2)\right)^{\frac{1}{\alpha+\beta-2}}dx\\&+\ldots+\int_{K_n}^{\infty}\left(\overline{\lambda}+\overline{\gamma_0}x+\overline{\gamma_1}x^2+\sum_{j=1}^{n}\overline{\xi_j}(x-K_j)\right)^{\frac{1}{\alpha+\beta-2}}dx=1\end{aligned}$$

which on further simplification gives

$$\begin{aligned}&\int_0^{K_1}\left(\overline{\lambda}+\overline{\gamma_0}x+\overline{\gamma_1}x^2\right)^{\frac{1}{\alpha+\beta-2}}dx+\int_{K_1}^{K_2}\left((\overline{\lambda}-\overline{\xi_1}K_1)+(\overline{\gamma_0}+\overline{\xi_1})x+\overline{\gamma_1}x^2\right)^{\frac{1}{\alpha+\beta-2}}dx\\&+\int_{K_2}^{K_3}\left((\overline{\lambda}-\sum_{j=1}^{2}\overline{\xi_j}K_j)+(\overline{\gamma_0}+\sum_{j=1}^{2}\overline{\xi_j})x+\overline{\gamma_1}x^2\right)^{\frac{1}{\alpha+\beta-2}}dx\\&+\ldots+\int_{K_n}^{\infty}\left((\overline{\lambda}-\sum_{j=1}^{n}\overline{\xi_j}K_j)+(\overline{\gamma_0}+\sum_{j=1}^{n}\overline{\xi_j})x+\overline{\gamma_1}x^2\right)^{\frac{1}{\alpha+\beta-2}}dx=1\end{aligned}$$

Without loss of generality, taking $K_0=0,\ K_{n+1}=\infty$ and $\overline{\xi_0}=0$, the above equation is written as

$$\sum_{i=0}^{n}\int_{K_i}^{K_{i+1}}\left[(\overline{\lambda}-\sum_{j=0}^{i}\overline{\xi_j}K_j)+(\overline{\gamma_0}+\sum_{j=0}^{i}\overline{\xi_j})x+\overline{\gamma_1}x^2\right]^{\frac{1}{\alpha+\beta-2}}dx=1$$

This expression is of the form

$$\sum_{i=0}^{n}\int_{K_i}^{K_{i+1}}\left(ax^2+b_ix+c_i\right)^{\frac{1}{\alpha+\beta-2}}dx=1 \tag{4.3.10}$$

where $a=\overline{\gamma_1},\ b_i=\overline{\gamma_0}+\sum_{j=0}^{i}\overline{\xi_j}$ and $c_i=\overline{\lambda}-\sum_{j=0}^{i}\overline{\xi_j}K_j$ for $i=0,1,...,n$.

Similarly, substituting the value of $p(x)$ from Eq.$(4.3.8)$ in Eqs.$(4.3.1),(4.3.2)$ and $(4.3.5)$, we get

$$\sum_{i=0}^{n}\int_{K_i}^{K_{i+1}}x\left(ax^2+b_ix+c_i\right)^{\frac{1}{\alpha+\beta-2}}dx=S_0e^{rT}, \tag{4.3.11}$$

$$\sum_{i=0}^{n}\int_{K_i}^{K_{i+1}}x^2\left(ax^2+b_ix+c_i\right)^{\frac{1}{\alpha+\beta-2}}dx=V_T \tag{4.3.12}$$

and

$$\sum_{i=l}^{n}\int_{K_i}^{K_{i+1}}(x-K_l)\left(ax^2+b_ix+c_i\right)^{\frac{1}{\alpha+\beta-2}}dx=C_le^{rT} \tag{4.3.13}$$

where $l=1,2,...,n$.

So the Eqs.$(4.3.10),(4.3.11),(4.3.12)$ and $(4.3.13)$ represent the simplified constraint equations. These constraints are solved for $1<\alpha+\beta<2$ by taking $\frac{1}{\alpha+\beta-2}=-q$, where $q(\geq 2)$ is assumed to be a positive integer. This gives $\alpha+\beta=\frac{2q-1}{q}$.

The Newton Raphson method is applied to find the value of the normalized Lagrange multipliers using $MATLAB2012b$. The run time is very small of the order of 10^{-1}s. The density function is calibrated using S&P 500 and FTSE 100 index options data for the options starting from January $4,2016$ with time to maturity 177 and 91 days. The initial price of the underlying asset of S&P 500 index is 2013.99 and of FTSE 100 index is 6093.43.

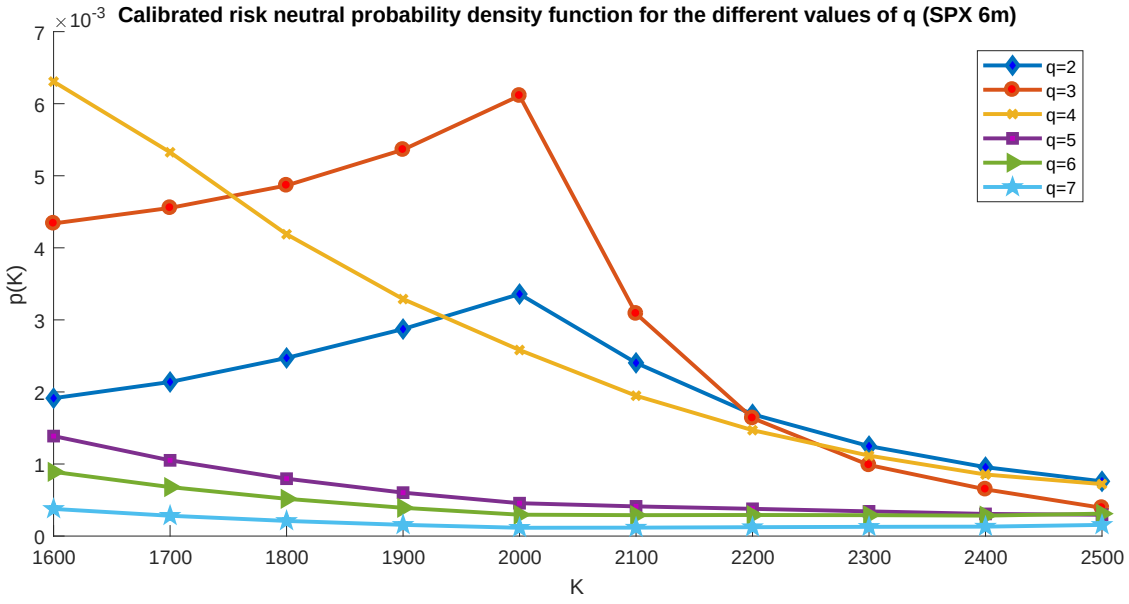

Figure 4.1: Calibrated risk-neutral density function p(K) for the different values of q, starting from $q=2$, using the S&P 500 index options data from January $4,2016$ with maturity 177 days.

The risk-neutral density function is plotted for the different values of q for both the indices at two different maturities. It is observed that with an increase in the value of q, the graph has a very small vertical displacement for both the data sets. This is given in Fig.4.1 and Fig.4.2 for S&P 500 index at two different maturities. Also, for FTSE 100 index, see Fig.4.3 and Fig.4.4 at two different maturities.

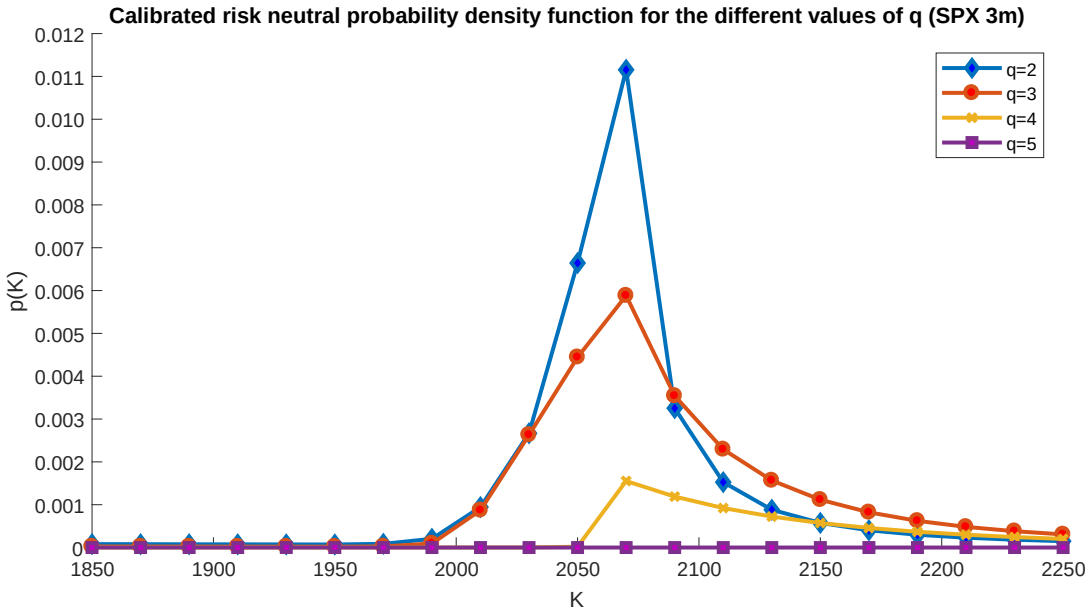

Figure 4.2: Calibrated risk-neutral density function p(K) for the different values of q, starting from $q = 2$, using the S&P 500 index options data from January $4, 2016$ with maturity 91 days.

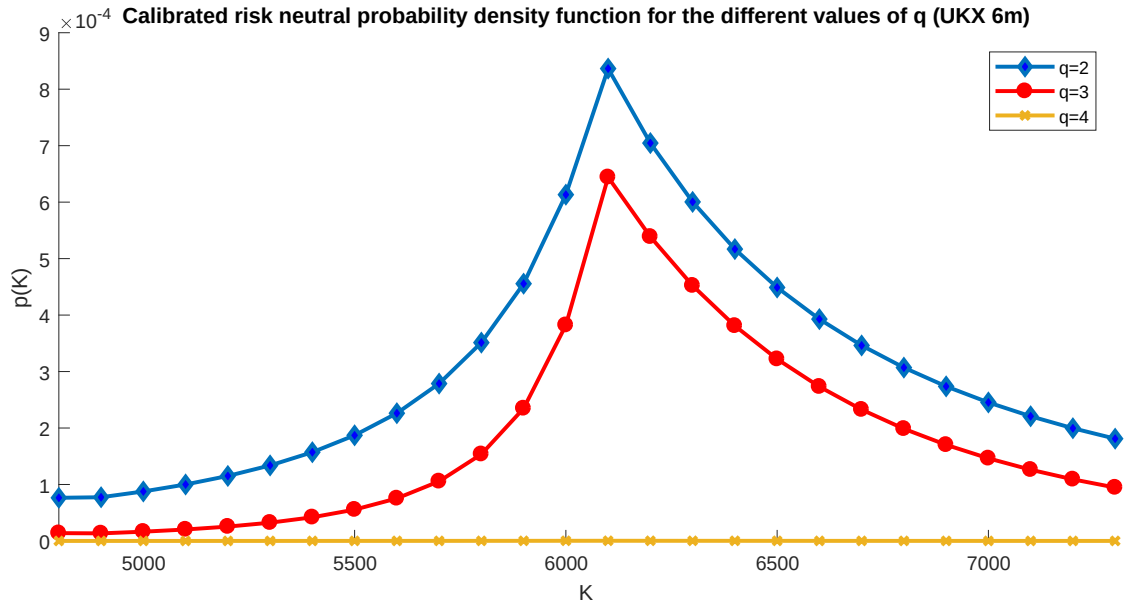

Figure 4.3: Calibrated risk-neutral density function p(K) for the different values of q, starting from $q = 2$, using the FTSE 100 index options data from January $4, 2016$ with maturity 177 days.

The range of $\alpha + \beta$ is governed by the nature and the number of constraints used i.e. by the expression of $G(x)$ used to impose the constraints. So it will be changed by the inclusion or exclusion of the new constraints. With the mean and the variance constraints and with the S&P 500 index options data for two different maturities, the calibrated risk-neutral probability density function is given in

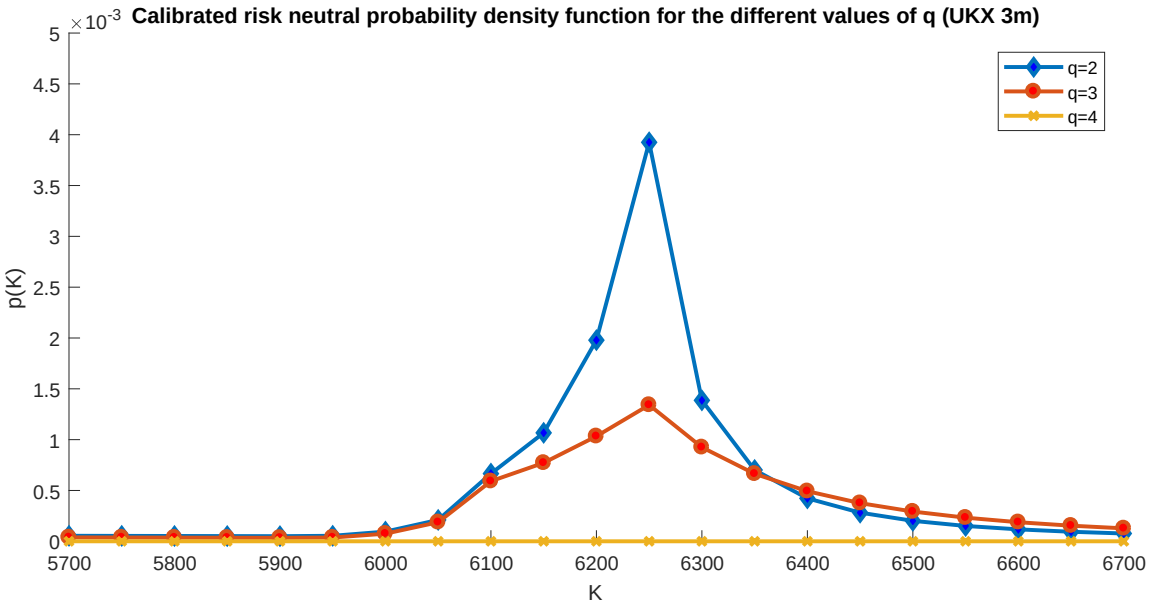

Figure 4.4: Calibrated risk-neutral density function p(K) for the different values of q, starting from $q = 2$, using the FTSE 100 index options data from January $4, 2016$ with maturity 91 days.

Fig.4.1 and Fig.4.2. Similarly, with the mean and the variance constraints and with the FTSE 100 index options data for two different maturities, the calibrated risk-neutral density function is given in Fig.4.3 and Fig.4.4. It is observed in both the data sets that the desired power law distribution is obtained for the small values of q for both the maturities. Particularly, for q ranging from 2 to 4 for S&P 500 index data set and q ranging from 2 to 3 for FTSE 100 index.

On considering $\alpha+\beta = \frac{2q-1}{q}$, the expression of $p(x)$ in Eq.$(4.3.8)$ becomes

$$p(x) = \left[\overline{\lambda} + \overline{\gamma_0}x + \overline{\gamma_1}x^2 + \sum_{j=1}^{n} \overline{\xi_j}(x-K_j)^+\right]^{-q} \tag{4.3.14}$$

with the power (exponent) of the tail distribution $2q$.

For S&P 500 index with $q = 2$ to 4, the power of x varies from 4 to 8 and $\alpha+\beta$ varies from 1.5 to 1.75. Here, α and β satisfy $\beta \geq 1$ and $\beta - 1 < \alpha < \beta$. For $\beta = 1$, the Varma entropy reduces to the Rényi entropy giving $0.5 \leq \alpha \leq 0.75$. Unlike the Varma entropy, the Rényi entropy is monotonically decreasing, so it is maximized for $\alpha = 0.5$ with exponent of the power law distribution equal to 4 for $q = 2$.

For $\beta > 1$, α takes possible values in the range $\beta - 1 < \alpha < \beta$. For example, if $\alpha+\beta = 1.5$, with $\beta = 1.1$ then $\alpha = 0.4$ (a unique value) in the range $0.1 < \alpha < 1.1$ so that their sum remains 1.5, and with $\beta = 1.2$, α becomes 0.3 which is well

within the range $0.2 < \alpha < 1.2$ so that their sum remains 1.5 and so on. Thus for a particular value of $\alpha+\beta$, infinite pairs (α,β) are obtained in accordance with the desired power law distribution.

For the FTSE 100 index, the range of $\alpha+\beta$ is $1.5 \leq \alpha+\beta \leq 1.66$ with the exponent of the tail distribution ranging from 4 to 6. For $\beta = 1$, the Varma entropy reduces to the Rényi entropy giving $0.5 \leq \alpha \leq 0.66$ which is maximized for $\alpha = 0.5$ with exponent of the power law distribution equal to 4 for $q = 2$.

The pricing of the European call options using the density function thus obtained is discussed in next section.

4.4 Option Price Calibration

The price of the European call option with strike price K and maturity time T is given as

$$C(K) = \left[\int_0^\infty (x-K)^+ p(x)dx\right] e^{-rT}$$

Using the expression of $p(x)$ given in Eq.$(4.3.8)$, it becomes

$$C(K) = \left[\int_K^\infty (x-K)\left(\overline{\lambda} + \overline{\gamma_0}x + \overline{\gamma_1}x^2 + \sum_{j=1}^{n} \overline{\xi_j}(x-K_j)^+\right)^{\frac{1}{\alpha+\beta-2}} dx\right] e^{-rT} \tag{4.4.1}$$

The strike price K can lie in any of the range $K_{l-1} \leq K < K_l, l = 1,2,...,n+1$ where $K_0 < K_1 < K_2 < ... < K_n < K_{n+1}$, $K_0 = 0$ and $K_{n+1} = \infty$. For $l = 1,2,...,n$, the integral on the right side of Eq.$(4.4.1)$ is simplified to give

$$\begin{aligned} C(K) = \Bigg[&\int_K^{K_l} (x-K)\left(ax^2 + b_{l-1}x + c_{l-1}\right)^{\frac{1}{\alpha+\beta-2}} dx + \\ &\sum_{i=l}^{n} \int_{K_i}^{K_{i+1}} (x-K)\left(ax^2 + b_i x + c_i\right)^{\frac{1}{\alpha+\beta-2}} dx\Bigg] e^{-rT}, \end{aligned} \tag{4.4.2}$$

and for $l = n+1$, it simply gives

$$C(K) = \left[\int_K^\infty (x-K)\left(ax^2 + b_n x + c_n\right)^{\frac{1}{\alpha+\beta-2}} dx\right] e^{-rT}$$

If $K = K_l$ for some $l = 1,2,...,n$, then $C(K_l) = C_l$ which is given by Eq.$(4.3.13)$.

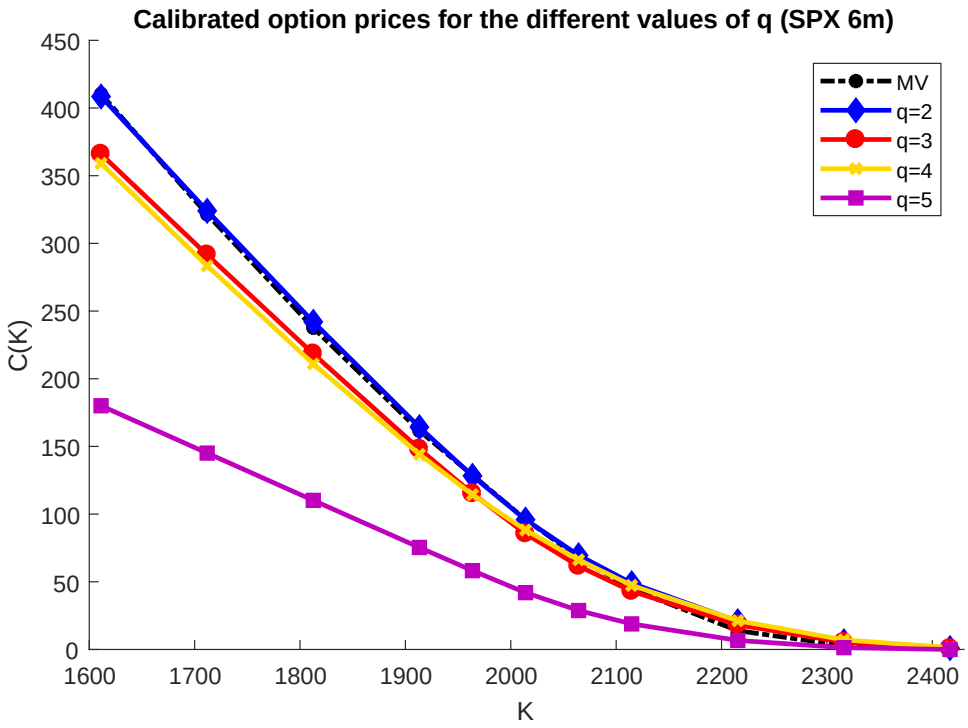

Figure 4.5: Calibrated option prices C(K) at the different values of q, starting from $q = 2$, for the S&P 500 index options from January $4, 2016$ with maturity 177 days.

The option prices are calibrated for S&P 500 index and FTSE 100 index with maturity 177 days and 91 days. For the S&P 500 index option data with maturity 177 days, Fig.4.5 is obtained. The corresponding market values (MV) of option with different strikes are given by the dotted line. For S&P 500 index with maturity 177 days, $q = 2$ fits better for in-the-money (ITM) and at-the-money (ATM) options whereas for out-the-money (OTM) options $q = 3$ gives the better fit. It is to be noted here that as the Rényi entropy is a particular case of the Varma entropy with $q = 2$ only, so it does not give the good fit for OTM options. Hence, the fit is much improved for the Varma entropy, obtained collaboratively with $q = 2$ and 3.

Similarly, for the input data of options with maturity 91 days, Fig.4.6 is obtained. Here also, the best fit is obtained for Varma entropy collaboratively with $q = 2$ and 3, showing an improvement over the one-parameter Rényi entropy.

Also, for FTSE 100 index options, as shown by Fig.4.7 and Fig.4.8, the best fit is given collaboratively with $q = 2$ and 3. This also supports the fact that the consideration of Varma entropy gives improved results over the one-parameter Rényi entropy.

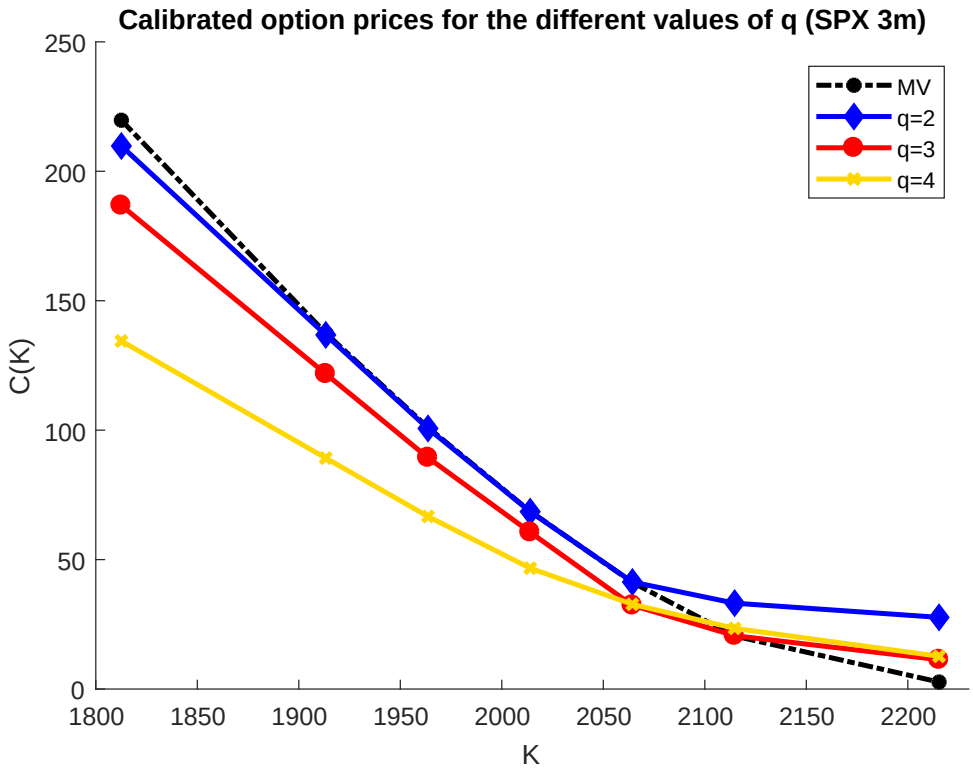

Figure 4.6: Calibrated option prices C(K) at the different values of q, starting from $q = 2$, for the S&P 500 index options from January $4, 2016$ with maturity 91 days.

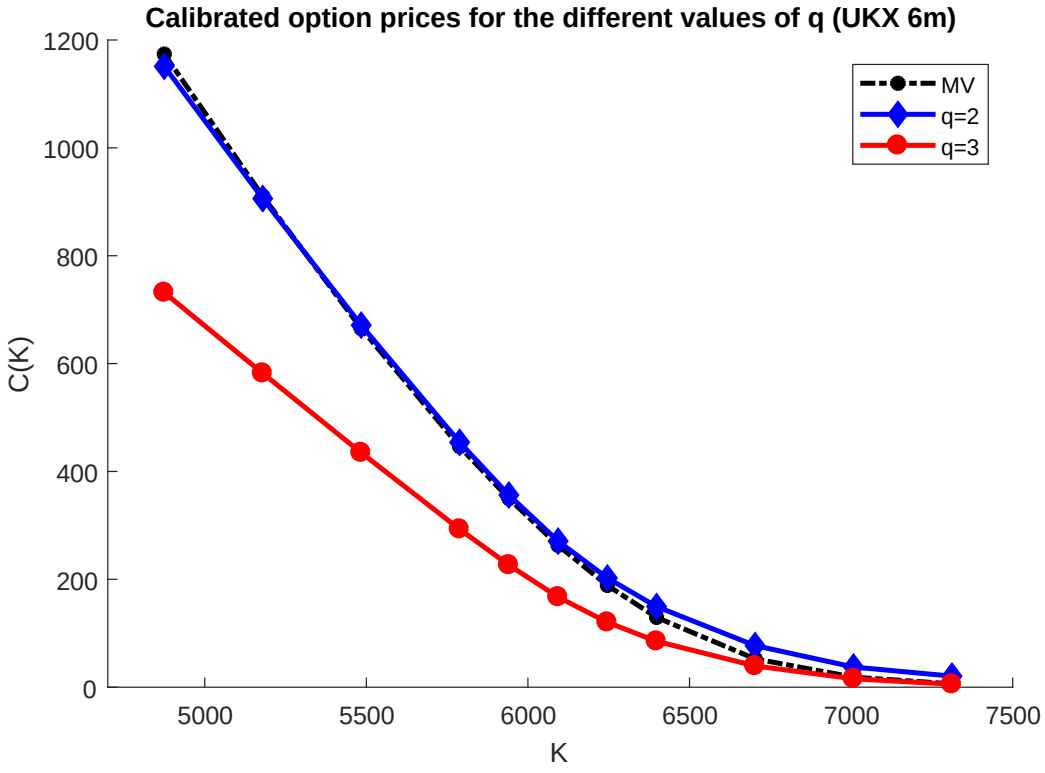

Figure 4.7: Calibrated option prices C(K) at the different values of q, starting from $q = 2$, for the FTSE 100 index options from January $4, 2016$ with maturity 177 days.

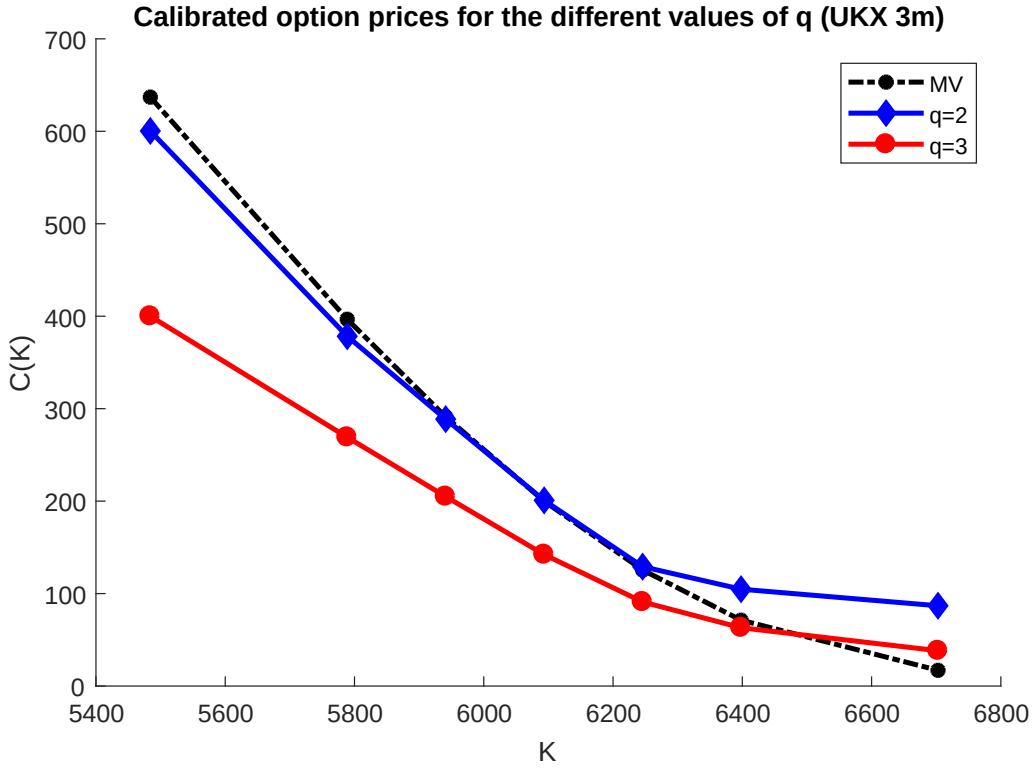

Figure 4.8: Calibrated option prices C(K) at the different values of q, starting from $q = 2$, for the FTSE 100 index options from January $4, 2016$ with maturity 177 days.

In the literature, much discussion is for the maximization of the Shannon entropy under certain constraints which gives the lognormal distribution of the future asset price. Brody et al. [16] extended this to the maximization of the one-parameter Rényi entropy under the first order moment constraint which gives the more realistic power law distribution for a single value of the entropy parameter α.

Here our contribution is two fold. One by maximization of the two-parameter Varma entropy and another by the introduction of the volatility constraint following a particular path. The benefit of the two-parameter formulation is the additional degrees of freedom and the better fit to market data than the single parametric formulation which in turn was better than the Shannon entropy framework.

Also, Brody et al. [16] has already established that under the same constraints, the maximization of the Tsallis entropy is equivalent to the maximization of the Rényi entropy. The maximization of the Rényi entropy with the additional volatility constraint is the particular case of the Varma entropy maximization with $\beta = 1$. Therefore, It can be inferred that the maximisation of the Tsallis entropy with additional volatility constraint is equivalent to the maximization of Varma entropy for $\beta = 1$.

4.5 Conclusion

The two-parameter Varma entropy is maximized with an additional volatility constraint. In this constraint, variance follows a mean-reverting quadratic path and its value is considered at the terminal time T. The entropy maximization gives the power law distribution of the future asset prices. The maximum entropy density function is calibrated against the options data of S&P 500 index and FTSE 100 index for maturity 177 days and 91 days. It is observed that, for S&P 500 index data set, the exponent of the power law lies in the range 4 to 8 and for FTSE 100 index it lies in range 4 to 6. For S&P 500 index data set, $\alpha+\beta$ lies in the range 1.5 to 1.75 and in the range 1.5 to 1.66 for FTSE 100 index. The results are also discussed for the Rényi entropy case giving an exponent of the tail distribution equal to 4, and $\alpha = 0.5$ for both the indices. For the data sets under consideration, Varma entropy gives the better fit to market option prices than the Rényi entropy, obtained collaboratively with $q = 2$ and 3. Though we understand that practitioners will be at convenience to use a single density function for the purpose of calibration of option prices, we observe that the fractional values of q will add complexity and hence not being recommended here. Further we are of the opinion, as exhibited by the computation and the graphs, considering two values of q to calibrate the option price is providing a better anatomy of the market for the data sets under consideration.

The improvement in the calibration results and the additional degrees of freedom provided by Varma entropy, also motivated us to apply this two-parameter entropy for the analysis of asset log-return series, because the entropy based measures are used in literature to quantify the complexity of a time series. So the financial time series analysis aspect is explored in the next chapter using the Varma entropy to introduce a two-parameter permutation entropy and its further extensions which include weights and multiscales.

Chapter 5

Analysis of the Financial Log-Return Time Series using Two-Parameter Permutation Entropy

---

In this chapter[1]*, a two-parameter permutation entropy is proposed. This entropy is extended to obtain a two-parameter multiscale permutation entropy by introducing a new coarse graining method of averaging the data points. Further, a two-parameter weighted multiscale permutation entropy is also introduced which captures the complexity of a financial time series on the multiple time scales, with the additional amplitude information captured by including weights. For calculating the weights of the neighbouring vectors, a new weighting scheme is proposed. An empirical analysis is conducted on S&P* 500 *index data by comparing these entropies at different values of embedding dimensions, scales and entropy parameters. The effect of change in entropy parameters on the entropy values is also discussed.*

---

[1]The work reported in this chapter is communicated under the titles **"Two-Parameter Multiscale Permutation Entropy of a Financial Time Series"** and **"Analysis of Financial Time Series Using a Two-Parameter Weighted Multiscale Permutation Entropy"**. Some of this work is presented in 'International Conference on Recent Advances in Pure and Applied Mathematics (ICRAPAM)-2018' held at Delhi Technological University, Delhi from October $23-25, 2018$.

5.1 Introduction

One of the interesting ways to analyse the complexity of any financial time series is by using the concept of entropy. As already mentioned in Subsection 1.5.1 of Chapter 1, to capture the multiple time scales inherent in healthy physiological dynamics, Costa et al. [24] introduced the concept of multiscale entropy using the coarse graining procedure given in Eq.(1.5.8). Yin and Shang [125] extended this concept to introduce a multiscale permutation entropy (MPE) by calculating the permutation entropy (PE) instead of sample entropy (SampEn) in the multiscale entropy procedure. They also proposed the modification of MPE as the weighted multiscale permutation entropy (WMPE) using the weighted permutation entropy of Fadlallah et al. [32] given in Eq.(1.5.11), which captures the amplitude information of a non-linear time series using a weighting scheme based on the variance of each neighbouring vector.

The MPE and WMPE procedures involve the calculation of Shannon entropy. Chen et al. [19] proposed the multiscale Rényi permutation entropy (MRPE) and weighted multiscale Rényi permutation entropy (WMRPE) using Rényi permutation entropy (RPE), which is a natural extension of PE to a one-parameter PE.

We have already used Varma entropy [117] in the previous chapter for the calibration of the risk-neutral probability density function, generalizing the results given by Buchen and Kelly [17] and Brody et al. [16] on Shannon and Rényi entropies respectively. In the present chapter, we have proposed a two parametric generalisation of PE by calculating the Varma entropy in place of Shannon entropy in the PE procedure given in Eq.(1.5.6) and have named it as *two-parameter permutation entropy* ($\mathrm{PE}_{\alpha,\beta}$).

For the inclusion of multiscales in $\mathrm{PE}_{\alpha,\beta}$, we have proposed a new averaging scheme as a modification of the conventional coarse graining procedure of Costa et al. [24] by taking the last data point of the present window in the next window while averaging. This gives the *two-parameter multiscale permutation entropy* ($\mathrm{MPE}_{\alpha,\beta}$) on overlapping scales.

To capture the amplitude information, the weights are included in $\mathrm{MPE}_{\alpha,\beta}$ procedure. By using the weighting scheme of Fadlallah et al. [32] given in Eq.(1.5.11), $\mathrm{MPE}_{\alpha,\beta}$ gives a *two-parameter weighted multiscale permutation*

entropy (WMPE$^{v}_{\alpha,\beta}$).

Along with this, a new weighting scheme is also proposed. For this, the overall change in value from initial to final component of a neighbouring vector is proposed as a weight of this vector. The resultant entropy using this new weighting scheme is named as a *two-parameter new weighted multiscale permutation entropy* (WMPE$^{w}_{\alpha,\beta}$).

An empirical analysis is conduced using the closing prices of S&P 500 index data. The two weighting schemes are compared in two-parameter permutation entropy framework. The new weighting scheme proposed in this chapter, successfully captures the amplitude information inherent in the financial log-return series. It is simple, robust, computationally fast and has less standard deviation than weighting scheme of Fadlallah et al. [32] of taking variance as weight. To show the advantage of taking overlapping average over non-overlapping average, the MPE$_{\alpha,\beta}$, WMPE$^{v}_{\alpha,\beta}$ and WMPE$^{w}_{\alpha,\beta}$ are calculated and compared on both overlapping and non-overlapping scales.

The effect of change of parameters α and β on the entropy values is also discussed. The MPE and WMPE methods of Yin and Shang [125] and MRPE and WMRPE methods of Chen et al. [19] become the particular cases of WMPE$^{v}_{\alpha,\beta}$ over the non-overlapping scales. Consideration of two-parameter entropy gives additional degrees of freedom to quantify the complexity of any non-linear time series.

The rest of the chapter is organized as follows: In Section 5.2, the end point overlapping average scheme has been introduced. Two-parameter permutation entropy and its extensions to include multiscales and weights have been proposed in Section 5.3. The new weighting scheme has also been introduced in this section. Section 5.4 includes the empirical analysis and discussion of the results. Finally, the conclusion has been given in Section 5.5.

5.2 The End Point Overlapping Average

The coarse graining procedure of Costa et al. [24], given in Eq.$(1.5.8)$, considers the average over disjoint windows to obtain a new time series. For a financial log-return series $\{x_i\}_{i=1}^{N}$ of length N, which is obtained from the daily closing price of an asset, such an average is represented in Fig.5.1 for scale 2 and 3.

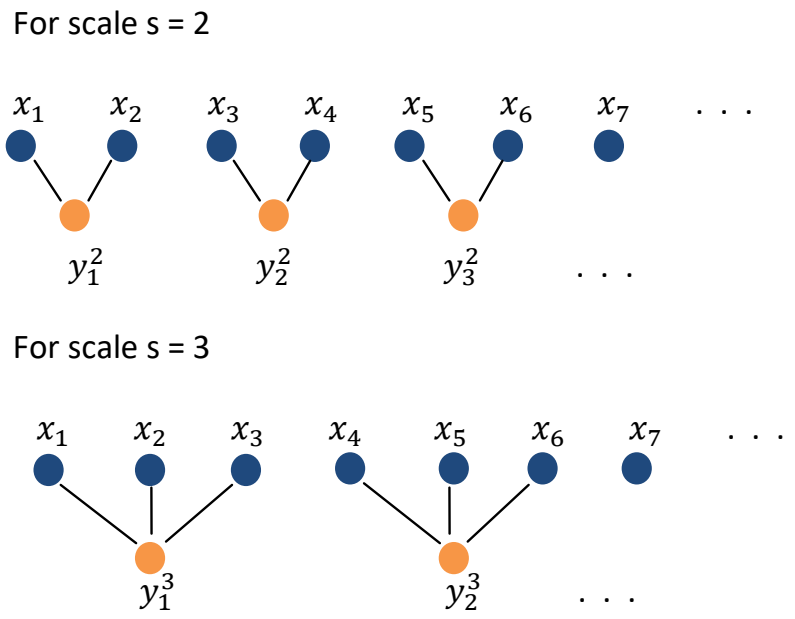

Figure 5.1: Non-overlapping average with scale 2 and 3.

For scale $s = 2$, the first data point of the new series ($y_1^2 = \frac{x_1+x_2}{2}$) accommodates the information about log-returns of the asset from day 1 to day 2. The next data point accommodates the information of asset log-returns from day 3 to day 4. No information is captured for the log-returns from day 2 to day 3. This results in the discontinuity and loss of information in the new data set thus generated. The same situation arises for the other values of scale factor s.

Thus, to maintain a continuity in the data set and to capture the information between the terminal points while switching from present window to the next window, a new averaging scheme is proposed. The new method involves the average over overlapping windows of length s (scale factor), with last data point of the present window to be considered in the next window while averaging. This averaging scheme is named as the end point overlapping (EPO) scheme. The procedure is explained as below:

Consider a one dimensional discrete time series $\{x_i\}_{i=1}^N$ from which a time series $\{z_j^s,\ j = 1,2,...,[\frac{N-1}{s-1}]\}$ is constructed by averaging the data points over the overlapping windows (with only end point overlapping) of length $s \geq 2$ given by

$$z_j^s = \frac{1}{s} \sum_{i=((j-1)(s-1))+1}^{j(s-1)+1} x_i \tag{5.2.1}$$

where $1 \leq j \leq \left[\frac{N-1}{s-1}\right]$ with $[.]$ as the greatest integer function.

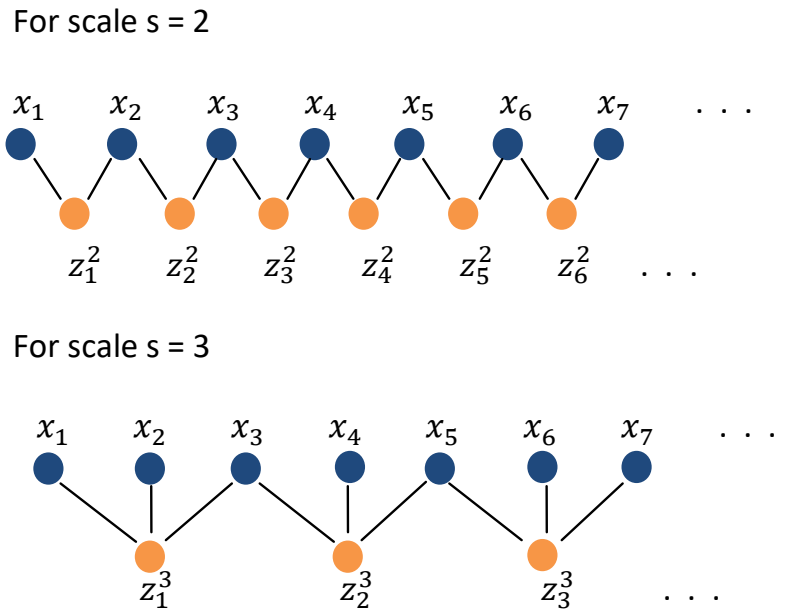

Figure 5.2: EPO average with scale 2 and 3.

For $s = 1$, there will be no end point overlapping average. So, $s = 1$ case is taken here as the original time series. This scheme is also shown in Fig.5.2 for scale 2 and 3.

The EPO scheme captures the information between the last day of a particular window to the first day of its next window which is not captured by considering non-overlapping scales.

Moreover, the average over the disjoint windows of length s reduces the length of the series to $\left[\frac{N}{s}\right]$. To get the reliable results in permutation entropy procedure, the length of the series should be significantly larger than the embedding dimension (m) (refer to Yin and Shang [125]). So, when the permutation entropy is calculated for a short time series it may lead to the unappropriate results at large value of embedding dimension. With the EPO scheme, the length of the new series obtained after averaging is $\left[\frac{N-1}{s-1}\right]$ which is larger than $\left[\frac{N}{s}\right]$.

5.3 Two Parametric Entropy Methods

In this section, we have proposed the two-parameter permutation entropy. This entropy is further extended to a two-parameter multiscale permutation entropy and a two-parameter weighted multiscale permutation entropy.

5.3.1 Two-Parameter Permutation Entropy

In Subsection 1.5.1 of Chapter 1, permutation entropy (PE) procedure is explained. We here propose the two-parameter permutation entropy ($PE_{\alpha,\beta}$) which is the refinement of PE, by calculating the Varma entropy (1.5.5) instead of the Shannon entropy in Eq.(1.5.6). It is given as

$$H(m,\tau,\alpha,\beta) = \frac{1}{\beta-\alpha}\log\left(\sum_{l=1}^{m!}(p(\pi_l))^{\alpha+\beta-1}\right) \tag{5.3.1}$$

where the relative frequencies $p(\pi_l)$ are given in Eq.(1.5.7). α and β satisfy the conditions $\beta \geq 1$, $\beta-1<\alpha<\beta$ and $\alpha+\beta \neq 2$. Clearly $\alpha+\beta>1$. For a particular value of m, $PE_{\alpha,\beta}$ gives a range of values with different combinations of α and β but the PE gives only single value. Thus $PE_{\alpha,\beta}$ generalizes PE. This is also discussed empirically in Subsection 5.4.2.

$PE_{\alpha,\beta}$ is a single scale entropy. To capture the multiple time scales inherent in the financial time series, this entropy is extended to a two-parameter multiscale permutation entropy as given in the next subsection.

5.3.2 Two-Parameter Multiscale Permutation Entropy

For the multiscale analysis, a new time series $\{z_j^s; j=1,2,...,[\frac{N-1}{s-1}]\}$ is obtained from the original time series $\{x_i\}_{i=1}^N$ by the EPO average scheme. It is represented in Eq.(5.2.1) as

$$z_j^s = \frac{1}{s}\sum_{i=((j-1)(s-1))+1}^{j(s-1)+1} x_i$$

where $s \geq 2$. For $s=1$, the results are discussed for the original time series $\{x_i\}_{i=1}^N$ because there will be no end point overlapping. For each new time series $\{z_j^s\}$, obtained at different values of scale factor s, $PE_{\alpha,\beta}$ is calculated as follows:

Consider the representation of data points of series $\{z_j^s\}$ as vectors

$$Z_t^s(m,\tau) = (z_t^s,\, z_{t+\tau}^s, ...,\, z_{t+(m-1)\tau}^s)$$

where $t=1,2,...,T-(m-1)\tau$ with $T=[\frac{N-1}{s-1}]$, embedding dimension m and time delay τ. Each of these $T-(m-1)\tau$ vectors has m components. As m different numbers can be ordered in $m!$ ways, so each vector is assigned a pattern out of

the $m!$ possible patterns $\{\pi_l\}_{l=1}^{m!}$. $\text{PE}_{\alpha,\beta}$ of the time series $\{z_j^s\}_{j=1}^{T}$ with $m \geq 2$ is defined in the discrete form as

$$H(m,\tau,\alpha,\beta) = \frac{1}{\beta-\alpha}\log\left(\sum_{l=1}^{m!}(p_z(\pi_l))^{\alpha+\beta-1}\right) \tag{5.3.2}$$

This entropy is called the two-parameter multiscale permutation entropy ($\text{MPE}_{\alpha,\beta}$) with EPO scales. The parameters α and β must satisfy the conditions $\beta-1<\alpha<\beta$, $\beta \geq 1$ and $\alpha+\beta \neq 2$ of Varma entropy. Clearly $\alpha+\beta>1$. Here, the relative frequency $p_z(\pi_l)$ is given as

$$p_z(\pi_l) = \frac{||\{t:\ t \leq T-(m-1)\tau,\ \ (z_t^s,\ z_{t+\tau}^s,...,\ z_{t+(m-1)\tau}^s)\ \ has\,the\,ordinal\,pattern\,\pi_l\}||}{T-(m-1)\tau} \tag{5.3.3}$$

It can be rewritten as

$$p_z(\pi_l) = \frac{\sum_{t\leq T-(m-1)\tau}\ I_{A_l}(Z_t^s(m,\tau))}{\sum_{t\leq T-(m-1)\tau}\ I_B(Z_t^s(m,\tau))} \tag{5.3.4}$$

where $I_X(Z)$ denotes the indicator function such that $I_X(z)=1$ if $z \in X$ otherwise $I_X(z)=0$, for an element z of Z. A_l is the set of all those vectors which have the ordinal pattern π_l. B is the set of all those vectors which have ordinal patterns in the set $\{\pi_l\}_{l=1}^{m!}$.

To compare the EPO scheme with the conventional coarse graining procedure, the $\text{MPE}_{\alpha,\beta}$ is also calculated over non-overlapping scales. The procedure involves the averaging of data points of the original time series $\{x_i\}_{i=1}^{N}$ over the non-overlapping windows of length s to get a coarse grained time series $\{y_r^s\}, r=1,2,...,[\frac{N}{s}]$ given as

$$y_r^s = \frac{1}{s}\sum_{i=(r-1)s+1}^{rs} x_i\ ;\ 1 \leq r \leq \left[\frac{N}{s}\right] \tag{5.3.5}$$

For the scale factor $s=1$, the time series in Eq.(5.3.5) becomes the original time series $\{x_i\}_{i=1}^{N}$. For each coarse grained series in Eq.(5.3.5), obtained at different values of scale factor s, the $\text{PE}_{\alpha,\beta}$ (5.3.2) is calculated with relative frequencies

$$p_y(\pi_l) = \frac{\sum_{t\leq M-(m-1)\tau}\ I_{A_l}(Y_t^s(m,\tau))}{\sum_{t\leq M-(m-1)\tau}\ I_B(Y_t^s(m,\tau))} \tag{5.3.6}$$

here $Y_t^s(m,\tau)=(y_t^s,y_{t+\tau}^s,...,y_{t+(m-1)\tau}^s)$ is the vector with $t=1,2,...,M-(m-1)\tau$. $M=[\frac{N}{s}]$ and I denotes the indicator function as explained earlier. This gives the

$\text{MPE}_{\alpha,\beta}$ over non-overlapping scales.

In the $\text{MPE}_{\alpha,\beta}$ over non-overlapping scales, when $\beta = 1$, MRPE of order α given by Chen et al. [19] is obtained. Moreover, for $\beta = 1$ and $\alpha = 1$, MPE of Yin and Shang [125] is obtained.

The $\text{MPE}_{\alpha,\beta}$ is extended to include the weights in the PE procedure over EPO and non-overlapping scales. For the inclusion of weights, a new weighting scheme is also proposed in the next subsection.

5.3.3 Two-Parameter New Weighted Multiscale Permutation Entropy

Fadlallah et al. [32] proposed the weighted permutation entropy given in Eq.$(1.5.11)$ to overcome the limitations of PE. Sometimes, variance as weights may not retain the correct amplitude information. For e.g., for the embedding dimension $m = 3$, consider the possible arrangement of data points as $(100, 101, 141)$, $(100, 140, 141)$ and $(100, 60, 101)$. In the first two arrangements, pattern followed by data points is $(0\,1\,2)$. In the last arrangement, the pattern of the data points is $(1\,0\,2)$. Despite of the different variation from initial to final point, these three arrangements have the same variance. So no correct amplitude information is obtained using variance.

In addition, sometimes for a particular pattern, one may be interested in the overall change in the value from the initial position and not on the fluctuations in between the initial and final time. For example, If an investor invests for n days, then his fortune will be the overall change in value of asset (or return) from day 1 to day n and not the fluctuations in between. Similarly, if a person is interested in trading an asset on day 3 from now (as in the European option contract), his return will be dependent on the value of asset on day 3 and not on the fluctuations in between.

For such path-independent patterns, a new weighting scheme is proposed here, to calculate the weights of neighbouring vectors in the weighted permutation entropy procedure. This method is simple and computationally fast. It gives better result than the case of variance as weight because the standard deviation of our new weighting scheme is less than than the standard deviation of weighting scheme of Fadlallah et al. [32] of taking variance as weight (see Table 5.14 in Subsection 5.4.4). The overall change in value from the initial point to final point is taken as the weight of a neighbouring vector ignoring the fluctuations in between

and is defined over EPO scales as:

$$w_t = \sum_{k=1}^{m-1} (z^s_{t+k\tau} - z^s_{t+(k-1)\tau}) \tag{5.3.7}$$

where $Z^s_t(m,\tau) = (z^s_t,\ z^s_{t+\tau},...,\ z^s_{t+(m-1)\tau})$ is a vector from the series $\{z^s_j\}^T_{j=1}$. We define the weighted relative frequencies as

$$p_w(\pi_l) = \frac{\left| \sum_{t \le T-(m-1)\tau} \ I_{A_l}(Z^s_t(m,\tau))\ w_t \right|}{G} \tag{5.3.8}$$

where

$$G = \sum_{l=1}^{m!} \left| \sum_{t \le T-(m-1)\tau} I_{A_l}(Z^s_t(m,\tau))\ w_t \right|$$

The value of $p_w(\pi_l)$ from (5.3.8) is used to calculate the weighted $\mathrm{PE}_{\alpha,\beta}$ given by

$$H_w(m,\tau,\alpha,\beta) = \frac{1}{\beta-\alpha} \log\left(\sum_{l=1}^{m!} p_w(\pi_l)^{\alpha+\beta-1} \right) \tag{5.3.9}$$

where $\beta - 1 < \alpha < \beta$, $\beta \ge 1$ and $\alpha + \beta \ne 2$. This is called the two-parameter new weighted multiscale permutation entropy ($\mathrm{WMPE}^w_{\alpha,\beta}$) with EPO average. On the same lines, $\mathrm{WMPE}^w_{\alpha,\beta}$ can be defined with non-overlapping average.

For comparing the results of this new weighting scheme with the weighting scheme of Fadlallah et al. [32], we define the two-parameter weighted multiscale permutation entropy ($\mathrm{WMPE}^v_{\alpha,\beta}$) using variance as weight for each neighbouring vector $Z^s_t(m,\tau)$. The variance of vector $Z^s_t(m,\tau)$ is

$$v_t = \frac{1}{m} \sum_{k=1}^{m} (z^s_{t+(k-1)\tau} - \overline{Z}^s_t(m,\tau))^2 \tag{5.3.10}$$

where $\overline{Z}_t(m,\tau))$ is the arithmetic mean of vector $Z_t(m,\tau)$. The corresponding weighted relative frequencies are

$$p_v(\pi_l) = \frac{\sum_{t \le T-(m-1)\tau} \ I_{A_l}(Z^s_t(m,\tau))\ v_t}{\sum_{t \le T-(m-1)\tau} \ I_B(Z^s_t(m,\tau))\ v_t} \tag{5.3.11}$$

which give the $\mathrm{WMPE}^v_{\alpha,\beta}$ with EPO scales as

$$H_v(m,\tau,\alpha,\beta) = \frac{1}{\beta-\alpha} \log\left(\sum_{l=1}^{m!} p_v(\pi_l)^{\alpha+\beta-1} \right) \tag{5.3.12}$$

where $\beta-1<\alpha<\beta, \beta \geq 1$ and $\alpha+\beta \neq 2$. Similarly, $\text{WMPE}^{v}_{\alpha,\beta}$ can be defined over non-overlapping scales. After proposing the theoretical framework of $\text{MPE}_{\alpha,\beta}$, $\text{WMPE}^{v}_{\alpha,\beta}$ and $\text{WMPE}^{w}_{\alpha,\beta}$ over non-overlapping and EPO scales, an empirical study is conducted in the next section using the financial market data.

5.4 Empirical Analysis and Discussion of Results

The $\text{PE}_{\alpha,\beta}$ generalizes the PE. For each value of embedding dimension m, only single value of PE is obtained but $\text{PE}_{\alpha,\beta}$ gives a range of values with different combinations of α and β. To show the advantage of considering $\text{PE}_{\alpha,\beta}$ over PE and to compare the $\text{MPE}_{\alpha,\beta}$, $\text{WMPE}^{v}_{\alpha,\beta}$ and $\text{WMPE}^{w}_{\alpha,\beta}$ over EPO scales and non-overlapping scales, an empirical analysis is conducted on the financial market data.

5.4.1 Data Used

The daily closing prices of S&P 500 index from November $1, 2009$ to October $31, 2018$ are considered. This time series contains 2320 data points. The daily logarithmic return of this data is calculated. For the multiscale analysis, the scale factor s is considered from 1 to 10 in both the averaging schemes. Scale factor $s=1$ gives the result for the original time series $\{x_i\}_{i=1}^{N}$.

Bandt and Pompe [8] suggested the range of embedding dimension m from $2, 3, \ldots 7$ for the practical purposes. Also, to obtain the reliable results, the length L of each time series must satisfy the constraint $L >> m!$ for the permutation analysis. Thus for calculating PE and $\text{PE}_{\alpha,\beta}$, m is chosen from 2 to 6 and for the multiscale analysis we have considered m from 2 to 5 to get the reliable results. The time delay τ is chosen 1 for simplicity. β is considered from 1.0 to 1.4 with step size 0.1 and α is considered from 0.1 to 0.9 with step size 0.1. *MATLAB2012b* is used to obtain the results. Only that combination of α and β is considered which satisfies the conditions of Varma entropy on α and β such that $\beta-1<\alpha<\beta, \beta \geq 1$ and $\alpha+\beta \neq 2$. The results obtained are discussed in the next subsections.

5.4.2 Comparison of $PE_{\alpha,\beta}$ with PE

For the data set under consideration, The PE and $PE_{\alpha,\beta}$ values are calculated at the different values of embedding dimension m. It is presented in Table 5.1 and Tables 5.2 to 5.5 respectively.

Table 5.1: Permutation Entropy (PE) for different values of embedding dimension m.

	m				
Entropy	2	3	4	5	6
PE	0.9966	2.5722	4.5584	6.8407	9.1987

Table 5.2: Two-parameter permutation entropy ($PE_{\alpha,\beta}$) at different values of α and β for m=2.

		β				
Entropy	α	1.0	1.1	1.2	1.3	1.4
$PE_{\alpha,\beta}$	0.1	0.9997	–	–	–	–
	0.2	0.9993	0.7770	–	–	–
	0.3	0.9990	0.7490	0.5546	–	–
	0.4	0.9986	0.7131	0.4990	0.3325	–
	0.5	0.9983	0.6653	0.4276	0.2493	0.1108
	0.6	0.9980	0.5986	0.3324	0.1424	–
	0.7	0.9976	0.4986	0.1994	–	–
	0.8	0.9973	0.3323	–	–	–
	0.9	0.9969	–	–	–	–

Table 5.3: Two-parameter permutation entropy ($PE_{\alpha,\beta}$) at different values of α and β for m=3.

		β				
Entropy	α	1.0	1.1	1.2	1.3	1.4
$PE_{\alpha,\beta}$	0.1	2.5837	–	–	–	–
	0.2	2.5824	2.0076	–	–	–
	0.3	2.5812	1.9349	1.4326	–	–
	0.4	2.5799	1.8419	1.2887	0.8587	–
	0.5	2.5786	1.7182	1.1040	0.6437	0.2859
	0.6	2.5773	1.5456	0.8583	0.3676	–
	0.7	2.5760	1.2874	0.5147	–	–
	0.8	2.5748	0.8578	–	–	–
	0.9	2.5735	–	–	–	–

Table 5.4: Two-parameter permutation entropy ($PE_{\alpha,\beta}$) at different values of α and β for m=4.

Entropy	α	β 1.0	1.1	1.2	1.3	1.4
$PE_{\alpha,\beta}$	0.1	4.5823	–	–	–	–
	0.2	4.5797	3.5599	–	–	–
	0.3	4.5770	3.4308	2.5399	–	–
	0.4	4.5744	3.2655	2.2845	1.5221	–
	0.5	4.5717	3.0461	1.9570	1.1409	0.5068
	0.6	4.5691	2.7399	1.5213	0.6516	–
	0.7	4.5664	2.2819	0.9122	–	–
	0.8	4.5638	1.5204	–	–	–
	0.9	4.5611	–	–	–	–

Table 5.5: Two-parameter permutation entropy ($PE_{\alpha,\beta}$) at different values of α and β for m=5.

Entropy	α	β 1.0	1.1	1.2	1.3	1.4
$PE_{\alpha,\beta}$	0.1	6.9002	–	–	–	–
	0.2	6.8935	5.3565	–	–	–
	0.3	6.8869	5.1602	3.8187	–	–
	0.4	6.8802	4.9097	3.4335	2.2868	–
	0.5	6.8736	4.5780	2.9402	1.7135	0.7608
	0.6	6.8670	4.1162	2.2846	0.9782	–
	0.7	6.8604	3.4269	1.3694	–	–
	0.8	6.8538	2.2824	–	–	–
	0.9	6.8472	–	–	–	–

Table 5.6: Two-parameter permutation entropy ($PE_{\alpha,\beta}$) at different values of α and β for m=6.

Entropy	α	β 1.0	1.1	1.2	1.3	1.4
$PE_{\alpha,\beta}$	0.1	9.3902	–	–	–	–
	0.2	9.3671	7.2679	–	–	–
	0.3	9.3445	6.9917	5.1670	–	–
	0.4	9.3223	6.6433	4.6397	3.08627	–
	0.5	9.3006	6.1862	3.9679	2.3095	1.0242
	0.6	9.2793	5.5551	3.0794	1.3169	–
	0.7	9.2585	4.6191	1.8436	–	–
	0.8	9.2381	3.0727	–	–	–
	0.9	9.2182	–	–	–	–

Each column of Tables 5.2 to 5.5 represents the entropy values for a particular β but α varying from 0.1 to 0.9. It is important to notice here that, entropies against only those values of α and β are given which satisfy the conditions $\beta - 1 < \alpha < \beta$, $\beta \geq 1$ and $\alpha + \beta \neq 2$. For a particular β, the entropy value decreases with an

increase in α value and same is the case for a fixed α.

It is clear that the $\text{PE}_{\alpha,\beta}$ generalizes the PE. For $\beta = 1$ and $\alpha \to 1$, the $\text{PE}_{\alpha,\beta}$ reduces to PE for all values of m. For $\beta = 1$, the first column in each of the Tables 5.2 to 5.5 gives the Rényi permutation entropy of Chen et al. [19].

In next subsection, the extensions of $\text{PE}_{\alpha,\beta}$ to $\text{MPE}_{\alpha,\beta}$, $\text{WMPE}^{v}_{\alpha,\beta}$ and $\text{WMPE}^{w}_{\alpha,\beta}$ are compared over EPO and non-overlapping scales.

5.4.3 Comparison of $\text{MPE}_{\alpha,\beta}$, $\text{WMPE}^{v}_{\alpha,\beta}$ and $\text{WMPE}^{w}_{\alpha,\beta}$

The $\text{MPE}_{\alpha,\beta}$, $\text{WMPE}^{v}_{\alpha,\beta}$ and $\text{WMPE}^{w}_{\alpha,\beta}$ on the non-overlapping and EPO scales are compared in this subsection using the data of S&P 500 index. Corresponding to a particular value of m and s, the $\text{MPE}_{\alpha,\beta}$, $\text{WMPE}^{v}_{\alpha,\beta}$ and $\text{WMPE}^{w}_{\alpha,\beta}$ on both non-overlapping and EPO scales, can be represented in a single table. By varying m from 2 to 5 and s from 2 to 10, total 36 such tables will be obtained. Additionally, for $s = 1$, which corresponds to the original time series $\{x_i\}_{i=1}^{N}$ (for both non-overlapping and EPO scales), there will be total 4 tables (one for each value of m). To avoid the excessive number of tables which will be arising out of calculation, we have confined ourselves to $m = 4, 5$ and $s = 1, 4, 7, 10$ in this chapter.

Table 5.7: Two parametric entropies at different values of α and β for s=1 and m=4,5.

		For m = 4					For m = 5				
		β					β				
Entropy	α	1.0	1.1	1.2	1.3	1.4	1.0	1.1	1.2	1.3	1.4
$\text{MPE}_{\alpha,\beta}$	0.1	4.5823	–	–	–	–	6.9002	–	–	–	–
	0.2	4.5797	3.5599	–	–	–	6.8935	5.3565	–	–	–
	0.3	4.5770	3.4308	2.5399	–	–	6.8869	5.1602	3.8187	–	–
	0.4	4.5744	3.2655	2.2845	1.5221	–	6.8802	4.9097	3.4335	2.2868	–
	0.5	4.5717	3.0461	1.9570	1.1409	0.5068	6.8736	4.5780	2.9402	1.7135	0.7608
	0.6	4.5691	2.7399	1.5213	0.6516	–	6.8670	4.1162	2.2846	0.9782	–
	0.7	4.5664	2.2819	0.9122	–	–	6.8604	3.4269	1.3694	–	–
	0.8	4.5638	1.5204	–	–	–	6.8538	2.2824	–	–	–
	0.9	4.5611	–	–	–	–	6.8472	–	–	–	–
$\text{WMPE}^{v}_{\alpha,\beta}$	0.1	4.5791	–	–	–	–	6.8896	–	–	–	–
	0.2	4.5733	3.5524	–	–	–	6.8725	5.3320	–	–	–
	0.3	4.5674	3.4212	2.5310	–	–	6.8555	5.1289	3.7899	–	–
	0.4	4.5616	3.2541	2.2749	1.5147	–	6.8386	4.8727	3.4026	2.2629	–
	0.5	4.5557	3.0333	1.9475	1.1346	0.5036	6.8218	4.5368	2.9094	1.6931	0.7507
	0.6	4.5499	2.7264	1.5127	0.6475	–	6.8052	4.0732	2.2574	0.9651	–
	0.7	4.5441	2.2691	0.9065	–	–	6.7886	3.3861	1.3512	–	–
	0.8	4.5382	1.5108	–	–	–	6.7722	2.2520	–	–	–
	0.9	4.5324	–	–	–	–	6.7559	–	–	–	–
$\text{WMPE}^{w}_{\alpha,\beta}$	0.1	4.5663	–	–	–	–	6.8778	–	–	–	–
	0.2	4.5477	3.5227	–	–	–	6.8493	5.3055	–	–	–
	0.3	4.5292	3.3830	2.4957	–	–	6.8213	5.0953	3.7593	–	–
	0.4	4.5107	3.2087	2.2369	1.4852	–	6.7938	4.8334	3.3701	2.2380	–
	0.5	4.4922	2.9826	1.9095	1.1093	0.4910	6.7667	4.4934	2.8774	1.6721	0.7403
	0.6	4.4738	2.6733	1.4791	0.6313	–	6.7401	4.0284	2.2295	0.9519	–
	0.7	4.4555	2.2187	0.8838	–	–	6.7140	3.3442	1.3326	–	–
	0.8	4.4373	1.4731	–	–	–	6.6884	2.2210	–	–	–
	0.9	4.4192	–	–	–	–	6.6631	–	–	–	–

The scale factor $s = 1$ gives the original time series $\{x_i\}_{i=1}^{N}$, reducing $\text{MPE}_{\alpha,\beta}$, $\text{WMPE}^{v}_{\alpha,\beta}$ and $\text{WMPE}^{w}_{\alpha,\beta}$ to $\text{PE}_{\alpha,\beta}$, two-parameter weighted permutation entropy ($\text{WPE}^{v}_{\alpha,\beta}$) and two-parameter new weighted permutation entropy ($\text{WPE}^{w}_{\alpha,\beta}$) respectively. For $s = 1$ and $m = 4$ and 5, the entropy values are given in Table 5.7.

In Table 5.7, for a particular value of α and β, the $\text{WMPE}^{w}_{\alpha,\beta}$ is the smallest among $\text{MPE}_{\alpha,\beta}$, $\text{WMPE}^{v}_{\alpha,\beta}$ and $\text{WMPE}^{w}_{\alpha,\beta}$. This justifies that the consideration of new weighting scheme captures more information than the weighting scheme of Fadlallah et al. [32], which in turn captures more information than $\text{MPE}_{\alpha,\beta}$. Further, for a particular value of β, as the α value increases, the $\text{WMPE}^{w}_{\alpha,\beta}$ values decline more rapidly than $\text{WMPE}^{v}_{\alpha,\beta}$.

Table 5.8: Two parametric entropies at different values of α and β for m=4 and s=4.

		NoO scales					EPO scales				
		β					β				
Entropy	α	1.0	1.1	1.2	1.3	1.4	1.0	1.1	1.2	1.3	1.4
$\text{MPE}_{\alpha,\beta}$	0.1	4.5811	–	–	–	–	4.5771	–	–	–	–
	0.2	4.5773	3.5572	–	–	–	4.5692	3.5476	–	–	–
	0.3	4.5736	3.4275	2.5369	–	–	4.5612	3.4149	2.5251	–	–
	0.4	4.5699	3.2617	2.2815	1.5198	–	4.5532	3.2466	2.2686	1.5097	–
	0.5	4.5664	3.0419	1.9541	1.1390	0.5059	4.5452	3.0248	1.9410	1.1302	0.5014
	0.6	4.5629	2.7357	1.5187	0.6504	–	4.5371	2.7174	1.5070	0.6447	–
	0.7	4.5595	2.2781	0.9106	–	–	4.5290	2.2605	0.9026	–	–
	0.8	4.5562	1.5176	–	–	–	4.5209	1.5043	–	–	–
	0.9	4.5529	–	–	–	–	4.5128	–	–	–	–
$\text{WMPE}^{v}_{\alpha,\beta}$	0.1	4.5766	–	–	–	–	4.5677	–	–	–	–
	0.2	4.5683	3.5467	–	–	–	4.5506	3.5261	–	–	–
	0.3	4.5601	3.4139	2.5243	–	–	4.5336	3.3876	2.5001	–	–
	0.4	4.5519	3.2455	2.2679	1.5092	–	4.5168	3.2144	2.2419	1.4892	–
	0.5	4.5438	3.0238	1.9404	1.1300	0.5013	4.5002	2.9892	1.9146	1.1129	0.4928
	0.6	4.5357	2.7166	1.5066	0.6446	–	4.4837	2.6805	1.4838	0.6336	–
	0.7	4.5277	2.2599	0.9024	–	–	4.4675	2.2257	0.8871	–	–
	0.8	4.5198	1.5040	–	–	–	4.4514	1.4785	–	–	–
	0.9	4.5120	–	–	–	–	4.4355	–	–	–	–
$\text{WMPE}^{w}_{\alpha,\beta}$	0.1	4.5688	–	–	–	–	4.5580	–	–	–	–
	0.2	4.5526	3.5284	–	–	–	4.5310	3.5030	–	–	–
	0.3	4.5365	3.3902	2.5022	–	–	4.5039	3.3576	2.4721	–	–
	0.4	4.5203	3.2172	2.2440	1.4907	–	4.4768	3.1784	2.2114	1.4653	–
	0.5	4.5041	2.9920	1.9166	1.1140	0.4933	4.4497	2.9485	1.8839	1.0923	0.4825
	0.6	4.4880	2.6832	1.4853	0.6343	–	4.4227	2.6375	1.4564	0.6204	–
	0.7	4.4720	2.2280	0.8880	–	–	4.3959	2.1846	0.8685	–	–
	0.8	4.4560	1.4800	–	–	–	4.3691	1.4475	–	–	–
	0.9	4.4401	–	–	–	–	4.3426	–	–	–	–

In Table 5.8, for $m = 4$ and $s = 4$, the $\text{MPE}_{\alpha,\beta}$, $\text{WMPE}^{v}_{\alpha,\beta}$ and $\text{WMPE}^{w}_{\alpha,\beta}$ values are compared on both non-overlapping (NoO) and EPO scales. Consideration of the EPO average decrease the entropy values in comparison to the corresponding entropies calculated on non-overlapping scales. Thus, the consideration of EPO average captures more information than the non-overlapping average.

Table 5.9 and 5.10 gives the entropy values for $m = 4$ and $s = 7$ and 10 respectively. For a particular m and a fixed value of α and β, the entropy values decrease with

an increase in the scale factor s. As s increases, the entropy values decrease more rapidly for a fixed β and increasing α from 0.1 to 0.9. This decline is more prominent for EPO scales. The $\text{WMPE}^{w}_{\alpha,\beta}$ decreases more quickly than $\text{MPE}_{\alpha,\beta}$ and $\text{WMPE}^{v}_{\alpha,\beta}$.

Table 5.11 to 5.13 gives the $\text{MPE}_{\alpha,\beta}$, $\text{WMPE}^{v}_{\alpha,\beta}$ and $\text{WMPE}^{w}_{\alpha,\beta}$ values with embedding dimension $m = 5$ and scale factor $s = 4, 7$ and 10 respectively. For $s = 4$, $\text{WMPE}^{w}_{\alpha,\beta}$ is smallest of all the three $\text{MPE}_{\alpha,\beta}$, $\text{WMPE}^{v}_{\alpha,\beta}$ and $\text{WMPE}^{w}_{\alpha,\beta}$. It is slightly high from $\text{WMPE}^{v}_{\alpha,\beta}$ for $s = 7$ and $s = 10$. The entropy values decreases more rapidly than in $m = 4$ case. For $m = 5$, the entropies on EPO scales are smaller than the corresponding entropies on non-overlapping scales for $s = 4$. These values start to increase for $s = 7$ and $s = 10$.

For $m = 5$ and $s = 7$ and 10 some fluctuations in the values of $\text{MPE}_{\alpha,\beta}$, $\text{WMPE}^{v}_{\alpha,\beta}$ and $\text{WMPE}^{w}_{\alpha,\beta}$ are observed, refer to Table 5.12 and Table 5.13. These fluctuations may perhaps be attributed due to more information being inherited by the proposed $\text{WMPE}^{w}_{\alpha,\beta}$ over $\text{WMPE}^{v}_{\alpha,\beta}$. The same is exhibited from Fig.5.7 and Fig.5.8 in the next subsection.

Table 5.9: Two parametric entropies at different values of α and β for m=4 and s=7.

		NoO scales					EPO scales				
		β					β				
Entropy	α	1.0	1.1	1.2	1.3	1.4	1.0	1.1	1.2	1.3	1.4
$\text{MPE}_{\alpha,\beta}$	0.1	4.5769	–	–	–	–	4.5774	–	–	–	–
	0.2	4.5690	3.5477	–	–	–	4.5701	3.5490	–	–	–
	0.3	4.5613	3.4154	2.5259	–	–	4.5630	3.4170	2.5274	–	–
	0.4	4.5538	3.2476	2.2698	1.5109	–	4.5561	3.2495	2.2713	1.5121	–
	0.5	4.5466	3.0264	1.9426	1.1315	0.5022	4.5493	3.0285	1.9441	1.1325	0.5026
	0.6	4.5396	2.7196	1.5087	0.6457	–	4.5427	2.7218	1.5100	0.6463	–
	0.7	4.5327	2.2630	0.9039	–	–	4.5363	2.2650	0.9048	–	–
	0.8	4.5260	1.5065	–	–	–	4.5300	1.5079	–	–	–
	0.9	4.5196	–	–	–	–	4.5238	–	–	–	–
$\text{WMPE}^{v}_{\alpha,\beta}$	0.1	4.5695	–	–	–	–	4.5748	–	–	–	–
	0.2	4.5543	3.5307	–	–	–	4.5649	3.5429	–	–	–
	0.3	4.5394	3.3936	2.5058	–	–	4.5552	3.4092	2.5201	–	–
	0.4	4.5248	3.2218	2.2482	1.4942	–	4.5456	3.2402	2.2635	1.5060	–
	0.5	4.5105	2.9976	1.9212	1.1173	0.4951	4.5363	3.0180	1.9363	1.1273	0.5001
	0.6	4.4965	2.6896	1.4898	0.6366	–	4.5271	2.7108	1.5031	0.6429	–
	0.7	4.4827	2.2347	0.8912	–	–	4.5180	2.2546	0.9001	–	–
	0.8	4.4693	1.4854	–	–	–	4.5092	1.5002	–	–	–
	0.9	4.4562	–	–	–	–	4.5005	–	–	–	–
$\text{WMPE}^{w}_{\alpha,\beta}$	0.1	4.5673	–	–	–	–	4.5631	–	–	–	–
	0.2	4.5494	3.5243	–	–	–	4.5419	3.5165	–	–	–
	0.3	4.5313	3.3847	2.4969	–	–	4.5212	3.3758	2.4897	–	–
	0.4	4.5129	3.2103	2.2378	1.4856	–	4.5010	3.2010	2.2311	1.4812	–
	0.5	4.4944	2.9838	1.9100	1.1094	0.4909	4.4814	2.9748	1.9044	1.1064	0.4898
	0.6	4.4756	2.6740	1.4792	0.6312	–	4.4623	2.6662	1.4752	0.6297	–
	0.7	4.4567	2.2187	0.8836	–	–	4.4436	2.2127	0.8816	–	–
	0.8	4.4375	1.4727	–	–	–	4.4255	1.4693	–	–	–
	0.9	4.4181	–	–	–	–	4.4078	–	–	–	–

Table 5.10: Two parametric entropies at different values of α and β for m=4 and s=10.

		NoO scales					EPO scales				
				β					β		
Entropy	α	1.0	1.1	1.2	1.3	1.4	1.0	1.1	1.2	1.3	1.4
	0.1	4.5734	–	–	–	–	4.5721	–	–	–	–
	0.2	4.5620	3.5393	–	–	–	4.5595	3.5366	–	–	–
	0.3	4.5506	3.4044	2.5155	–	–	4.5471	3.4012	2.5129	–	–
	0.4	4.5392	3.2343	2.2584	1.5019	–	4.5350	3.2308	2.2558	1.5001	–
$MPE_{\alpha,\beta}$	0.5	4.5280	3.0112	1.9310	1.1237	0.4982	4.5231	3.0077	1.9287	1.1223	0.4976
	0.6	4.5168	2.7034	1.4982	0.6406	–	4.5115	2.7001	1.4964	0.6398	–
	0.7	4.5057	2.2474	0.8968	–	–	4.5002	2.2446	0.8957	–	–
	0.8	4.4947	1.4946	–	–	–	4.4892	1.4928	–	–	–
	0.9	4.4839	–	–	–	–	4.4784	–	–	–	–
	0.1	4.5652	–	–	–	–	4.5490	–	–	–	–
	0.2	4.5464	3.5221	–	–	–	4.5149	3.4865	–	–	–
	0.3	4.5284	3.3835	2.4972	–	–	4.4827	3.3391	2.4573	–	–
	0.4	4.5113	3.2107	2.2396	1.4881	–	4.4521	3.1594	2.1979	1.4566	–
$WMPE^{v}_{\alpha,\beta}$	0.5	4.4950	2.9862	1.9132	1.1124	0.4929	4.4231	2.9305	1.8728	1.0863	0.4802
	0.6	4.4793	2.6785	1.4832	0.6337	–	4.3957	2.6219	1.4484	0.6174	–
	0.7	4.4642	2.2249	0.8871	–	–	4.3698	2.1726	0.8644	–	–
	0.8	4.4497	1.4786	–	–	–	4.3452	1.4406	–	–	–
	0.9	4.4357	–	–	–	–	4.3219	–	–	–	–
	0.1	4.5611	–	–	–	–	4.5491	–	–	–	–
	0.2	4.5369	3.5098	–	–	–	4.5132	3.4824	–	–	–
	0.3	4.5126	3.3660	2.4796	–	–	4.4774	3.3312	2.4477	–	–
	0.4	4.4880	3.1880	2.2192	1.4711	–	4.4416	3.1470	2.1851	1.4448	–
$WMPE^{w}_{\alpha,\beta}$	0.5	4.4633	2.9589	1.8914	1.0970	0.4848	4.4058	2.9134	1.8576	1.0747	0.4737
	0.6	4.4383	2.6480	1.4627	0.6233	–	4.3701	2.6007	1.4330	0.6091	–
	0.7	4.4133	2.1940	0.8726	–	–	4.3345	2.1495	0.8527	–	–
	0.8	4.3881	1.4543	–	–	–	4.2990	1.4212	–	–	–
	0.9	4.3628	–	–	–	–	4.2636	–	–	–	–

Table 5.11: Two parametric entropies at different values of α and β for m=5 and s=4.

		NoO scales					EPO scales				
				β					β		
Entropy	α	1.0	1.1	1.2	1.3	1.4	1.0	1.1	1.2	1.3	1.4
	0.1	6.8757	–	–	–	–	6.8696	–	–	–	–
	0.2	6.8573	5.3196	–	–	–	6.8448	5.3050	–	–	–
	0.3	6.8395	5.1167	3.7810	–	–	6.8207	5.0978	3.7633	–	–
	0.4	6.8223	4.8612	3.3949	2.2581	–	6.7970	4.8385	3.3757	2.2431	–
$MPE_{\alpha,\beta}$	0.5	6.8057	4.5265	2.9032	1.6898	0.7494	6.7740	4.5009	2.8840	1.6770	0.7430
	0.6	6.7897	4.0645	2.2531	0.9635	–	6.7514	4.0376	2.2359	0.9553	–
	0.7	6.7742	3.3796	1.3489	–	–	6.7294	3.3539	1.3374	–	–
	0.8	6.7592	2.2482	–	–	–	6.7078	2.2289	–	–	–
	0.9	6.7446	–	–	–	–	6.6868	–	–	–	–
	0.1	6.8431	–	–	–	–	6.8393	–	–	–	–
	0.2	6.7946	5.2492	–	–	–	6.7867	5.2398	–	–	–
	0.3	6.7490	5.0294	3.7028	–	–	6.7369	5.0174	3.6918	–	–
	0.4	6.7059	4.7607	3.3131	2.1963	–	6.6898	4.7466	3.3015	2.1877	–
$WMPE^{v}_{\alpha,\beta}$	0.5	6.6650	4.4174	2.8239	1.6383	0.7243	6.6453	4.4020	2.8127	1.6312	0.7210
	0.6	6.6261	3.9534	2.1845	0.9313	–	6.6031	3.9378	2.1750	0.9270	–
	0.7	6.5890	3.2767	1.3038	–	–	6.5630	3.2625	1.2978	–	–
	0.8	6.5534	2.1730	–	–	–	6.5250	2.1629	–	–	–
	0.9	6.5191	–	–	–	–	6.4888	–	–	–	–
	0.1	6.8360	–	–	–	–	6.8398	–	–	–	–
	0.2	6.7830	5.2377	–	–	–	6.7864	5.2381	–	–	–
	0.3	6.7342	5.0163	3.6917	–	–	6.7346	5.0134	3.6866	–	–
	0.4	6.6884	4.7465	3.3018	2.1878	–	6.6845	4.7400	3.2944	2.1810	–
$WMPE^{w}_{\alpha,\beta}$	0.5	6.6451	4.4024	2.8129	1.6312	0.7208	6.6360	4.3926	2.8042	1.6247	0.7173
	0.6	6.6035	3.9381	2.1749	0.9267	–	6.5889	3.9259	2.1662	0.9222	–
	0.7	6.5635	3.2624	1.2974	–	–	6.5431	3.2493	1.2911	–	–
	0.8	6.5248	2.1624	–	–	–	6.4986	2.1518	–	–	–
	0.9	6.4872	–	–	–	–	6.4553	–	–	–	–

Table 5.12: Two parametric entropies at different values of α and β for m=5 and s=7.

		NoO scales					EPO scales				
				β					β		
Entropy	α	1.0	1.1	1.2	1.3	1.4	1.0	1.1	1.2	1.3	1.4
	0.1	6.7151	–	–	–	–	6.7985	–	–	–	–
	0.2	6.6895	5.1835	–	–	–	6.7773	5.2552	–	–	–
	0.3	6.6645	4.9801	3.6759	–	–	6.7567	5.0524	3.7316	–	–
	0.4	6.6402	4.7261	3.2969	2.1906	–	6.7365	4.7978	3.3489	2.2263	–
$MPE_{\alpha,\beta}$	0.5	6.6166	4.3959	2.8165	1.6376	0.7255	6.7169	4.4651	2.8624	1.6652	0.7381
	0.6	6.5938	3.9430	2.1835	0.9328	–	6.6977	4.0074	2.2203	0.9490	–
	0.7	6.5717	3.2752	1.3060	–	–	6.6790	3.3304	1.3286	–	–
	0.8	6.5504	2.1766	–	–	–	6.6609	2.2144	–	–	–
	0.9	6.5299	–	–	–	–	6.6432	–	–	–	–
	0.1	6.6743	–	–	–	–	6.7679	–	–	–	–
	0.2	6.6136	5.1010	–	–	–	6.7193	5.1907	–	–	–
	0.3	6.5584	4.8811	3.5900	–	–	6.6738	4.9734	3.6617	–	–
	0.4	6.5081	4.6158	3.2098	2.1268	–	6.6312	4.7079	3.2766	2.1724	–
$WMPE^{v}_{\alpha,\beta}$	0.5	6.4621	4.2797	2.7344	1.5859	0.7010	6.5911	4.3688	2.7931	1.6207	0.7167
	0.6	6.4196	3.8282	2.1146	0.9013	–	6.5532	3.9103	2.1610	0.9215	–
	0.7	6.3803	3.1718	1.2619	–	–	6.5172	3.2415	1.2901	–	–
	0.8	6.3437	2.1031	–	–	–	6.4830	2.1501	–	–	–
	0.9	6.3094	–	–	–	–	6.4503	–	–	–	–
	0.1	6.6757	–	–	–	–	6.7581	–	–	–	–
	0.2	6.6139	5.0986	–	–	–	6.7003	5.1694	–	–	–
	0.3	6.5553	4.8748	3.5814	–	–	6.6463	4.9466	3.6375	–	–
	0.4	6.4997	4.6047	3.1979	2.1157	–	6.5955	4.6767	3.2509	2.1527	–
$WMPE^{w}_{\alpha,\beta}$	0.5	6.4466	4.2639	2.7202	1.5751	0.6950	6.5474	4.3345	2.7678	1.6041	0.7085
	0.6	6.3958	3.8083	2.1001	0.8936	–	6.5017	3.8749	2.1388	0.9109	–
	0.7	6.3471	3.1502	1.2511	–	–	6.4581	3.2082	1.2753	–	–
	0.8	6.3003	2.0851	–	–	–	6.4164	2.1255	–	–	–
	0.9	6.2553	–	–	–	–	6.3764	–	–	–	–

Table 5.13: Two parametric entropies at different values of α and β for m=5 and s=10.

		NoO scales					EPO scales				
				β					β		
Entropy	α	1.0	1.1	1.2	1.3	1.4	1.0	1.1	1.2	1.3	1.4
	0.1	6.5013	–	–	–	–	6.6899	–	–	–	–
	0.2	6.4790	5.0218	–	–	–	6.6655	5.1654	–	–	–
	0.3	6.4565	4.8256	3.5620	–	–	6.6413	4.9629	3.6629	–	–
	0.4	6.4341	4.5797	3.1946	2.1222	–	6.6172	4.7094	3.2847	2.1820	–
$MPE_{\alpha,\beta}$	0.5	6.4116	4.2594	2.7286	1.5861	0.7024	6.5932	4.3796	2.8054	1.6307	0.7222
	0.6	6.3891	3.8200	2.1148	0.9031	–	6.5695	3.9276	2.1743	0.9286	–
	0.7	6.3667	3.1721	1.2644	–	–	6.5460	3.2614	1.3000	–	–
	0.8	6.3443	2.1073	–	–	–	6.5228	2.1666	–	–	–
	0.9	6.3219	–	–	–	–	6.4999	–	–	–	–
	0.1	6.4631	–	–	–	–	6.6425	–	–	–	–
	0.2	6.4057	4.9398	–	–	–	6.5732	5.0604	–	–	–
	0.3	6.3512	4.7246	3.4724	–	–	6.5062	4.8310	3.5435	–	–
	0.4	6.2995	4.4646	3.1019	2.0532	–	6.4413	4.5560	3.1586	2.0859	–
$WMPE^{v}_{\alpha,\beta}$	0.5	6.2504	4.1359	2.6398	1.5294	0.6753	6.3783	4.2114	2.6819	1.5500	0.6826
	0.6	6.2038	3.6957	2.0392	0.8682	–	6.3171	3.7546	2.0666	0.8777	–
	0.7	6.1596	3.0588	1.2155	–	–	6.2577	3.0999	1.2287	–	–
	0.8	6.1176	2.0259	–	–	–	6.1998	2.0479	–	–	–
	0.9	6.0777	–	–	–	–	6.1436	–	–	–	–
	0.1	6.4707	–	–	–	–	6.6503	–	–	–	–
	0.2	6.4206	4.9566	–	–	–	6.5919	5.0849	–	–	–
	0.3	6.3728	4.7452	3.4906	–	–	6.5377	4.8652	3.5771	–	–
	0.4	6.3270	4.4879	3.1203	2.0665	–	6.4869	4.5991	3.1965	2.1165	–
$WMPE^{w}_{\alpha,\beta}$	0.5	6.2830	4.1604	2.6569	1.5398	0.6800	6.4388	4.2620	2.7212	1.5769	0.6964
	0.6	6.2405	3.7196	2.0531	0.8743	–	6.3931	3.8096	2.1025	0.8953	–
	0.7	6.1994	3.0797	1.2240	–	–	6.3494	3.1537	1.2535	–	–
	0.8	6.1594	2.0401	–	–	–	6.3075	2.0891	–	–	–
	0.9	6.1203	–	–	–	–	6.2673	–	–	–	–

Thus, Table 5.7 to 5.13 gives the $\text{MPE}_{\alpha,\beta}$, $\text{WMPE}^{v}_{\alpha,\beta}$ and $\text{WMPE}^{w}_{\alpha,\beta}$ for different values of α and β with some selective values of m and s.

Consideration of two parameters generalize the results of non parametric and one parametric entropies giving additional degrees of freedom to analyse the time series under observation. For instance, for $\beta = 1$ and varying α, the Rényi permutation entropy results are obtained. The comparison of these entropies is also studied on some selected range of parameters α and β in the next subsection.

5.4.4 Comparison of Entropies at Different Values of Parameters

In Section 4.3 of the previous chapter, for S&P 500 index, the calibrated density function is obtained for α and β in the range $1.5 \leq \alpha+\beta \leq 1.75$. Here also, the entropies are compared by considering different combinations of α and β such that $\alpha+\beta = 1.5, 1.6$ and 1.7. The impact of changing α and β on entropy values with different m and s values is given in Fig.5.3 to Fig.5.28.

Firstly, for a close observation, at a fixed $\alpha = 0.5$ and $\beta = 1.0$ and for each value of m, the two-parameter entropy values are plotted in Fig.5.3 to Fig.5.8 with both non-overlapping and EPO average. For $m = 2$, the entropy values were very insignificant different so we have demonstrated the case of $m = 3, 4$ and 5 only.

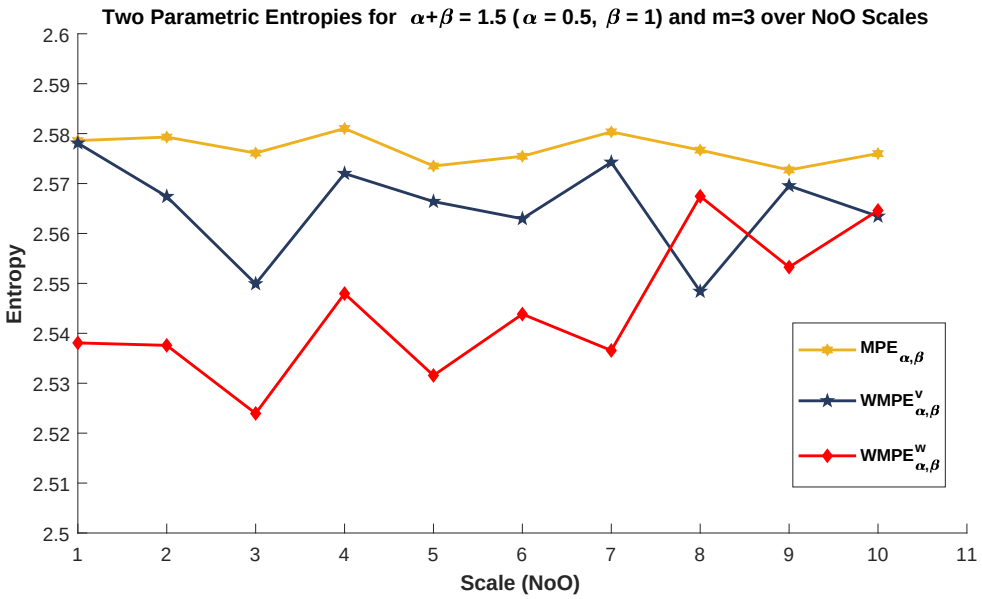

Figure 5.3: Entropies for $m = 3$ over non-overlapping scales at $(\alpha, \beta) = (0.5, 1.0)$.

Fig.5.3 and Fig.5.4 gives the $\text{MPE}_{\alpha,\beta}$, $\text{WMPE}^{v}_{\alpha,\beta}$ and $\text{WMPE}^{w}_{\alpha,\beta}$ values at $m = 3$ for non-overlapping and EPO scales respectively with $\alpha = 0.5$ and $\beta = 1.0$.

The difference in entropy patterns for non-overlapping and EPO scales is clearly observable. Fig.5.4 considers the scale factor $s \geq 2$ as $s = 1$ (original time series) is already covered in non-overlapping scales in Fig.5.3.

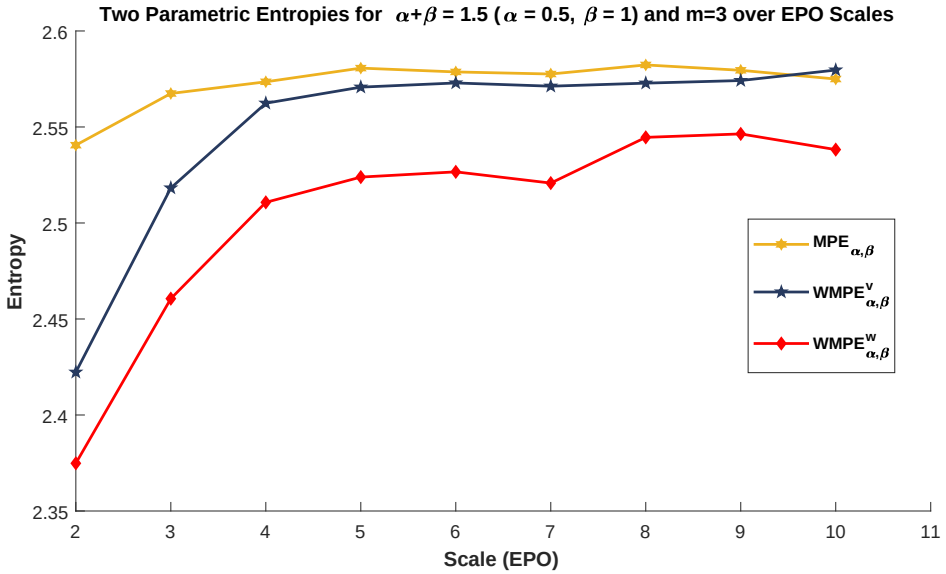

Figure 5.4: Entropies for $m = 3$ over EPO scales at $(\alpha, \beta) = (0.5, 1.0)$.

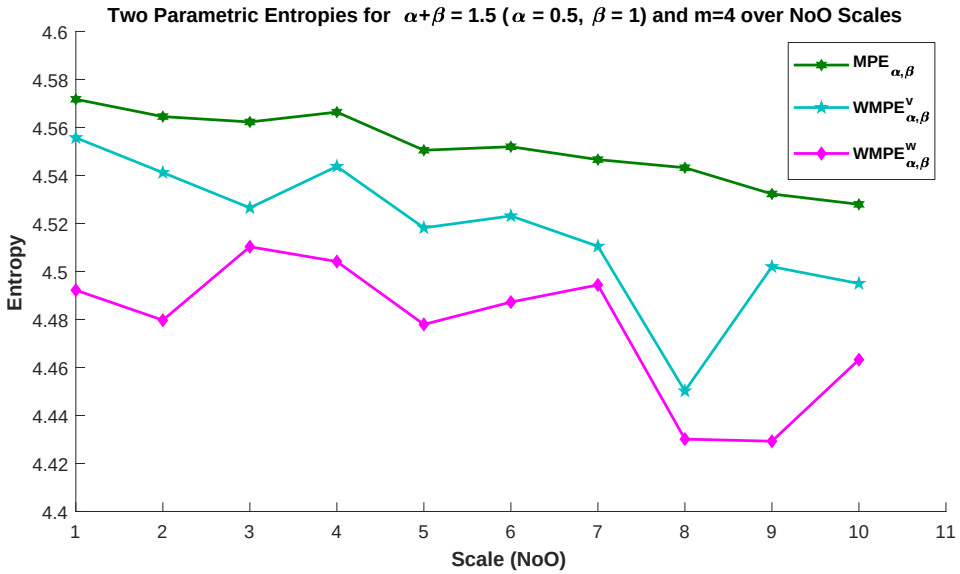

Figure 5.5: Entropies for $m = 4$ over non-overlapping scales at $(\alpha, \beta) = (0.5, 1.0)$.

In Fig.5.5 and Fig.5.6, $\text{MPE}_{\alpha,\beta}$, $\text{WMPE}^{v}_{\alpha,\beta}$ and $\text{WMPE}^{w}_{\alpha,\beta}$ values are given for $m = 4$ over non-overlapping and EPO scales respectively with $\alpha = 0.5$ and $\beta = 1.0$. For $m = 4$, the entropy values start to decrease with increase in s on non-overlapping scales.

For non-overlapping scales, there are more fluctuations in $\text{WMPE}^{v}_{\alpha,\beta}$ and $\text{WMPE}^{w}_{\alpha,\beta}$ than in $\text{MPE}_{\alpha,\beta}$. For EPO scales these entropies firstly increase then decrease. For $m = 3$ and 4, the $\text{WMPE}^{w}_{\alpha,\beta}$ is smallest of the three.

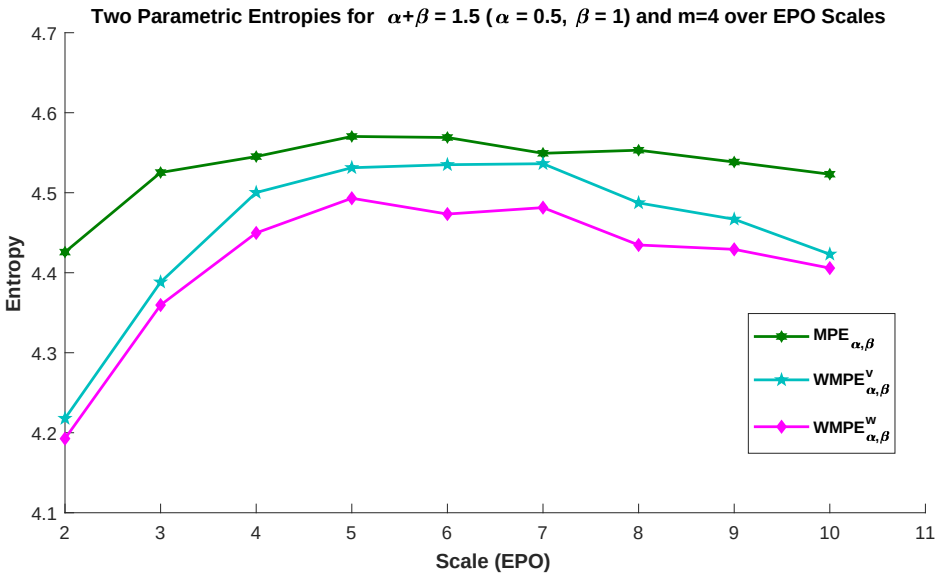

Figure 5.6: Entropies for $m = 4$ over EPO scales at $(\alpha, \beta) = (0.5, 1.0)$.

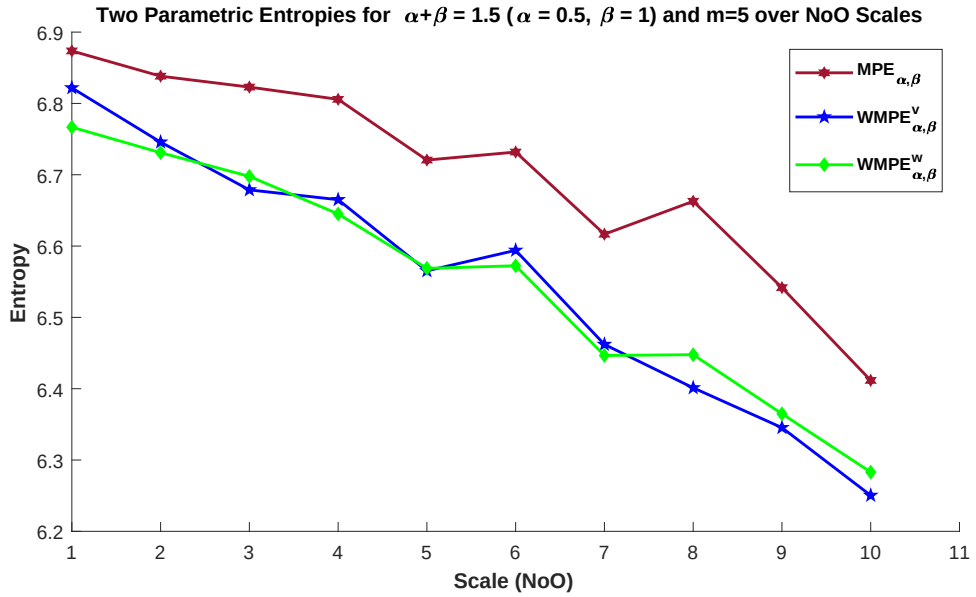

Figure 5.7: Entropies for $m = 5$ over non-overlapping scales at $(\alpha, \beta) = (0.5, 1.0)$.

In Fig.5.7 and Fig.5.8, $\text{MPE}_{\alpha,\beta}$, $\text{WMPE}^{v}_{\alpha,\beta}$ and $\text{WMPE}^{w}_{\alpha,\beta}$ values are given at $m = 5$ for non-overlapping and EPO scales respectively with $\alpha = 0.5$ and $\beta = 1.0$.

For $m = 5$, the entropies on non-overlapping scales are decreasing with increase in scale factor s and the corresponding entropies on EPO scales follow a parabolic path.

The $WMPE^{v}_{\alpha,\beta}$ and $WMPE^{w}_{\alpha,\beta}$ are smaller than $MPE_{\alpha,\beta}$ on both non-overlapping and EPO scales supporting the fact that the inclusion of weight captures more information.

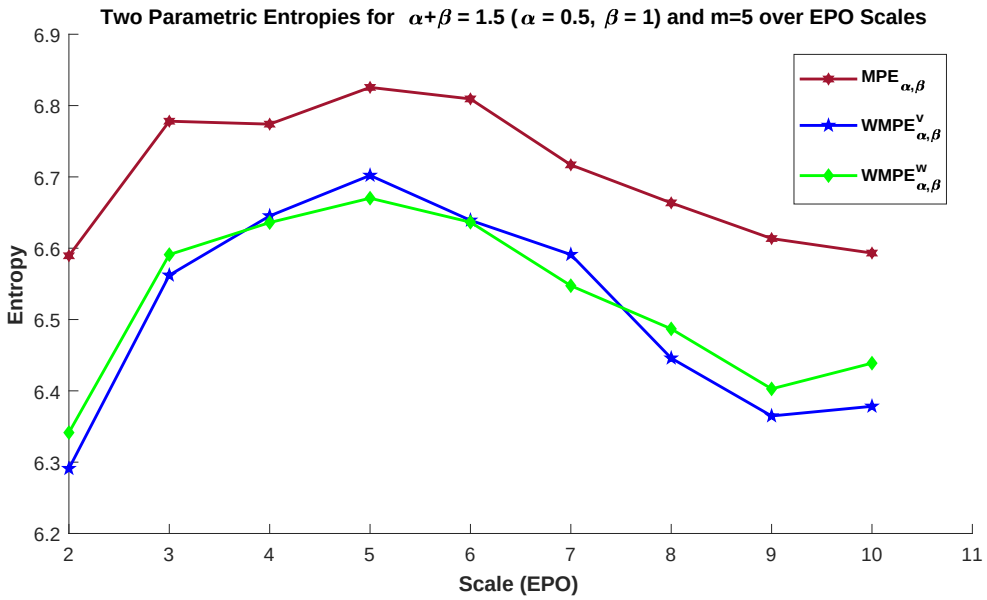

Figure 5.8: Entropies for $m = 5$ over EPO scales at $(\alpha, \beta) = (0.5, 1.0)$.

Further, for $m = 5$, although the $WMPE^{w}_{\alpha,\beta}$ and $WMPE^{v}_{\alpha,\beta}$ gives the equivalent results, but $WMPE^{w}_{\alpha,\beta}$ is more simple, computationally fast and robust than $WMPE^{v}_{\alpha,\beta}$ on both non-overlapping and EPO scales.

Now, Fig.5.9 to Fig.5.28 are considered where the entropies are compared on different m and scales s by taking different combinations of α and β.

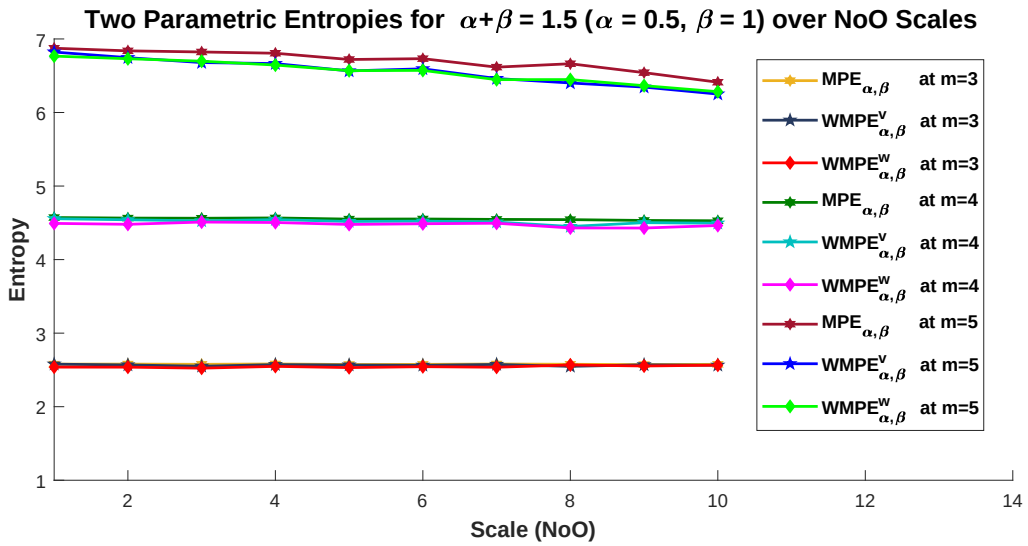

Figure 5.9: Entropies over non-overlapping scales for $\alpha = 0.5$ and $\beta = 1.0$

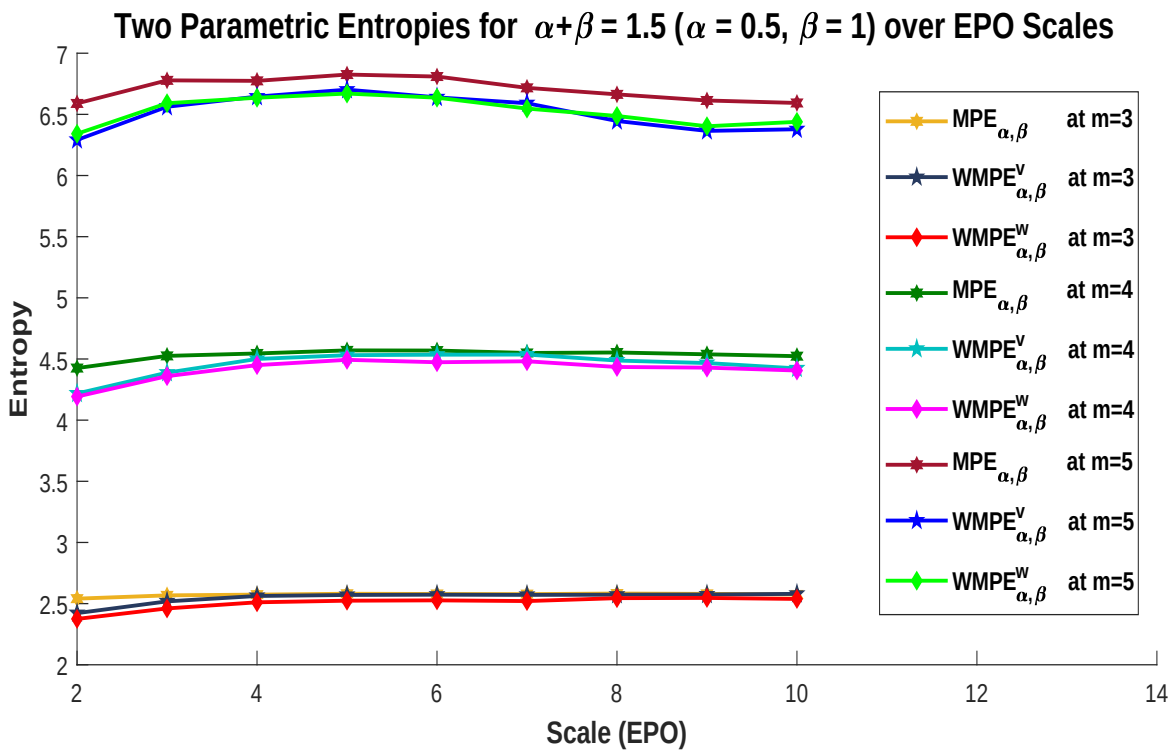

Figure 5.10: Entropies over EPO scales for $\alpha = 0.5$ and $\beta = 1.0$

In Fig.5.9 and Fig.5.10, the entropies at different m values for $\alpha+\beta = 1.5$ with $\alpha = 0.5$ and $\beta = 1.0$ are given on non-overlapping and EPO scales respectively. For $m = 3$, there is almost no difference visible in the entropy values but this difference was visible in Fig.5.3. As the m increases from 3 to 5, the $\text{WMPE}^{v}_{\alpha,\beta}$ and $\text{WMPE}^{w}_{\alpha,\beta}$ begin to separate from $\text{MPE}_{\alpha,\beta}$. This separation is more visible on EPO scales than on non-overlapping scales.

Fig.5.11 and Fig.5.12 gives the entropy values at different m values for $\alpha+\beta = 1.5$ but with $\alpha = 0.4$ and $\beta = 1.1$ on non-overlapping and EPO scales respectively. This decrease in α and increase in β, to maintain $\alpha+\beta = 1.5$, decreases the entropy value. This decrease in entropy value is more prominent for $\alpha = 0.3$ and $\beta = 1.2$ in Fig.5.13 and Fig.5.14.

Similarly, for $\alpha+\beta = 1.6$, all the possible combinations of (α,β) are $(0.6,1),(0.5,1.1)$ and $(0.4,1.2)$, giving Fig.5.15 to Fig.5.20 for both non-overlapping and EPO scales. For $\alpha+\beta = 1.7$, all the possible combinations of (α,β) are $(0.7,1),(0.6,1.1),(0.5,1.2)$ and $(0.4,1.2)$, giving Fig.5.21 to Fig.5.28 for both non-overlapping and EPO scales.

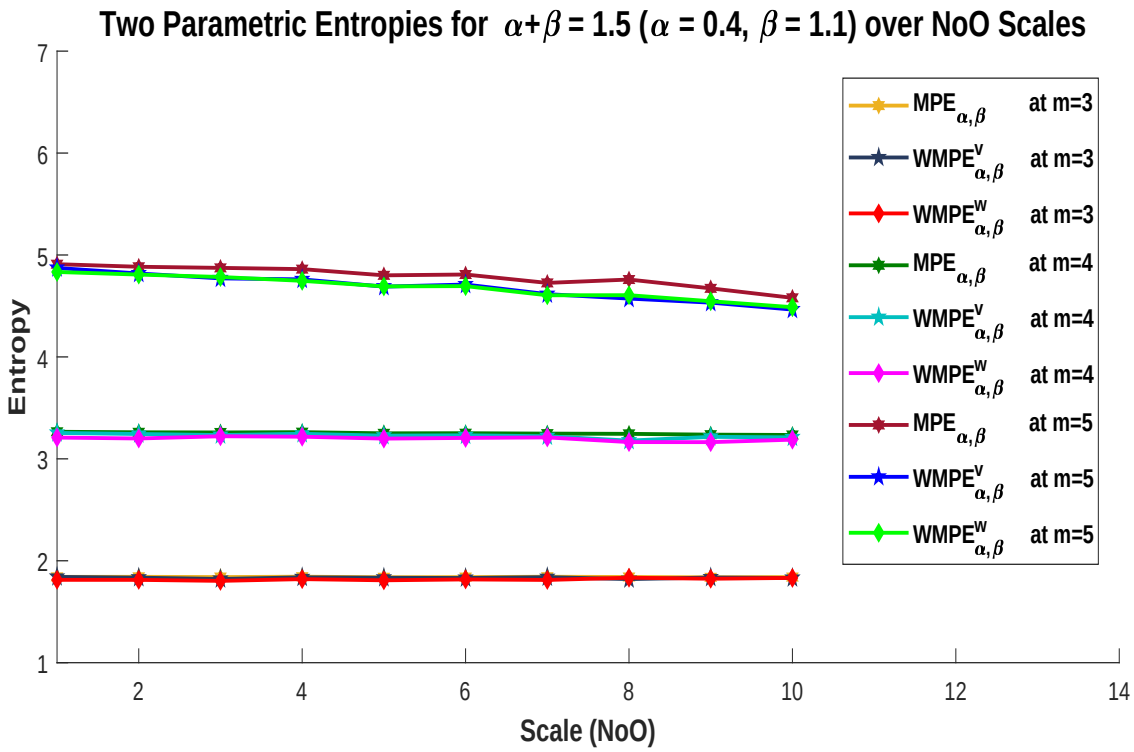

Figure 5.11: Entropies over non-overlapping scales for $\alpha = 0.4$ and $\beta = 1.1$

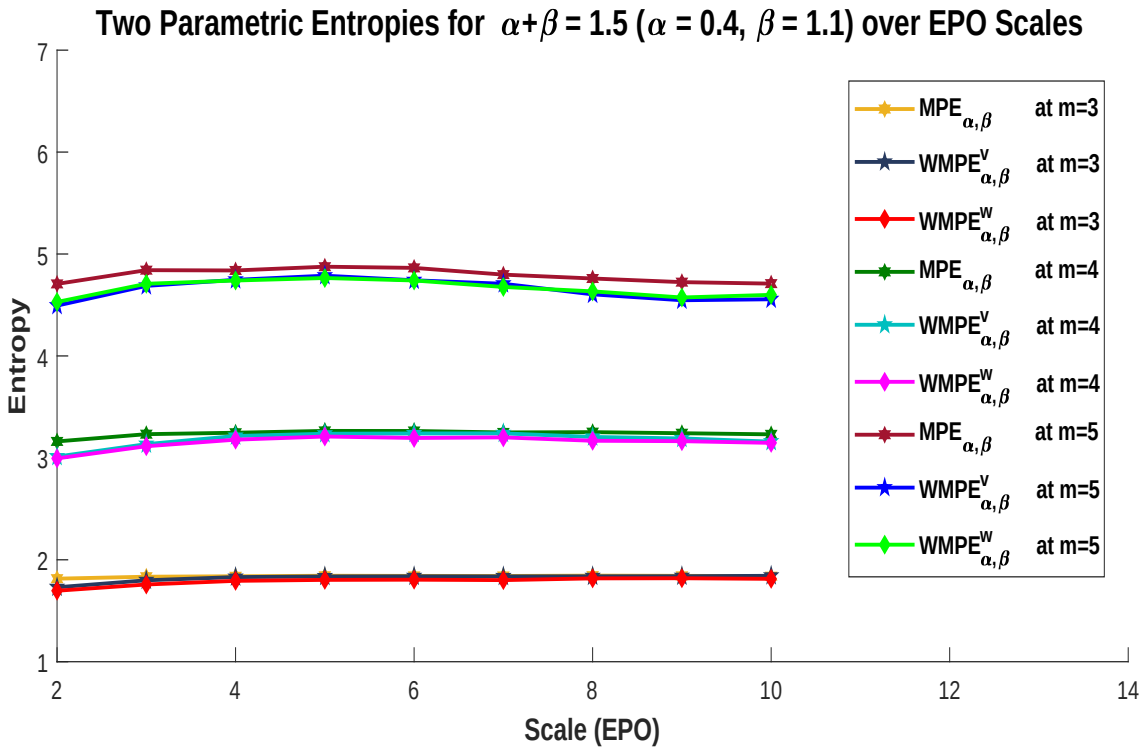

Figure 5.12: Entropies over EPO scales for $\alpha = 0.4$ and $\beta = 1.1$

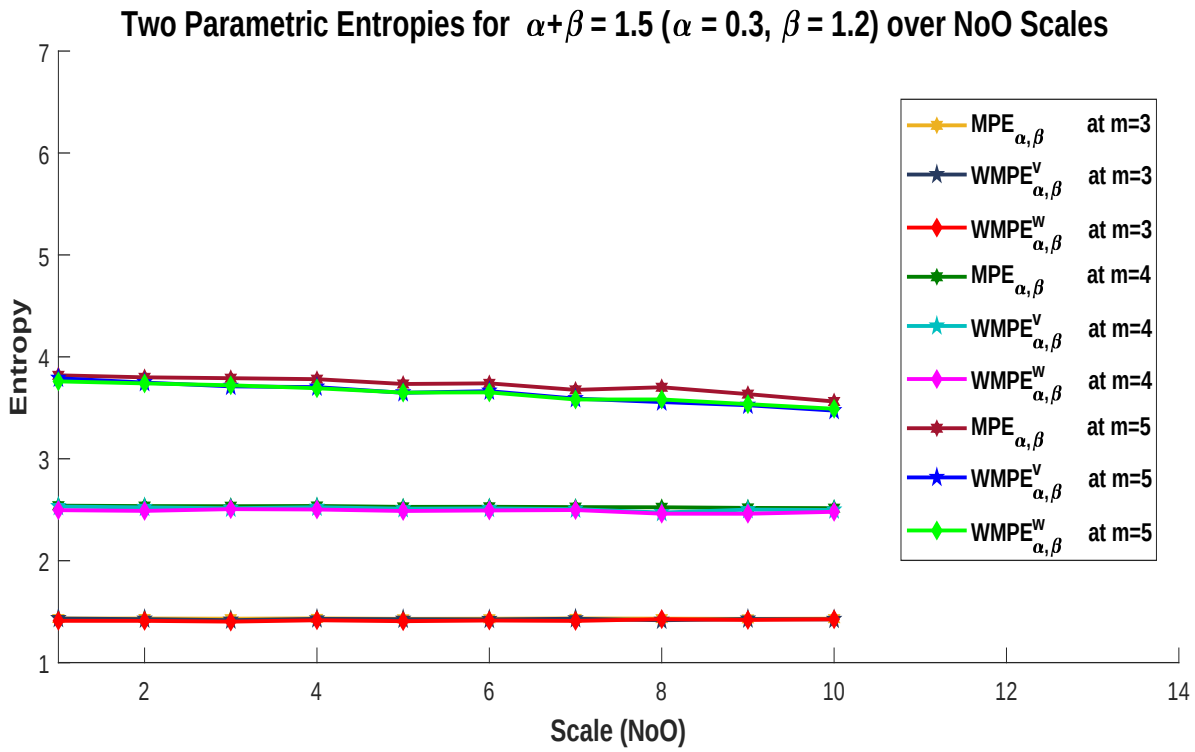

Figure 5.13: Entropies over non-overlapping scales for $\alpha = 0.3$ and $\beta = 1.2$

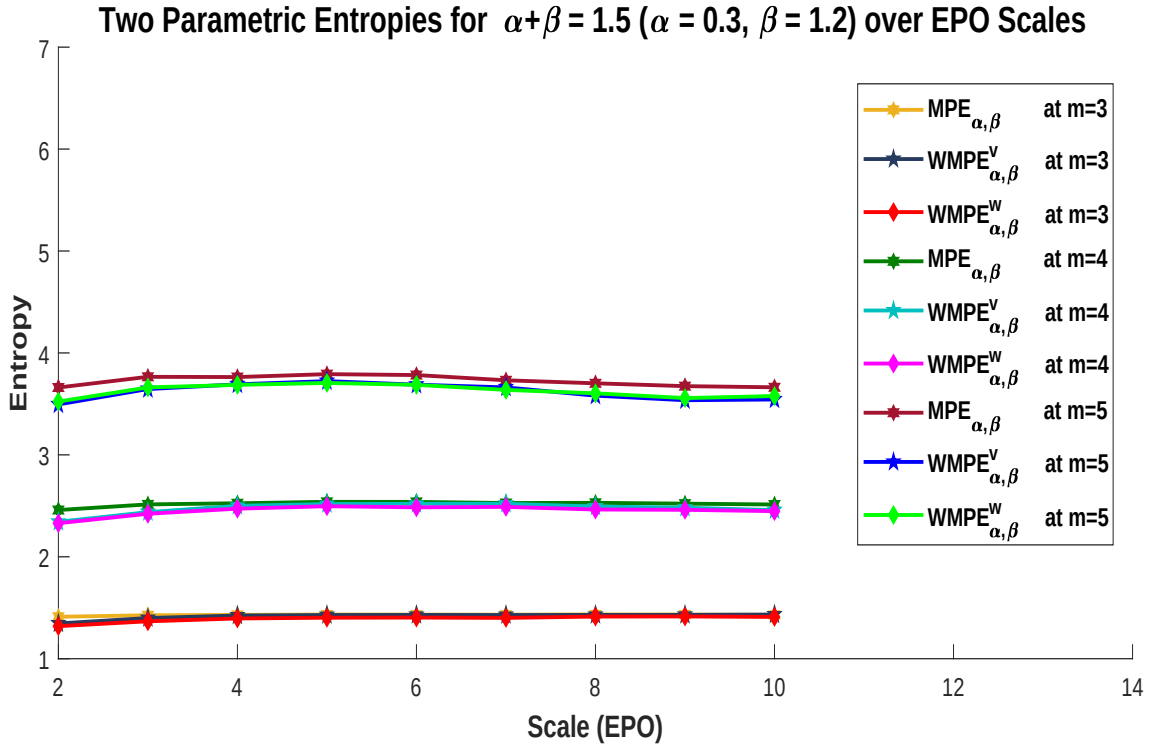

Figure 5.14: Entropies over EPO scales for $\alpha = 0.3$ and $\beta = 1.2$

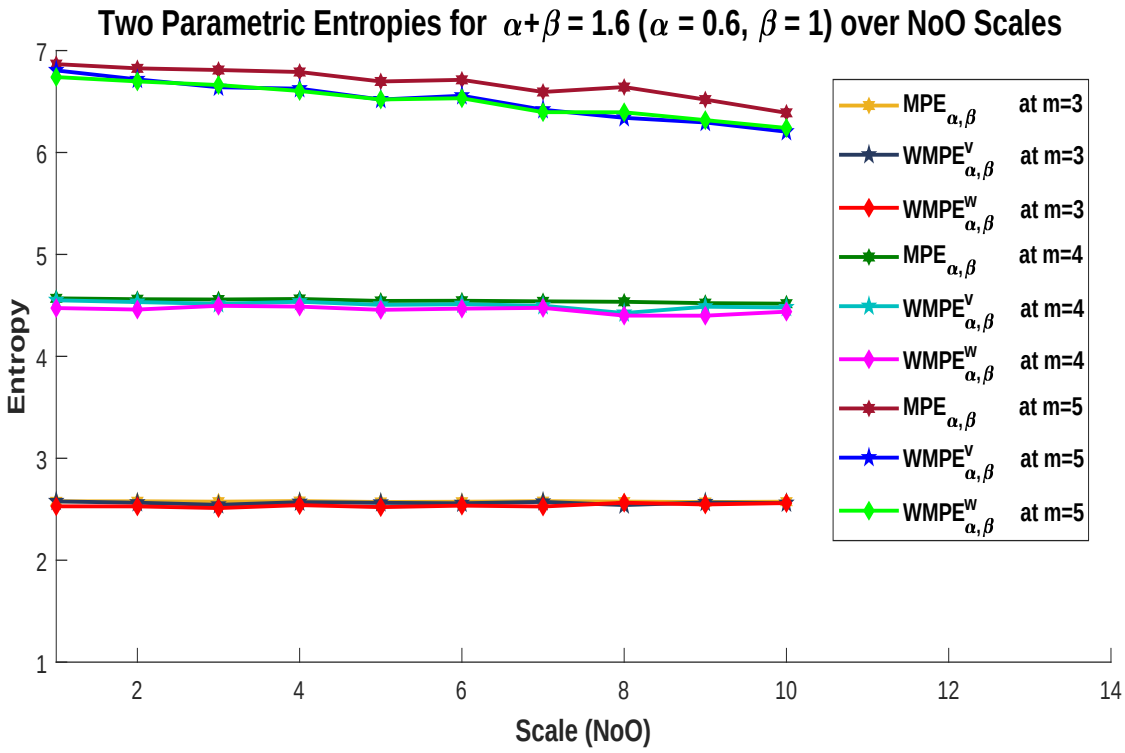

Figure 5.15: Entropies over non-overlapping scales for $\alpha = 0.6$ and $\beta = 1.0$

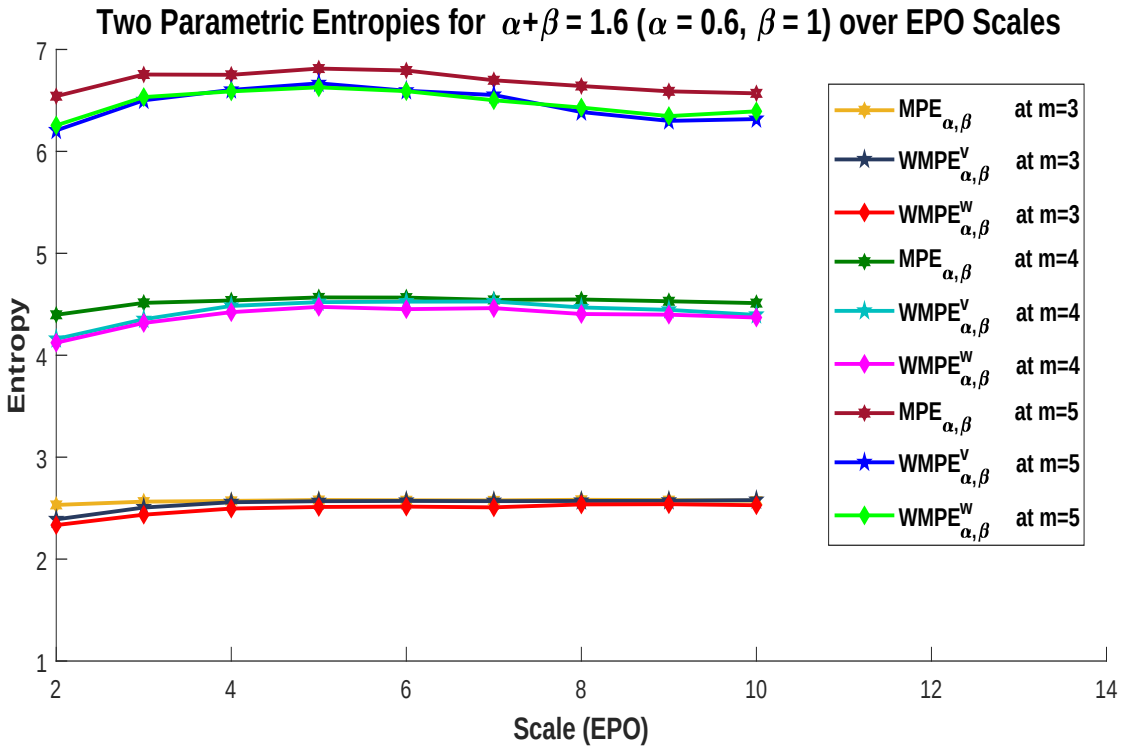

Figure 5.16: Entropies over EPO scales for $\alpha = 0.6$ and $\beta = 1.0$

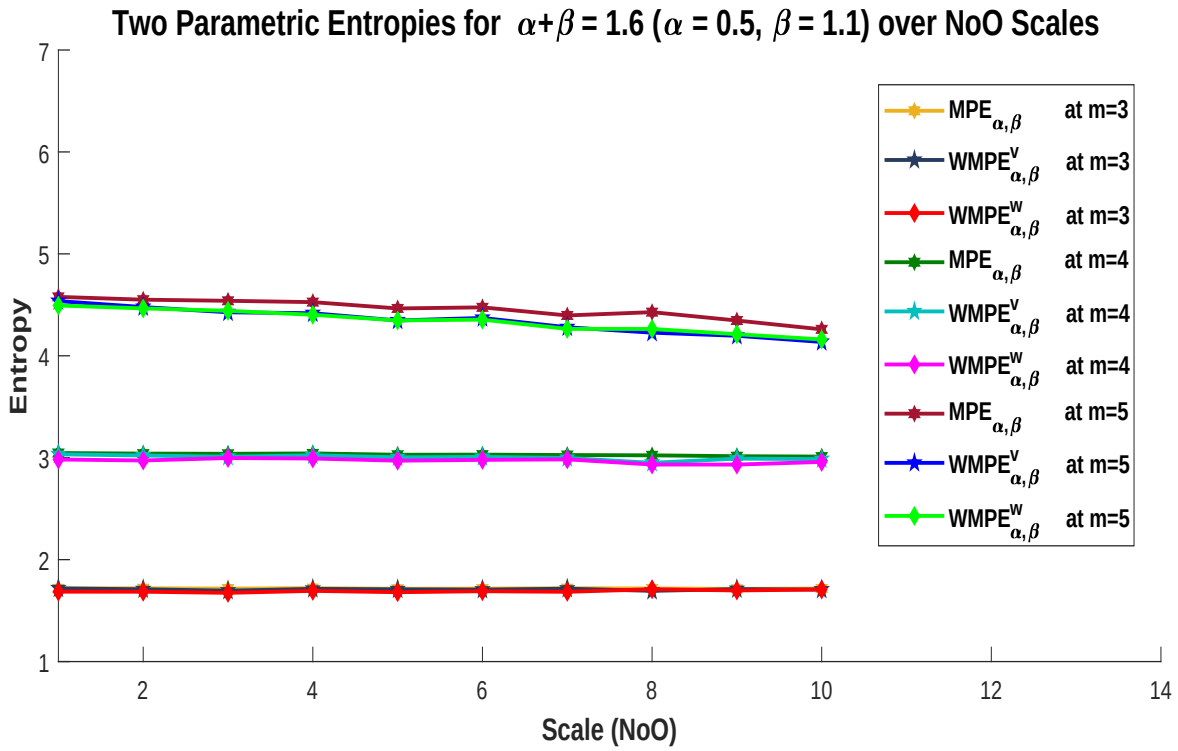

Figure 5.17: Entropies over non-overlapping scales for $\alpha = 0.5$ and $\beta = 1.1$

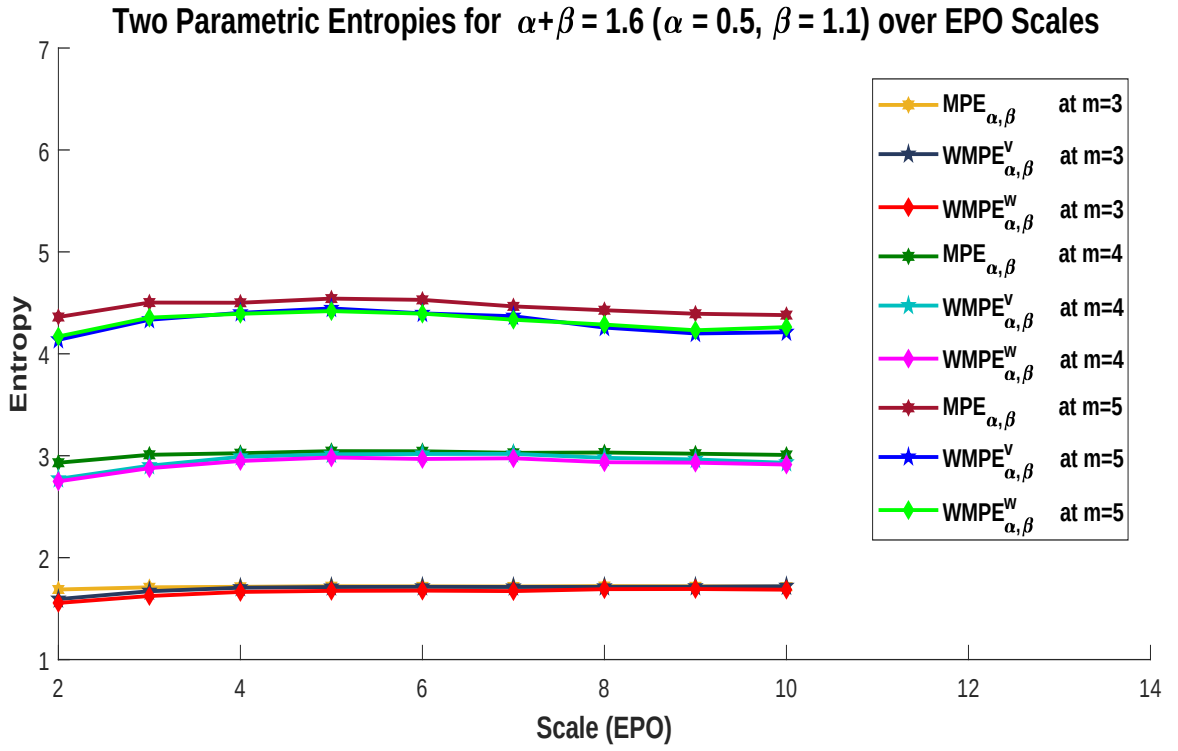

Figure 5.18: Entropies over EPO scales for $\alpha = 0.5$ and $\beta = 1.1$

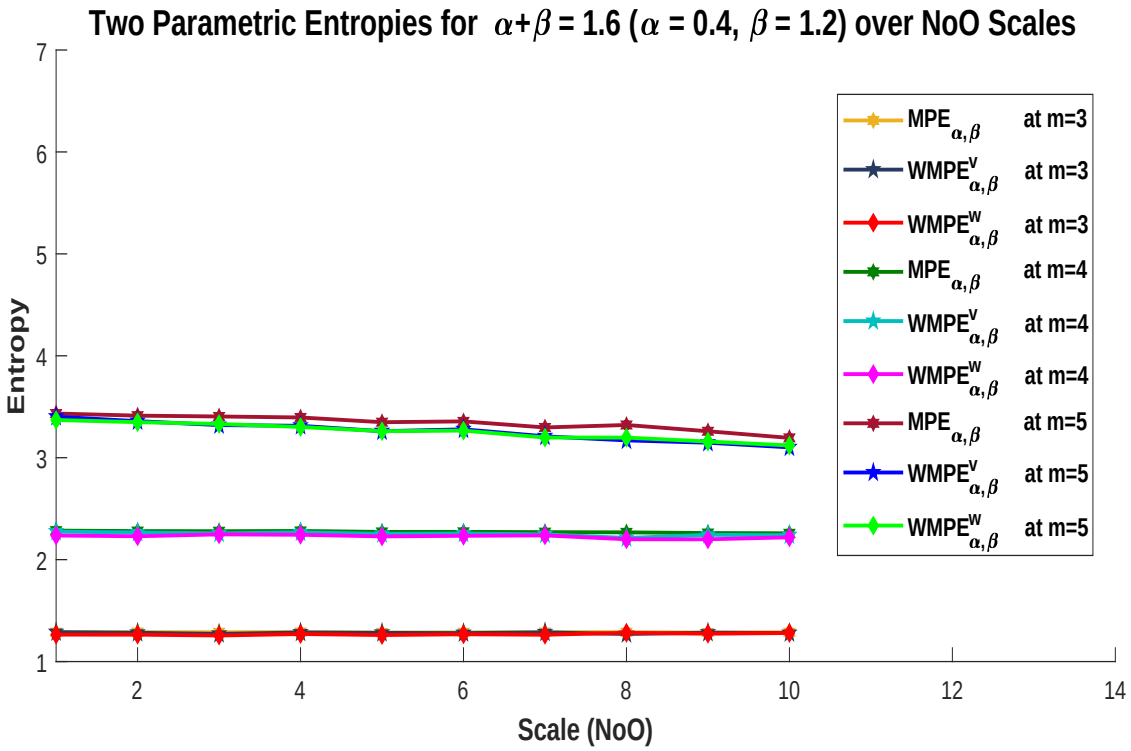

Figure 5.19: Entropies over non-overlapping scales for $\alpha = 0.4$ and $\beta = 1.2$

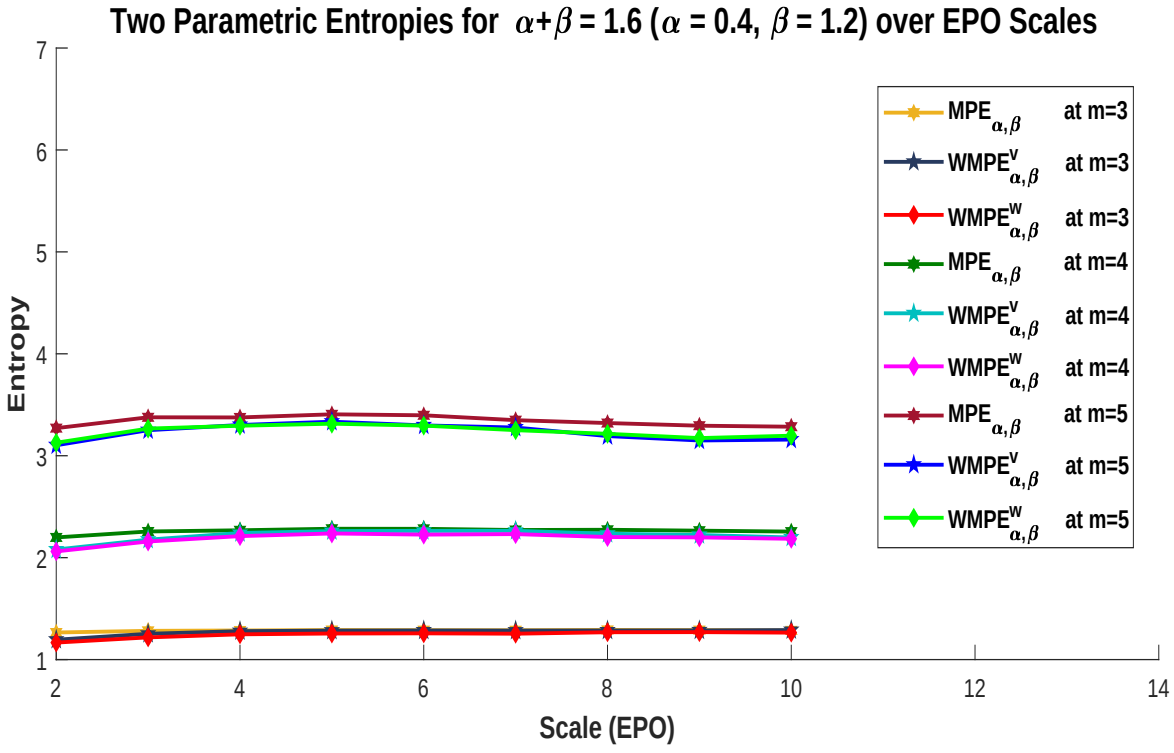

Figure 5.20: Entropies over EPO scales for $\alpha = 0.4$ and $\beta = 1.2$

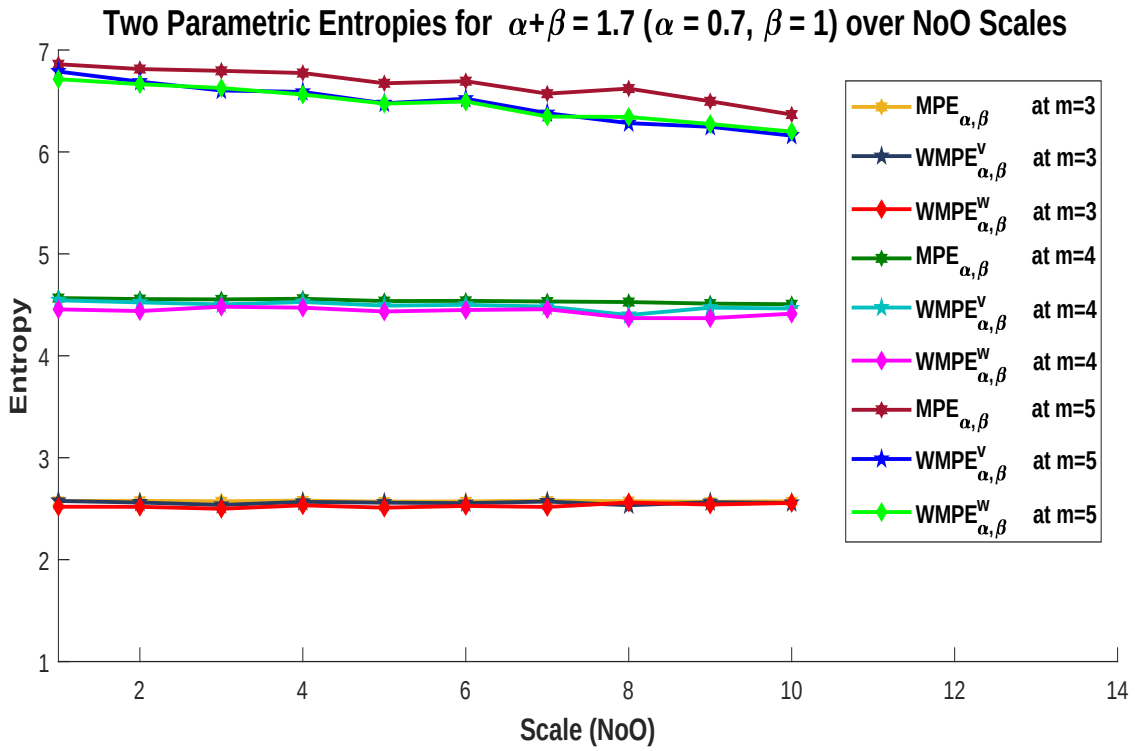

Figure 5.21: Entropies over non-overlapping scales for $\alpha = 0.7$ and $\beta = 1.0$

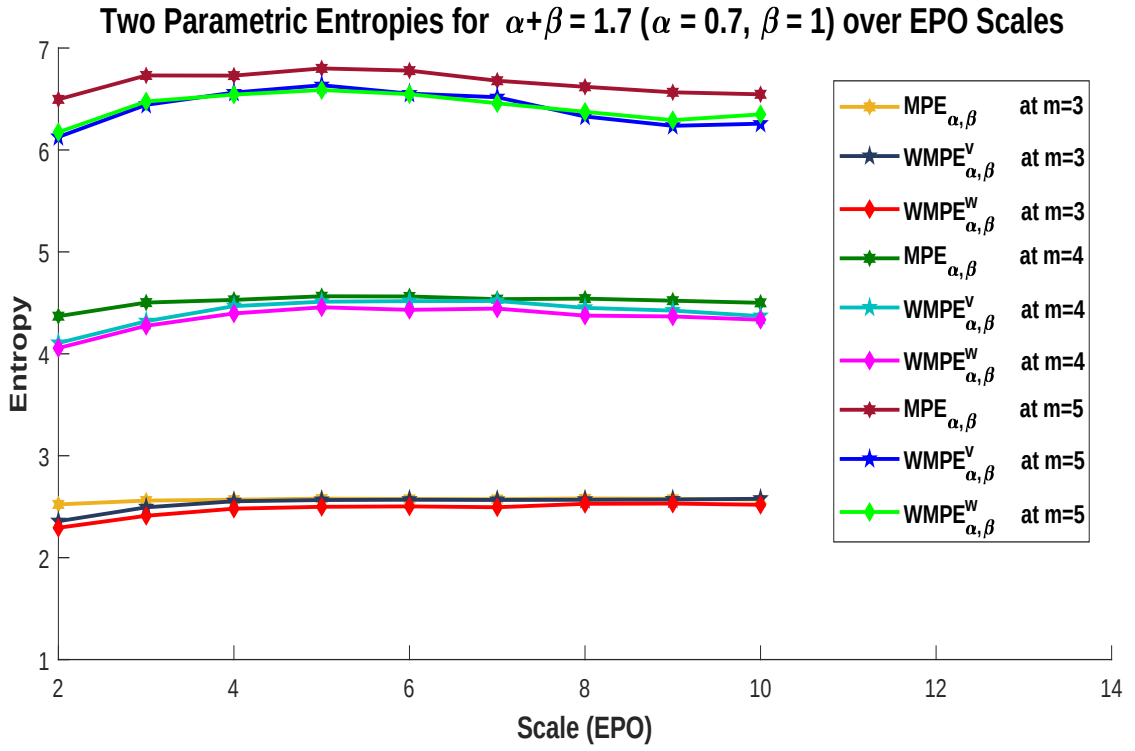

Figure 5.22: Entropies over EPO scales for $\alpha = 0.7$ and $\beta = 1.0$

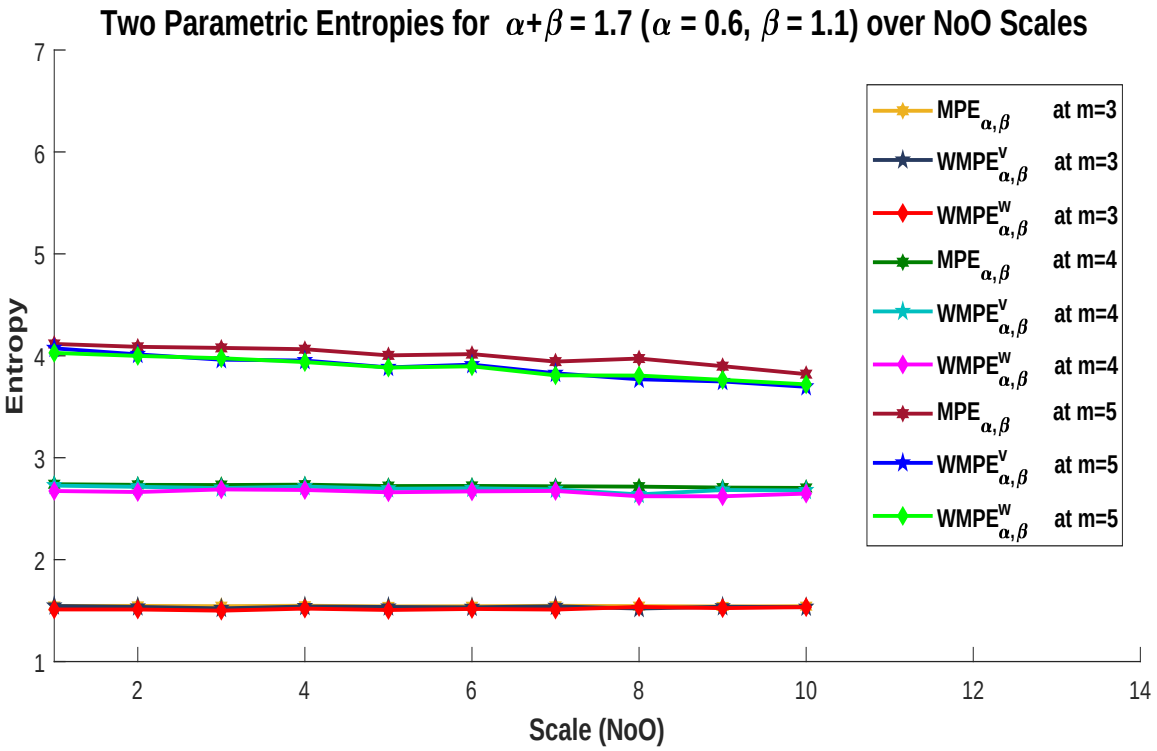

Figure 5.23: Entropies over non-overlapping scales for $\alpha = 0.6$ and $\beta = 1.1$

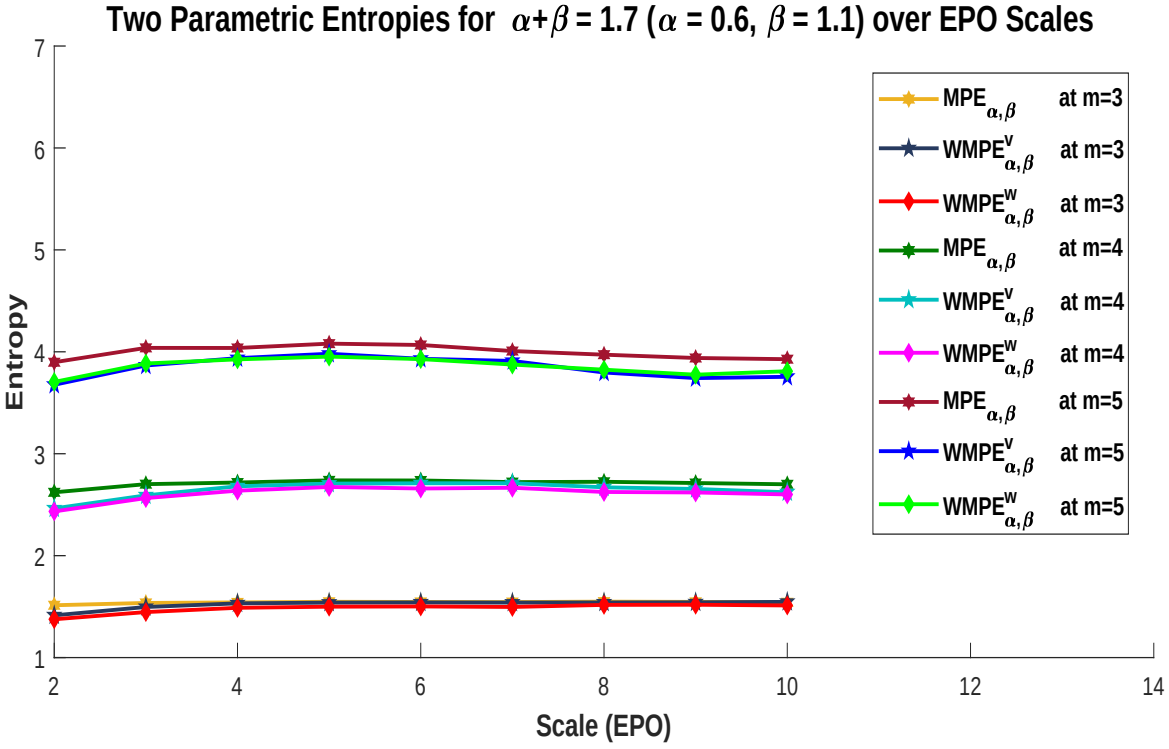

Figure 5.24: Entropies over EPO scales for $\alpha = 0.6$ and $\beta = 1.1$

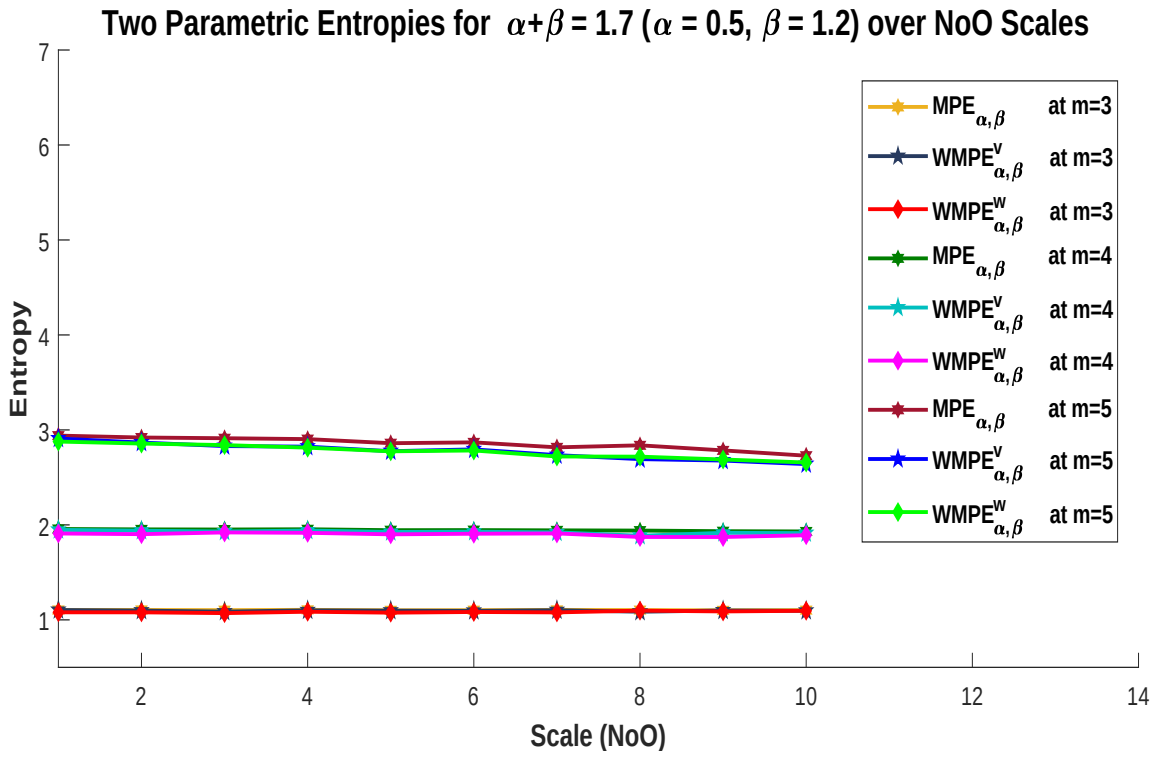

Figure 5.25: Entropies over non-overlapping scales for $\alpha = 0.5$ and $\beta = 1.2$

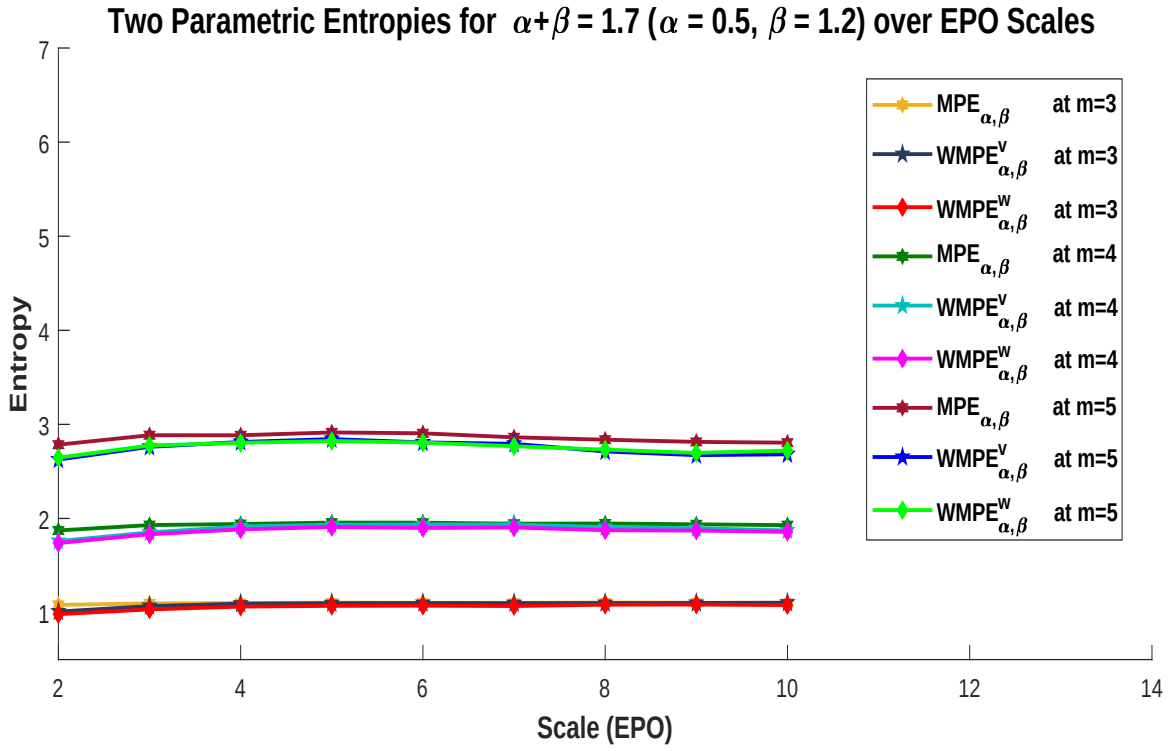

Figure 5.26: Entropies over EPO scales for $\alpha = 0.5$ and $\beta = 1.2$

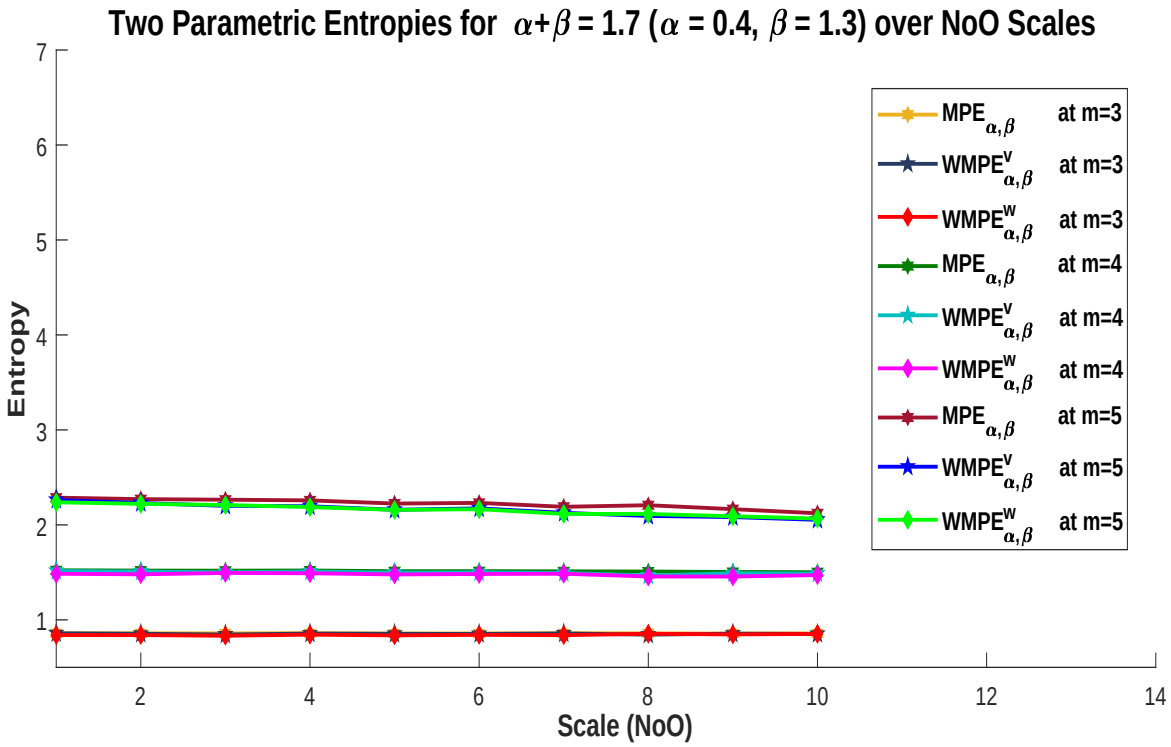

Figure 5.27: Entropies over non-overlapping scales for $\alpha = 0.4$ and $\beta = 1.3$

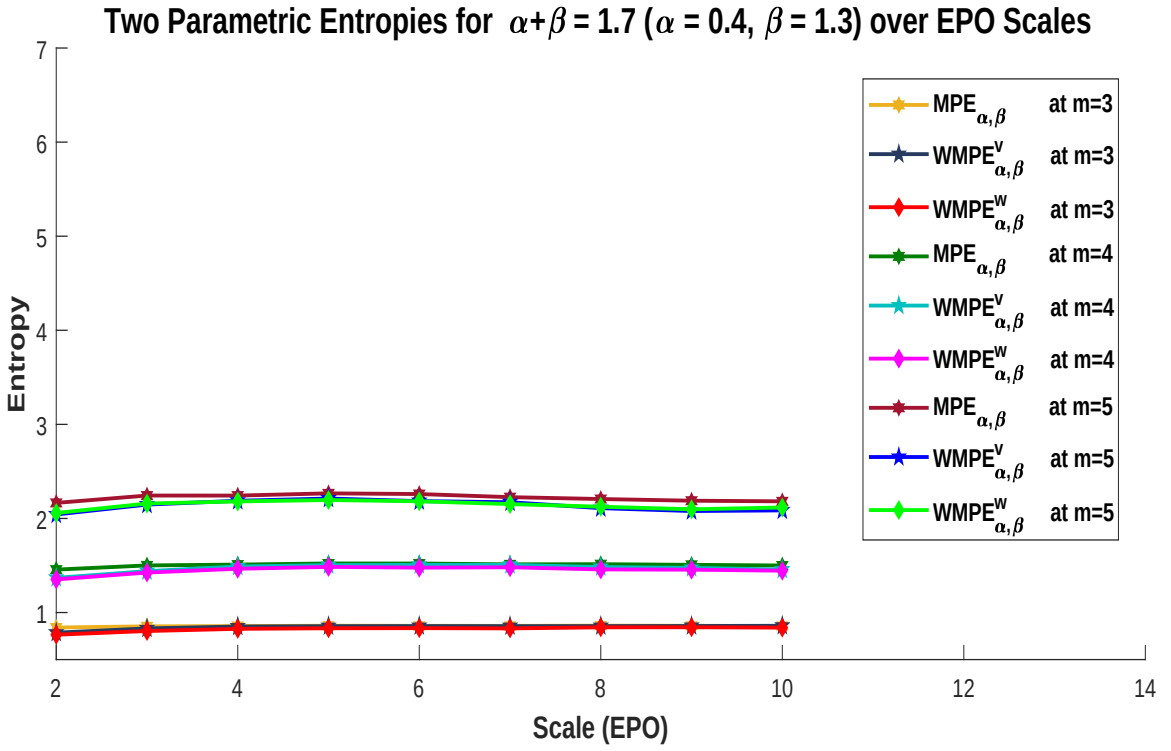

Figure 5.28: Entropies over EPO scales for $\alpha = 0.4$ and $\beta = 1.3$

The $WMPE^{w}_{\alpha,\beta}$ shows a significant improvement over $MPE_{\alpha,\beta}$ and $WMPE^{v}_{\alpha,\beta}$. Moreover, the standard deviation (S.D.) of $WMPE^{w}_{\alpha,\beta}$ is smaller than the S.D. of $MPE_{\alpha,\beta}$ and $WMPE^{v}_{\alpha,\beta}$ over both non-overlapping and EPO scales and has the lower values on EPO scales than on non-overlapping scales. For instance, the S.D. of $WMPE^{v}_{\alpha,\beta}$ and $WMPE^{w}_{\alpha,\beta}$ are given for $m = 5$ over non-overlapping and EPO scales at the different combinations of α and β in Table 5.14.

Table 5.14: Standard deviation of $WMPE^{v}_{\alpha,\beta}$ and $WMPE^{w}_{\alpha,\beta}$ on $m = 5$.

	NoO scales		EPO scales	
(α,β)	$WMPE^{v}_{\alpha,\beta}$	$WMPE^{w}_{\alpha,\beta}$	$WMPE^{v}_{\alpha,\beta}$	$WMPE^{w}_{\alpha,\beta}$
(0.5,1.0)	0.174812039	0.154298455	0.160385345	0.126272746
(0.4,1.1)	0.124865742	0.110213182	0.114560961	0.090194818
(0.3,1.2)	0.097117799	0.085721364	0.08910297	0.070151525
(0.6,1.0)	0.184345756	0.160191144	0.177987598	0.138318245
(0.5,1.1)	0.122897171	0.106794096	0.118658399	0.092212163
(0.4,1.2)	0.092172878	0.080095572	0.088993799	0.069159122
(0.7,1.0)	0.193246981	0.165702303	0.194411586	0.149869569
(0.6,1.1)	0.115948189	0.099421382	0.116646951	0.089921741
(0.5,1.2)	0.082820135	0.071015273	0.083319251	0.064229815
(0.4,1.3)	0.06441566	0.055234101	0.064803862	0.049956523

5.5 Conclusion

The $PE_{\alpha,\beta}$ is proposed and extended to give $MPE_{\alpha,\beta}$, $WMPE^{v}_{\alpha,\beta}$ and $WMPE^{w}_{\alpha,\beta}$ over non-overlapping and EPO scales. Consideration of EPO scales captures more information than non-overlapping scales, which commendably improves the entropies and gives the visible difference in $MPE_{\alpha,\beta}$, $WMPE^{v}_{\alpha,\beta}$ and $WMPE^{w}_{\alpha,\beta}$ even at $m = 3$ and $m = 4$. $WMPE^{v}_{\alpha,\beta}$ and $WMPE^{w}_{\alpha,\beta}$ values are always lower than $MPE_{\alpha,\beta}$, supporting that the inclusion of weights capture more information.

It is also obtained that the $WMPE^{w}_{\alpha,\beta}$, which is proposed using a new weighting scheme, gives the improved results than $MPE_{\alpha,\beta}$ and $WMPE^{v}_{\alpha,\beta}$. This scheme can be used as an alternate to variance for calculating the weights of neighbouring vectors. The new proposed weighting scheme is comparatively fast and has simple computations. The effect of change of parameters α and β on the entropy values is also studied. Different combinations of α and β result in to a wide range of entropy values. With an increase in α or β value, the entropy reduces.

Chapter 6

Comparative Study of Two Extensions of Heston Stochastic Volatility Model

Present chapter[1] *contemplates two extensions of the Heston stochastic volatility model. Out of which, one considers the addition of jumps to the stock price process (a stochastic volatility jump diffusion model) and another considers an additional stochastic volatility factor varying at a different time scale (a multiscale stochastic volatility model), in the Heston's model. An empirical analysis is carried out on the market data of options with different strike prices and maturities, to do a comparison in the pricing performance of these models and to capture their implied volatility fit. The unknown parameters of these models are calibrated using the non-linear least square optimization. It has been found that the multiscale stochastic volatility model performs better than the Heston stochastic volatility model and the stochastic volatility jump diffusion model for the data set under consideration.*

[1]The work reported in this chapter has been communicated in a research paper titled **"Comparative Study of a Stochastic Volatility Jump Model and a Multifactor Stochastic Volatility Model"**. Some of this work is presented in 'International Conference on Interdisciplinary Mathematics, Statistics and Computational Techniques' held at Manipal University, Jaipur from December 22-24, 2016 and in 'International Conference on Advanced Production and Industrial Engineering' held at Delhi Technological University, Delhi from October 6-7, 2017.

6.1 Introduction

In Chapter 1, we discussed in detail that the derivative pricing model proposed by Black and Scholes [14] assumes volatility to be constant and asset log-return distributions as Gaussian. Empirically, the volatility is not constant and the asset log-return distributions are non-Gaussian in nature characterised by heavy tails and high peaks [48]. A wide range of research has been done to improve upon classical Black-Scholes model. The model has been expanded to include either constant volatility with jumps (e.g. jump diffusion models given by Merton [83] and Kou [73]) or volatility itself a dynamic quantity as discussed in Subsection 1.3.4 of Chapter 1.

In the consideration of dynamic volatility, the most realistic models are the stochastic volatility models which allow the volatility to fluctuate randomly and are able to explain many empirical characteristics of volatility namely volatility smile (or skew), mean-reversion and leverage etc.

The Heston stochastic volatility (HSV) model [59] is most popular and successful among the single factor stochastic volatility models because it gives a fast and easily implemented semi closed form solution for the European call options, as described in Eq.(1.3.18) to Eq.(1.3.23) of Chapter 1. Computationally, it is very economical. But, despite its success and popularity, it has some shortcomings. The model is not efficiently able to give the volatility fit for all maturities and strike prices, particularity for the options with short expiry [48]. Shu and Zhang [110] obtained that the Heston model overprices OTM and short-term options and it underprices ITM options.

The single factor stochastic volatility models has been improved in many ways. One of these ways is to consider the stochastic volatility jump diffusion (SVJD or simply SVJ) models, which explain the distributional characteristics of return and implied volatility smile for the short term options (see Bakshi et al. [6]). An alternate approach is to consider the multifactor stochastic volatility (MSV) models. These models contemplate the multiple factors of volatility which vary at different time scales, thus sometimes named as the multiscale stochastic volatility models. These models give the improved fit for the market implied volatility.

This motivated us to study and compare these two approaches in context of Heston stochastic volatility model. So in this chapter, we have considered two

extensions of Heston stochastic volatility model. One model is the stochastic volatility jump diffusion model proposed in Yan and Hanson [124] where they considered the log-uniform distribution for the jump amplitude in the stock price process. The another model is the multiscale stochastic volatility model of Fouque and Lorig [37] in which a fast mean-reverting volatility factor is additionally considered in the framework of Heston stochastic volatility model.

These two models are compared with each other, and also with the Heston stochastic volatility model using S&P 500 index options data. Firstly, the model parameters are calibrated using non-linear least square optimization. Then the models' fit to the market implied volatility is captured against log moneyness at different time to maturity. The mean relative error of models' prices with market data is also calculated. We have obtained that the MSV model performs better than the other two models.

The rest of the chapter is organized as follows: The underlying models has been explained in Section 6.2. The empirical analysis has been conducted in Section 6.3 to compare these models, where the calibration of the models' parameters, models' fit to market implied volatility and mean relative error of model prices with market data has been reported and the results obtained are discussed. The conclusion has been given in Section 6.4.

6.2 Models Under Consideration

We explain the two models to be considered for the empirical analysis.

6.2.1 Stochastic Volatility Jump Diffusion Model

Yan and Hanson [124] proposed a SVJ model which considers the log-uniform distribution of the jump amplitudes in the stock price process. The model is explained below:

Let X_t be the stock price at time t whose dynamics under the risk-neutral probability measure P^* is

$$dX_t = X_t((r-\lambda\bar{J})dt + \sqrt{V_t}dW_t^x + J(U)dN_t) \tag{6.2.1}$$

where r is the risk free interest rate and $J(U)$ is the Poisson jump-amplitude with mean $\overline{J}$. The variance V_t follows the CIR process given by

$$dV_t = \kappa(\theta - V_t)dt + \sigma\sqrt{V_t}dW_t^v \tag{6.2.2}$$

with κ as the rate of mean-reversion, θ as the long-run mean value and σ as the volatility of variance. The condition $2\kappa\theta \geq \sigma^2$ must be satisfied to ensure the positivity of the process (6.2.2). W_t^x and W_t^v are the standard Brownian motions for the stock price process and the volatility process respectively with correlation

$$E[dW_t^x.dW_t^v] = \rho_{xv}dt$$

U is the amplitude mark process which is assumed to be uniformly distributed with density

$$\varphi_U(u) = \begin{cases} \frac{1}{n-m} & \text{if } m \leq u \leq n, \\ 0 & \text{otherwise} \end{cases}$$

and is given by

$$U = \ln(J(U)+1)$$

N_t is the standard Poisson jump counting process with jump intensity λ, $J(U)dN_t$ is the Poisson sum which is given as

$$J(U)dN_t = \sum_{i=1}^{dN_t} J(U_i)$$

here U_i is the ith jump-amplitude random variable and $\overline{J}$, the mean of jump-amplitude J, is given as

$$\overline{J} = E[J(U)] = \frac{e^n - e^m}{n-m} - 1.$$

Under this model, the pricing formula for the European call option, in terms of log stock price $s = \ln(x)$, is given as:

$$C_{svj} = e^s P_1(s,v,t,K,T) - Ke^{-r(T-t)}P_2(s,v,t,K,T) \tag{6.2.3}$$

where $v = V_t$ is the variance at time t, T is the maturity time, K is the strike price and r is the risk free interest rate. The subscript svj in the price C_{svj} is just to

specify the price obtained from SVJ model. The same convention is also followed for Heston and MSV model.

For $j = 1, 2$,

$$P_j(s,v,t,K,T) = \frac{1}{2} + \frac{1}{\pi}\int_0^\infty Re\left[\frac{e^{-i\phi \ln K} f_j(s,v,t,\phi,T)}{i\phi}\right] d\phi, \tag{6.2.4}$$

where the characteristic function f_j of P_j is

$$f_j(s,v,t,\phi,t+\tau) = e^{A_{(1j)}(\tau,\phi)+A_{(2j)}(\tau,\phi)v+i\phi s+\beta_j(\tau)} \tag{6.2.5}$$

with $\tau = T-t$ and $\beta_j(\tau) = r\tau\delta_{j,2}$; $\delta_{j,2} = 1$ for $j = 2$ and 0 for $j = 1$. The other terms are

$$A_{(1j)}(\tau,\phi) = r\phi i\tau - (\lambda\overline{J}i\phi + \lambda\overline{J}\delta_{j,1} + r\delta_{j,2})\tau + \lambda\tau\left[\frac{e^{(i\phi+\delta_{j,1})n} - e^{(i\phi+\delta_{j,1})m}}{(n-m)(i\phi+\delta_{j,1})} - 1\right] + A'_{(1j)}(\tau,\phi), \tag{6.2.6}$$

$$A_{(2j)}(\tau,\phi) = \frac{b_j - \rho\sigma\phi i + d_j}{\sigma^2}\left(\frac{1-e^{d_j\tau}}{1-g_j e^{d_j\tau}}\right), \tag{6.2.7}$$

and

$$A'_{(1j)}(\tau,\phi) = \frac{\kappa\theta}{\sigma^2}\left[(b_j - \rho\sigma\phi i + d_j)\tau - 2\ln\left(\frac{1-g_j e^{d_j\tau}}{1-g_j}\right)\right] \tag{6.2.8}$$

with

$$g_j = \frac{b_j - \rho\sigma\phi i + d_j}{b_j - \rho\sigma\phi i - d_j},$$

$$d_j = \sqrt{(\rho\sigma\phi i - b_j)^2 - \sigma^2(2\alpha_j\phi i - \phi^2)},$$

and

$$\alpha_1 = \frac{1}{2},\ \alpha_2 = \frac{-1}{2},\ b_1 = \kappa - \rho\sigma,\ b_2 = \kappa \tag{6.2.9}$$

The unknown parameters of this model are κ, θ, σ, ρ, v, λ, m and n.

After the SVJ model, we give the MSV model of Fouque and Lorig [37].

6.2.2 Multiscale Stochastic Volatility Model

Fouque and Lorig [37] extended the Heston stochastic volatility model to a MSV model by considering an additional fast mean-reverting volatility factor in the Heston stochastic volatility model. This model is given below.

Under P^*, the dynamics of stock price X_t is given as

$$dX_t = rX_t dt + \eta_t X_t dW_t^x \tag{6.2.10}$$

here $\eta_t = \sqrt{V_t} f(Y_t)$. Y_t and V_t are respectively the fast and the slow scale factors of volatility with their dynamics given as

$$dY_t = \frac{V_t}{\varepsilon}(m - Y_t)dt + \mu\sqrt{2}\sqrt{\frac{V_t}{\varepsilon}}dW_t^y \tag{6.2.11}$$

and

$$dV_t = \kappa(\theta - V_t)dt + \sigma\sqrt{V_t}dW_t^v \tag{6.2.12}$$

W_t^x ,W_t^y and W_t^v are the standard Brownian motions for the stock price process and for the fast and the slow factors of volatility respectively with $E(dW_t^x.dW_t^y) = \rho_{xy}dt$, $E(dW_t^x.dW_t^v) = \rho_{xv}dt$, and $E(dW_t^y.dW_t^v) = \rho_{yv}dt$. ρ_{xy}, ρ_{xv} and ρ_{yv} are constants which satisfy $\rho_{xy}^2 < 1, \rho_{xv}^2 < 1, \rho_{yv}^2 < 1$ and $\rho_{xy}^2 + \rho_{xv}^2 + \rho_{yv}^2 - 2\rho_{xy}\rho_{xv}\rho_{yv} < 1$.

The fast factor of volatility, Y_t follows the OU process with the mean-reversion rate V_t/ε and volatility of volatility parameter $\mu\sqrt{2}\sqrt{\frac{V_t}{\varepsilon}}$. $\varepsilon > 0$ is very small so that Y_t is fast mean-reverting towards its long-run mean m. The slow volatility factor V_t, as already explained for SVJ model, is the square root process. It slowly reverts to its long-run mean θ.

Fouque and Lorig [37] used the perturbation technique to obtain the expression for European call option prices. The asymptotic expansion of price in powers of $\sqrt{\varepsilon}$ is given as

$$C_{msv}^{\varepsilon}(x,y,v,t) = C_0 + \sqrt{\varepsilon}C_1 + \varepsilon C_2 + ... \tag{6.2.13}$$

They obtained the first order approximation to the price of the European call option as

$$C_{msv}^{\varepsilon}(x,v,t) \approx C_0(x,v,t) + \sqrt{\varepsilon}C_1(x,v,t)$$

This price approximation is clearly independent of the fast factor of volatility and depends only on the slow volatility factor v. The approximated price is perturbed around the Heston price C_0 at the effective correlation $\rho_{xv} < f >$, where $< f >$ is the average of $f(y)$ with respect to long-run distribution of the volatility factor Y_t.

The first order approximation term C_1 is

$$C_1 = e^s Q_1(s,v,t,K,T) - Ke^{-r(T-t)}Q_2(s,v,t,K,T) \tag{6.2.14}$$

where $s = \ln x$. For $j = 1, 2$

$$Q_j(s,v,t,K,T) = \frac{1}{2} + \frac{1}{\pi}\int_0^\infty Re\left[\frac{e^{-i\phi \ln K} q_j(s,v,t,\phi,T)}{i\phi}\right] d\phi \tag{6.2.15}$$

The characteristic function q_j of Q_j is

$$q_j(s,v,t,\phi,t+\tau) = (\kappa\theta\hat{q_0}(\tau,\phi) + v\hat{q_1}(\tau,\phi))(e^{A'_{(1j)}(\tau,\phi)+A_{(2j)}(\tau,\phi)v+i\phi s}) \tag{6.2.16}$$

here

$$\hat{q_0}(\tau,\phi) = \int_0^\tau \hat{q_1}(z,\phi)dz,$$
$$\hat{q_1}(\tau,\phi) = \int_0^\tau B(z,\phi)e^{A_{(3j)}(\tau,\phi,z)}dz$$

with

$$A_{(3j)}(\tau,\phi,z) = (b_j - \rho\sigma\phi i + d_j)\frac{1-g_j}{d_j g_j}\ln\left(\frac{g_j e^{d_j\tau}-1}{g_j e^{d_j z}-1}\right)$$
$$B(\tau,\phi) = -(V_1 A_{(2j)}(\tau,\phi)(2\alpha_j\phi i - \phi^2) + V_2 A^2_{(2j)}(\tau,\phi)(\phi i) + V_3(2\alpha_j\phi^3 i + \phi^2)$$
$$+ V_4 A_{(2j)}(\tau,\phi)(-\phi^2)) \tag{6.2.17}$$

All the other terms are already given in Eq.(6.2.8) to Eq.(6.2.9). The unknown parameters of this model are κ, θ, σ, ρ, v, V_1, V_2, V_3 and V_4.

In the next section, the empirical analysis is conducted to compare these models.

6.3 Empirical Analysis and Discussion of Results

For the empirical analysis, the data of S&P 500 index options is considered from January 4, 2016 with maturity ranging from 30 days to 180 days and moneyness from 75% to 125%. The risk free rate of interest is the yield on 3-month "U.S. government treasury bill". Firstly, the unknown parameters of each model are calibrated using non-linear least square optimization. Once the parameters are obtained, the models' fit to the market implied volatilities for the S&P 500 index are captured and plotted against log moneyness. To compare the pricing performance, the mean relative error of each model price is calculated corresponding to the market option price data. These methods are explained in following subsections.

6.3.1 Calibration of Model Parameters

The unknown parameters of Heston stochastic volatility model, SVJ model and MSV model are calibrated using the data of S&P 500 index options. Let M_1, M_2 and M_3 denote the parameter sets of unknown parameters of Heston, SVJ and MSV model respectively , such that

$$\begin{aligned} M_1 &= (\zeta, \rho, \sigma, \theta, v) \\ M_2 &= (\zeta, \rho, \sigma, \theta, v, \lambda, m, n) \\ M_2 &= (\zeta, \rho, \sigma, \theta, v, V_1, V_2, V_3, V_4) \end{aligned} \tag{6.3.1}$$

here all of these unknown parameters are already mentioned in Section 6.2 except ζ, which is obtained from the condition $2\kappa\theta \geq \sigma^2$ of the CIR process $(6.2.2)$ such that $\zeta = \kappa - \frac{\sigma^2}{2\theta}, \quad \zeta \geq 0$. Thus, the rate of mean-reversion $\kappa = \zeta + \frac{\sigma^2}{2\theta}$ is obtained from the calibrated values of ζ, σ and θ.

These parameters are calibrated by non-linear least square optimization using $MATLAB2012b$. The objective function is defined as:

$$\Delta_h^2(M_1) = \sum_j \sum_{i(j)} (C_{mkt}(T_j, K_{i(j)}) - C_h(T_j, K_{i(j)}, M_1))^2 \tag{6.3.2}$$

$$\Delta_{svj}^2(M_2) = \sum_j \sum_{i(j)} (C_{mkt}(T_j, K_{i(j)}) - C_{svj}(T_j, K_{i(j)}, M_2))^2 \tag{6.3.3}$$

$$\Delta_{msv}^2(M_3) = \sum_j \sum_{i(j)} (C_{mkt}(T_j, K_{i(j)}) - C_{msv}(T_j, K_{i(j)}, M_3))^2 \tag{6.3.4}$$

where $C_{mkt}(T_j, K_{i(j)})$ is the market price of call option with maturity T_j. For each expiration T_j, the available collection of strike prices is $K_{i(j)}$. Similarly, for a particular value of T_j and $K_{i(j)}$, $C_h(T_j, K_{i(j)}, M_1)$, $C_{svj}(T_j, K_{i(j)}, M_2)$ and $C_{msv}(T_j, K_{i(j)}, M_3)$ are the prices of the European call options with expiration date T_j and exercise price $K_{i(j)}$, calculated from the Heston stochastic volatility model with parameter set M_1, SVJ model with the parameter set M_2 and MSV model with the parameter set M_3 respectively.

The optimal set of parameters M_1^*,M_2^* and M_3^* is obtained which satisfies

$$\begin{aligned}
\Delta_h^2(M_1^*) &= min_{M_1}(\Delta_h^2(M_1)) \\
\Delta_{svj}^2(M_2^*) &= min_{M_2}(\Delta_{svj}^2(M_2)) \\
\Delta_{msv}^2(M_3^*) &= min_{M_3}(\Delta_{msv}^2(M_3))
\end{aligned} \tag{6.3.5}$$

Firstly, the optimal parameter set for the Heston stochastic volatility model, M_1^*, is calibrated. Once the M_1^* is obtained, the initial iteration for SVJ model is taken as $(M_1^*,\ 50,\ -0.01,\ 0.01)$ with the lower and upper bounds for the last three components as $(1,\ -1,\ 0)$ and $(100,\ 0,\ 1)$ respectively. Similarly, the initial iteration for MSV model is taken as $(M_1^*,\ 0.0001,\ 0,\ 0,\ 0)$ with the lower and upper bounds for last four components as $(-0.05,\ -0.05,\ -0.05,\ -0.05)$ and $(0.05,\ 0.05,\ 0.05,\ 0.05)$ respectively.

Using the optimal parameter set, the implied volatility fit for all the three models is obtained and is plotted against log moneyness ($log\frac{K}{X}$). The models fit are compared relative to market implied volatility (MV) data. It is given in Fig.6.1 to Fig.6.3 for time to maturity 30 days, 90 days and 180 days respectively.

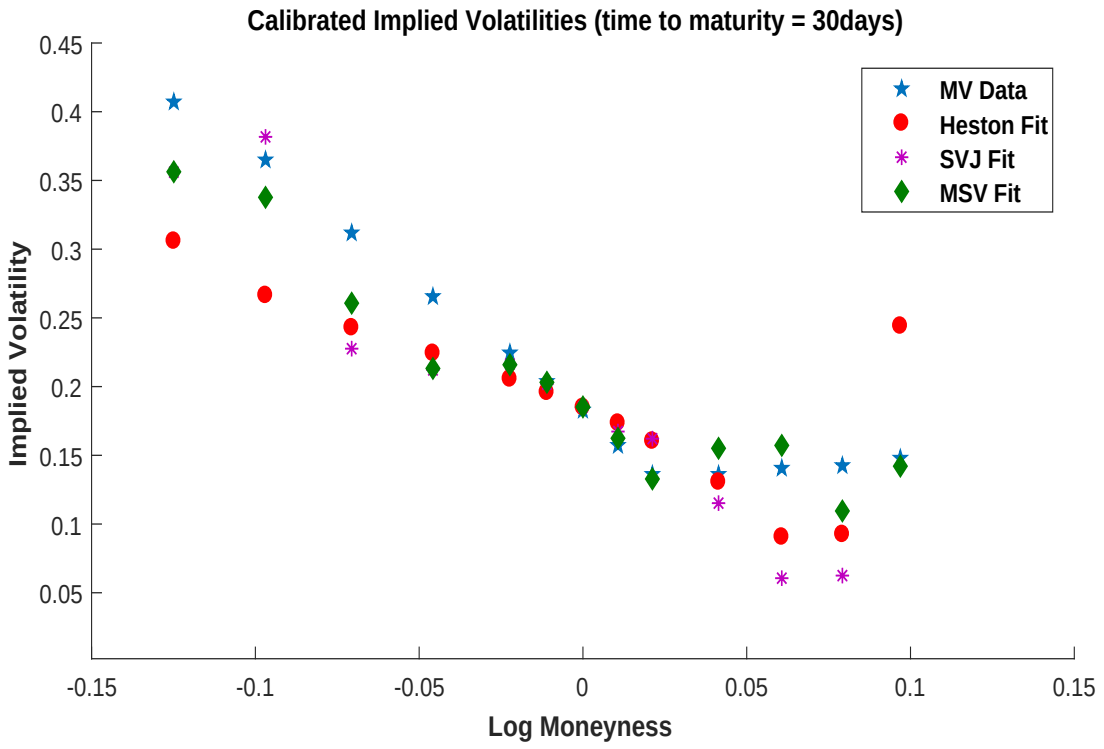

Figure 6.1: Models' fit to the implied volatilities of S&P 500 index with 30 days to maturity

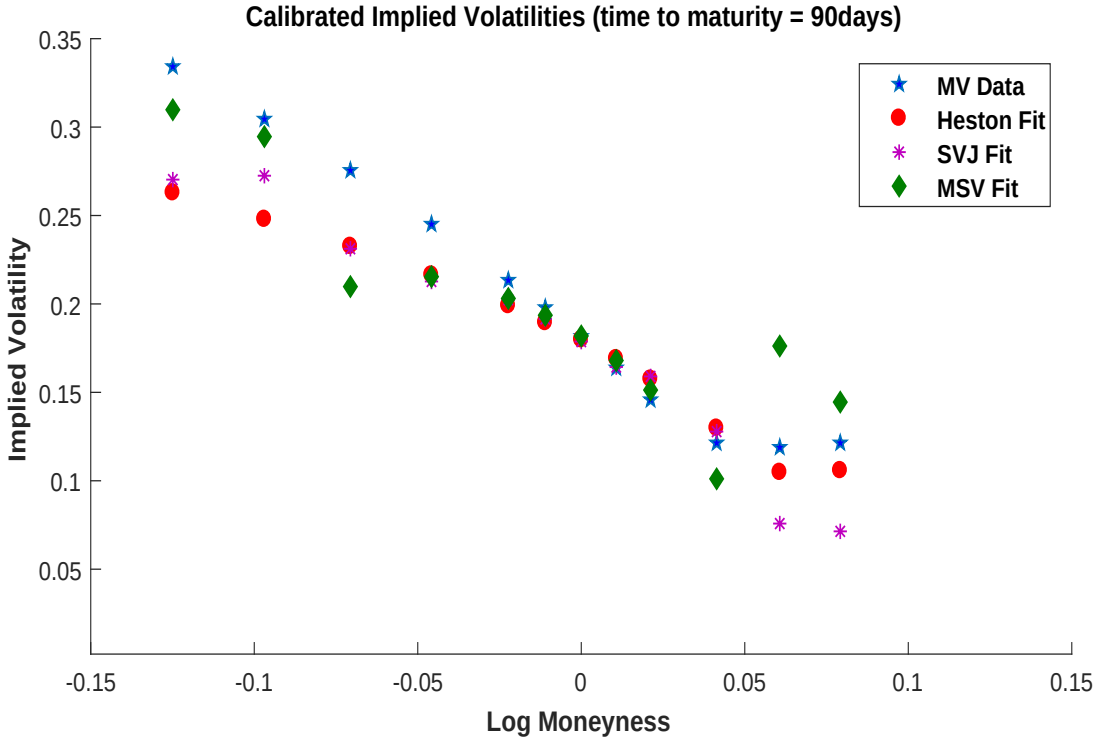

Figure 6.2: Models' fit to the implied volatilities of S&P 500 index with 90 days to maturity

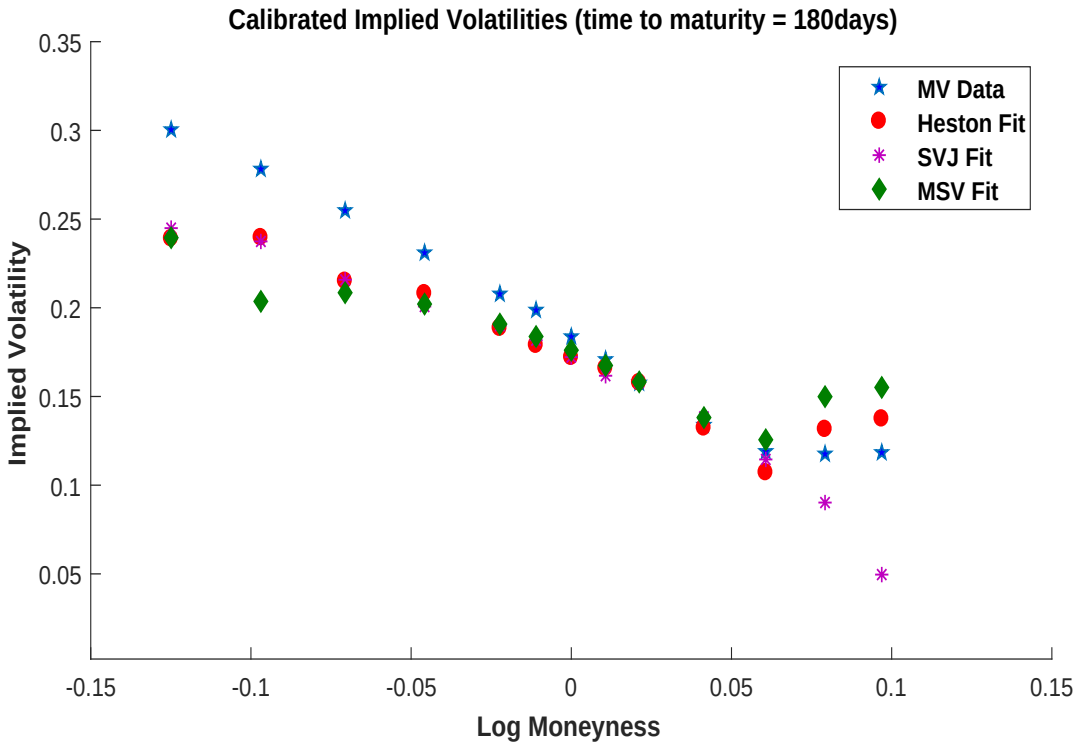

Figure 6.3: Models' fit to the implied volatilities of S&P 500 index with 180 days to maturity

The parameters are calibrated from the whole data but the results are given and discussed for the different maturity times, separately.

Along with this, the mean relative error of the prices obtained from Heston stochastic volatility model, SVJ model and MSV model, with the market data of S&P 500 index option, is calculated at different maturity time. It is given in Subsection 6.3.2.

6.3.2 Mean Relative Error

For a particular model with price $C_{model}(T_j, K_{i(j)}, \Theta)$ at different values of T_j and $K_{i(j)}$, the mean relative error (MRE) of model price with respect to market price, at time to maturity T_j is given as

$$MRE(j) = \frac{1}{N_j} \sum_{i(j)} \frac{|C_{model}(T_j, K_{i(j)}, \Theta) - C_{mkt}(T_j, K_{i(j)})|}{C_{mkt}(T_j, K_{i(j)})} \tag{6.3.6}$$

where N_j is the different number of call options that has expiry at time T_j, Θ is the optimal parameter set for the given model.

The mean relative error of Heston stochastic volatility model, SVJ model and MSV model is calculated for S&P 500 index data set. The maturity time is taken from 30 days to 180 days. Corresponding to a particular maturity, the strike prices range from 75% to 125%. The results are given in Table 6.1.

Table 6.1: The mean relative error of models prices with respect to market data.

	Models		
Maturity Time (T)	Heston	SVJ	MSV
30 days	0.0697	0.0499	0.0225
90 days	0.0874	0.0987	0.0456
180 days	0.0284	0.1070	0.0380

Now, we discuss the results obtained in Fig.6.1 to Fig.6.3 and in Table6.1. From the models fit to the implied volatility given in Fig.6.1 to Fig.6.3, it is clearly observable that the MSV model performs in an improved way in comparison to Heston stochastic volatility model and the SVJ model. For ATM and near the money options, all the three models give equivalent results. The difference is observable for ITM and OTM options.

In Fig.6.1, the maturity time is short, that is 30 days. For such options, the Heston model fit to market implied volatility is not good. This supports the empirical findings that the Heston model poorly performs for short term options. The SVJ model performs better than Heston model and MSV model for deep ITM options, but as the log moneyness value increases, MSV model outperforms both Heston model and SVJ model.

In Fig.6.2, the maturity time is medium, that is 90 days. The implied volatility fit of Heston model is improved for the OTM options. For ITM options, implied volatility fit of MSV model is better than the implied volatility fit of Heston model. The Heston model fit is equivalent to the SVJ model fit to market implied volatility.

In Fig.6.3, at the longer maturity, which is 180 days, all of the three models give almost similar fit for ITM options but for OTM options the Heston model outperforms the other two models. The implied volatility fit of MSV model is better than the fit of SVJ model to the market implied volatilities.

Thus, out of SVJ model and MSV model, the overall fit of MSV model to the market implied volatility is better than SVJ model.

Additionally, from Table6.1, the pricing performance of three models is compared in terms of mean relative error of models prices with the market option price data. For the short and medium term options with maturity 30 and 90 days respectively, the mean relative error of MSV model is least. Thus the MSV model performs better than the SVJ model and Heston model in pricing. For maturity time 30 days, SVJ model performs better than Heston model in pricing, but for maturity 90 days, Heston model gives better pricing performance.

For the long term options with maturity 180 days, the MSV model performs better than SVJ model and Heston model outperforms the SVJ and MSV model.

Thus, out of SVJ model and MSV model, the overall pricing performance of MSV model is better than SVJ model for the data set under consideration.

6.4 Conclusion

The two extensions of Heston stochastic volatility model, already proposed in literature, are studied and compared in this chapter on the basis of their fit to the market implied volatility and pricing performance. An empirical analysis is conducted on S&P 500 index options data and the results are obtained for all the

three models. We obtained that for the data set under consideration and out of the two models considered in this study, multiscale stochastic volatility performs better than the stochastic volatility jump model. Thus, we conclude that the inclusion of additional volatility factor to a stochastic volatility model enhances its fit to the market implied volatility and improves its pricing performance in comparison to the addition of jump factors to the underlying stock price process.

Conclusion and Further Scope of the Work

The motive of the work reported in this thesis was to mathematically study the risk in the financial markets. The standard measure of risk is volatility and an alternate measure of risk is entropy which is also an uncertainty measure. We have explored both these aspects for the asset pricing and analysis of financial log-return series.

The Black-Scholes model for pricing European options was a turning point in the history of option pricing. The model considered volatility to be constant and lognormal distribution for the asset returns. Empirically, it was obtained that these assumptions did not hold good in the actual market scenario. After 1987 stock market crash, the model was extended in numerous ways. Many models were proposed to capture the dynamic behaviour of volatility for the better accuracy of the option pricing. Among these extensions, the stochastic volatility models were the much reformed models because of their ability to capture many empirical characteristics of volatility. The Heston stochastic volatility model became a very popular single factor stochastic volatility model. These stochastic volatility models with single factor of volatility were further improved, either by the addition of jumps in the stock price or (and) the volatility process, or by the inclusion of additional factors of volatility in the model, to capture the time varying nature of volatility. The models with the additional factors of volatility, which varies at different time scales, were named as the multifactor stochastic volatility models.

Amid these multifactor stochastic volatility models, Fouque et al. [39] proposed a model with two factors of volatility, one varying on the fast time scale and another on the slow time scale. Their model considered the diffusion of slow volatility factor resulting from a simple time change. They did not emphasize much on the dynamics of slow scale volatility factor which is the persistent volatility factor.

This motivated us to introduce a new multifactor stochastic volatility model where we have proposed to approximate slow volatility factor with a quadratic arc. This model is firstly used to obtain the pricing formula and to capture the volatility smiles for the European options. With this model, we have obtained a very simple and easily implemented pricing formula for the European options with only one unknown parameter which has been estimated from the implied volatility calibration. To see the performance of this model for the path-dependent Asian options, the model has further been extended to include additional factor of randomness arose by geometric averaging in the pricing of floating and fixed strike GAOs. A comparative study of a stochastic volatility jump model and a multifactor stochastic volatility model has also been done to capture the market implied volatility and for the pricing of European options, where we have found that the multifactor stochastic model performs better than the stochastic volatility jump model.

Entropy has widely been used for the asset pricing, portfolio selection and time series analysis. Therefore, along with the stochastic volatility modeling, we have worked on the entropy approach for the financial asset pricing and analysis of asset log-return series. The concept of approximation of slow volatility factor has been infused with the entropy maximization. For this, we have proposed to calibrate the risk-neutral density function by the maximization of two-parameter (Varma) entropy with the mean and variance constraint. For the variance constraint, we have considered the quadratic expression of volatility. The maximum entropy density function thus obtained has been used to price the European options. The maximization of Varma entropy with additional volatility constraint has generalized the maximization results of Shannon, Rényi and Tsallis entropies for the calibration of risk-neutral density function and pricing of European options. Also, the consideration of two-parameter entropy has given the additional degrees of freedom. Additionally, for the analysis of asset log-return series, two-parameter permutation entropy has been proposed and extended to include multiscales and weights. The end point overlapping scheme for averaging the time series has been proposed. A new weighting scheme has also been proposed. The two-parameter multiscale permutation entropy and two-parameter weighted multiscale permutation entropies thus proposed have been used to analyse the asset log-return series.

Throughout this thesis, we have verified our results on the actual market data of stock indices. We have mainly used S&P 500 index closing price data, and S&P 500 index options data with different maturity and strike prices for both European and geometric Asian call options. Along with this, FTSE 100 index options data with different maturity and strike prices is also used for the empirical analysis. We have used *MATLAB2012b* and *Excel2013* for the numerical computations and graphical representation of the results.

Further Scope of the Work

While working on this thesis several ideas have come up in our minds, which could be of great potential to study further.

The proposed multifactor stochastic volatility model can be extended for the pricing of American and other path-dependent options.

The foreign exchange options market is the deepest, largest and the most liquid market for options of any kind. In 1983, Garman and Kohlhagen [47] extended the Black-Scholes model for the foreign exchange option pricing to cope with the presence of two interest rates. The model proposed in Chapter 2 has been used to price only stock index options and can be extended for the pricing of foreign exchange options.

The interesting issue of the relationship between the densities generated by the stochastic volatility model and the maximum entropy density function can be explored in the future work.

We have introduced a two-parameter permutation entropy and have shown empirically with S&P 500 index data set that the two-parameter weighted multiscale permutation entropy using new weighting scheme and using end point overlapping average gives improved results. This entropy can be further used for the comparative analysis of different stock indices.

Bibliography

[1] Alizadeh, S., Brandt, M.W. and Diebold, F.X. (2002). Range-Based Estimation of Stochastic Volatility Models. *Journal of Finance*, **57**, 1047 – 1091.

[2] Angus, J.E. (1999). A Note on Pricing Asain Derivatives with Continuous Geometric Averaging. *Journal of Futures Markets*, **19**, 845 – 858.

[3] Avellaneda, M. (1998). Minimum-Relative-Entropy Calibration of Asset-Pricing Models. *International Journal of Theoretical and Applied Finance*, **1**, 447 – 472.

[4] Ayres, H.F. (1963). Risk Aversion in the Warrants Market. *Industrial Management Review*, **4**, 497 – 505.

[5] Bachelier, L. (1900). Théorie de la spéculation. *Annales Scientifiques de l'École Normale Supérieure*, **17**, 21 – 86.

[6] Bakshi, G., Cao, C. and Chen, Z. (1997). Empirical Performance of Alternative Option Pricing Models. *Journal of Finance*, **52**, 2003 – 2049.

[7] Ball, C.A. and Roma, A. (1994). Stochastic Volatility Option Pricing. *Journal of Financial and Quantitative Analysis*, **29**, 589 – 607.

[8] Bandt, C. and Pompe, B. (2002). Permutation Entropy: A Natural Complexity Measure for Time Series. *Physical Review Letters*, **88**, 174102.

[9] Bates, D.S. (2000). Post-'87 Crash Fears in the S&P500 Futures Option Market. *Journal of Econometrics*, **94**, 181 – 238.

[10] Baumol, W.J., Malkiel, B.G. and Quandt, R.E. (1966). The Valuation of Convertible Securities. *Quarterly Journal of Economics*, **80**, 48 – 59.

[11] Benedetto, F., Giunta, G. and Mastroeni, L. (2015). A Maximum Entropy Method to Assess the Predictability of Financial and Commodity Prices. *Digital Signal Processing*, **46**, 19 – 31.

[12] Bentes, S.R. and Menezes, R. (2012). Entropy: A New Measure of Stock Market Volatility? *Journal of Physics: Conference Series*, **394**, 012033.

[13] Bera, A.K. and Park, S.Y. (2008). Optimal Portfolio Diversification Using the Maximum Entropy Principle. *Econometric Reviews*, **27**, 484 – 512.

[14] Black, F. and Scholes, M. (1973). The Pricing of Options and Corporate Liabilities. *Journal of Political Economy*, **81**, 637 – 654.

[15] Boness, A.J. (1964). Elements of a Theory of Stock-Option Value. *Journal of Political Economy*, **72**, 163 – 75.

[16] Brody, D.C., Buckley, I.R.C. and Constantinou, I.C. (2007). Option Price Calibration from Rényi Entropy. *Physics Letters A*, **366**, 298 – 307.

[17] Buchen, P.W. and Kelly, M. (1996). The Maximum Entropy Distribution of an Asset Inferred from Option Prices. *Journal of Financial and Quantitative Analysis*, **31**, 143 – 159.

[18] Chen, A.H.Y. (1970). A Model of Warrant Pricing in a Dynamic Market. *Journal of Finance*, **25**, 1041 – 1059.

[19] Chen, S., Shang, P. and Wu, Y. (2018). Weighted Multiscale Rényi Permutation Entropy of Nonlinear Time Series. *Physica A: Statistical Mechanics and Its Applications*, **496**, 548 – 570.

[20] Chernov, M. and Ghysels, E. (2000). A Study Towards a Unified Approach to the Joint Estimation of Objective and Risk Neutral Measures for the Purpose of Options Valuation. *Journal of Financial Economics*, **56**, 407 – 458.

[21] Chong, W.F., Hu, Y., Liang, G. and Zariphopoulou, T. (2019). An Ergodic BSDE Approach to Forward Entropic Risk Measures: Representation and Large-Maturity Behavior. *Finance and Stochastics*, **23**, 239 – 273.

[22] Christoffersen, P., Heston, S. and Jacobs, K. (2009). The Shape and Term Structure of the Index Option Smirk: Why Multifactor Stochastic Volatility Models Work So Well. *Management Science*, **55**, 1914 – 1932.

[23] Cont, R. and Tankov, P. (2004). *Financial Modelling with Jump Processes*. USA: CRC Press LLC.

[24] Costa, M., Goldberger, A.L. and Peng, C.K. (2002). Multiscale Entropy Analysis of Complex Physiologic Time Series. *Physical Review Letters*, **89**, 068102.

[25] Cox, J.C. and Ross, S.A. (1976). The Valuation of Options for Alternative Stochastic Processes. *Journal of Financial Economics*, **3**, 145 – 166.

[26] Cozzolino, J.M. and Zahner, M.J. (1973). The Maximum-Entropy Distribution of the Future Market Price of a Stock. *Operations Research*, **21**, 1200 – 1211.

[27] Csiszár, I. (1975). I-Divergence Geometry of Probability Distributions and Minimization Problems. *The Annals of Probability*, **3**, 146 – 158.

[28] Derman, E. and Kani, I. (1994). Riding On a Smile. *Risk*, **7**, 32 – 39.

[29] Dupacova, J., Hurt, J. and Stepan, J. (2003). *Stochastic Modeling in Economics and Finance*. Kluwer Academic Publishers.

[30] Dupire, B. (1994). Pricing With a Smile. *Risk*, **7**, 18 – 20.

[31] Engle, R.F. and Patton, A.J. (2001). What Good is a Volatility Model? *Quantitative Finance*, **1**, 237 – 245.

[32] Fadlallah, B., Chen, B., Keil, A. and Principe, J. (2013). Weighted-Permutation Entropy: A Complexity Measure for Time Series Incorporating Amplitude Information. *Physcal Review E*, **87**, 022911.

[33] Fatone, L., Mariani, F., Recchioni, M.C. and Zirilli, F. (2009). An Explicitly Solvable Multi-Scale Stochastic Volatility Model: Option Pricing and Calibration Problems. *Journal of Futures Markets*, **29**, 862 – 893.

[34] Friedman, A. (1975). *Stochastic Differential Equations and Applications (Volume 1)*. New York: Academic Press.

[35] Fonseca, J.D., Grasselli, M. and Tebaldi, C. (2008). A Multifactor Volatility Heston Model. *Quantitative Finance*, **8**, 591 – 604.

[36] Fouque, J.P. and Han, C.H. (2003). Pricing Asian Options with Stochastic Volatility. *Quantitative Finance*, **3**, 353 – 362.

[37] Fouque, J.P. and Lorig, M.J. (2011). A Fast Mean-Reverting Correction to Heston's Stochastic Volatility Model. *SIAM Journal of Financial Mathematics*, **2**, 221 – 254.

[38] Fouque, J.P., Lorig,M. and Sircar, R. (2016). Second Order Multiscale Stocahstic Volatility Asymptotics: Stochastic Terminal Layer Analysis and Calibration. *Finance and Stochastics*, **20**, 543 – 588.

[39] Fouque, J.P., Papanicolaou, G., Sircar, R. and Solna, K. (2003). Multiscale Stochastic Volatility Asymptotics. *Multiscale Modeling and Simulation*, **2**, 22 – 42.

[40] Fouque, J.P., Papanicolaou, G., Sircar, R. and Solna, K. (2003). Singular Perturbations in Option Pricing. *SIAM Journal on Applied Mathematics*, **63**, 1648 – 1665.

[41] Fouque, J.P., Papanicolaou, G., Sircar, R. and Solna, K. (2011). *Multiscale Stochastic Volatility for Equity, Interest Rate and Credit Derivatives*. New York, USA: Cambridge University Press.

[42] Frittelli, M. (2000). The Minimal Entropy Martingale Measure and Valuation Problem in Incomplete Markets. *Mathematical Finance*, **10**, 39 – 52.

[43] Frittelli, M. and Gianin, E.R. (2004). Dynamic Convex Risk Measures. *Risk Measures for the* 21^{st} *Century*, 227 – 248.

[44] Fu, M.C., Madan, D.B. and Wang, T. (1999). Pricing Continuous Asian Options: A Comparison of Monte Carlo and Laplace Transform Inversion Methods. *Journal of Computational Finance*, **2**, 49 – 74.

[45] Gabaix, X., Gopikrishnan, P., Plerou, V. and Stanley, H.E. (2003). A Theory of Power-Law Distributions in Financial Market Fluctuations. *Nature*, **423**, 267 – 270.

[46] Gabaix, X. (2009). Power Laws in Economics and Finance. *The Annual Review of Economics*, **1**, 255 – 294.

[47] Garman, M.B. and Kohlhagen, S.W. (1983). Foreign Currency Option Values. *Journal of International Money and Finance*, **2**, 231 – 237.

[48] Gatheral, J. (2006). *The Volatility Surface: A Practitioner's Guide*. Hoboken, NJ: Wiley.

[49] Geman, H. and Yor, M. (1993). Bessel Processes, Asian Options and Perpetuities. *Mathematical Finance*, **3**, 349 – 375.

[50] Goncalves, B.A., Carpi, L., Rosso, O.A., Ravetti, M.G. and Atman, A.P.F. (2019). Quantifying Instabilities in Financial Markets. *Physica A: Statistical Mechanics and Its Applications*, **525**, 606 – 615.

[51] Gopikrishnan, P., Plerou, V., Amaral, L.A.N., Meyer, M. and Stanley, H.E. (1999). Scaling of the Distribution of Fluctuations of Financial Market Indices. *Physical Review E*, **60**, 5305 – 5316.

[52] Gulko, L. (1997). Dart Boards and Asset Prices. *Advances in Econometrics*, **12**, 237 – 276.

[53] Gulko, L. (1999). The Entropy Theory of Stock Option Pricing. *International Journal of Theoretical and Applied Finance*, **2**, 331 – 355.

[54] Gulko, L. (2002). The Entropy Theory of Bond Option Pricing. *International Journal of Theoretical and Applied Finance*, **5**, 355 – 383.

[55] Hafner, R. (2004). *Stochastic Implied Volatility (A Factor-Based Model)*. Springer-Verlag Berlin Heidelberg.

[56] Harrison, M.J. and Pliska, S.R. (1981). Martingales and Stochastic Integrals in the Theory of Continuous Trading. *Stochastic Processes and their Applications*, **11**, 215 – 260.

[57] Havrda, J. and Charvát, F. (1967). Quantification Method of Classification Processes. Concept of Structural α-Entropy. *Kybernetika*, **3**, 30 – 35.

[58] Henry, M. and Judge, G. (2019). Permutation Entropy and Information Recovery in Nonlinear Dynamic Economic Time Series. *Econometrics*, **7**, 10.

[59] Heston, S.L. (1993). A Closed-Form Solution for Options with Stochastic Volatility with Applications to Bond and Currency Options. *The Review of Financial Studies*, **6**, 327 – 343.

[60] Huang, C.S., O'Hara, J.G. and Mataramvura, S. (2017). Efficient Pricing of Discrete Arithmetic Asian Options under Mean Reversion and Jumps based on Fourier-Cosine Expansions. *Journal of Computational and Applied Mathematics*, **311**, 230 – 238.

[61] Huang, X. (2012). An Entropy Method for Diversified Fuzzy Portfolio Selection. *International Journal of Fuzzy Systems*, **14**, 160 – 165.

[62] Hubalek, F. and Sgarra, C. (2011). On the Explicit Evaluation of the Geometric Asian Options in Stochastic Volatility Models with Jumps. *Journal of Computational and Applied Mathematics*, **235**, 3355 – 3365.

[63] Hull, J.C. and Basu, S. (2016). *Options, Futures and Other Derivatives,* 9^{th} *edition*. Pearson India Education Services Pvt. Ltd.

[64] Hull, J. and White, A. (1987). The Pricing of Options on Assets with Stochastic Volatilities. *Journal of Finance*, **42**, 281 – 300.

[65] Ito, K. (1942). Differential Equations Determining Markov Processes (in Japanese). *Zenkoku Shijo Sugaku Danwakai*, **244**, 1352 – 1400.

[66] Ito, K. (1944). Stochastic Integral. *Proceedings of the Imperial Academy*, **20**, 519 – 524.

[67] Javid, A.A. (2012). Entropic Value-At-Risk: A New Coherent Risk Measure. *Journal of Optimization Theory and Applications*, **155**, 1105 – 1123.

[68] Jaynes, E.T. (1958). Probability Theory in Science and Engineering, Colloquium Lectures in Pure and Applied Science, Field Research Laboratory, Socony Mobil Oil Company, Dallas, Texas.

[69] Jiang, J., Shang, P., Zhang, Z. and Li, X. (2017). Permutation Entropy Analysis based on Gini-Simpson Index for Financial Time Series. *Physica A: Statistical Mechanics and Its Applications*, **486**, 273 – 283.

[70] Karatzas, I. and Shreve, S.E. (1991). *Brownian Motion and Stochastic Calculus*. New York, USA: Springer-Verlag.

[71] Kemna, A.G.Z. and Vorst, A.C.F. (1990). A Pricing Method for Options based on Average Asset Values. *Journal of Banking and Finance*, **14**, 113 – 129.

[72] Kim, B. and Wee, I.S. (2014). Pricing of Geometric Asian Options under Heston's Stochastic Volatility Model. *Quantitative Finance*, **14**, 1795 – 1809.

[73] Kou,S.G. (2002). A Jump Diffusion Model for Option Pricing. *Management Science*, **48**, 1086 – 1101.

[74] Kullback, S. and Leibler, R.A. (1951). On Information and Sufficiency. *The Annals of Mathematical Statistics*, **22**, 79 – 86.

[75] Kwok, Y.K. (2008). *Mathematical models of financial derivatives (2nd edition)*. Springer Berlin Heidelberg.

[76] Lefebvre, M. (2007). *Applied Stochastic Processes*. Springer Science & Business Media LLC.

[77] Li, B., Zhu, Y., Sun, Y., Aw, G. and Teo, K.L. (2018). Multi-Period Portfolio Selection Problem under Uncertain Environment with Bankruptcy Constraint. *Applied Mathematical Modelling*, **56**, 539 – 550.

[78] Linetsky, V. (2004). Spectral Expansions for Asian (Average Price) Options. *Operations Research*, **52**, 856 – 867.

[79] Luenberger, D.G. (1998). *Investment Science*. Oxford University Press: New York.

[80] Makate, N. and Sattayatham, P. (2011). Stochastic Volatility Jump-Diffusion Model for Option Pricing. *Journal of Mathematical Finance*, **1**, 90 – 97.

[81] Martina, E., Rodriguez, E., Perez, R.E. and Ramirez, J.A. (2011). Multiscale Entropy Analysis of Crude Oil Price Dynamics. *Energy Economics*, **33**, 936 – 947.

[82] Merton, R.C. (1973). Theory of Rational Option Pricing. *Bell Journal of Economics and Management Science*, **4**, 141 – 183.

[83] Merton,R.C. (1976). Option Pricing when Underlying Stock Returns are Discontinuous. *Journal of Financial Economics*. **3**, 125 – 144.

[84] Mikosch, T. (1998). *Elementary Stochastic Calculus (with Finance in View)*. World Scientific.

[85] Mitra, S. (2011). A Review of Volatility and Option Pricing. *International Journal of Financial Markets and Derivatives*, **2**, 149 – 179.

[86] Molgedey, L. and Ebeling, W. (2000). Local Order, Entropy and Predictability of Financial Time Series. *The European Physical Journal B - Condensed Matter and Complex Systems*, **15**, 733 – 737.

[87] Molina, G., Han, C.H. and Fouque, J.P. (2010). MCMC Estimation of Multiscale Stochastic Volatility Models. *Handbook of Quantitative Finance and Risk Management*, 1109 – 1120.

[88] Neri, C. and Schneider, L. (2012). Maximum Entropy Distributions Inferred from Option Portfolios on an Asset. *Finance and Stochastics*, **16**, 293 – 318.

[89] Neri, C. and Schneider, L. (2013). A Family of Maximum Entropy Densities Matching Call Option Prices. *Applied Mathematical Finance*, **20**, 548 – 577.

[90] Neri, C. and Schneider, L. (2014). The Impact of the Prior Density on a Minimum Relative Entropy Density: A Case Study with SPX Option Data. *Entropy*, **16**, 2642 – 2668.

[91] Ning, Y., Ke, H. and Fu, Z. (2015). Triangular Entropy of Uncertain Variables with Application to Portfolio Selection. *Soft Computing*, **19**, 2203 – 2209.

[92] Niu, H. and Wang, J. (2015). Quantifying Complexity of Financial Short-Term Time Series by Composite Multiscale Entropy Measure. *Communications in Nonlinear Science and Numerical Simulation*, **22**, 375 – 382.

[93] Øksendal, B. (2003). *Stochastic Differential Equations (An Introduction with Applications)*, Springer-Verlag, Heidelberg.

[94] Ormos, M. and Zibriczky, D. (2014). Entropy-Based Financial Asset Pricing. *PloS One*, **9**, e115742.

[95] Pan, J. (2002). The Jump-Risk Premia Implicit in Options: Evidence from an Integrated Time-Series Study. *Journal of Financial Economics*, **63**, 3 – 50.

[96] Peng, B. (2006). Pricing Geometric Asian Options under the CEV Process. *International Economic Journal*, **20**, 515 – 522.

[97] Pichler, A. and Schlotter, R. (2019). Entropy Based Risk Measures. *European Journal Of Operational Research*, (In Press).

[98] Qin, Z., Li, X. and Ji, X. (2009). Portfolio Selection Based on Fuzzy Cross-Entropy. *Journal of Computational and Applied Mathematics*, **228**, 139 – 149.

[99] Ramirez, J.A., Rodriguez, E. and Alvarez, J. (2012). A Multiscale Entropy Approach for Market Efficiency. *International Review of Financial Analysis*, **21**, 64 – 69.

[100] Rényi, A. (1961). On Measures of Entropy and Information. *Proceedings of the 4th Berkeley Symposium on Mathematical Statistics and Probability*, **1**, 547 – 561.

[101] Richman, J.S. and Moorman, J.R. (2000). Physiological Time-Series Analysis Using Approximate Entropy and Sample Entropy. *American Journal of Physiology - Heart and Circulatory Physiology*, **278**, H2039 – H2049.

[102] Rogers, L.C.G. and Shi, Z. (1995). The Value of an Asian Option. *Journal of Applied Probability*, **32**, 1077 – 1088.

[103] Ross, S.M. (1996). *Stochastic Processes*. John Wiley & Sons.

[104] Rouge, R. and Karoui, N.E. (2000). Pricing via Utility Maximization and Entropy. *Mathematical Finance*, **10**, 259 – 276.

[105] Samuelson, P.A. (1965). Rational Theory of Warrant Pricing. *Industrial Management Review*, **6**, 13 – 31.

[106] Samuelson, P.A. (1965). Proof that Properly Anticipated Prices Fluctuate Randomly. *Industrial Management Review*, **6**, 41 – 49.

[107] Scott, L.O. (1987). Option Pricing When the Variance Changes Randomly: Theory, Estimation, and an Application. *Journal of Financial and Quantitative Analysis*, **22**, 419 – 438.

[108] Scott, L.O. (1997). Pricing Stock Options in a Jump-Diffusion Model with Stochastic Volatility and Interest Rates: Applications of Fourier Inversion Methods. *Mathematical Finance*, **7**, 413 – 426.

[109] Shannon, C.E. (1948). A Mathematical Theory of Communication. *Bell System Technical Journal*, **27**, 379 – 423.

[110] Shu, J. and Zhang, J.E. (2004). Pricing S&P 500 Index Options under Stochastic Volatility with the Indirect Inference Method. *Journal of Derivatives Accounting*, **1**, 171 – 186.

[111] Sprenkle, C.M. (1961). Warrant Prices as Indicators of Expectations and Preferences. *Yale Economic Essays*, **1**, 178 – 231.

[112] Stein, E.M. and Stein, J.C. (1991). Stock Price Distributions with Stochastic Volatility: An Analytic Approach. *The Review of Financial Studies*, **4**, 727 – 752.

[113] Stutzer, M. (1996). A Simple Nonparametric Approach to Derivative Security Valuation. *Journal of Finance*, **51**, 1633 – 1652.

[114] Tunaru, R. (2016). Entropy Concepts Applied to Option Pricing. *Annals of the University of Craiova, Mathematics and Computer Science Series*, **43**, 108 – 117.

[115] Tsallis, C. (1988). Possible Generalization of Boltzmann-Gibbs Statistics. *Journal of Statistical Physics*, **52**, 479 – 487.

[116] Turnbull, S.M. and Wakeman, L.M. (1991). A Quick Algorithm for Pricing European Average Options. *Journal of Financial and Quantitative Analysis*, **26**, 377 – 389.

[117] Varma, R.S. (1966). Generalizations of Renyi's Entropy of Order α. *Journal of Mathematical Sciences*, **1**, 34 – 48.

[118] Vecer, J. (2001). A New PDE Approach for Pricing Arithmetic Average Asian Options. *Journal of Computational Finance*, **4**, 105 – 113.

[119] Vecer, J. (2002). Unified Pricing of Asian Options. *Risk*, **15**, 113 – 116.

[120] Wong, H.Y. and Cheung, Y.L. (2004). Geometric Asian Options: Valuation and Calibration with Stochastic Volatility. *Quantitative Finance*, **4**, 301 – 314.

[121] Xia, J. and Shang, P. (2012). Multiscale Entropy Analysis of Financial Time Series. *Fluctuation and Noise Letters*, **11**, 1250033.

[122] Xia, J., Shang, P., Wang, J. and Shi, W. (2014). Classifying of Financial Time Series Based on Multiscale Entropy and Multiscale Time Irreversibility. *Physica A: Statistical Mechanics and Its Applications*, **400**, 151 – 158.

[123] Xu, M., Shang, P. and Zhang, S. (2019). Multiscale Analysis of Financial Time Series by Rényi Distribution Entropy. *Physica A: Statistical Mechanics and Its Applications*, **120916**, (In Press).

[124] Yan, G. and Hanson, F.B. (2006). Option Pricing for a Stocahstic Volatility Jump-Diffusion Model with Log-Uniform Jump Amplitudes. *Proceedings of the 2006 American control conference,USA*, 2989 – 2994.

[125] Yin, Y. and Shang, P. (2014). Weighted Multiscale Permutation Entropy of Financial Time Series, *Nonlinear Dynamics*, **78**, 2921 – 2939.

[126] Zhang, J.E. (2003). Pricing Continuously Sampled Asian Options with Perturbation Method. *Journal of Futures Markets*, **23**, 535 – 560.

[127] Zhang, Y. and Shang, P. (2017). Permutation Entropy Analysis of Financial Time Series based on Hill's Diversity Number. *Communications in Nonlinear science and Numerical Simulation*, **53**, 288 – 298.

[128] Zhang, Y. and Shang, P. (2018). Refined Composite Multiscale Weighted-Permutation Entropy of Financial Time Series. *Physica A: Statistical Mechanics and Its Applications*, **496**, 189 – 199.

[129] Zhou, R., Cai, R. and Tong, G. (2013). Applications of Entropy in Finance: A Review. *Entropy*, **15**, 4909 – 4931.

[130] Zunino, L., Zanin, M., Tabak, B.M., Pérez, D.G. and Rosso, O.A. (2009). Forbidden Patterns, Permutation Entropy and Stock Market Inefficiency. *Physica A: Statistical Mechanics and Its Applications*, **388**, 2854 – 2864.

List of Research Papers

Papers Published/Communicated

1. **Gifty Malhotra**, R. Srivastava and H. C. Taneja. Quadratic Approximation of the Slow Factor of Volatility in a Multifactor Stochastic Volatility Model. *Journal of Futures Markets*, **38**, 607 – 624 (2018). https://doi.org/10.1002/fut.21895

2. **Gifty Malhotra**, R. Srivastava and H. C. Taneja. Calibration of the Risk-Neutral Density Function by Maximization of a Two-Parameter Entropy. *Physica A*, **513**, 45–54 (2019). https://doi.org/10.1016/j.physa.2018.08.148

3. **Gifty Malhotra**, R. Srivastava and H. C. Taneja. Pricing of the Geometric Asian Options Under a Multifactor Stochastic Volatility Model, Communicated.

4. **Gifty Malhotra**, R. Srivastava and H. C. Taneja. Comparative Study of a Stochastic Volatility Jump Model and a Multifactor Stochastic Volatility Model, Communicated.

5. **Gifty Malhotra**, H. C. Taneja and R. Srivastava. Two-Parameter Multiscale Permutation Entropy of a Financial Time Series, Communicated.

6. **Gifty Malhotra**, H. C. Taneja and R. Srivastava. Analysis of Financial Time Series Using a Two-Parameter Weighted Multiscale Permutation Entropy, Communicated.

Papers Presented in Conferences

1. **Gifty Malhotra**, R. Srivastava and H. C. Taneja. Comparison Between Multiscale Stochastic Volatility Model and Stochastic Volatility Jump Model, Presented in *International Conference on Interdisciplinary Mathematics, Statistics and Computational Techniques* held at Manipal University, Jaipur, December 22-24, 2016.

2. **Gifty Malhotra**, R. Srivastava and H. C. Taneja. Pricing of Geometric Asian Options Under a Multiscale Stochastic Volatility Model, Presented in *National Seminar on Recent Developments In Mathematical Sciences* held at Maharshi Dayanand University, Rohtak, March 07-08, 2017.

3. **Gifty Malhotra**, R. Srivastava and H. C. Taneja. Pricing of Geometric Asian Options Under a Multiscale Stochastic Volatility Model, Presented in *FIM&ISME 2017* Conference held at Kitakyushu International Conference Center, Kitakyushu, Japan, August 25-28, 2017.

4. **Gifty Malhotra**, R. Srivastava and H. C. Taneja. Comparative Study of Addition of Jump and Stochastic Volatility Factor in the Heston Model for Option Pricing, Presented in *International Conference on Advanced Production and Industrial Engineering* held at Delhi Technological University, Delhi, October 6-7, 2017.

5. **Gifty Malhotra**, H. C. Taneja and R. Srivastava. Information - Theoretic Approach to Study the Volatility of Stock Markets, Presented in *International Conference on Recent Advances in Pure and Applied Mathematics* held at Delhi Technological University, Delhi, October 23-25, 2018.